UNIVERSIDAD DE EXTREMADURA

TESIS DOCTORAL

Estrategias fisiológicas y comportamentales subyacentes a las respuestas de las aves al calentamiento global

Physiological and behavioural strategies underlying the responses of birds to global warming

Dña. Núria Playà Montmany

Programa de doctorado en Modelización y Experimentación en Ciencia y Tecnología

Conformidad del director y coodirectora en su caso

Dr. D. José Antonio Masero Osorio	Dra. Dña. Mª Auxiliadora Villegas Sánchez

Esta tesis cuenta con la autorización del director y coodirectora de la misma y de la Comisión Académica del programa. Dichas autorizaciones constan en el Servicio de la Escuela Internacional de Doctorado de la Universidad de Extremadura.

2022

To my parents

Acknowledgements

I could have never conducted this research without the support of my supervisors, colleagues, friends and family. Firstly, I would like to thank my supervisors Dr. José A. Masero ('Jose') and Dra. Auxiliadora Villegas ('Auxi'). Jose, your love and devotion for science are contagious and make all challenges that came across the way be accepted with the claim "We can!". Thank you for your willingness to discuss any aspect of the research, to listen to my ideas and for providing me with the guidance and help to convert them into high-quality scientific work. Your humour has made difficult times lighter and to someone with attention placed on the ocean, you have shown me the beauty that exists in the air. I will certainly carry the Great tit as my banner! Auxi, you were the first person who welcomed me, who accompanied me through every corner of the university and who showed me which would be my new home, Badajoz. From the beginning, you have accompanied me in what would be one of the biggest challenges of my life. Along the way, I have messed up in some calculations and measurements, but you were always patient and helped me to solve them. Your support and knowledge in statistics along with your guidance in all laboratory protocols have been crucial to successfully conducting this research and to increasing my expertise enormously, and I would like to add, you have been an example that women have no limits in science! In short, thank you both, for your mentorship and friendship.

Special thanks must go to Juan M. Sánchez-Guzmán ('Juanma'). Thank you for providing me with the funding and resources needed so I could conduct this research, for allowing me this opportunity and for the time you always had to attend to all my concerns. Throughout these years you have provided me with a lot of advice and opinions so that I could grow beyond the professional sphere. I am hugely grateful for your patience, interest and honesty. Along the way, there always came up questions to me, doubts and uncertainties that generated a lot of adrenaline, but your talks always helped me to calm my fears and to move forward. Thank you.

My field would not have been possible without the valuable work and assistance of Dr. Jose M. Abad ('Pipe') and Dr. Manuel Parejo ('Manolo') and I would like to highlight that I was also a witness (at least in the final phase) of the effort and hard work both of you displayed to become doctors, which made me realise the hardness of the way, but also how gratifying would be to achieve it too! In addition, I must include Julián (soon to be Dr. Julián Cabello-Vergel!) and Dr. Erick González-Medina ('Erick') with whom I shared most of the fieldwork, and I could learn, laugh and why not to say it, suffer when in those late afternoons no birds fell in the mist nets! Thank you for your friendship, assistance and for all the fun you brought along the way. All of you delved me into the wonderful world of ornithology and I am truly grateful for your help. I would like to make a special mention to Erick and his patience, you always were available to advise and guide me, thank you.

Being an introvert means finding difficulties in perhaps the simplest tasks, so I feel fortunate to have had the opportunity to teach under the guidance of the Dra. Mercedes Morales ('Merche') and Prof. Carlos de la Cruz ('Carlos'). Taking their advice and examples gave me the self-confidence to enjoy teaching and now, I know how rewarding teaching is when at the end of the class a student says to me that they enjoyed the class.

I would also like to thank Dr. Glenn Tattersall ('Glenn') for allowing me to work in his laboratory at Brock University (as long as the pandemic permitted it) and for training me in infrared thermography! My sincere gratitude for your guidance, support and commitment to carrying out the 'spot size' study herein as Chapter 6 and for understanding the inconveniences that the unusual pandemic situation brought. I must also thank the time you took to ensure I took the maximum profit from my visit to Canada. Thank you for planning all collaborations and visits, and thus, I would also like to thank Kyna Intini, for not only accompanying us during the data collection of Trumpeter swans but also for showing us the valuable work you do in rehabilitating injured individuals. Thanks to Dr. Kennet Welch for allowing me to visit your laboratory and to Erich Ebberts for his assistance and help in the use of the thermal cameras and respirometry system during my stay in Toronto. I must include how grateful I am for giving me the chance to work with hummingbirds! Thanks also to Katharine Yagi and Nicholas Sakich for their kindness and attention, and Dr. Joshua Kenneth Robertson for scheduling a visit to Toronto Zoo to use thermal cameras, although the pandemic prevented it.

I would also like to thank Dr. Vito M. R. Muggeo for answering numerous questions along with helping modify the R-segmented package, Juan Varela for the drawings here shown in the Chapter 2, Saúl Martín for the digital illustration and the Facility of Bioscience Applied Techniques of Research Support Service (SAIUEX) for the technical and human support provided.

During the development of this work, I have received the support of many colleagues and friends: María, Sofía, Jorge, Casimiro, Pablo, Deseada, Pepa, Pablo, Gregorio, Adriel, Jordi, Jose, Sara, Irene, Marcos, Andreu, Georgina, Rocío, … and please, feel included all of you who showed interest in this research over the years, thank you all!

Juan Carlos, my peace in the storm, thank you for your unconditional support and your endless words of encouragement. Despite you being concerned about the huge amount of time I spent developing this research, or even it was hard for you to understand the 'sacrifice' that this implied, you were always caring, empathic, thoughtful and supportive. I feel so grateful to you and your family who provided me with a place to recharge myself, feel relaxed and beloved.

Last, but not less important, I would like to thank my parents for the support I have never lacked from them. You taught me what hard work and perseverance are, and that there is no win without effort and constancy. There are been some years since I left home, but you have always been there for me, thank you. This achievement is also yours.

Abstract

Anthropogenic activity is leading to a global warming due to the continued and increasing emission of greenhouse effect gases. Consequently, the mean surface temperature of Earth is rising since the early 19th century and extreme weather events, such as heat waves, are becoming more intense, frequent and long-lasting. This has a major impact on biodiversity, which has experienced alterations in its distribution, demography, phenology, physiology, behaviour and morphology, along with dramatic consequences related to heat waves such as mass die-offs events. This poses biodiversity at a great risk highlighting the need and the urgency to delve into species' biological knowledge in order to better predict responses of avifauna to global change.

One of the most endangered regions on the planet due to climate change is the Mediterranean basin. In the last 30 years, Mediterranean habitats have experienced an increasing trend of maximum environmental temperature (T_a) along with more frequent and severe heat waves. However, the thermoregulatory demands of Mediterranean bird species to high T_a remain largely unexplored. Thus, the main goal of this thesis is to gain a better understanding of the major physiological and behavioural strategies underlying the responses of birds to global warming. Phenotypic flexibility allows individuals to reversibly modify thermoregulatory traits in response to environmental changes. Current and future selection pressures driven by climate change may favour species with higher physiological flexibility, resulting in greater resilience to environmental changes. According to the climatic variability hypothesis, individuals inhabiting more heterogeneous environments should exhibit a greater capacity to perform physiological adjustments. Here, (i) we tested this hypothesis by investigating seasonal differences in key thermoregulatory traits in resident Mediterranean songbirds. Additionally, we compared thermoregulatory traits between resident and trans-Saharan migratory species during summer. We found that Mediterranean resident songbirds seasonally adjusted key thermoregulatory traits in response to environmental conditions, with short-term benefits in terms of energy and water savings under thermally stressful conditions. Migratory songbirds, on the other hand, had more efficient thermoregulation mechanisms and evaporative cooling at high temperatures than resident songbirds. Overall, the results reveal that phenotypic flexibility in the thermoregulatory traits of Mediterranean songbirds may be crucial for their resilience to global warming. Birds inhabiting open landscapes are exposed to extreme cold and heat loads forcing them to develop a suite of behavioural and physiological adjustments to

successfully maintain homeothermy. Both types of responses could be influenced by relative bill and leg sizes, but experimental data are lacking. To achieve this goal, we experimentally evaluated (ii) how body postural adjustments (back rest, unipedal resting and sitting), panting and locomotor activity in the Dunlin *Calidris alpina* can be explained by the T_a, microhabitat use and relative bill and leg sizes. Additionally, resting metabolic rates (RMR) and evaporative water loss (EWL) were measured at different temperatures to assess potential relationships between thermal physiological traits and relative appendage size. We found Dunlins faced cold temperatures (< 20°C) mainly by increasing locomotor activity, while body postural adjustments (back rest and unipedal resting) were used less than expected. Under hot conditions (>30°C), locomotor activity strongly decreased, and dunlins rested on wet substrate (sand) in the sitting posture. Panting was ultimately used while wet-sitting when challenged with temperatures above 37 °C. No significant relationship was found between behavioural and physiological traits with relative bill and leg size, probably due to the low intraspecific variation. Our experimental findings emphasized the role of favourable substrates (wetland margins) in minimising heat stress in wetland species. Highly vascularized and unfeathered appendages exert a role in birds' thermoregulation by functioning as effective 'thermal windows', although this role in Mediterranean bird species remains largely unexplored and undescribed. To fulfil this gap and provide further information about physiological thermoregulatory aspects in small-sized Mediterranean birds in the context of global warming, we explored (iii) the potential relationship between several thermoregulatory traits (RMR, EWL, the lower critical temperature [T_{lc}], the upper critical temperature [T_{uc}], the breadth of the thermoneutral zone [TNZ], the T_a inflection point of EWL and the evaporative cooling efficiency) to the relative bill and leg surface areas in Mediterranean Great tits *Parus major*. The T_{lc} and T_{uc} of our Mediterranean population were ~17°C and ~34°C, respectively, being the T_a inflection point of EWL ~32°C. Overall, our modelling approach did not show any evidence of bill and leg relative sizes playing a significant role in thermoregulation physiology in this Mediterranean bird species. Our Great tit population occupies habitats with free-standing water, so active heat dissipation by EWL might be favoured instead of dry heat loss through the bill surface. Nevertheless, great tit males (but not females) with larger tarsi areas showed higher cooling efficiencies at 40°C. We argue that male dominance behaviour could imply a greater dependence on cutaneous EWL through the upper legs surfaces as a consequence of higher exposure to harsh environmental conditions than faced by females. The increase in long-lasting, more intense and frequent heat waves are leading to large scale die-offs around the globe, but concomitant sublethal effects on survivors are poorly known and remain largely undescribed in wild birds. Thus, we evaluated (iv) the potential effects of exposure to a simulated realistic summer heat wave scenario (39 ºC-42 ºC) in a Mediterranean population of Great tits at the physiological and morphological level while assessing the potential role of the phenotypic flexibility in bird capability to buffer heat stress. We showed Great tits to display slightly higher T_b values during heat waves simulations with reduced BMR (by 17%) and increased oxidative damage (by 56%) at the end of the experiment. Simultaneously, T_a appeared to shape contour feathers by decreasing barb and barbule density of the plumulaceous and pennaceous sections while eliciting more yellowish feathers in experimental birds. Great tits seem to possess efficient machinery at both, physiological and morphological levels, to plastically responded to heat, but not without potential adverse effects. Infrared thermography is a growing tool in the study of thermal ecology. However, the various pitfalls associated with this technique are still not fully appreciated or remain ignored in many biological thermography research studies. Therefore, it is vital to know and understand the main sources of error that can impact the collection of accurate data. Through the use of two cameras and three lenses, we aimed (v) to determine the inter-camera measurement differences of a known temperature object, the potential effect of spot size and object distance on temperature estimates, and the angle of incidence effect on emissivity measurements of different biological materials, in order to ultimately provide methodological advice to ecologist interested in thermal imaging. Distance greatly impacted on temperature obtained by thermal cameras. Increasing distance led to an increment of the apparent error in temperature, resulting in an underestimation up to 6ºC at 10 m. In addition, the angle of incidence also impacted the emissivity of biological materials, obtaining a decrease in emissivity at angles over 50º and more notoriously on smooth surfaces. In order to reduce both potential source of errors and thus obtain accurate data, we recommend thermal camera to be close enough to target object while maintaining the angle of incidence to the minimum.

Resumen

La actividad antropogénica está provocando un calentamiento global debido a la continua y creciente emisión de gases de efecto invernadero. En consecuencia, la temperatura media de la superficie de la Tierra está aumentando desde principios del siglo XIX y los fenómenos meteorológicos extremos, como las olas de calor, son cada vez más intensos, frecuentes y duraderos. Esto tiene un gran impacto en la biodiversidad, que ha experimentado alteraciones en su distribución, demografía, fenología, fisiología, comportamiento y morfología, junto con consecuencias mucho más dramáticas relacionadas con las olas de calor, como eventos de mortalidad masiva. Esto supone un gran riesgo para la biodiversidad, lo que pone de manifiesto la necesidad y la urgencia de profundizar en el conocimiento biológico de las especies para poder predecir de forma más precisa las respuestas de las aves al cambio global.

Una de las regiones del planeta más amenazadas por el camio climático es la cuenca mediterránea. En los últimos 30 años, los hábitats mediterráneos han experimentado una tendencia al aumento de la temperatura ambiental (T_a) máxima, junto con olas de calor más frecuentes y severas. Sin embargo, las demandas termorreguladoras de las especies de aves mediterráneas frente a altas T_a y olas de calor permanecen en gran medida inexploradas. Por lo tanto, el objetivo principal de esta tesis es comprender mejor las principales estrategias fisiológicas y comportamentales que subyacen a las respuestas de las aves frente al calentamiento global. La flexibilidad fenotípica permite a los individuos modificar reversiblemente los rasgos termorreguladores en respuesta a los cambios ambientales. Las presiones de selección actuales y futuras, impulsadas por el cambio climático, pueden favorecer a las especies con mayor flexibilidad fisiológica, lo que se traduce en una mayor resiliencia a los cambios ambientales. Según la hipótesis de variabilidad climática, los individuos que habitan entornos más heterogéneos deberían mostrar una mayor capacidad a la hora de realizar ajustes fisiológicos. Aquí, (i) examinamos esta hipótesis investigando las diferencias estacionales en rasgos termorreguladores clave en paseriformes mediterráneos residentes. Además, comparamos estos rasgos termorreguladores entre especies residentes y migratorias transaharianas durante el verano. Encontramos que los paseriformes residentes mediterráneos ajustan estacionalmente de manera muy significativa los rasgos termorreguladores en respuesta a las condiciones ambientales, con beneficios a corto plazo en términos de ahorro de energía y agua en condiciones de estrés térmico. Las especies migratorias, por otro lado, mostraron mecanismos de termorregulación y de eficiencia de enfriamiento más eficientes a altas temperaturas que las especies

residentes. En general, estos resultados destacan que la flexibilidad fenotípica en los rasgos termorreguladores de las aves paseriformes mediterráneas puede ser crucial para su resiliencia al calentamiento global. Las aves que habitan en paisajes abiertos están expuestas a cargas extremas de frío y calor, lo que les obliga a desarrollar un conjunto de ajustes conductuales y fisiológicos para mantener con éxito la homeotermia. Ambos tipos de respuestas podrían estar influidas por el tamaño relativo del pico y las patas, pero se carece, en general, de datos experimentales. Para lograr este objetivo evaluamos experimentalmente (ii) cómo los ajustes posturales (*back rest*, descanso sobre una pata y sentarse), el jadeo y la actividad locomotora del Correlimos común *Calidris alpina* pueden explicarse por la T_a, el uso del microhábitat y el tamaño relativo del pico y de las patas. Además, se midieron las tasas metabólicas en reposo (RMR) y la pérdida de agua por evaporación (EWL) a diferentes temperaturas para evaluar las posibles relaciones entre ambos rasgos termorreguladores y el tamaño relativo de los apéndices. Encontramos que los Correlimos comunes se enfrentaron a temperaturas frías (< 20ºC) aumentando principalmente la actividad locomotora, mientras que los ajustes corporales (*back rest* y descanso sobre una pata) se utilizaron menos de lo esperado. En condiciones de calor (> 30ºC), la actividad locomotora disminuyó hasta desaparecer y los correlimos descansaron sentados sobre el sustrato húmedo (arena). El jadeo se utilizó en última instancia, mientras se mantenían sentados y las temperaturas superaban los 37ºC. No se encontró ninguna relación significativa entre los rasgos conductuales y fisiológicos con el tamaño relativo del pico y de las patas, probablemente debido a la escasa variación intraespecífica. Nuestros resultados experimentales destacan el papel que los sustratos favorables (los márgenes de los humedales) juegan en la reducción del estrés térmico de las especies que ocupan estos hábitats. Los apéndices altamente vascularizados y desprovistos de plumas ejercen un papel en la termorregulación de las aves al funcionar como eficaces "ventanas térmicas", aunque este papel en las especies de aves mediterráneas permanece en gran medida inexplorado. Para intentar paliar esta falta de información sobre los aspectos fisiológicos de la termorregulación de las aves mediterráneas de pequeño tamaño en el contexto de calentamiento global, exploramos (iii) la posible relación entre varios rasgos termorreguladores (RMR, EWL, la temperatura crítica inferior [T_{lc}], la temperatura crítica superior [T_{uc}], la amplitud de la zona termoneutral [TNZ], el punto de inflexión de la T_a de la EWL y la eficiencia de enfriamiento por evaporación) con la superficie relativa del pico y de las patas en los Carboneros comunes *Parus major* mediterráneos. La T_{lc} y T_{uc} de nuestra población mediterránea fueron de ~17ºC y ~34ºC, respectivamente, siendo el punto de inflexión de la T_a de la EWL de ~32ºC. En general, nuestros modelos no mostraron evidencias de que los tamaños relativos del pico y de las patas desempeñen un papel significativo en el balance de calor y agua en esta especie mediterránea, ya que no se encontraron relaciones significativas entre el tamaño relativo de estos apéndices desprovistos de plumas y varios rasgos térmicos. Nuestra población de Carbonero común ocupa hábitats dónde hay agua disponible, lo cual podría favorecerse la disipación activa de calor corporal por medio de la EWL. Sin embargo, en los machos (pero no en las hembras) con mayor superficie de tarso encontramos una mayor eficiencia de enfriamiento a ~40ºC. Hemos argumentado que el comportamiento dominante de los machos podría implicar una mayor dependencia de la EWL a través de las patas, ya que este comportamiento le hace exponerse a condiciones ambientales más duras que a las que se enfrentan las hembras. El incremento de la T_a, junto con el mencionado aumento de olas de calor de larga duración, más intensas y frecuentes, está provocando grandes mortalidades de fauna en todo el globo, pero los efectos subletales concomitantes son poco conocidos y permanecen en gran medida sin describir en uno de los grupos más vulnerables, los paseriformes mediterráneos y otras especies silvestres. Hemos evaluado (iv) los efectos potenciales de olas de calor de intensidad creciente (39 ºC-42 ºC) a nivel fisiológico y morfológico en una población mediterránea de Carbonero común. Demostramos que los Carboneros comunes incrementan su T_b durante las simulaciones de olas de calor, junto con una disminución de la BMR (en un 17%) y un mayor daño oxidativo (en un 56%) al final del experimento. Al mismo tiempo, la olas de calor afectaron la estructura de las plumas de contorno, disminuyendo la densidad de las bárbulas y barbas de la sección plumulacea y pennacea, al tiempo que hubo un efecto en su coloración, siendo más amarillentas en los individuos experimentales. Los Carboneros comunes parecen poseer una gran flexibilidad en ciertos rasgos termorregulatorios que les permitiría hacer frente a estos eventos extremos de calor. Sin embargo, los individuos experimentales mostraron un mayor daño oxidativo, por lo que no podemos excluir posibles efectos acumulativos en la eficacia biológica. La termografía infrarroja es una herramienta cada vez más utilizada en el estudio de la ecología térmica. Sin embargo, los diversos problemas asociados a esta técnica aún no se conocen del todo o siguen siendo ignorados en muchos estudios. Por lo tanto, es vital conocer y comprender las principales fuentes de error que pueden afectar a la recogida de datos precisos cuando se usa esta técnica. Mediante el uso de dos cámaras térmicas y tres lentes, nos propusimos (v) determinar el efecto potencial del *spot size* y la distancia a un objeto de temperatura conocida en las estimaciones de temperatura, así como el efecto del ángulo de incidencia en las mediciones de emisividad de diferentes materiales biológicos,

con el fin de proporcionar, en última instancia, asesoramiento metodológico a los ecólogos interesados en la termografía. La distancia al objeto tuvo un gran impacto en la temperatura obtenida por las cámaras térmicas. El aumento de la distancia conllevó un incremento del error aparente en la temperatura, resultando en una subestimación de 6ºC a 10m. Además, el ángulo de incidencia impactó en la emisividad de los materiales biológicos, obteniéndose una disminución de la misma en ángulos superiores a 50º y de forma más notoria en superficies lisas. Estos resultados ponen de manifiesto que parámetros como la distancia al objeto de estudio o el ángulo de incidencia pueden ser grandes fuentes de error cuando se utiliza la termografía infrarroja. Para reducir ambas fuentes potenciales de error y obtener datos precisos, se recomienda que la cámara térmica esté lo suficientemente cerca del objeto y que el ángulo de incidencia sea el mínimo.

List of abbreviations

BMR – Basal metabolic rate
CORT – Corticosterone
CORT$_{f}$ – Corticosterone in feathers
CEWL – Cutaneous evaporative heat loss
EHL – Evaporative heat loss
EHL/MHP – Evaporative cooling efficiency
EWL – Evaporative water loss
fGCM – Faecal glucocorticoid metabolites
M$_{b}$ – Body mass
MHP – Metabolic heat production
MR – Metabolic rate
RMR – Resting metabolic rate
ROS – Reactive oxygen species
T$_{a}$ – Environmental temperature
T$_{b}$ – Body temperature
TL – Telomere length
T$_{lc}$ – Lower critical temperature of thermoneutrality
TNZ – Thermoneutral zone
T$_{uc}$ – Upper critical temperature of thermoneutrality
VO$_{2}$ – Oxygen consumption

Content

1. **Introduction 3**

Phenotypic flexibility in bird thermoregulation 5

Behavioural strategies to face thermal stress 6

The role of morphology in facing thermal stress................................. 9

General responses of birds to global warming................................... 13

New recent techniques in the study of thermoregulation in birds................. 15

Thesis objectives 18

References 18

2. **Mediterranean songbirds show pronounced variation in thermoregulatory traits...31**

Abstract 32

Introduction.. 33

Materials and methods 35

  Bird captures 35

  Experimental setup 36

  Gas exchange measurements.. 37

  Statistical analyses.. 37

  Phylogenetic comparative analyses 38

Results... 39

  Seasonal variation across resident species 39

  Comparisons across migratory and resident species..................... 40

Discussion 42

References 45

Appendix 1: Supplementary Material.. 54

3. **Behavioural and physiological responses to experimental temperature changes in a long-billed and long-legged bird: a role for relative appendage size 63**
  - Abstract 64
  - Introduction 65
  - Materials and Methods 67
    - Bird capture and maintenance 67
    - Metabolic measurement protocol 67
    - Gas exchange measurements 68
    - Behavioural data collection 68
    - Data analysis 69
  - Results 71
  - Discussion 75
  - References 79

4. **The thermoregulatory role of relative bill and leg surface areas in a Mediterranean population of Great tit (*Parus major*) 87**
  - Introduction 89
  - Materials and methods 91
    - Capture and biometric measurements 91
    - Gas exchange measurements 92
    - Data collection protocol 93
    - Data analysis 94
    - Results 95
    - Discussion 102
  - References 104

5. **How do Mediterranean bird species cope with extreme weather events? Physiological and morphological responses to simulated heat waves in Great tits (*Parus* major) 113**
  - Abstract 114
  - Introduction 115

Materials and methods 118
  Capture and housing 118
  Experimental setup 118
  Thermoregulatory traits and body mass 119
  Corticosterone, oxidative status and telomere length measurements 121
  Contour feather measurements 123
  Data analysis 124
Results 125
  Thermoregulatory traits and body mass 126
  Feather CORT, oxidative status and telomere length 136
  Feather structure and colouration 136
Discussion 139
References 142
Supplementary material: Appendix 2 152

6. Spot size, distance and emissivity errors in field applications of infrared thermography 155

Abstract 156
Introduction 157
Material and Methods 163
  Thermal Infrared Cameras 163
  Study System 164
  Distance and Spot Size Effects on Camera Offset (ΔT) 165
  Spot Size Calculations 166
  Accuracy Assessment 166
  Field Test of Distance Effects in Trumpeter Swans 167
  Angle Effects on Emissivity 168
Results 171
  Camera Accuracy and Thermal Resolution 171
  Distance and Spot Size Effects on ΔT 171

Distance Effects in Wild Birds ... 173
Angle Effects on Emissivity ... 175
Discussion ... 176
Camera Accuracy and Thermal Resolution ... 178
Distance and Spot Size Underestimate Temperature ... 178
Spot Size Effects ... 179
Angle of Incidence and Emissivity of Biological Surfaces ... 180
Recommendations for data reporting in field thermography ... 180
References ... 183
Appendix 3: Supplementary Material ... 186
7. General conclusions ... 193
General conclusions ... 194
Conclusiones generales ... 196
Addresses of co-authors ... 198

1

Introduction

Earth's climate is warming at an unprecedented rate since the early 19th century due to increased emissions of greenhouse gases (IPCC 2021). The global mean surface temperature has increased by more than 0.75°C since the 1960s (see Figure 1), with the sharpest increments occurring in the last decades and most dramatically in the continents of the northern hemisphere (IPCC 2021). These changes in mean environmental temperatures (T_a) are linked to increasing long-lasting, intense and frequent extreme weather events recorded since the late 20th century (Møller *et al.* 2010; Stillman 2019; IPCC 2021). The Mediterranean basin is one of the most affected areas by global warming (Herrero *et al.* 2021; IPCC 2021), and climatic models anticipate longer and more severe heat waves exceeding 45°C in the Iberian Peninsula (Viceto *et al.* 2019) by the end of this century. This raises the question of whether Mediterranean fauna, including an especially vulnerable group as birds, will be able to buffer heat stress through behavioural, physiological and morphological adjustments.

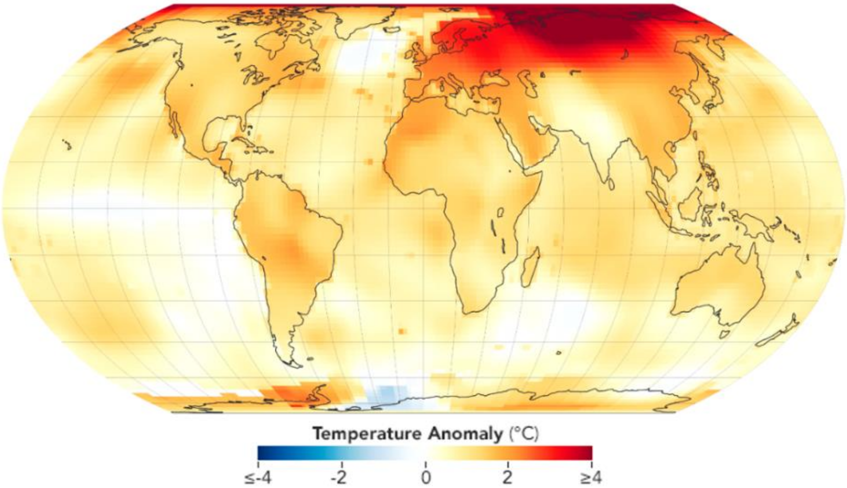

Figure 1. Global averaged temperature anomaly in 2020 over the last 50 years relative to 1951-1980 mean. Global averaged temperature is increasing since the baseline period, being in 2020 1.02°C warmer (NASA's Goddard Institute for Space Studies; photo from NASA Earth Observatory: https://earthobservatory.nasa.gov).

Phenotypic flexibility in bird thermoregulation

A major mechanism of response by organisms to environmental changes is phenotypic flexibility (Bonamour *et al.* 2019; Piersma & van Gils 2011, see **Chapter 2**). This property can be defined as those changes in individuals' behavioural, physiological or morphological traits triggered by changes in the environment, that are reversible and transitory, and can confer adaptive advantages (Piersma & Drent 2003). Phenotypic flexibility may allow birds to acclimatize to spatially and temporally heterogeneous environments (e.g., Cavieres & Sabat 2008; Stager *et al.* 2021), as well as cope with the environmental variability elicited by climate change (Bonamour *et al.* 2019; Piersma & van Gils 2011). One of the physiological traits where flexibility has been extensively documented is the basal metabolic rate (BMR), which is known to be adjusted according to body mass (M_b), diet, climate, latitude, altitude, circadian rhythm, life-history traits or season (see Cooper *et al.* 2002; Vézina *et al.* 2006; Thompson 2014; Thompson *et al.* 2015). For example, birds inhabiting seasonal climates showed an upregulation of the BMR during the colder months, since this may improve thermogenic capacity (McKechnie *et al.* 2015; Swanson *et al.* 2020), while in warmer months birds reduce the BMR to avoid thermal stress and conserve water (Tieleman & Williams 2000; Tieleman *et al.* 2002, 2003; Thompson 2014). The metabolic rate of endotherms is inherently related to the thermoneutral zone (TNZ; the range of T_a where individuals that remain inactive, post-absorptive, non-reproductive and in a resting state show basal energy consumption. Below the lower [T_{lc}] and above the upper [T_{uc}] critical limits of TNZ additional water and energy is needed to thermoregulate (McNab 2002; see an example of a TNZ representation in **Chapter 3, Figure 1**) (McNab 2002). This way, the breadth of the TNZ may imply contrasting phenotypic flexibilities to deal with environmental changes (Thompson 2014; Pollock *et al.* 2021; **Chapter 2**).

Despite the well-known capacity of small-sized bird species to acclimate to seasonality by commonly upregulating metabolic rate in winter (Thompson 2014; McKechnie *et al.* 2015), there exist variability in the physiological adjustments adopted (Bush *et al.* 2008; Smit et al. 2008). For example, it has been registered a downregulation of metabolic rates in southern hemisphere birds in summer (Smit *et al.* 2008), whilst several temperate-zone species showed an increase in BMR rates in winter (McKechnie *et al.* 2015). Therefore, the physiological responses that birds adopt to respond to challenging environmental conditions differ between species and have not been clearly determined. This imposes the necessity to conduct intra- and interspecific studies to better describe and characterize the thermal physiological flexibility of birds displaying contrasting life-history strategies and inhabiting seasonal climates in the context of climate change.

The climatic variability hypothesis (CVH) predicts the strongest selection for plasticity in those species inhabiting more variable climates at both, temporal and spatial scales (Stevens 1989). Thus, the CVH forecasts species from higher latitudes would display a pronounced thermal plasticity and acclimation capacity due to they inhabit more thermally heterogeneous environments (Schlichting & Pigliucci 1998; Cavieres & Sabat 2008; Stager *et al.* 2021). Similarly, migratory species are expected to exhibit greater phenotypic flexibility as they are exposed to diverse biotic and abiotic variables, including thermal niche (see **Chapter 2**) by moving between geographic localizations that are several thousand kilometres apart (Kvist & Lindström 2001; Lindström & Klaassen 2003; Piersma & van Gils 2011). The physiological strategies that bird adopt shape their capacity to respond to changing environmental conditions, which may differ between species from different climates and species displaying contrasting life-history traits (see **Chapter 2**). For example, previous interspecific differences in thermoregulation physiology have been documented between small-sized migratory and resident songbirds in China (Qiao *et al.* 2016). Then, comparative studies evaluating life-history strategies along with seasonality are needed to evaluate phenotypic flexibility in different thermoregulatory traits like BMR, TNZ breadth and evaporative water loss (EWL) to provide further information on previous mixed results obtained (**Chapter 2**).

Behavioural strategies to face thermal stress

Endotherms maintain high core body temperatures (hereafter referred to as T_b) by generating large amounts of heat through metabolism (i.e., food oxidation, basal cellular metabolism and muscular contraction (Daan *et al.* 1990; Piersma *et al.* 1996; Burness *et al.* 1998; Clarke 2017). Birds' T_b (39 to 42°C; Bartholomew & Cade 1963) commonly surpasses that of mammals and that of the environment, which allows them to carry fine control over T_b regulation as they can easily modify thermal conductance (e.g., changes in the peripheral blood supply of the bare skin surfaces, insulation depth or body postures) (McNab 2012; Tattersall *et al.* 2012; Sturkie 2015; Lovette & Fitzpatrick 2016; Clarke 2017). Under thermal stress, the literature indicates behaviour to be the main strategy shared by a wide variety of bird species to cope with it as being less energetically costly than physiological adjustments (Wolf 2000; Lovette & Fitzpatrick 2016). However, despite the relevance of behaviour in birds' thermoregulation, research empirically characterizing avifauna responses to challenging T_a still focuses mainly on physiological responses (e.g., Smith *et al.* 2015; Whitfield *et al.* 2015; McKechnie *et al.* 2017).

The thermoregulatory behaviours that birds adopt are, commonly, non-mutually exclusive. For example, they can adopt various body postures simultaneously (e.g., exposition of both bare surfaces: the bill and the legs) (see Ryeland *et al.* 2017, 2019, 2021). In cold conditions, birds are observed to huddle, squat, "fluffing feathers", change unfeathered areas exposed to the environment or select favourable microhabitats (Stukie 2015; Smit *et al.* 2016; Ryeland *et al.* 2017, 2019, 2021). On the other hand, in hot environments, birds usually adopt behaviours that promote body heat loss such as seeking shade, body postural adjustments or minimizing locomotor activity (Sturkie 2015; Ryeland *et al.* 2017, 2019, 2021; Thompson *et al.* 2018; Funghi *et al.* 2019). Curiously, birds can potentially adopt the same body posture to deal with cold and heat stress (Sturkie 2015; Ryeland *et al.* 2017, 2019, 2021). For example, sitting has been observed to minimize around 20-50% of body heat loss in domestic fowls in cold conditions (Sturkie 2015) whereas it is also adopted by several shorebird species at high T_a to favour body heat loss through conduction when resting in colder surfaces (Ryeland *et al.* 2021). Extreme T_a (e.g., T_a beyond thermoneutrality) exposes birds to the risk of not being capable of maintaining T_b at a level where physiological performance is optimal, so minimizing exposition of unfeathered appendages along with selecting suitable microclimates allows them to maintain thermal balance (Ryeland *et al.* 2017, 2019, 2021). Therefore, as mentioned above, birds exert certain control on the heat that is retained by the body or lost to the environment (Brodsky & Weatherheat 1984; Wiersma & Piersma 1994; Ryeland *et al.* 2017, 2019, 2021).

Figure 2. Dunlins *Calidris alpina* resting while adopting diverse body postures in the coastline (photo by Georg Wietschorke).

Recent studies performed with Charadriiform species showed how individuals adjust body posture ('back rest' – individuals tucked the bill under scapular feathers -, standing on one or two legs and sitting; see an example of resting Dunlins in Figure 2) in accordance with T_a and microhabitat (Ryeland *et al.* 2017, 2019, 2021). By adopting different body postures birds modify the unfeathered surfaces of appendages to surroundings and change the surface area to volume ratio (Brodsky & Weatherhead 1984; Wiersma & Piersma 1994; Ryeland *et al.* 2017, 2019, 2021), allowing individuals to regulate heat to maintain homeothermy (Sturkie 2015). Moreover, shorebirds occupying water-logged wetlands buffer high T_a while sitting on wet surfaces to increase body heat loss (Ryeland *et al.* 2021).

It should be noted that the availability of microclimates greatly differs between habitats, as the opportunities for birds to occupy thermal refugia in deserts are reduced or even inexistent compared to those inhabiting forests. This highlights a behavioural response that has been overlooked when studying the effects of heat stress on birds: the level of locomotor activity. To avoid overheating, it is well-known that many diurnal species confine their activity to cold periods as locomotor activity increases metabolic heat production (Davies 1982). For example, the Roadrunner *Geococcyx californianus* reduced locomotor activity during the hottest hours of the day (Calder 1968). Keeping immobile during high T_a may allow birds to avoid dramatic and fatal increments of T_b (Davies 1982; Ryeland *et al.* 2017, 2019; see **Chapter 3**). Behavioural thermoregulation (e.g., body postural adjustments or locomotor activity) can also inflict large costs as this minimizes opportunities to employ other crucial activities such as reproduction, foraging or being aware of predators (Clarke 2017; Cunningham *et al.* 2021), and these costs could be exacerbated in a context of global warming (Cunningham *et al.* 2021).

The role of morphology in facing thermal stress

Species morphology is related to climate and shows a great intra- and interspecific variation across the latitudinal gradient (Bergmann 1847; Allen 1877). One of the most known 'ecogeographical rules' is Bergmann's rule which established endotherms from warmer climates (i.e., tropics) are smaller than their counterparts from colder environments (i.e., poles), since smaller bodies possess a greater body surface/volume ratio that enables animals to dissipate higher rates of body heat (Bergmann 1847; Ryding *et al.* 2021). In the context of global warming, over the last years, a reduction in body size has been documented in both terrestrial and aquatic species including endotherms and ectotherms, pointing to the reduction in body size and changes in animal body shape as additional responses to increasing T_a (Gardner *et al.* 2011; Ryding *et al.* 2021). Allen's rule predicts a reduced size of appendages of those species inhabiting higher altitudes and latitudes, as a minimized size of these appendages diminishes body heat loss being advantageous in cold environments (Allen 1877; Symonds & Tattersall 2010; Greenberg *et al.* 2012; Gardner *et al.* 2016). Thus, an increase in the relative size of appendages of individuals would be expected (for example in the size of bills or legs in birds) as a result of increasing heat waves (Gardner *et al.* 2011, 2016; Ryding *et al.* 2021). For example, the Starling *Sturnus vulgaris* showed an increase in body and bill sizes which relates to the increment of summer maximum T_a (Cardilini *et al.* 2016) and the Dark-eyed junco *Junco hyemalis* individuals displayed an increment in bill size as a result of extreme weather events along with gradual T_a increase (LaBarbera *et al.* 2020). To better predict the impacts of global warming on wildlife is key to understanding the role that morphology exerts on thermal balance and thus, the relevance and the function that appendages have on avifauna thermoregulation (see **Chapter 3** and **Chapter 4**).

Birds successfully maintain a relatively constant T_b at thermoneutrality due to effective thermal conductance adjustments where the role of "thermal windows" becomes key (Tattersall *et al.* 2009, 2017). Two essential characteristics of structures are required to be able to function as thermal windows: a bare surface and a network of superficial blood vessels (Steen & Steen 1965; Tattersall *et al.* 2009, 2012, 2017; Lovette & Fitzpatrick 2016). In birds, the unfeathered and highly vascularized appendages (i.e., bill and legs; see Figure 3 and Figure 4) are recognized to be effective thermal windows due to they function as potent heat exchangers to the environment via non-evaporative means (i.e., radiation, convection and conduction; see Figure 5 for further details) (Tattersall *et al.* 2009, 2017), although both appendages display a different vascular network (Symonds & Tattersall 2010; Tattersall *et al.* 2017). The vascular vessels supplying blood to the dermis, allocated between the body and the rhamphotheca in the bill, dilate or contract to increase or decrease, respectively, the blood supply to match the environmental conditions (Tattersall *et al.* 2009, 2017; Van de Ven *et al.* 2016; Janse van Vuuren *et al.* 2020). The vascular arrangement found in the bill seems to be more random than in the legs (Steen & Steen 1965; Hagan & Heath 1980; Mitgård 1981; Arad *et al.* 1989; Tattersall *et al.* 2012, 2016). Legs are irrigated by a counter-current system, a well-known thermoregulatory system (Steen & Steen 1965; Mitgård 1981; Maloney & Dawson 1994). In cold environments, the warm blood of arteries that irrigates the foot and feet lose heat through the adjacent veins that return cool blood from the extremities to the core body, while in warm environments venous vessels dilate to increase blood volume favouring body heat loss to surroundings (Steen & Steen 1965; Mitgård 1981; Maloney & Dawson 1994). Thus, both unfeathered surfaces regulate the superficial volume of blood to reduce or favour body heat loss in accordance with T_a (Steen & Steen 1965; Mitgård 1981; Maloney & Dawson 1994; Sturkie 2015).

Figure 3. A Southern yellow-billed hornbill *Tockus leucomelas* where it can be appreciated the extensive vascularization of the bill (Photo by Petr Kratochvil).

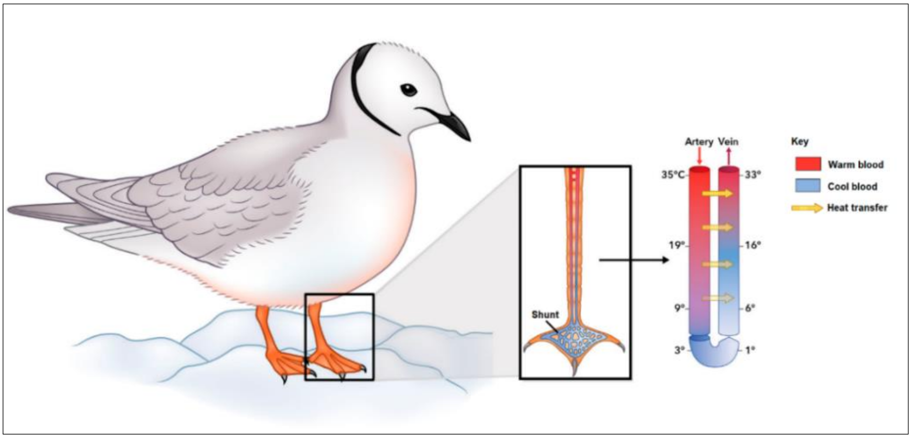

Figure 4. The body heat loss through feet surface as a result of the direct contact with cold grounds (e.g., ice) is reduced by an effective counter-current blood system that saves huge amounts of body heat by maintaining higher temperatures on the leg and cooler feet temperatures (Adapted from Randall *et al.* 2002).

Convection Heat loss is due to the actual movement of air molecules. The layer in direct contact to the skin warms up and thus, rises while the cooler and denser air comes to contact the skin. This is known as "natural convection", but when air speed increases, this prevents air from heating up, so the gradient between T_a and T_b increases and heat loss is enhanced.

Radiation Heat radiation in form of electromagnetic waves (i.e., infrared) is transferred from the skin surface or the plumage to the cooler surroundings when they are not in contact. However, heat flux is reversed when biological surfaces surpass environment temperature.

Conduction The transfer of heat occurs from molecule to molecule, implying a direct contact of bird surfaces (e.g., legs) to the surroundings (e.g., surface).

Figure 5. Nonevaporative avenues (convection, radiation and conduction) to maintain thermal balance.

In the last years, the role in birds' thermoregulation of both appendages has attracted considerable interest as they can potentially act as effective heat radiators above the T_{uc} (see Tattersall *et al.* 2009, 2017, 2018; Greenberg *et al.* 2012; Gardner *et al.* 2016; Van de Ven *et al.* 2016; Janse van Vuuren *et al.* 2020). This is possible due to the thermal gradient that exists between the environment and the body (T_a-T_b) since this allows a heat flux from the individual to the surroundings when T_b surpasses T_a, although if reversed, the unfeathered appendages could become heat sinks (Greenberg & Danner 2012; Gardner *et al.* 2016; Ryeland *et al.* 2017; Probst *et al.* 2021). The bill has been proven to act as an effective thermal radiator at high T_a in different long-billed species such as the Toco toucan *Ramphastos toco* (Tattersall *et al.* 2009), the Southern yellow-billed hornbill *Tockus leucomelas* (Van de Ven *et al.* 2016; Figure 3) or the Southern ground-hornbill *Bucorvus leadbeateri* (Janse van Vuuren *et al.* 2020). However, this role has also been found in small-sized birds whose bill only represents ~2% of total body size (Greenberg *et al.* 2012). On the other hand, the role of legs in thermoregulation has been largely described in 21 orders and 66 species of birds (see Mitgård 1981) being the counter-current system found in several species, such as the Rea *Rhea americana*, the Eider *Somateria mollissima*, the Painted stork *Mycteria leucocephalus,* the Japanise quail *Coturnis japonica* or the Greater flamingo *Phoenicopterus roseus*. However, contrary to bill structure, studies analysing leg role in bird thermal balance have been mainly focused on their function in retaining body heat at low T_a whereas its role in hot conditions has been largely overlooked (Steen & Steen 1965; Baudinette *et al.* 1976; Maloney & Dawson 1994; Cabello-Vergel *et al.* 2021). Thus, the function of both appendages in the thermoregulation of small-sized birds (<200 g) like songbirds is poorly known and it is completely unexplored in species like the Great tit inhabiting Mediterranean habitats (see **Chapter 4**).

General responses of birds to global warming

Global warming has turn into one of the worldwide known greatest threats to biodiversity (Sala *et al.* 2000; Tilman *et al.* 2017) and it has been related with alterations in fitness and changes in distribution, demography, phenology, physiology, behaviour and even, the morphology of several species, including birds (e.g., Hughes 2000; Parmesan & Yohe 2003; Root *et al.* 2003; Parmesan 2006; Møller *et al.* 2010; Gardner *et al.* 2011). Predicted scenarios of global change anticipate birds will experience in the next decades harsher environmental conditions as being exposed most frequently to hot days and heat waves where maximum T_a will be outside or further outside the T_{uc} of their TNZ (McNab 2002). When T_a overcomes T_b, passive pathways to lose body heat (Figure 5) are no longer viable, being the EWL the only avenue birds can employ to maintain T_b within safe limits (Calder & King 1974; McNab 2002). In this context, the thermal gradient may be potentially minimized or even eliminated, forcing birds to enhance energetically costly mechanisms (e.g., panting) to face concomitant thermal stress (e.g., Calder & King; McKechnie & Wolf 2019) and thus, becoming much more vulnerable to rising T_a (McKechnie & Wolf 2010, 2019; Lovette & Fitzpatrick 2016). In last years, extreme events such as heat waves are leading to large-scale die-offs of several marine and terrestrial species (McKechnie & Wolf 2010; Saunders *et al.* 2011; McKechnie *et al.* 2012; Marvel *et al.* 2019) including bats and birds (McKechnie & Wolf 2010; McKechnie *et al.* 2021). Concretely, in 2010 in Australia, a heat wave led to thousands of Carnaby's black cockatoos *Calyptorhynchus latirostris* dead (Saunders *et al.* 2011; McKechnie *et al.* 2012) and recently, the carcasses of 47 birds of 14 species were found dead consequently of experiencing consecutive days above 37°C in eastern South Africa (McKechnie *et al.* 2021). These episodes highlight the potential of heat waves to drive catastrophic declines in wild living populations across the globe, and so, the severe consequences associated with anthropogenic climate change (McKechnie & Wolf 2010, 2019; Saunders *et al.* 2011; McKechnie *et al.* 2012).

In this framework, survivors are likely to experience sublethal effects associated with conducting behavioural, physiological or morphological adjustments in order to buffer heat stress, which may impact fitness in the long-term future (McKechnie & Wolf 2010; Saunders *et al.* 2011; Stillman 2019;

McKechnie *et al.* 2012, 2021; Conradie *et al.* 2019; Danner *et al.* 2021). This is not surprising as many biological processes and structures are thermally sensitive, such as energetics (McNab 2002), water balance (Calder & King 1974; Wolf & Walsberg 1996), endocrine activity (Sapolsky *et al.* 2000; Xie *et al.* 2017), oxidative status (Mujahid *et al.* 2005; Lin *et al.* 2008; Jacobs *et al.* 2020), telomere dynamics (Simide *et al.* 2016; Zhang *et al.* 2018; Fitzpatrick *et al.* 2021) or feather structure and colouration (Burtt & Ichida 2006; Broggi *et al.* 2011; Sándor *et al.* 2022). Thus, the literature indicates a broad repertoire of adjustments that may occur to maintain thermal homeostasis in response to heat, but these are poorly known and understood (e.g., Simide *et al.* 2016; Zhang *et al.* 2018). Previous studies have shown mixed effects resulting from exposition to high T_a (>35°C) in birds. For example, Ton et al. (2021) found no effect on growth rate or body mass in juvenile Zebra finches *Taeniopygia guttata*, which is consistent with previous reports on other small-sized passerines species (Dawson *et al.* 2005; Hsu *et al.* 2020), but Andreasson et al. (2018) registered lower mass gain in individuals from heat-exposed nests. Moreover, it has been reported an increment in corticosterone levels in the Diamond dove *Geopelia cuneata* following exposure to 45°C, but this was not observed in Budgerigars *Melopsittacus undulatus* or in Zebra finches suggesting heat is not perceived as a stressor in the latter two species (Xie *et al.* 2017). To fulfil this gap, further research is needed to shed some light on potential sublethal consequences derived from exposition to sustained exposure to heat stress like heat waves.

Moreover, physiological and morphological traits responses to hot temperatures (**Chapter 5**) have been mainly studied on avian species inhabiting arid and semi-arid environments such as hot deserts, where freestanding water and thermally buffered microclimates are scarce (McKechnie & Wolf 2010; du Plessis *et al.* 2012; Van de Ven *et al.* 2019). Mediterranean climate is characterized by hot, dry summers with frequent heat waves and cool, wet winters where T_a of the warmest month and the coldest month is ~35°C and ~4°C respectively (Allam *et al.* 2019; Coelho & Pinto 2019). So, despite the milder conditions that Mediterranean birds experience as compared to those inhabiting deserts, in the last 30 years the Mediterranean region has experienced an increasing trend of summer maximum T_a along with more frequent and severe heat waves (Acero *et al.* 2014, 2018; Viceto *et al.* 2019; IPCC 2021). However, the thermoregulatory demands of Mediterranean bird species to high T_a and the impact of heat waves on bird physiology and morphology remain largely unexplored (**Chapter 5**).

New recent techniques in the study of thermoregulation in birds

Thermal imaging was born in the 1960s as a tool used in the USA for military purposes (Vollmer & Möllmann 2010), but this later become accessible to a broader public, including scientists, becoming broadly used in several fields of science such as animal ecology and physiology (e.g., McCafferty 2013; Tattersall 2016; Tabh *et al.* 2021; Tapper *et al.* 2021). With this technique, the surface temperature of individuals can be obtained at distance without interfering with natural processes (Tattersall 2016). Its main advantage is that it neither requires the capture nor the handling of individuals, avoiding birds' stress that could translate into higher metabolic rates, increased T_b and abnormal behaviour (McCafferty 2013; Tattersall 2016). Thermal imaging has been widely applied in avian thermal physiology and has provided further insight into this topic by allowing the obtention of several thermal traits and ratios such as heat net flux, body surface temperature, thermal conductance of the skin or plumage, and determining the role of unfeathered appendages in thermal balance (e.g., Tattersall *et al.* 2009, 2016, 2018; Greenberg *et al.* 2012; Tabh *et al.* 2021; Tapper *et al.* 2021). Thermal imaging may be a powerful tool to characterize the physiological responses of birds to thermal stress. For example, Tattersall et al. (2018) showed bills function as effective heat dissipators under hot environmental conditions by using thermal cameras.

All matter is in constant motion, atoms are continuedly vibrating and emitting radiation (Tattersall 2016). The infrared radiation (heat) can be detected by infrared cameras that detect electromagnetic radiation in the spectral band (~8-12μm) in any object whose temperature is above absolute zero (-273.15°C or 0°K). Thermal cameras measure emitted infrared radiation (R; W m^{-2}) and calculate temperature (T; °K) using the Stefan-Boltzmann equation: $R=\varepsilon\sigma T^4$, where σ is the Stefan-Boltzmann constant (5.67×10^{-8} W m^{-2} K^{-2}) and ε is the emissivity (i.e., the radiant energy emitted by a surface) (McCafferty 2013). An object with an emissivity of one (a black body) is a perfect emitter, this reflects no energy, but in nature, most biological surfaces are recorded in the range of 0.95-0.98 (Hammel 1956; Best & Fowler 1981).

A thermal camera uses a unique lens (Box 1 for thermal camera specifications) that allows the pass of radiation which is detected by internal sensors that scan the information and generate a thermogram. All data contained in the thermogram are transformed for visualization. Thermal images are constituted by a set of pixels where each contains a registered temperature (Figure 6; McCafferty 2013). Potential sources of error and uncertainties (**Chapter 6 Figure 1**) may be exacerbated when using thermal cameras without taking into account the specifications which may critically affect the quality of thermal data obtained (Faye *et al.* 2016; Tattersall 2016). For example, Faye et al. (2016) showed that increased distance to the object could lead to underestimating temperatures specifically due to the effect of solar radiation, atmospheric composition and pixel size effect.

Figure 6 Thermal image of a hummingbird *Archilochus colubris* inside a metabolic chamber equipped with a germanium glass to allow heat transfer (photo by Núria Playà-Montmany).

The field of view (FOV) is related to spatial thermal image resolution as this is typically divided into a concrete number of pixels. A related parameter the instantaneous field of view (IFOV) refers to the smallest detail that can be detected in the FOV. Both parameters are greatly affected by distance leading to a huge impact on data accuracy (Fernandez-Cuevas *et al.* 2015; Faye *et al.* 2016; Tattersall 2016). The plumage is not a smooth surface, feathers that cover birds' bodies constitute a conjunction of different layers that lead to data obtention of the same target surface, but different profundities and angles (McCafferty 2013). This emphasizes the relevance of taking into account distance and angle effect when conducting ecophysiological studies with the thermal camera both in the field and laboratory, as this can be a huge source of error and led to the obtention of non-accurate data (**Chapter 6**).

Box 1. Thermal cameras' specifications:

Lens: Lenses of infrared cameras are made out of germanium or alternative materials that display low absorption of infrared spectrum to allow the electromagnetic wave to pass through.

Sensor: The infrared camera detects the infrared energy of each object focused and converts infrared data to an electronic image. This electronic image shows the apparent surface temperature. Each pixel of the array sensors reacts to the infrared energy and produces an electronic signal, which is mathematically converted to a colour map. This way, each temperature value is associated to a specific colour. The result is a matrix of colours which is displayed by the thermal camera.

Thermogram: This is the thermal image displayed by the thermal cameras where each colour is associated to an apparent temperature, which results the amount of heat an object has emitted, transmitted and reflected.

Components that constitute a thermal camera (image obtained from Dräger®)

Thesis objectives

The main goal of this thesis is to gain a better understanding of the main physiological and behavioural strategies underlying the responses of birds to global warming. To achieve this goal, we divided the study in five specific aims:

- **Objective 1:** To appraise thermoregulatory traits variation in migratory and resident songbird species in Southern Iberia (**Chapter 2**).
- **Objective 2:** To evaluate the behavioural and physiological responses in relation to environmental temperature changes, microhabitat availability and relative appendage size in the Dunlin *Calidris alpina* (**Chapter 3**).
- **Objective 3:** To investigate the role of relative appendage size in the thermoregulation physiology of Mediterranean Great tits *Parus major* (**Chapter 4**).
- **Objective 4:** To assess the physiological and morphological effects of simulated heat waves in adult Great tits (**Chapter 5**).
- **Objective 5:** To provide methodological advice to ecologists interested in employing thermography (**Chapter 6**).

References

Acero, F. J., Fernández-Fernández, M. I., Carrasco, V. M. S., Parey, S., Hoang, T. T. H., Dacunha-Castelle, D., & García, J. A. (2018) Changes in heat wave characteristics over Extremadura (SW Spain). Theoretical and Applied Climatology 133(1), 605-617.

Acero, F. J., García, J. A., Gallego, M. C., Parey, S., & Dacunha-Castelle, D. (2014) Trends in summer extreme temperatures over the Iberian Peninsula using nonurban station data. Journal of Geophysical Research: Atmospheres 119(1), 39-53.

Allam, A., Moussa, R., Najem, W., & Bocquillon, C. (2019) Mediterranean specific climate classification and future evolution under RCP scenarios. Hydrology and Earth System Sciences Discussions 1-25.

Allen, J. A. (1877) The influence of physical conditions in the genesis of species (1877). Radical Review 1, 108–140.

Andreasson, F., Nord, A., & Nilsson, J. Å. (2018) Experimentally increased nest temperature affects body temperature, growth and apparent survival in blue tit nestlings. Journal of Avian Biology 49(2), jav-01620.

Arad, Z., Midtgård, U., & Bernstein, M. H. (1989) Thermoregulation in turkey vultures: vascular anatomy, arteriovenous heat exchange, and behavior. The Condor 91(3), 505-514.

Bartholomew, G. A. & Cade, T. J. (1963) The water economy of land birds. Auk 80, 504-539.

Baudinette, R. V., Loveridge, J. P., Wilson, K. J., Mills, C. D., & Schmidt-Nielsen, K. N. U. T. (1976) Heat loss from feet of herring gulls at rest and during flight. American Journal of Physiology-Legacy Content 230, 920–924.

Bergmann, C. (1847) Ueber die Verhältnisse der Wärmeökonomie der Thiere zu ihrer Grösse. Göttinger Studien 1, 595–708.

Best, R. & Fowler, R. (1981) Infrared emissivity and radiant surface temperatures of canada and snow geese. Journal of Wildlife Managament 45(4), 1026–1029.

Bonamour, S., Chevin, L. M., Charmantier, A., & Teplitsky, C. (2019) Phenotypic plasticity in response to climate change: the importance of cue variation. Philosophical Transactions of the Royal Society B 374(1768), 20180178.

Boyles, J. G., Seebacher, F., Smit, B. & McKechnie, A. E. (2011) Adaptive thermoregulation in endotherms may alter responses to climate change. Integrative and Comparative Biology 51, 676-690.

Brodsky, L. M., & Weatherhead, P. J. (1984) Behavioral and ecological factors contributing to American black duck-mallard hybridization. The Journal of wildlife management, 846-852.

Broggi, J., Gamero, A., Hohtola, E., Orell, M., & Nilsson, J. Å. (2011) Interpopulation variation in contour feather structure is environmentally determined in great tits. PLoS One 6(9), e24942.

Burness, G., P., Ydenberg, R. C., Hochachka, P. W. (1998) Interindividual variability in body composition and resting oxygen consumption rates in breeding tree swallows, *Trachycineta bicolor*. Physiological Zoology 71, 247-256.

Burtt Jr, E. H., & Ichida, J. M. (2006) Selection for feather structure. Acta Zoologica Sinica 52, 131-135.

Bush, N. G., Brown, M., & Downs, C. T. (2008) Seasonal effects on thermoregulatory responses of the rock kestrel, *Falco rupicolis*. Journal of Thermal Biology 33(7), 404-412.

Cabello-Vergel, J., Soriano-Redondo, A., Villegas, A., Masero, J. A., Guzmán, J. M. S., & Gutiérrez, J. S. (2021) Urohidrosis as an overlooked cooling mechanism in long-legged birds. Scientific reports 11(1), 1-11.

Calder, W. A. (1968) The diurnal activity of the Roadrunner, *Geococcyx californianus*. The Condor 70(1), 84-85.

Calder, W. A. and King, J. R. (1974) Thermal and caloric relations of birds. In Avian Biology, Vol. 4 (ed. D. S. Farner and J. R. King), pp. 259-413. New York: Academic Press.

Cardilini, A., Buchanan, K. L., Sherman, C. D., Cassey, P., & Symonds, M. R. (2016) Tests of ecogeographical relationships in a non-native species: what rules avian morphology?. Oecologia 181(3), 783-793.

Cavieres, G. & Sabat, P. (2008) Geographic variation in the response to thermal acclimation in rufous-collared sparrows: are physiological flexibility and environmental heterogeneity correlated? Functional Ecology 22(3), 509-515.

Cavieres, G., & Sabat, P. (2008) Geographic variation in the response to thermal acclimation in rufous-collared sparrows: are physiological flexibility and environmental heterogeneity correlated?. Functional Ecology 22(3), 509-515.

Clarke, A. (2017) Principles of thermal ecology: Temperature, energy and life. Oxford University Press.

Coelho, J. C., & Pinto, P. A. (2019) Brief Characterization And Analysis Of Soils And Climate And An Analysis Of Suitability To Irrigation Of The Portuguese Continental Territory.

Conradie, S. R., Woodborne, S. M., Cunningham, S. J., & McKechnie, A. E. (2019) Chronic, sublethal effects of high temperatures will cause severe declines in southern African arid-zone birds during the 21st century. Proceedings of the National Academy of Sciences 116(28), 14065-14070.

Cooper, C.E., Withers, P.C., Mawson, P.R., Bradshaw, S.D., Prince, J. & Robertson, H. (2002) Metabolic ecology of cockatoos in the south-west of Western Australia. Australian Journal of Zoology 50, 67-76

Cunningham, S. J., Gardner, J. L., & Martin, R. O. (2021) Opportunity costs and the response of birds and mammals to climate warming. Frontiers in Ecology and the Environment 19(5), 300-307.

Daan, S., Masman, D. & Growenewold, A. (1990) Avian basal metabolic rates: their association with body composition and energy expenditure in nature. American Journal of Physiology 28, R333–R340

Danner, R. M., Coomes, C. M., & Derryberry, E. P. (2021) Simulated heat waves reduce cognitive and motor performance of an endotherm. Ecology and evolution 11(5), 2261-2272.

Davies, S. J. J. F. (1982) Behavioural adaptations of birds to environments where evaporation is high and water is in short supply. Comparative Biochemistry and Physiology 71, 557–566

Dawson, R. D., Lawrie, C. C., & O'Brien, E. L. (2005) The importance of microclimate variation in determining size, growth and survival of avian offspring: experimental evidence from a cavity nesting passerine. Oecologia 144(3), 499-507.

du Plessis, K. L., Martin, R. O., Hockey, P. A., Cunningham, S. J., & Ridley, A. R. (2012) The costs of keeping cool in a warming world: implications of high temperatures for foraging, thermoregulation and body condition of an arid-zone bird. Global Change Biology 18(10), 3063-3070.

Faye, E., Dangles, O., & Pincebourde, S. (2016) Distance makes the difference in thermography for ecological studies. Journal of Thermal Biology 56, 1-9.

Fernandez-Cuevas, I., Marins, J.C.B., Lastras, J.A., Carmona, P.M.G., Carlo, S.P., Garcia Concepcion, M.A. & Sillero-Quintana, M. (2015) Classification of factors influencing the use of infrared thermography in humans: A review. Infrared Physics & Technology 71**,** 28-55

Fitzpatrick, L. J., Olsson, M., Pauliny, A., While, G. M., & Wapstra, E. (2021) Individual telomere dynamics and their links to life history in a viviparous lizard. Proceedings of the Royal Society B 288(1951), 20210271.

Funghi, C., McCowan, L. S., Schuett, W., & Griffith, S. C. (2019) High air temperatures induce temporal, spatial and social changes in the foraging behaviour of wild zebra finches. Animal Behaviour 149, 33-43.

Gardner, J. L., Peters, A., Kearney, M. R., Joseph, L., & Heinsohn, R. (2011) Declining body size: a third universal response to warming?. Trends in ecology & evolution 26(6), 285-291.

Gardner, J. L., Symonds, M. R., Joseph, L., Ikin, K., Stein, J., & Kruuk, L. E. (2016) Spatial variation in avian bill size is associated with humidity in summer among Australian passerines. Climate Change Responses 3(1), 1-11.

Greenberg, R., & Danner, R. M. (2012) The influence of the California marine layer on bill size in a generalist songbird. Evolution: International Journal of Organic Evolution 66(12), 3825-3835.

Greenberg, R., Cadena, V., Danner, R. M., & Tattersall, G. (2012) Heat loss may explain bill size differences between birds occupying different habitats. PloS one 7(7), e40933.

Hagan, A. A., & Heath, J. E. (1980) Regulation of heat loss in the duck by vasomotion in the bill. Journal of Thermal Biology 5(2), 95-101.

Hammel, H. T. (1956). Infrared emissivities of some arctic fauna. Journal of Mammalogy 37(3), 375-378.

Herrero, A., Ruiz-Benito, P., Andivia, E., Madrigal-González, J., Villar-Salvador, P., Ratcliffe, S., & Zavala, M. A. (2021) Mediterranean pine forest distribution: assessing vulnerability and resilience under climate change. In Pines and Their Mixed Forest Ecosystems in the Mediterranean Basin (pp. 251-277). Springer, Cham.

Hsu, B. Y., Sarraude, T., Cossin-Sevrin, N., Crombecque, M., Stier, A., & Ruuskanen, S. (2020) Testing for context-dependent effects of maternal thyroid hormones on offspring survival and physiology: an experimental approach manipulating temperature in a wild bird species. bioRxiv.

Hughes, L. (2000) Biological consequences of global warming: is the signal already present? Trends in Ecology and Evolution 15, 56-61.

IPCC (2021) Summary for Policymakers. In: Climate Change 2021: The Physical Science Basis. Contribution of Working Group I to the Sixth Assessment Report of the Intergovernmental Panel on Climate Change. Cambridge University Press. https://www.ipcc.ch/report/ar6/wg1

Jacobs, P. J., Oosthuizen, M. K., Mitchell, C., Blount, J. D., & Bennett, N. C. (2020) Heat and dehydration induced oxidative damage and antioxidant defenses following incubator heat stress and a simulated heat wave in wild caught four-striped field mice *Rhabdomys dilectus*. PloS one 15(11), e0242279.

Janse van Vuuren, A. K., Kemp, L. V., & McKechnie, A. E. (2020) The beak and unfeathered skin as heat radiators in the Southern Ground-hornbill. Journal of Avian Biology, 51(6).

Kvist, A., & Lindström, Å. (2001) Basal metabolic rate in migratory waders: intraindividual, intraspecific, interspecific and seasonal variation. Functional Ecology 15, 465–473

LaBarbera, K., Marsh, K. J., Hayes, K. R., & Hammond, T. T. (2020) Context-dependent effects of relative temperature extremes on bill morphology in a songbird. Royal Society open science 7(4), 192203.

Lin, H., De Vos, D., Decuypere, E., & Buyse, J. (2008) Dynamic changes in parameters of redox balance after mild heat stress in aged laying hens (Gallus gallus domesticus). Comparative Biochemistry and Physiology Part C: Toxicology & Pharmacology 147(1), 30-35.

Lindström, Å. & Klaassen, M. (2003) High basal metabolic rates of shorebirds while in the Arctic: a circumpolar view. Condor 105, 420–427

Lovette, I. J. & Fitzpatrick, J. W. (2016) Handbook of bird biology (3rd ed.). Chichester, UK: John Wiley & Sons Inc.

Maloney, S. K., & Dawson, T. J. (1994) Thermoregulation in a large bird, the emu (*Dromaius novaehollandiae*). Journal of Comparative Physiology B 164(6), 464-472.

Marvel, K., Cook, B. I., Bonfils, C. J., Durack, P. J., Smerdon, J. E., & Williams, A. P. (2019) Twentieth-century hydroclimate changes consistent with human influence. Nature 569(7754), 59-65.

McCafferty, D. J. (2013) Applications of thermal imaging in avian science. Ibis 155(1), 4-15.

McKechnie, A. E. (2008) Phenotypic flexibility in basal metabolic rate and the changing view of avian physiological diversity: a review. Journal of Comparative Physiology B 178(3), 235-247.

McKechnie, A. E., & Lovegrove, B. G. (2002) Avian facultative hypothermic responses: a review. The Condor 104(4), 705-724.

McKechnie, A. E., & Wolf, B. O. (2010) Climate change increases the likelihood of catastrophic avian mortality events during extreme heat waves. Biology letters 6(2), 253-256.

McKechnie, A. E., & Wolf, B. O. (2019) The physiology of heat tolerance in small endotherms. Physiology 34(5), 302-313.

McKechnie, A. E., Gerson, A. R., McWhorter, T. J., Smith, E. K., Talbot, W. A., & Wolf, B. O. (2017) Avian thermoregulation in the heat: evaporative cooling in five Australian passerines reveals within-order biogeographic variation in heat tolerance. Journal of Experimental Biology 220(13), 2436-2444.

McKechnie, A. E., Hockey, P. A., & Wolf, B. O. (2012) Feeling the heat: Australian landbirds and climate change. Emu-Austral Ornithology 112(2), i-vii.

McKechnie, A. E., Noakes, M. J., & Smit, B. (2015) Global patterns of seasonal acclimatization in avian resting metabolic rates. Journal of Ornithology 156(1), 367-376.

McNab, B. K. (2002) The Physiological Ecology of Vertebrates: A View from Energetics. Ithaca, New York: Cornell University Press. p. 587.

McNab, B. K. (2012) Extreme measures: the ecological energetics of bird and mammals. University of Chicago Press, Chicago.

Midtgård, U. (1981) The rete tibiotarsale and arteriovenous association in the hind limb of birds: a compartive morphological study on counter-current heat exchange systems. Acta Zoologica 62(2), 67-87.

Møller, A. P., Fiedler, W., & Berthold, P. (Eds.). (2010). Effects of climate change on birds. OUP Oxford.

Mujahid, A., Yoshiki, Y., Akiba, Y., & Toyomizu, M. (2005) Superoxide radical production in chicken skeletal muscle induced by acute heat stress. Poultry Science 84(2), 307-314.

Parmesan, C. & Yohe, G. (2003) A globally coherent fingerprint of climate change impacts across natural systems. Nature 421, 37-42.

Parmesan, C. (2006) Ecological and evolutionary responses to recent climate change. Annual Review of Ecology, Evolution, and Systematics 37, 637-669

Piersma, T., & Drent, J. (2003) Phenotypic flexibility and the evolution of organismal design. Trends in Ecology & Evolution 18(5), 228-233.

Piersma, T., & Van Gils, J. A. (2011) The flexible phenotype. A body-centred integration of ecology, physiology, and behaviour. Oxford University Press, Oxford

Piersma, T., Bruinzeel, L., Drent, R., Kersten, M., Van der Meer, J. & Wiersma, P. (1996) Variability in basal metabolic rate of a long-distance migrant shorebird (red knot, *Calidris canutus*) reflects shifts in organ sizes. *Physiological Zoology* 69, 191–217.

Pollock, H. S., Brawn, J. D., & Cheviron, Z. A. (2021) Heat tolerance of temperate and tropical birds and their implications for susceptibility to climate warming. Functional Ecology 35(1), 93-104.

Probst, C. M., Ralston, J., & Bentley, I. (2021) Effects of climate on bill morphology within and across Toxostoma thrashers. Journal of Avian Biology 2022(1).

Qing-Gang, Q., Liang, H. J., Min-Lan, Ba., Zheng, W. H., & Jin-Song, L. (2016) Interspecific variation of thermoregulation between small migratory and resident passerines in Wenzhou. Zoological Research 37(3), 167.

Randall, D., W. Burggren, & French, K. (2002) Eckert Animal Physiology: Mechanisms and Adaptation, 5th Edition. W. H. Freeman and Co., New York, NY.

Root, T. L., Price, J. T., Hall, K. R., Schneider, S. H., Rosenzweig, C. & Pounds, J. A. (2003) Fingerprints of global warming on wild animals and plants. Nature 421, 57-60

Ryding, S., Klaassen, M., Tattersall, G. J., Gardner, J. L., & Symonds, M. R. (2021) Shape-shifting: changing animal morphologies as a response to climatic warming. Trends in Ecology & Evolution 36(11), 1036-1048.

Ryeland, J., Weston, M. A. & Symonds, M. R. (2017) Bill size mediates behavioural thermoregulation in birds. Functional Ecology 31(4), 885-893.

Ryeland, J., Weston, M. A., & Symonds, M. R. (2019) Leg length and temperature determine the use of unipedal roosting in birds. Journal of avian biology 50(5), e02008.

Ryeland, J., Weston, M. A., & Symonds, M. R. (2021) The importance of wetland margin microhabitat mosaics; the case of shorebirds and thermoregulation. Journal of Applied Ecology 58(2), 382-391.

Sala, O. E., Chapin III, F. S., Armesto, J. J., Berlow, E., Bloomfield, J., Dirzo, R., Huber-Sanwald, E., Huenneke L. F., Jackson R. B., Kinzig A., Leemans, R., Modge, D. M., Mooney, H. A., Oesterheld, M., Poff, N. L., Sykes, M. T., Walker B. H., Walker, M. & Wall, D. H. (2000) Global biodiversity scenarios for the year 2100. science 287(5459), 1770-1774.

Sándor, K., Seress, G., Sinkovics, C., Péter, Á., & Liker, A. (2022) Differences in feather structure between urban and forest great tits: constraint or adaptation?. Journal of Avian Biology, e02922.

Sapolsky, R. M., Romero, L. M., & Munck, A. U. (2000) How do glucocorticoids influence stress responses? Integrating permissive, suppressive, stimulatory, and preparative actions. Endocrine reviews 21(1), 55-89.

Saunders, D. A., Mawson, P., & Dawson, R. (2011) The impact of two extreme weather events and other causes of death on Carnaby's black cockatoo: a promise of things to come for a threatened species?. Pacific Conservation Biology 17(2), 141-148.

Schlichting, C. D., & Pigliucci, M. (1998) Phenotypic evolution: a reaction norm perspective. Sinauer associates incorporated.

Simide, R., Angelier, F., Gaillard, S., & Stier, A. (2016) Age and heat stress as determinants of telomere length in a long-lived fish, the Siberian sturgeon. Physiological and Biochemical Zoology 89(5), 441-447.

Smit, B., Brown, M., & Downs, C. T. (2008) Thermoregulatory responses in seasonally acclimatized captive southern white-faced scops-owls. Journal of Thermal Biology 33(2), 76-86.

Smit, B., Zietsman, G., Martin, R. O., Cunningham, S. J., McKechnie, A. E., & Hockey, P. A. R. (2016) Behavioural responses to heat in desert birds: implications for predicting vulnerability to climate warming. Climate Change Responses 3(1), 1-14.

Smit. B., Brown, M., & Downs, C. T. (2008) Thermoregulatory responses in seasonally acclimatized captive southern white-faced scops-owls. Journal of Thermal Biology 33, 76–86

Smith, E. K., O'Neill, J., Gerson, A. R., & Wolf, B. O. (2015) Avian thermoregulation in the heat: resting metabolism, evaporative cooling and heat tolerance in Sonoran Desert doves and quail. Journal of Experimental Biology 218(22), 3636-3646.

Stager, M., Senner, N. R., Swanson, D. L., Carling, M. D., Eddy, D. K., Greives, T. J., & Cheviron, Z. A. (2021) Temperature heterogeneity correlates with intraspecific variation in physiological flexibility in a small endotherm. Nature Communications 12(1), 1-11.

Steen, I. & Steen, J. B. (1965) The Importance of the Legs in the Thermoregulation of Birds. Acta Physiologica Scandinavica 63, 285–291

Stevens, G.C. (1989) The latitudinal gradient in geographicalrange–how so many species coexist in the tropics.TheAmerican Naturalist133, 240–256

Stier, A., Hsu, B. Y., Cossin-Sevrin, N., Garcin, N., & Ruuskanen, S. (2021) From climate warming to accelerated cellular ageing: an experimental study in wild birds. bioRxiv.

Stillman, J. H. (2019) Heat waves, the new normal: summertime temperature extremes will impact animals, ecosystems, and human communities. Physiology 34(2), 86-100.

Sturkie, P. D. (2015) Avian Physiology. Springer, Berlin.

Swanson, D. L., Agin, T. J., Zhang, Y., Oboikovitz, P., & DuBay, S. (2020) Metabolic flexibility in response to within-season temperature variability in house sparrows. Integrative Organismal Biology 2(1), obaa039.

Symonds, M. R., & Tattersall, G. J. (2010) Geographical variation in bill size across bird species provides evidence for Allen's rule. The American Naturalist 176(2), 188-197.

Tabh, J. K., Burness, G., Wearing, O. H., Tattersall, G. J., & Mastromonaco, G. F. (2021) Infrared thermography as a technique to measure physiological stress in birds: Body region and image angle matter. Physiological reports 9(11), e14865.

Tapper, S., Tabh, J., Tattersall, G. J., & Burness, G. (2021) Changes in body surface temperature play an under-appreciated role in the avian immune response. Physiological and Biochemical Zoology 95(2), 152-167.

Tattersall, G. J. (2016) Infrared thermography: A non-invasive window into thermal physiology. Comparative Biochemistry and Physiology Part A: Molecular & Integrative Physiology, 202, 78-98.

Tattersall, G. J., Andrade, D. V., & Abe, A. S. (2009) Heat exchange from the toucan bill reveals a controllable vascular thermal radiator. Science 325(5939), 468-470.

Tattersall, G. J., Arnaout, B., & Symonds, M. R. (2017) The evolution of the avian bill as a thermoregulatory organ. Biological Reviews 92(3), 1630-1656.

Tattersall, G. J., Chaves, J. A., & Danner, R. M. (2018) Thermoregulatory windows in Darwin's finches. Functional Ecology 32(2), 358-368.

Tattersall, G. J., Sinclair, B. J., Withers, P. C., Fields, P. A., Seebacher, F., Cooper, C. E., & Maloney, S. K. (2012) Coping with thermal challenges: physiological adaptations to environmental temperatures. Comprehensive Physiology 2(3), 2151-2202.

Thompson, L. J. (2014) Flexibility in metabolic rate in a small Afrotropical bird *Zosterops virens* (Doctoral dissertation).

Thompson, L. J., Brown, M., & Downs, C. T. (2015) The potential effects of climate-change-associated temperature increases on the metabolic rate of a small Afrotropical bird. The Journal of experimental biology 218(10), 1504-1512.

Thompson, M. L., Cunningham, S. J., & McKechnie, A. E. (2018) Interspecific variation in avian thermoregulatory patterns and heat dissipation behaviours in a subtropical desert. Physiology & behavior 188, 311-323.

Tieleman, B. I., & Williams, J. B. (2000) The adjustment of avian metabolic rates and water fluxes to desert environments. Physiological and Biochemical Zoology 73(4), 461-479.

Tieleman, B. I., Williams, J. B., & Bloomer, P. (2003) Adaptation of metabolism and evaporative water loss along an aridity gradient. Proceedings of the Royal Society of London. Series B: Biological Sciences 270(1511), 207-214.

Tieleman, B. I., Williams, J. B., & Buschur, M. E. (2002) Physiological adjustments to arid and mesic environments in larks (Alaudidae). Physiological and Biochemical Zoology 75(3), 305-313.

Tilman, D., Clark, M., Williams, D. R., Kimmel, K., Polasky, S., & Packer, C. (2017) Future threats to biodiversity and pathways to their prevention. Nature 546(7656), 73-81.

Ton, R., Stier, A., Cooper, C. E., & Griffith, S. C. (2021) Effects of heat waves during post-natal development on mitochondrial and whole body physiology: an experimental study in zebra finches. Frontiers in physiology 12, 554.

Van de Ven, T. M. F. N., Martin, R. O., Vink, T. J. F., McKechnie, A. E., & Cunningham, S. J. (2016) Regulation of heat exchange across the hornbill beak: functional similarities with toucans?. PLoS One 11(5), e0154768.

Van de Ven, T. M., McKechnie, A. E., & Cunningham, S. J. (2019). The costs of keeping cool: behavioural trade-offs between foraging and thermoregulation are associated with significant mass losses in an arid-zone bird. Oecologia 191(1), 205-215.

Vézina, F., Jalvingh, K. M., Dekinga, A. & Piersma, T. (2006) Acclimation to different thermal conditions in a northerly wintering shorebird is driven by body mass-related changes in organ size. Journal of Experimental Biology 209, 3141–3154.

Viceto, C., Cardoso Pereira, S., & Rocha, A. (2019) Climate change projections of extreme temperatures for the Iberian Peninsula. Atmosphere 10(5), 229.

Viceto, C., Cardoso Pereira, S., & Rocha, A. (2019) Climate change projections of extreme temperatures for the Iberian Peninsula. Atmosphere 10(5), 229.

Vollmer, M., & Möllmann, K.P. (2010) Infrared Thermal Imaging: Fundamentals, Research and Applications. John Wiley and Sons, New York.

Whitfield, M. C., Smit, B., McKechnie, A. E., & Wolf, B. O. (2015) Avian thermoregulation in the heat: scaling of heat tolerance and evaporative cooling capacity in three southern African arid-zone passerines. The Journal of experimental biology 218(11), 1705-1714.

Wiersma, P., & Piersma, T. (1994) Effects of microhabitat, flocking, climate and migratory goal on energy expenditure in the annual cycle of red knots. The Condor 96(2), 257-279.

Williams, J. B., & Tieleman, B. I. (2000) Flexibility in basal metabolic rate and evaporative water loss among hoopoe larks exposed to different environmental temperatures. Journal of Experimental Biology 203, 3153–3159

Wolf, B. (2000) Global warming and avian occupancy of hot deserts: a physiological and behavioral perspective. Revista Chilena De Historia Natural 73, 395-400.

Wolf, B., & Walsberg, G. (1996) Respiratory and cutaneous evaporative water loss at high environmental temperatures in a small bird. The Journal of Experimental Biology 199(2), 451-457.

Xie, S., Romero, L. M., Htut, Z. W., & McWhorter, T. J. (2017) Stress responses to heat exposure in three species of Australian desert birds. Physiological and Biochemical Zoology 90(3), 348-358.

Yom-Tov, Y., Yom-Tov, S., Wright, J., JR Thorne, C., & Du Feu, R. (2006) Recent changes in body weight and wing length among some British passerine birds. Oikos 112(1), 91-101.

Zhang, Q., Han, X., Hao, X., Ma, L., Li, S., Wang, Y., & Du, W. (2018) A simulated heat wave shortens the telomere length and lifespan of a desert lizard. Journal of thermal biology 72, 94-100.

2

Mediterranean songbirds show pronounced variation in thermoregulatory traits

Núria Playà-Montmany, Erick González-Medina, Julián Cabello-Vergel, Manuel Parejo, José M. Abad-Gómez, Juan M. Sánchez-Guzmán, Auxiliadora Villegas, Jorge S. Gutiérrez and José A. Masero

Submitted to Ecology letters

Abstract

The climatic variability hypothesis proposes that individuals inhabiting more heterogeneous environments should exhibit broader ranges of tolerance to changing environmental temperatures. Here we investigated seasonal differences in key thermoregulatory traits of Mediterranean songbirds and tested this hypothesis by comparing thermal tolerance ranges between resident and trans-Saharan migratory species. Resident songbirds seasonally adjusted all the measured thermoregulatory traits — except the upper critical temperature slope — to environmental conditions, with short-term benefits in terms of energy and water savings under thermally stressful conditions. Migrants had more efficient thermoregulation mechanisms and evaporative cooling at high temperatures than residents. These findings reveal that phenotypic flexibility in the thermoregulatory traits of Mediterranean songbirds is crucial for their resilience to environmental changes and that migratory species may be more resilient to climate change as they have a higher efficiency in thermoregulation mechanisms at high temperatures than resident species, which is consistent with the climatic variability hypothesis prediction.

Keywords: climate change, climatic variability hypothesis, passerines, phenotypic flexibility, thermoregulatory traits, thermoneutral zone.

Introduction

Climate change is one of the main threats to biodiversity, causing detrimental effects more rapidly than predicted (Bellard *et al.*, 2012; Xu *et al.* 2018). Indeed, scientists expect negative cumulative impacts on wildlife (Ceballos *et al.* 2017; Spooner *et al.* 2018). Globally, the gradual increase in mean environmental temperature is occurring jointly with rises in the intensity, duration and frequency of heat waves (Coumou & Robinson 2013). Notably, the Mediterranean basin is warming up 20% faster than the global average (Herrero *et al.* 2021; IPCC 2021). This raises the question of whether Mediterranean wildlife species would be able to adapt fast enough to keep up with their warming environments. The ability of species and populations to respond to changing environmental conditions is critical for their survival in a climate change context (Fox *et al.* 2019; Visser 2008).

Phenotypic flexibility is a major mechanism of response to environmental variability, as it may allow organisms to cope with rapid environmental changes, including global change (Piersma & van Gils 2011; Bonamour *et al.* 2019;). Despite the potential importance of thermoregulatory physiological traits for understanding and predicting the effects of climate change on animals, data on their phenotypic flexibility are still very limited, especially for Mediterranean species (Thomas *et al.* 2001). Ignoring phenotypic flexibility in thermoregulatory traits could potentially lead to under- or overestimating the actual thermal risk of species with different life-history strategies. Although phenotypic flexibility can increase resilience to thermal stress, trade-offs during acclimation can have hidden costs (including maintenance costs of plasticity) that reduce the net benefits of acclimation or increase susceptibility to other environmental stressors (Pörtner *et al.* 2006; Burraco *et al.* 2022;). These trade-offs are difficult to detect, but they are critical to predicting whole-organism responses to environmental changes (Bozinovic & Pörtner 2015; Riddell *et al.* 2018; Burraco *et al.* 2022;).

The physiological "tool-kit" that endotherms have at their disposal to generate rapid plastic responses to temperature comprises metabolic traits such as basal metabolic rate (BMR), thermoneutral zone breath (TNZ), and evaporative water loss (EWL). BMR is a good example of a flexible physiological trait that can be seasonally modulated through adjustments at several levels in small vertebrates (McKechnie 2008; Książek *et al.* 2009; Swanson 2010; Zheng *et al.* 2014; Boratyński *et al.* 2016), with most studies showing BMR upregulation in birds inhabiting regions with cold winter climates (McKechnie *et al.* 2015; Swanson *et al.* 2020). TNZ breath, defined as the environmental temperature (T_a) range at which an endotherm does not expend energy for thermoregulation, is another flexible physiological trait with clear implications for sensitivity to climate warming (McNab 2002: Araújo *et al.* 2013; Pollock *et al.* 2021). Beyond TNZ thresholds (lower and upper critical temperature, T_{lc} and T_{uc}, respectively), an endotherm must allocate energy to maintain normothermic core temperature (McNab 2002). Several bird species showed a broader TNZ breadth during winter than in the summer season (Bush *et al.* 2008; Wu *et al.* 2015; Pollock *et al.* 2019), while others displayed an opposite pattern or no variations (Maddocks & Geiser 2000; Nzama *et al.* 2010; Wilson *et al.* 2011; Pollock et al., 2019). These contrasting patterns probably arise from the scarcity of comparative multispecies studies. Indeed, only one study has assessed whether birds can modulate their TNZ breadth according to their life-history strategies (Pollock *et al.* 2019). There are important gaps in knowledge about the flexibility of these metabolic traits.

Another important thermoregulatory trait linked to an animal's metabolic rate is EWL, which is fundamental to balancing energy flux with the environment and reducing thermal and hydric stress (McNab 2002). EWL is the major avenue of water efflux in small endotherms, especially in birds whose EWL is five times greater than urinary and faecal water losses (Williams & Tieleman 2005). Birds can, to some degree, tolerate temperatures above their T_{uc} by increasing their EWL rate and thus enhancing evaporative cooling (e.g., Huey *et al.* 2012; Talbot *et al.* 2017). Some studies revealed seasonal variation in EWL, with EWL increasing exponentially at high T_a during summer and at low T_a during winter (Cooper & Gessaman 2004; Noakes *et al.* 2016; Oswald *et al.* 2018). Among passerines, regularly drinking species have a greater capacity to elevate rates of EWL above minimal levels compared to non-drinking species, allowing the former to achieve greater heat tolerances (Czenze *et al.* 2020). Since summer in the Mediterranean is typically hot and dry, it could be hypothesized that Mediterranean resident songbirds show a higher capacity to improve evaporative cooling efficiency during summer.

The climatic variability hypothesis (CVH) predicts that phenotypic flexibility in thermoregulatory traits will be greater in animals coping with greater temperature variability (e.g., Cavieres & Sabat 2008; Stager *et al.* 2021). Migratory birds breeding outside the tropics typically experience greater variability in climatic conditions than closely related resident species (Eyres *et al.* 2020), so we would expect long-distance migratory species to exhibit broader thermal tolerance ranges than closely related resident species. Songbirds (Passeriformes) represent the largest identifiable radiation of birds (over 50% of all bird species), showing astonishing ecological and behavioural diversity (Barker *et al.* 2004). They are an excellent model for exploring intra- and interspecific variation in thermoregulatory traits because they exhibit a certain degree of phenotypic flexibility in these traits, including body temperature (T_b), BMR, EWL and TNZ breadth (e.g., Swanson 1990; Tieleman *et al.* 2003; McKechnie *et al.* 2007; Swanson 2010; Zheng *et al.* 2013; Noakes *et al.* 2017; Pollock *et al.* 2019; Wang *et al.* 2019; Oboikovitz & Swanson 2021). In this study, we investigated patterns of variation in thermoregulatory traits of Mediterranean songbirds across seasons and migratory strategies. Specifically, we investigated whether Mediterranean resident songbirds adjust key thermoregulatory traits during summer and winter. We also compared thermoregulatory traits in migratory and resident songbirds. Based on the CVH hypothesis, we predicted that (i) resident songbirds would exhibit strong seasonal variation in thermoregulatory traits and (ii) Palearctic-African songbirds (i.e., trans-Saharan migratory species) would have broader TNZ breadth thermal tolerance ranges and a higher EWL inflection point on the breeding grounds than resident songbirds. Our analysis revealed that resident songbirds seasonally adjusted almost all the measured thermoregulatory traits with short-term benefits in terms of energy and water savings under thermally stressful conditions. Migrants had more efficient thermoregulation mechanisms and evaporative cooling at high temperatures than residents, which is consistent with the climatic variability hypothesis prediction.

Materials and methods

Bird captures

Adults and juveniles of both resident and migratory species were captured over four years (2018–2021) near Badajoz city (SW Spain; 38° 56’ N, 6° 56’ W). This site has a Mediterranean climate with a mean monthly/annual temperature of 24.6 °C during summer and 10.5 °C during winter (AEMET 2022). Resident species (n = 10) were captured in winter (December - early March) and summer (June - early September), while migratory species (n = 5) were captured in summer (sample sizes per species and seasons are shown in Supplementary Tables 1–2). We captured birds using mist nets before sunset, and individuals were ringed with a numbered aluminium ring. During summer, we selected individuals with non-active moult in their flight feathers and with light body moult (less than 20% of the body feathers). During winter, all individuals showed freshly moulted feathers. Upon capture, birds were transported to the facilities of the University of Extremadura in Badajoz, where metabolic trials were conducted at night in the respirometry laboratory. All birds were released at the capture site the day (early morning) following capture.

Experimental setup

Individuals were weighed (±0.1 g) and placed into polypropylene metabolic chambers (232 × 165 × 162 mm; effective volume = 3.9 L) whose floor was covered with a mineral oil layer of 1 cm to avoid evaporation from excreta. A wire mesh platform was placed 3 cm above the oil layer to allow individuals to perch without touching the oil. Metabolic chambers were placed (see Gas exchange measurements below) inside a temperature-controlled cabinet (ICP, 750 Memmert GmbH, Schwabach, Germany) where they were exposed to stepped T_a profiles previously programmed using control software. To determine T_{lc}, six birds were simultaneously exposed alternatively to an increasing or a decreasing stepped T_a profile ranging from 10 to 30 °C or vice versa (at 5 °C increments). All individuals were exposed to each T_a for a minimum of 65 min. For T_{uc} determination, two birds were simultaneously exposed to an increasing profile of T_a (35, 37, and 40 °C); they were exposed to each T_a for a minimum of 25 min. We introduced a calibrated thermistor probe (±0.001 °C) inside the metabolic chambers to monitor the T_a during the metabolic trials. The first 65 min or 25 of the stepped T_a profiles of each protocol were used to ensure that the individuals were acclimated to the metabolic chambers (i.e., stable VO_2 and EWL traces) after handling. Immediately after each metabolic trial, individuals were weighed, hydrated, and then released at the site of capture. All individuals were measured at night (resting phase of the circadian cycle of all species) under post-prandial conditions (without food for at least 2 h). Bird behaviour and activity levels inside the chambers were monitored using infrared cameras to ensure that the birds remained calm during the metabolic measurements. We included only data from birds that remained calm and resting throughout the measurements in our subsequent analysis (58 individuals were discarded from the analysis).

We calculated body mass (M_b) as the mean of the pre- and post-metabolic trial weights. A common practice used to control for mass-specific BMR during calculations is to use the residuals of the M_b–BMR regression as data in subsequent analyses, but this methodology can lead to biased parameter estimates if M_b is correlated with other variables of interest in subsequent analyses (Freckleton 2009). To calculate mass-adjusted BMR, we opted for an alternative approach proposed by Pollock et al. (2019). Briefly, we empirically calculated the allometric scaling relationship between M_b and BMR (Stager *et al.*, 2016), which is described by the equation BMR = aM_b^b, where *a* is the y-intercept and *b* is the scaling exponent. We obtained values of *b* = 0.85 (winter) and *b* =

0.63 (summer) and calculated mass-adjusted BMR by dividing each BMR measurement by M_b^b using the season-specific scaling exponents.

Gas exchange measurements

Rates of O_2 consumption and EWL were measured using an open flow-through respirometry system (see details in Gonzalez-Medina *et al.* 2020) following the protocols used by Playà-Montmany et al. (2021). Briefly, exterior ambient dry air (<1 kPa WVP) was pumped from an air dryer compressor (MESTRA®) into a carboy and then directed to the metabolic chambers using mass flow controllers (MFS, Sable Systems International) at a rate of 1,000 or 3,000 ml min^{-1} (T_{lc} and $T_{uc,}$ respectively). Excurrent airstreams from the chambers flowed through an eight-channel multiplexer (RM-8, Sable Systems International), which automatically alternated every 360 s between metabolic chambers containing birds and an additional chamber left empty to obtain baseline values. Measurements from the latter were obtained for 300 s at the start of every trial and following two metabolic chamber measurements. We subsampled the downstream air at 200 ml min^{-1} (SS3 subsampler, Sable Systems International) and pulled it sequentially through an H_2O analyser (RH300, Sable Systems), a Drierite® column, and an O_2 analyser (FC- 10 Oxygen Analyzer, Sable Systems). The data were digitalized using an analogue-to-digital converter (UI2 model, Sable Systems) and recorded with a sampling interval of 1 s using Expedata software (version 1.9.14, Sable Systems).

The VO_2 and EWL values at each T_a were estimated as the lowest stable 2-min (see, for example, Boratyński *et al.* 2016) values using Eqs. 10.2 and 10.9 from Lighton (2018), respectively, with a custom macro designed in Expedata. We used a respiratory quotient of 0.70 (e.g., Kvist & Lindström 2001) and converted VO_2 to metabolic rates (Watt, W) using an energy equivalent of 20.08 kJ 1^{-1} O_2 (Schmidt-Nielsen 1997). The drift of water and O_2 traces was corrected using the Catmull-Rom spline correction applied to baselines.

Statistical analyses

To estimate the limits of the TNZ breadth (T_{lc} or T_{uc}) of a given species, we used a generalized estimating equation (GEE) approach to simultaneously identify the population limits of the TNZ breadth (T_{lc} or T_{uc}) following Playà-Montmany et al. (2021). The mean value of VO_2 within the TNZ was considered to be the BMR, and the TNZ breadth of each species was calculated as the difference between the mean T_{uc} and mean T_{lc} (TNZ = $T_{uc} - T_{lc}$; Khaliq *et al.* 2014). The inflection point of EWL was also calculated by using piecewise linear regression (Muggeo 2009) with the 'lme4' and 'segmented' packages. As a proxy for thermal conductance, we calculated the slope of the relationship between T_a and VO_2 below T_{lc} (T_{lc} slope) and above T_{uc} (T_{uc} slope) using the 'segmented' package (Muggeo 2008). Last, we also calculated the slope of the relationship between T_a and EWL (EWL slope) above the inflection point.

Phylogenetic comparative analyses

We used phylogenetic comparative analyses to control for the phylogenetic autocorrelation introduced by shared ancestry (Harvey & Pagel 1991). We used the most complete bird phylogeny available, i.e., that from Jetz et al. (2012), available at http://birdtree.org/). We obtained 10,000 trees with different topologies from the Bird Tree project for the species in our dataset (15 species of migratory/resident and eight species of Mediterranean resident songbirds), using 'Hackett All Species' as the backbone. We then derived an ultrametric and rooted consensus tree using the package phytools (Revell 2012).

First, we fitted Bayesian phylogenetic mixed models to examine the links between seasonality (winter/summer) and variation in thermoregulatory traits (TNZ breadth, T_{uc}, T_{lc}, T_{uc} slope, T_{lc} slope, mass-adjusted BMR, EWL inflection point and EWL slope). Thermoregulatory traits of Mediterranean resident songbirds were used as response variables (Gaussian error distribution), with seasonality (winter or summer) and M_b as predictors (each species had a value for winter and summer). We included M_b to control for any effect of size on the different species tested.

Second, we also fitted similar phylogenetic mixed models to assess whether and how migratory strategy (migratory/resident) influences thermoregulatory traits during the summer season (when both migratory and resident species were measured). Thermoregulatory traits were used as response variables (Gaussian error distribution), with migratory strategy (migratory/resident) and M_b as predictors (with a single value per species).

All the models were fitted using the MCMCglmm R package v2.32 (Hadfield 2010; Hadfield & Nakagawa 2010). In all the models, a consensus tree was included as a random effect to control for phylogenetic relatedness. For all analyses, we used weakly informative priors (a normal distribution with a mean of zero and a variance of 1,000). For each model, we ran MCMC chains for 5 million iterations, with a burn-in of 100,000 and a thinning interval of 2,500, resulting in a posterior distribution of >1,500 samples. We checked that the autocorrelation of samples was <0.1 and ran each model twice, assessing proper convergence using the Gelman–Rubin statistic, requiring models to have a scaling reduction factor below 1.1 (Gelman & Rubin 1992). We report the posterior mean and the 95% credible intervals (CIs) for each variable and assess significance according to pMCMC, which is the proportion of samples in the posterior distribution not overlapping with zero. We estimated the importance of shared evolutionary history among species by using heritability (h^2), a measure of phylogenetic signal ranging between 0 and 1 (with values close to 0 indicating low phylogenetic signal) that can be calculated from the estimated phylogenetic variance in the model (Hadfield 2010). We calculate h^2 across the entire posterior distribution of model variances. All analyses were performed in R (R Core Team 2021).

Results

Seasonal variation across resident species

The TNZ breadth limits for resident songbirds ranged between 18.7° and 32.8 °C during summer and between 20.0° and 32.6 °C during winter (Figure 1), resulting in a net increase in TNZ breadth of ~1.5 °C during summer. Resident songbirds increased their mass-adjusted BMR, which was 71% higher in winter, while the T_{lc} slope decreased by 43% from summer to winter. The EWL slope above the inflection point increased by 55% from summer to winter. Finally, the songbirds had a higher EWL inflection point in summer (0.29 °C) than wintering songbirds.

Our phylogenetic mixed models showed that seasonality was a strong predictor of all thermoregulatory traits except T_{uc} slope (Supplementary Table 1, Figures 1–4). Resident songbirds during winter had a significantly higher mass-adjusted BMR ($\beta = 0.02$, CI = 0.009, 0.03) and EWL slope ($\beta = 15.31$, CI = −0.37, 30.64; Figure 4) but a significantly lower T_{lc} slope ($\beta = -0.04$, CI = −0.07, 0.02; Figure 1). Additionally, resident songbirds during summer showed a greater T_{uc} ($\beta = 33.32$, CI = 29.27, 37.04), TNZ breath ($\beta = 13.24$, CI = 7.64, 18.50), and EWL ($\beta = 34.91$, CI = 32.44, 38.06) but lower T_{lc} ($\beta = 19.88$, CI = 16.34, 24.16; Supplementary Table 1, Figures 1–4).

Comparisons across migratory and resident species

The TNZ breadth limits ranged between 24.1 and 36.6 °C in migratory species and between 18.9 and 32.9 °C in resident species (Figure 1). Migratory species exhibited greater T_{lc} (+5.1 °C) and T_{uc} (+3.7 °C) values than resident species. They also exhibited a higher EWL inflection point (+1.5 °C) than resident species.

We found that migratory birds showed a greater T_{uc} (β = 37.03, CI = 34.39, 39.32), TNZ breadth (β = 10.56, CI = 5.67, 15.24) and EWL (β = 36.87, CI = 32.97, 40.59) but lower T_{lc} (β = 26.54, CI = 22.49, 30.49) than resident species (Supplementary Table 1, Figures 1–4).

Based on the migratory strategy and seasonal comparisons of thermoregulatory traits across species, we showed that h^2 varied substantially (ranging from 0.055 to 0.653 in the seasonal comparisons and from 0.393 to 0.725 in the migratory strategy comparisons; Supplementary Table 1). Overall, this indicates an important role of shared ancestry and the need to incorporate phylogenetic information when studying thermoregulatory traits across bird species.

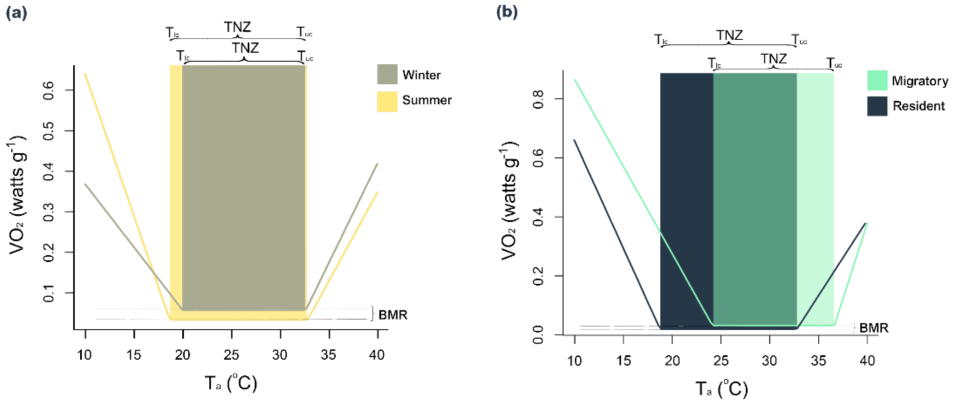

Figure 1 The relationship between oxygen consumption and the environmental temperature (T_a) of songbird species (a) during two seasons, winter and summer, and (b) with different migratory strategies (migratory or resident). The thermoneutral zone breadth (TNZ) is delimited by the lower (T_{lc}) and upper (T_{uc}) critical temperatures.

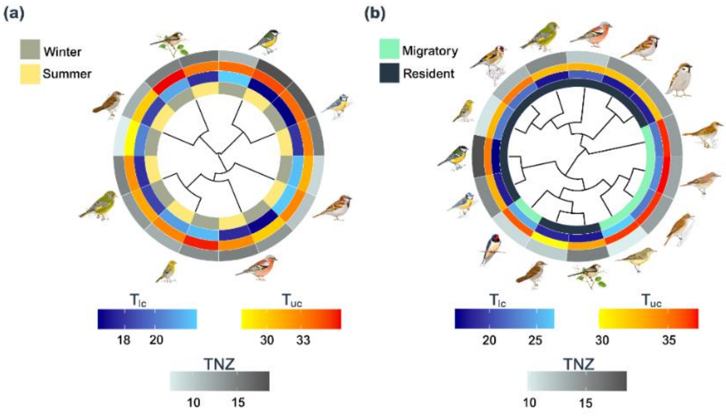

Figure 2 Consensus phylogenetic tree of the songbird species used in this study. We illustrate the lower and upper critical temperatures (T_{lc} and T_{uc}) and TNZ breadth in all the bird species included in this study (a) during two seasons, winter and summer, and (b) with different migratory strategies (migratory or resident). Temperatures are in degrees Celsius (°C). Credits for all the bird drawings: Juan Varela Simó.

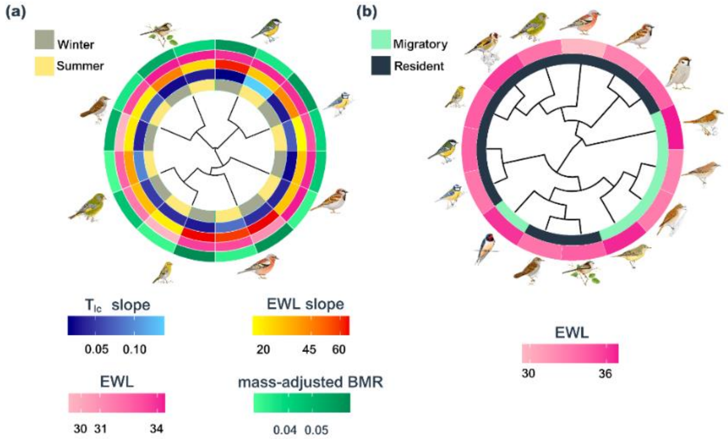

Figure 3 Consensus phylogenetic tree of the songbird species used in this study. We illustrate thermoregulatory traits (mass-adjusted BMR [watts g^{-1}], EWL inflection point [°C], T_{lc} slope [the slope of the metabolic rate below T_{lc}; ml min^{-1} °C^{-1}], and EWL slope [the slope of the evaporative water loss inflection point; mg hr^{-1} °C^{-1}]) in all the bird species included in this study (a) during two seasons, winter and summer, and (b) with different migratory strategies (migratory or resident). Credits for all the bird drawings: Juan Varela Simó.

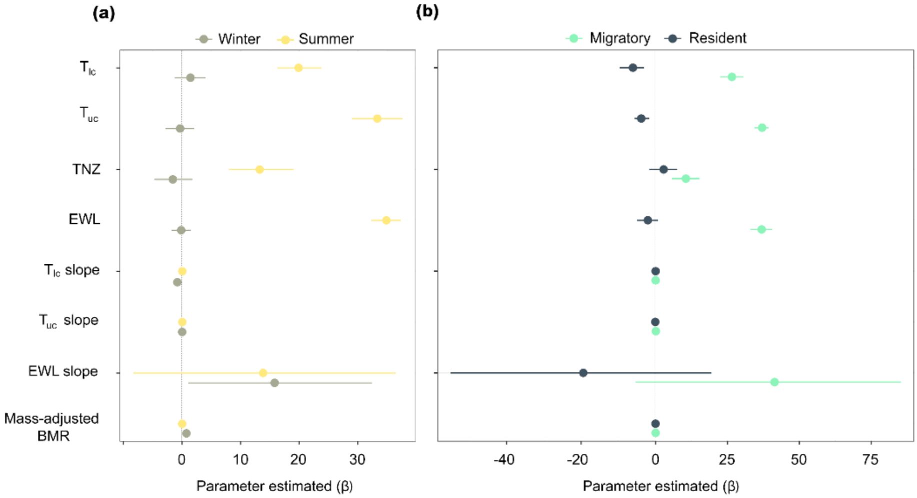

Figure 4 Posterior distributions of the parameter estimates (with 95% CI) of (a) seasonality (winter or summer) and (b) migratory strategy (migratory or resident). The posterior distribution of an independent variable with a negligible effect on a given thermoregulatory trait is expected to be centred on zero (dotted line); conversely, the distribution of an influential variable is expected to be substantially shifted from 0.

Discussion

Here, we present a phylogenetic comparative framework for examining how thermoregulatory traits of Mediterranean songbirds vary according to season and life-history strategy (residents versus long-distance migrants). After controlling for phylogenetic and body size effects, we found resident songbirds to seasonally adjust a suite of key thermoregulatory physiological traits, including winter upregulation of BMR (+71%), EWL slope (+55%), and T_{lc} slope (+43%), compared with summer values. We also found that in the summer, migratory songbirds had a greater T_{uc}, TNZ breadth and EWL inflection point than resident species, indicating that they have more efficient thermoregulation mechanisms and evaporative cooling at high temperatures, which was consistent with our CVH prediction.

Our findings showed that resident songbirds strongly increased their BMR during winter. Such metabolic adjustments to cold conditions reflect a common reaction norm of small endotherms to seasonal changes in energy demands (Nzama *et al.* 2010; Smit & McKechnie 2010; Wilson *et al.* 2011; Van de

Ven *et al.* 2013; Wu *et al.* 2015; Zhou *et al.* 2016). In small endotherms with high metabolic rates, such as songbirds, a higher BMR during winter than in summer generally implies a greater thermogenic capacity in colder winters and/or reduced metabolic heat production under warmer summer conditions (Arens & Cooper 2005; Nzama *et al.* 2010). The strong seasonal variation in the BMR of Mediterranean resident small songbirds confirmed this assertion. At the same time, the shallower T_{lc} slope (a proxy for thermal conductance) in winter should increase thermal tolerance to cold winters and reduce heat loss and promote energy savings under cold temperatures (Beason 1995), suggesting that Mediterranean resident songbirds adjust this thermoregulatory trait simultaneously with BMR as an adaptive strategy for coping with the contrasting temperatures experienced in Mediterranean habitats. Finally, contrary to our predictions, resident songbirds exhibited an increase (+1.3 °C) in T_{lc} during winter, which, a priori, could be an indicator of an early increase in energy expenses to upregulate thermogenesis as temperature decreases. However, they had a shallower T_{lc} slope in winter than in summer, which, in terms of energy expenditure, has greater relevance than the increase in the T_{lc} inflection point. For example, Mediterranean songbirds at ~10 °C (average T_a during winter in the study area) would spend half as much energy as in summer to maintain homeothermy (see Figure 1a).

Additionally, the strong increase in EWL during winter but elevated EWL inflection point in summer (+0.29 °C) is a strategy for increasing water conservation in summer, which could be related to facultative hyperthermia in summer (Noakes *et al.* 2016). Water balance may be under selective pressures similar to those for energy expenditure, especially in birds exposed to high T_a or with limited drinking water (Versteegh *et al.* 2008; Czenze *et al.* 2020), as is the case in our study area during summer. The observed increase in the EWL inflection point in summer was similar to that found in other species outside the Mediterranean, which was related to the flexibility of this thermoregulatory trait to enhance evaporative cooling efficiency in hot environments (Cooper & Gessaman 2004; Oswald *et al.* 2018). Our Mediterranean resident songbirds also exhibited a moderate increase (+0.2 °C) in T_{uc} during summer. The pattern of change in T_{uc} was similar to that found in bird species outside the Mediterranean basin (most of them belonging to the passerines; Bush *et al.* 2008; Pollock *et al.* 2019), but other bird species have shown the opposite pattern (Wu *et al.* 2015; Pollock *et al.* 2019). A higher T_{uc} in hot environments may be an indicator of energy conservation to downregulate thermogenesis at T_a above the TNZ during summer. This phenotypic flexibility in thermoregulatory traits likely enables small songbirds to cope physiologically with climatic variation in Mediterranean habitats, which is particularly important for species inhabiting geographical areas where warming is faster than the global average (Herrero *et al.* 2021; IPCC 2021).

When comparing the thermoregulatory traits of migratory and resident bird species during summer, we found that migratory species exhibited greater T_{lc} and T_{uc} and narrower TNZ breadths than resident species. Pollock (2016) found similar results when comparing temperate residents and migratory bird species in North America, which indicates that migratory tendency predicts interspecific variation in avian thermoregulatory traits. Our migratory songbirds showed more efficient thermoregulation mechanisms at high temperatures than resident songbirds, which supports the hypothesis that trans-Saharan migrants are exposed to a wide range of climatic conditions (Culp *et al.* 2017; Eyres *et al.* 2020). T_{uc} was 33 °C and 36.6 °C for resident and migratory birds, respectively, implying an advantage for migratory birds in terms of energy savings when temperatures exceed 33 °C. Beyond 33 °C, resident songbirds must allocate extra energy to maintain their normothermic core temperature, while migratory birds do not have to expend energy for thermoregulation until temperatures exceed 36.6 °C. The average maximum summer temperature in the study area was 34.2 °C, so resident species would be allocating significantly more energy for thermoregulation. Additionally, these Afro-Palearctic migrants exhibited a higher EWL inflection point (+1.5 °C), indicating that they have a higher evaporative cooling efficiency. These results also suggest that Mediterranean migratory songbirds would be more resilient to global warming than resident songbirds.

Contrary to our expectations, we found no differences in summer BMR between migratory and resident birds. A global comparative study in birds found that migratory bird species have higher mass-adjusted BMRs than resident species, yet the differences became non-significant after accounting for environmental variables such as average annual temperature or temperature range (Jetz *et al.* 2008). We measured migratory and resident birds from the same location and same periods, so our results support that migratory behaviour *per se* is not a strong driver of increased metabolic rate (but see Kvist & Lindström 2001). Rather, they support the idea that T_a is a major environmental predictor of BMR (see White *et al.* 2007; Jetz *et al.* 2008). This is consistent with the findings of a previous study in songbirds (family Fringillidae), which did not find significant differences in mass-adjusted BMR between migratory and resident species (McNab 2012). Nonetheless, further empirical work on BMR across different species and environments is needed to determine the full extent of variation in BMR across migratory and resident species.

Overall, our study demonstrates that Mediterranean resident songbirds exhibit pronounced seasonal variation in some key thermoregulatory traits. Such physiological adjustments might promote the resilience of organisms and populations to environmental changes, with short-term benefits in terms of energy and water savings under thermally stressful conditions. We have also shown that migratory species have higher efficiency in thermoregulation mechanisms at high temperatures, which could confer a greater thermal tolerance compared to that of resident ones; therefore, they would have a greater resilience against global warming. Current and future selection pressures driven by climate change may favour species with higher physiological flexibility, resulting in greater thermal tolerance (Calosi *et al.* 2008; Somero 2010). Our study indicates that these characteristics may apply especially to Mediterranean migratory songbirds. However, this flexibility also has associated costs in terms of trade-offs that result from changes in energy allocation among organismal functions (Riddell *et al.* 2018; Fox *et al.* 2019; Burraco *et al.* 2022). For instance, reductions in EWL rates during thermal acclimation can be associated with simultaneous reductions in metabolic rates (Riddell et al., 2018), which may structure whole-organism strategies for responding to environmental stressors and constrain phenotypic variation. Thus, the balance between the costs and benefits of flexibility in thermoregulatory traits will determine the capacity of species to cope with and adapt to changing environments (Angilletta *et al.* 2002; Pörtner *et al.* 2006; Angilletta *et al.* 2010; Bozinovic & Pörtner 2015;). Finally, the large observed seasonal variation in some thermoregulatory traits (namely, BMR, TNZ breadth, EWL, and T_{lc} slope) reveals some methodological implications for comparative studies of avian energetics and thermoregulation using birds captured and measured in different seasons and environments. Consequently, it is essential to note the local environmental conditions under which such traits are measured, especially when metabolic comparisons are made between animals at different places over the course of their annual cycle (Kvist & Lindström 2001).

References

AEMET (2022) Climate statistics. Badajoz Airport (1981–2010). Agencia Estatal de Meteorología. Gobierno de España. http://www.aemet.es/es/serviciosclimaticos/datosclimatologicos/valoresclimatologicos?l=4452&k=ext

Angilletta, M. J., Cooper, B. S., Schuler, M. S. & Boyles, J. G. (2010) The evolution of thermal physiology in endotherms. Frontiers in Bioscience (Elite Ed), 2, 861–881.

Angilletta, M. J. Jr, Niewiarowski, P. H. & Navas, C. A. (2002) The evolution of thermal physiology in ectotherms. Journal of Thermal Biology 27(4), 249–268.

Araújo, M. B., Ferri-Yáñez, F., Bozinovic, F., Marquet, P. A., Valladares, F. & Chown, S. L. (2013) Heat freezes niche evolution. Ecology Letters 16(9), 1206–1219.

Arens, J. R. & Cooper, S. J. (2005) Metabolic and ventilatory acclimatization to cold stress in house sparrows (*Passer domesticus*) Physiological and Biochemical Zoology 78(4), 579–589.

Barker, F. K., Cibois, A., Schikler, P., Feinstein, J. & Cracraft, J. (2004) Phylogeny and diversification of the largest avian radiation. Proceedings of the National Academy of Sciences 101(30), 11040–11045.

Beason, R. C. (1995) Horned Lark: Eremophila Alpestris (Vol. 195) Philadelphia, PA, USA: American Ornithologists' Union.

Bellard, C., Bertelsmeier, C., Leadley, P., Thuiller, W. & Courchamp, F. (2012) Impacts of climate change on the future of biodiversity. Ecology Letters 15(4), 365–377.

Bonamour, S., Chevin, L. M., Charmantier, A. & Teplitsky, C. (2019) Phenotypic plasticity in response to climate change: the importance of cue variation. Philosophical Transactions of the Royal Society B 374(1768), 20180178.

Boratyński, J. S., Jefimow, M. & Wojciechowski, M. S. (2016) Phenotypic flexibility of energetics in acclimated Siberian hamsters has a narrower scope in winter than in summer. Journal of Comparative Physiology B 186(3), 387–402.

Bozinovic, F. & Pörtner, H.O. (2015) Physiological ecology meets climate change. Ecology and Evolution, 5(5), 1025–1030.

Burraco, P., Rendón, M. A., Díaz-Paniagua, C. & Gomez-Mestre, I. (2022) Maintenance of phenotypic plasticity is linked to oxidative stress in spadefoot toad larvae. Oikos, e09078.

Bush, N. G., Brown, M. & Downs, C. T. (2008) Seasonal effects on thermoregulatory responses of the rock kestrel*, Falco rupicolis*. Journal of Thermal Biology 33(7), 404–412.

Calosi, P., Bilton, D. T. & Spicer, J. I. (2008) Thermal tolerance, acclimatory capacity and vulnerability to global climate change. Biology Letters 4(1), 99–102.

Cavieres, G. & Sabat, P. (2008) Geographic variation in the response to thermal acclimation in rufous-collared sparrows: are physiological flexibility and environmental heterogeneity correlated? Functional Ecology 22(3), 509–515.

Ceballos, G., Ehrlich, P. R. & Dirzo, R. (2017) Biological annihilation via the ongoing sixth mass extinction signaled by vertebrate population losses and declines. Proceedings of the National Academy of Sciences 114(30), E6089–E6096.

Cooper, S. J. & Gessaman, J. A. (2004) Thermoregulation and habitat preference in Mountain Chickadees and Juniper Titmice. The Condor 106(4), 852–861.

Coumou, D. & Robinson, A. (2013) Historic and future increase in the global land area affected by monthly heat extremes. Environmental Research Letters 8(3), 034018.

Culp, L. A., Cohen, E. B., Scarpignato, A. L., Thogmartin, W. E. & Marra, P. P. (2017) Full annual cycle climate change vulnerability assessment for migratory birds. Ecosphere 8(3), e01565.

Czenze, Z. J., Kemp, R., Van Jaarsveld, B., Freeman, M. T., Smit, B., Wolf, B. O. & McKechnie, A. E. (2020) Regularly drinking desert birds have greater evaporative cooling capacity and higher heat tolerance limits than non-drinking species. Functional Ecology 34(8), 1589–1600.

Eyres, A., Böhning-Gaese, K., Orme, C. D. L., Rahbek, C. & Fritz, S. A. (2020) A tale of two seasons: The link between seasonal migration and climatic niches in passerine birds. Ecology and Evolution 10(21), 11983-11997.

Fox, R. J., Donelson, J. M., Schunter, C., Ravasi, T. & Gaitán–Espitia, J. D. (2019) Beyond buying time: the role of plasticity in phenotypic adaptation to rapid environmental change. Philosophical Transactions of the Royal Society B: Biological Sciences 374, 20180174.

Freckleton, R. P. (2009) The seven deadly sins of comparative analysis. Journal of Evolutionary Biology 22(7), 1367–1375.

Gelman, A. & Rubin, D. B. (1992) Inference from iterative simulation using multiple sequences. Statistical Science 7(4), 457–472.

González-Medina, E., Cabello-Vergel, J., Playà-Montmany, N., Villegas, A., Parejo, M., Abad-Gómez, J. M., Sánchez-Guzmán J. M. & Masero, J.A. (2020) Going to sleep with a full belly: Thermal substitution by specific dynamic action in shorebirds. Comparative Biochemistry and Physiology Part A: Molecular & Integrative Physiology 244, 110689.

Hadfield, J. D. & Nakagawa, S. (2010) General quantitative genetic methods for comparative biology: phylogenies, taxonomies and multi-trait models for continuous and categorical characters. Journal of Evolutionary Biology 23(3), 494–508.

Hadfield, J. D. (2010) MCMC methods for multi–response generalized linear mixed models: the MCMCglmm R package. Journal of Statistical Software 33, 1–22.

Harvey, P. H. & Pagel, M. D. (1991) The comparative method in evolutionary biology. Oxford: Oxford University Press.

Herrero, A., Ruiz–Benito, P., Andivia, E., Madrigal–González, J., Villar–Salvador, P., Ratcliffe, S. & Zavala, M. A. (2021) Mediterranean pine forest distribution: assessing vulnerability and resilience under climate change. In: Ne`eman, G. & Osem Y. (Eds.) Pines and their mixed forest ecosystems in the Mediterranean basin. Springer, pp. 251–277.

Huey, R. B., Kearney, M. R., Krockenberger, A., Holtum, J. A., Jess, M. & Williams, S.E. (2012) Predicting organismal vulnerability to climate warming: roles of behaviour, physiology and adaptation. Philosophical Transactions of the Royal Society B: Biological Sciences 367(1596), 1665–1679.

IPCC (2021) Climate Change 2021: The Physical Science Basis. Contribution of Working Group I to the Sixth Assessment Report of the Intergovernmental Panel on Climate Change. In: Masson-Delmotte, V., P. Zhai, A. Pirani, S.L. Connors, C. Péan, S. Berger, N. Caud, Y. Chen, L. Goldfarb, M.I. Gomis, M. Huang, K. Leitzell, E. Lonnoy, J.B.R. Matthews, T.K. Maycock, T. Waterfield, O. Yelekçi, R. Yu, and B. Zhou (Eds.) Cambridge University Press. Available from: https://www.ipcc.ch/report/ar6/wg1/downloads/report/IPCC_AR6_WGI_Full_Report_smaller.pdf [accessed 10 December 2021].

Jetz, W., Freckleton, R. P. & McKechnie, A. E. (2008) Environment, migratory tendency, phylogeny and basal metabolic rate in birds. PLoS One 3(9), e3261.

Jetz, W., Thomas, G. H., Joy, J. B., Hartmann, K. & Mooers, A. O. (2012) The global diversity of birds in space and time. Nature 491(7424), 444–448.

Khaliq, I., Hof, C., Prinzinger, R., Böhning–Gaese, K. & Pfenninger, M. (2014) Global variation in thermal tolerances and vulnerability of endotherms to climate change. Proceedings of the Royal Society B: Biological Sciences 281(1789), 20141097.

Książek, A., Czerniecki, J. & Konarzewski, M. (2009) Phenotypic flexibility of traits related to energy acquisition in mice divergently selected for basal metabolic rate (BMR) Journal of Experimental Biology 212(6), 808–814.

Kvist, A. & Lindström, Å. (2001) Basal metabolic rate in migratory waders: intra–individual, intraspecific, interspecific and seasonal variation. Functional Ecology 15(4),465–473.

Lighton, J. R. (2018) Measuring metabolic rates: a manual for scientists. Oxford Oxford University Press.

Maddocks, T. A. & Geiser, F. (2000) Seasonal variations in thermal energetics of Australian silvereyes (*Zosterops lateralis*) Journal of Zoology 252(3), 327–333.

McKechnie, A.E. (2008) Phenotypic flexibility in basal metabolic rate and the changing view of avian physiological diversity: a review. Journal of Comparative Physiology B 178(3), 235–247.

McKechnie, A. E., Chetty, K. & Lovegrove, B. G. (2007) Phenotypic flexibility in the basal metabolic rate of laughing doves: responses to short–term thermal acclimation. Journal of Experimental Biology 210(1), 97–106.

McKechnie, A. E., Noakes, M. J. & Smit, B. (2015) Global patterns of seasonal acclimatization in avian resting metabolic rates. Journal of Ornithology 156(1), 367–376.

McNab, B. K. (2002) The physiological ecology of vertebrates: a view from energetics. Cornell: Cornell University Press.

McNab, B. K. (2012) Extreme measures: the ecological energetics of birds and mammals. The University of Chicago Press.

Muggeo, V. M. (2008) Segmented: an R package to fit regression models with broken–line relationships. *R* news 8(1), 20–25.

Muggeo, V. M. (2009) Segmented: segmented relationships in regression models. – R package ver. 0.2–6.

Noakes, M. J., Wolf, B. O. & McKechnie, A. E. (2016) Seasonal and geographical variation in heat tolerance and evaporative cooling capacity in a passerine bird. Journal of Experimental Biology 219(6), 859-869.

Noakes, M. J., Wolf, B. O. & McKechnie, A. E. (2017) Seasonal metabolic acclimatization varies in direction and magnitude among populations of an Afrotropical passerine bird. Physiological and Biochemical Zoology 90(2), 178–189.

Nzama, S. N., Downs, C. T. & Brown, M. (2010) Seasonal variation in the metabolism–temperature relation of house sparrows (*Passer domesticus*) in KwaZulu–Natal, South Africa. Journal of Thermal Biology 35(2), 100–104.

Oboikovitz, P. & Swanson, D. L. (2021) Seasonal metabolic flexibility is correlated with microclimate variation in horned larks and house sparrows. Current Zoology 68(2), 199–210.

Oswald, K. N., Evlambiou, A. A., Ribeiro, Â. M. & Smit, B. (2018) Tag location and risk assessment for passive integrated transponder-tagging passerines. Ibis 160(2), 453-457.

Piersma, T. & Van Gils, J.A. (2011) The flexible phenotype: a body–centred integration of ecology, physiology, and behaviour. Oxford: Oxford University Press.

Playà-Montmany, N., González-Medina, E., Cabello-Vergel, J., Parejo, M., Abad-Gómez, J. M., Sánchez-Guzmán, J. M., Villegas, A. & Masero, J.A. (2021) The thermoregulatory role of relative bill and leg surface areas in a Mediterranean population of Great tit (*Parus major*). Ecology and Evolution 11(22), 15936–15946.

Pollock, H. S. (2016) The influence of spatiotemporal variation in ambient temperature on the ecology and physiology of birds. – PhD thesis, University of Illinois, Urbana-Champaign.

Pollock, H. S., Brawn, J. D. & Cheviron, Z. A. (2021) Heat tolerances of temperate and tropical birds and their implications for susceptibility to climate warming. *Functional Ecology*, 35(1), 93–104.

Pollock, H. S., Brawn, J. D., Agin, T. J. & Cheviron, Z. A. (2019) Differences between temperate and tropical birds in seasonal acclimatization of thermoregulatory traits. Journal of Avian Biology 50(4), e02067.

Pörtner, H. O., Bennett, A. F., Bozinovic, F., Clarke, A., Lardies, M. A., Lucassen, M., Pelster, B., Schiemer, F. & Stillman, J. H. (2006) Trade–offs in thermal adaptation: the need for a molecular to ecological integration. Physiological and Biochemical Zoology, 79(2), 295–313.

R Core Team (2021) R: A Language and Environment for Statistical Computing. (ed. Computing, RFfS) Vienna, Austria.

Revell, L. J. (2012) phytools: an R package for phylogenetic comparative biology (and other things). Methods in Ecology and Evolution 3(2), 217–223.

Riddell, E. A., McPhail, J., Damm, J. D. & Sears, M. W. (2018) Trade-offs between water loss and gas exchange influence habitat suitability of a woodland salamander. Functional Ecology 32(4), 916–925.

Schmidt-Nielsen, K. (1997) Animal physiology: adaptation and environment. Cambridge University Press.

Smit, B. & McKechnie, A. E. (2010) Avian seasonal metabolic variation in a subtropical desert: basal metabolic rates are lower in winter than in summer. Functional Ecology 24(2), 330–339.

Somero, G. N. (2010) The physiology of climate change: how potentials for acclimatization and genetic adaptation will determine 'winners' and 'losers'. Journal of Experimental Biology 213(6), 912–920.

Spooner, F. E., Pearson, R. G. & Freeman, R. (2018) Rapid warming is associated with population decline among terrestrial birds and mammals globally. Global Change Biology 24(10), 4521–4531.

Stager, M., Pollock, H. S., Benham, P. M., Sly, N. D., Brawn, J. D. & Cheviron, Z. A. (2016) Disentangling environmental drivers of metabolic flexibility in birds: the importance of temperature extremes versus temperature variability. Ecography 39(8), 787–795.

Stager, M., Senner, N. R., Swanson, D. L., Carling, M. D., Eddy, D. K., Greives, T. J. & Cheviron, Z. A. (2021) Temperature heterogeneity correlates with intraspecific variation in physiological flexibility in a small endotherm. Nature Communications 12(1), 1–11.

Swanson, D. L. (1990) Seasonal variation in cold hardiness and peak rates of cold–induced thermogenesis in the dark–eyed junco (*Junco hyemalis*). The Auk 107(3), 561–566.

Swanson, D. L. (2010) Seasonal metabolic variation in birds: functional and mechanistic correlates. In: Thompson, C. (Eds.) *Current Ornithology Volume 17*. Springer, pp. 75–129.

Swanson, D. L., Agin, T. J., Zhang, Y., Oboikovitz, P. & DuBay, S. (2020) Metabolic flexibility in response to within–season temperature variability in house sparrows. Integrative Organismal Biology 2(1), obaa039.

Talbot, W. A., McWhorter, T. J., Gerson, A. R., McKechnie, A. E. & Wolf, B. O. (2017) Avian thermoregulation in the heat: evaporative cooling capacity of arid–zone Caprimulgiformes from two continents. *Journal of Experimental Biology*, 220(19), 3488–3498.

Thomas, D. W., Blondel, J. & Perret, P. (2001) Physiological ecology of Mediterranean Blue Tits (*Parus caeruleus*) I. A test for inter–population differences in resting metabolic rate and thermal conductance as a response to hot climates. Zoology 104(1), 33–40.

Tieleman, B. I., Williams, J. B. & Bloomer, P. (2003) Adaptation of metabolism and evaporative water loss along an aridity gradient. Proceedings of the Royal Society of London. Series B: Biological Sciences 270(1511), 207–214.

Van de Ven, T. M., Mzilikazi, N. & McKechnie, A. E. (2013) Seasonal metabolic variation in two populations of an Afrotropical euplectid bird. Physiological and Biochemical Zoology 86(1), 19–26.

Versteegh, M. A., Helm, B., Dingemanse, N. J. & Tieleman, B. I. (2008) Repeatability and individual correlates of basal metabolic rate and total evaporative water loss in birds: a case study in European stonechats. Comparative Biochemistry and Physiology Part A: Molecular & Integrative Physiology 150(4), 452–457.

Visser, M. E. (2008) Keeping up with a warming world; assessing the rate of adaptation to climate change. Proceedings of the Royal Society B: Biological Sciences 275(1635), 649–659.

Wang, Y., Shan, S., Zhang, H., Dong, B., Zheng, W. & Liu, J. (2019) Physiological and biochemical thermoregulatory responses in male Chinese hwameis to seasonal acclimatization: phenotypic flexibility in a small passerine. Zoological Studies 58,6

White, C. R., Blackburn, T. M., Martin, G. R. & Butler, P. J. (2007) Basal metabolic rate of birds is associated with habitat temperature and precipitation, not primary productivity. Proceedings of the Royal Society B: Biological Sciences 274(1607), 287–293.

Williams, J. B. & Tieleman, B. I. (2005) Physiological adaptation in desert birds. Bioscience 55(5), 416–425.

Wilson, A. L., Brown, M. & Downs, C. T. (2011) Seasonal variation in metabolic rate of a medium–sized frugivore, the knysna turaco (*Tauraco corythaix*). Journal of Thermal Biology 36(3), 167–172.

Wu, M. X., Zhou, L. M., Zhao, L. D., Zhao, Z. J., Zheng, W. H. & Liu, J. S. (2015) Seasonal variation in body mass, body temperature and thermogenesis in the hwamei, *Garrulax canorus*. Comparative Biochemistry and Physiology Part A: Molecular & Integrative Physiology 179, 113–119.

Xu, Y., Ramanathan, V. & Victor, D. G. (2018) Global warming will happen faster than we think. Nature 564, 30–32.

Zheng, W. H., Lin, L., Liu, J. S., Pan, H., Cao, M. T. & Hu, Y. L. (2013) Physiological and biochemical thermoregulatory responses of Chinese bulbuls *Pycnonotus sinensis* to warm temperature: Phenotypic flexibility in a small passerine. Journal of Thermal Biology 38(5), 240–246.

Zheng, W. H., Liu, J. S. & Swanson, D. L. (2014) Seasonal phenotypic flexibility of body mass, organ masses, and tissue oxidative capacity and their relationship to resting metabolic rate in chinese bulbuls. Physiological and Biochemical Zoology 87(3), 432–444.

Zhou, L. M., Xia, S. S., Chen, Q., Wang, R. M., Zheng, W. H. & Liu, J. S. (2016) Phenotypic flexibility of thermogenesis in the hwamei (*Garrulax canorus*): responses to cold acclimation. American Journal of Physiology–Regulatory, Integrative and Comparative Physiology 310(4), R330–R336.

Appendix 1: Supplementary Material

Supplementary Table 1. Posterior distributions of the parameter estimates (with 95% CI) of migratory strategy (migratory or resident) and seasonality (winter or summer). The posterior distribution of an independent variable with a negligible effect on a given thermoregulatory trait is expected to be centered on zero (dotted line); conversely, the distribution of an influential variable is expected to be substantially shifted from 0. Significant predictors are in bold.

Thermal Traits		**Post.mean (lower and upper CI)**	h^2	**pMCMC**
Migratory strategy (migratory/resident)				
T_{lc}	**(Intercept)**	**26.54 (22.49, 30.49)**	**0.644**	**<5e-04**
	***Strategy resident**	**-6.08 (-9.67, -3.07)**		**<5e-04**
	Body mass	-0.13 (-0.27, 0.049)		0.105
T_{uc}	**(Intercept)**	**37.03 (34.39, 39.32)**	**0.398**	**< 5e-04**
	***Strategy resident**	**-3.82 (-5.71, -1.74)**		**0.002**
	Body mass	-0.02 (-0.12, 0.098)		0.732
TNZ breath	**(Intercept)**	**10.56 (5.67, 15.24)**	**0.560**	**0.001**
	*Strategy resident	2.17 (-1.73, 5.87)		0.223
	Body mass	0.11 (-0.07, 0.31)		0.242
EWL	**(Intercept)**	**36.87 (32.97, 40.59)**	**0.393**	**<5e-04**
	*Strategy resident	-2.07 (-4.97, 0.62)		0.123
	Body mass	-0.09 (-0.25, 0.06)		0.217
T_{lc} slope	(Intercept)	0.01 (-0.06, 0.08)	0.579	0.644
	*Strategy resident	0.017 (-0.03, 0.07)		0.508
	Body mass	0.002 (-0.0004, 0.006)		0.068
T_{uc} slope	(Intercept)	0.086 (-0.008, 0.19)	0.564	0.074
	*Strategy resident	-0.06 (-0.13, 0.02)		0.102
	Body mass	0.002 (-0.002, 0.006)		0.326

(Continues)

Supplementary Table 1. (Continued)

Thermal Traits		**Post.mean (lower and upper CI)**	h^2	**pMCMC**
Seasonality (winter and summer)				
EWL slope	(Intercept)	41.36 (-6.93, 85.23)	0.725	0.081
	*Strategy resident	-19.43 (-55.13, 15.03)		0.258
	Body mass	0.70 (-0.86, 2.20)		0.358
Mass-adjusted BMR	(Intercept)	0.04 (-0.008, 0.09)	0.557	0.072
	*Strategy resident	-0.0004 (-0.04, 0.03)		0.986
	Body mass	-0.0007 (-0.003, 0.001)		0.486
T_{lc}	**(Intercept)**	**19.88 (16.34, 24.16)**	**0.093**	**<5e-04**
	†Season Winter	1.31 (-1.18, 3.8)		0.296
	Body mass	-0.08 (-0.32, 0.12)		0.441
T_{uc}	**(Intercept)**	**33.32 (29.27, 37.04)**	**0.298**	**<5e-04**
	†Season Winter	-0.29 (-2.45, 2.19)		0.776
	Body mass	-0.02 (-0.25, 0.19)		0.820
TNZ breadth	**(Intercept)**	**13.24(7.64, 18.50)**	**0.273**	**<5e-04**
	†Season Winter	-1.60 (-5.04, 1.41)		0.270
	Body mass	0.068 (-0.23, 0.40)		0.656
EWL	**(Intercept)**	**34.91 (32.44, 38.06)**	**0.167**	**<5e-04**
	†Season Winter	-0.19 (-1.862, 1.49)		0.819
	Body mass	-0.12 (-0.29, 0.01)		0.093
T_{lc} slope	(Intercept)	0.04 (-0.02, 0.09)	0.434	0.120
	†Season Winter	**-0.04 (-0.07, 0.02)**		**0.004**
	Body mass	0.002 (-0.001, 0.005)		0.190
T_{uc} slope	(Intercept)	0.04 (-0.04, 0.12)	0.396	0.309
	†Season Winter	0.009 (-0.03, 0.05)		0.624
	Body mass	-7.9e-05 (-4.4e-03, 4.8e-03)		0.947
EWL slope	(Intercept)	13.81 (-7.3, 36.8)	0.055	0.21
	†Season Winter	**15.31 (-0.37, 30.64)**		**0.049**
	Body mass	1.0 (-0.2, 2.31)		0.105

(Continues)

Supplementary Table 1. (Continued)

Thermal Traits		**Post.mean (lower and upper CI)**	***h^2***	**pMCMC**
Seasonality (winter and summer)				
Seasonality (winter and summer)	(Intercept)	0.03 (7.7e-04, 0.06)	0.653	0.061
	†Season Winter	**0.02 (0.009, 0.03)**		**<5e-04**
	Body mass	2.6e-05 (-0.001, 0.002)		0.973

*Reference category is "Migratory".

†Reference category is "Summer"

Supplementary Table 2. Thermoregulatory traits of songbirds linked to their migratory strategy (migratory/resident).

Scientific name	Common name	Family	Strategy	n	EWL (°C)	EWL slope (mg hr^{-1} °C^{-1})	Body mass (g)
Cettia cetti	Cetti's warbler	Sylviidae	Resident	10	33.25	18.662	12.26
Aegithalos caudatus	Long-tailed tit	Aegithalidae	Resident	12	34.36	24.386	6.17
Cyanistes caeruleus	Blue tit	Paridae	Resident	16	33.16	14.824	8.93
Carduelis carduelis	Goldfinch	Fringillidae	Resident	10	35.85	41.055	13.33
Serinus serinus	Serin	Fringillidae	Resident	5	34.41	29.508	10.17
Hirundo rustica	Barn swallow	Hirundinidae	Migratory	11	36.21	50.543	17.50
Acrocephalus arundinaceus	Great reed warbler	Sylviidae	Migratory	10	32.85	29.319	29.12
Hippolais polyglotta	Melodious warbler	Sylviidae	Migratory	9	36.59	37.796	10.14
Acrocephalus scirpaceus	Reed warbler	Sylviidae	Migratory	13	32.47	8.868	9.63
Chloris chloris	Greenfinch	Fringillidae	Resident	19	33.34	58.621	21.49
Parus major	Great tit	Paridae	Resident	10	34.16	28.571	16.59
Fringilla coelebs	Common chaffinch	Fringillidae	Resident	14	29.38	18.962	19.28
Passer montanus	Eurasian tree sparrow	Passeridae	Resident	8	34.13	55.594	17.90
Passer domesticus	House sparrow	Passeridae	Resident	6	32.51	37.958	25.377
Luscinia megarhynchos	Nightingale	Turdidae	Migratory	9	36.92	92.322	19.32

(Continues)

Supplementary Table 2 (Continued)

Scientific name	BMR (W)	Mass-adjusted BMR (watts g^{-1})	T_{lc} (°C)	T_{uc} (°C)	T_{uc} slope (ml min^{-1} $°C^{-1}$)	T_{lc} slope (ml min^{-1} $°C^{-1}$)	TNZ breath (°C)
Cettia cetti	0.275	0.034	18.4	30.0	0.014	0.069	11.6
Aegithalos caudatus	0.192	0.041	17.7	33.5	0.046	0.032	15.8
Cyanistes caeruleus	0.2613	0.041	17.9	33.1	0.016	0.068	15.2
Carduelis carduelis	0.327	0.036	22.1	35.0	0.065	0.056	12.9
Serinus serinus	0.205	0.029	22.6	32.9	0.024	0.037	10.3
Hirundo rustica	0.399	0.035	25	35.8	0.078	0.063	10.9
Acrocephalus arundinaceus	0.359	0.021	22.7	36.7	0.102	0.077	14.0
Hippolais polyglotta	0.233	0.033	26.8	36.6	0.072	0.025	9.8
Acrocephalus scirpaceus	0.239	0.038	23.5	37.2	0.052	0.045	13.7
Chloris chloris	0.416	0.030	17.5	32.7	0.074	0.082	15.2
Parus major	0.370	0.034	16.4	35.0	0.038	0.139	18.6
Fringilla coelebs	0.353	0.028	21.2	33.0	0.117	0.042	11.8
Passer montanus	0.392	0.034	18.1	32.3	0.082	0.091	14.2
Passer domesticus	0.397	0.025	17.7	32.4	0.023	0.094	14.7
Luscinia megarhynchos	0.408	0.033	22.6	36.8	0.213	0.088	14.2

Supplementary Table 3. Seasonality of thermoregulatory traits in resident songbirds in the study area.

Scientific name	Common name	Family	Season	n	EWL (°C)	EWL slope (g hr^{-1} °C^{-1})	Body-mass (g)
Aegithalos caudatus	Long-tailed tit	Aegithalidae	Summer	12	34.36	24.386	6.17
Chloris chloris	Greenfinch	Fringillidae	Summer	19	33.34	58.621	21.49
Cettia cetti	Cetti's warbler	Sylviidae	Summer	10	33.25	18.662	12.27
Fringilla coelebs	Common chaffinch	Fringillidae	Summer	14	29.38	18.962	19.28
Cyanistes caeruleus	Blue tit	Paridae	Summer	16	33.16	14.824	8.926
Parus major	Great tit	Paridae	Summer	10	34.16	28.571	16.60
Passer domesticus	House sparrow	Passeridae	Summer	6	32.51	37.958	25.38
Serinus serinus	serin	Fringillidae	Summer	5	34.41	29.508	10.17
Aegithalos caudatus	Long-tailed tit	Aegithalidae	Winter	12	34.37	45.176	6.163
Chloris chloris	Greenfinch	Fringillidae	Winter	13	30.90	64.428	22.93
Cettia cetti	Cetti's warbler	Sylviidae	Winter	8	29.35	19.752	13.27
Fringilla coelebs	Common chaffinch	Fringillidae	Winter	11	33.67	64.069	20.74
Parus caeruleus	Blue tit	Paridae	Winter	13	34.01	43.178	9.24
Parus major	Great tit	Paridae	Winter	10	34.02	62.050	16.79
Passer domesticus	House sparrow	Passeridae	Winter	8	31.75	30.860	26.31
Serinus serinus	Serin	Fringillidae	Winter	4	34.20	29.370	10.38

(Continues)

Supplementary Table 3 (Continued)

Scientific name	BMR (W)	Mass-adjusted BMR (watts g^{-1})	T_{lc} (°C)	T_{uc} (°C)	T_{uc} slope (ml min^{-1} °C^{-1})	T_{lc} slope (ml min^{-1} °C^{-1})	TNZ breath (°C)
Aegithalos caudatus	0.192	0.041	17.7	33.5	0.046	0.032	15.8
Chloris chloris	0.416	0.030	17.5	32.7	0.074	0.082	15.18
Cettia cetti	0.276	0.034	18.4	30.0	0.014	0.069	11.6
Fringilla coelebs	0.353	0.028	21.2	33.0	0.117	0.042	11.8
Cyanistes caeruleus	0.261	0.041	17.9	33.1	0.016	0.069	15.2
Parus major	0.370	0.034	16.4	35.0	0.038	0.139	18.6
Passer domesticus	0.397	0.025	17.7	32.4	0.023	0.095	14.7
Serinus serinus	0.206	0.029	22.6	32.9	0.024	0.037	10.3
Aegithalos caudatus	0.174	0.055	21.5	36.5	0.118	0.024	15.0
Chloris chloris	0.454	0.063	16.5	30.0	0.038	0.042	13.47
Cettia cetti	0.271	0.053	20.4	27.8	0.009	0.035	7.4
Fringilla coelebs	0.445	0.066	22.1	36.1	0.048	0.030	14.0
Parus caeruleus	0.246	0.060	16.2	34.0	0.080	0.030	17.8
Parus major	0.364	0.061	22.77	33.9	0.064	0.014	11.17
Passer domesticus	0.396	0.046	18.4	31.6	0.008	0.050	13.2
Serinus serinus	0.196	0.045	22.2	31.1	0.032	0.021	8.9

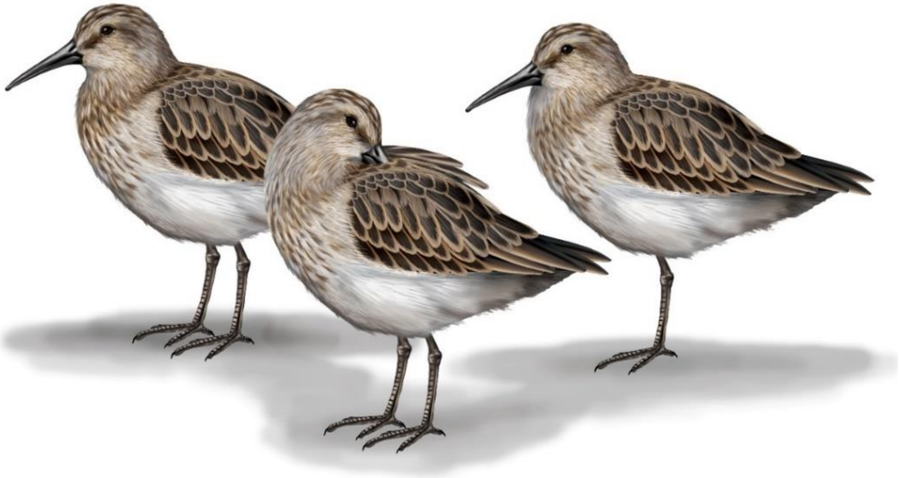

3

Behavioural and physiological responses to experimental temperature changes in a long-billed and long-legged bird: a role for relative appendage size

Núria Playà-Montmany, Erick González-Medina, Julián Cabello-Vergel, Manuel Parejo, José M. Abad-Gómez, Juan M. Sánchez-Guzmán, Auxiliadora Villegas and José A. Masero

Submitted to Behavioral Ecology and Sociobiology

Abstract

Bird species occupying open landscapes are inherently exposed to acute external cold and heat loads, which force them to adopt a suite of behavioural and physiological strategies to maintain homeothermy. Both types of responses could be influenced by relative bill and leg sizes, but experimental data are lacking. Here, we evaluated how variations in body postural adjustments, panting, and locomotor activity in the Dunlin *Calidris alpina* can be explained by the environmental temperature, microhabitat use and relative bill and leg sizes. Additionally, we estimated resting metabolic rate and evaporative water loss to assess potential links between both physiological traits and relative appendage size. Temperatures below the thermoneutral zone (< 20°C) were faced by enhancing metabolic heat production through increased locomotor activity, while body postural adjustments were used less than expected. Within the thermoneutral zone, back rest posture and unipedal resting were selected by Dunlins, probably as being more comfortable for resting. At high temperatures (>35°C), Dunlins were inactive and increased the time of bill exposure and wet-sitting and ultimately panting while wet-sitting when challenged with temperatures above 37°C. We did not find support for a role of relative appendage size in explaining behavioural or physiological responses. The low intraspecific variation in relative bill and leg surfaces could explain the lack of explanatory power of these morphological traits. The substrate type available for roosting in wetland margins was assumed to be important for bird thermoregulation. Our findings confirmed the key role of this factor in minimising heat stress in wetland species.

Keywords: bill size, evaporative water loss, leg size, metabolic rate, shorebirds, thermal behaviour.

Introduction

Many birds living in open landscapes are regularly exposed to acute external cold and heat loads, and they have evolved specific behavioural and physiological responses to cope with these thermal challenges (Luskick *et al.* 1978; Brodsky & Weatherhead 1984; Tieleman *et al.* 2002; Amat & Masero 2004; Gutiérrez *et al.* 2015; González-Medina *et al.* 2020). Groups such as shorebirds, waterfowl and gulls rely on exposed intertidal areas for foraging, but at high tide, they are forced to move to alternative sites, which are usually open, non-vegetated beaches or mudflats near the tide line (e.g., Rogers *et al.* 2006), where they rest for long periods of time while waiting for the next low-tide period (e.g., Rosa *et al.* 2006). To minimise the high metabolic costs associated with resting in these open habitats, they adjust, for example, body postures by altering both the unfeathered appendage area exposed to the surrounding air and the surface-to-volume ratio in a behavioural strategy that seems to be key to adjusting the pattern of heat transfer between their bodies and the environment (Brodsky & Weatherhead 1984; Wiersma & Piersma 1994; Ryeland *et al.* 2017, 2019, 2021). Other (non-mutually exclusive) behaviours include selecting microhabitats that maximise metabolic efficiency, such as resting in wet substrates at high temperatures (Walsberg *et al.* 1993; Wolf & Walsberg 1996; van de Ven *et al.* 2019; Ryeland *et al.* 2021). In addition to these behavioural adjustments, these species may rely on metabolically costly processes such as panting or gular fluttering to regulate their thermal balance in challenging environmental temperatures (T_a) (Bartholomew *et al.* 1968; Amat & Masero 2004; du Plessis *et al.* 2012).

Unfeathered bills, legs and feet are bird appendages that are highly vascularized, and their potential roles in regulating thermal balance is well recognised (e.g., Hagan & Heath 1980; Steen & Steen, 1965; Tattersall *et al.* 2009; 2017; Carr & Lima 2012; Cabello-Vergel *et al.* 2021; Playà-Montmany *et al.* 2021). An appendage's size may vary among populations of the same bird species according to the thermal environment, and it has been suggested, for example, that a larger bill surface area could be an adaptation to increase dry heat loss in hot climatic conditions (Greenberg *et al.* 2012). However, these appendages may also be a source of heat gain for birds living in extremely hot environments, where the environmental temperature (T_a) can approach or surpass the body temperature (T_b), or of heat loss when exposed to cold (Hagan & Heath 1980; Tattersall *et al.* 2009; Greenberg & Danner 2012; Gardner *et al.* 2016), although these aspects of bird thermoregulation are less-known (Gardner *et al.* 2016; van de Ven *et al.* 2016; Ryeland *et al.* 2017, 2019; Playà-Montmany *et al.* 2021).

In the case of shorebirds (Charadrii), the role of these appendages as 'thermal windows' for dry heat exchange may be particularly important, since these birds generally have large relative bill and leg sizes. Thus, for example, shorebirds with smaller legs expend less energy to maintain homeothermy in cold environments than individuals with longer leg lengths (Cartar & Morrison 2005). Within this context, Ryeland et al. (2017, 2019, 2021) using field observations of several shorebirds' species across a wide range of T_a (10-45 °C) shown that thermal behaviour in nonbreeding shorebirds while resting at high tide can be mediated by bill and leg sizes. These studies supported back rest and unipedal posture at high tide as effective strategies for reducing heat loss at low temperatures, while sitting in wet substrates favours body heat loss in hot conditions. They also found evidence for the use of back rest as a strategy to minimise heat gain through the bill at the examined upper temperature limits (Ryeland *et al.* 2017, 2019). In contrast, they did not find support for the use of unipedal standing to insulate against heat gain, although its use at extremely high T_a values cannot be discarded (Ryeland *et al.* 2017, 2019). In this framework, experimental data are needed to test the correlations that predict bird postural adjustments according to T_a.

Here, we experimentally challenged a migratory shorebird with relatively large bill and leg sizes, the Dunlin *Calidris alpina*, with a wide range of T_a values to model behavioural and physiological responses to environmental temperature change, microhabitat use and relative bill al leg sizes while resting. As birds adjust body posture, they adopt heat dissipating/conservating behaviours and select specific microhabitats to maintain thermal homeostasis (Ryeland *et al.* 2017, 2019, 2021; Pavlovic *et al.* 2019). We predicted that (i) Dunlins would reduce the exposed unfeathered area to minimise body heat loss and body heat gain under cold and extremely hot conditions (where T_a approaches T_b), respectively; and (ii) Dunlins would initiate metabolically costly processes, such as panting, only in extremely hot environments. Furthermore, it is well established that one of the strategies used to dissipate body heat and minimise evaporative water loss (EWL) in endotherms is to reduce locomotor activity (Wolf 2000; Thompson *et al.* 2018). Thus, for example, the White-backed mousebird *Colius colius*, the Cape glossy starling *Lamprotornis nitens* and the Sociable weaver *Philetarius socius* decrease their locomotor activity as T_a increases (Thompson *et al.* 2018). We also predicted, therefore, that (iii) Dunlins would decrease their locomotor activity as T_a increased to decrease body heat production. Last, we measured the resting metabolic rate (RMR) and EWL of Dunlins at different T_a values to assess the potential role of relative bill and tarsi sizes in explaining variations in both rates. We expected that individuals with larger relative appendage sizes would be favoured at high T_a values and disadvantaged under cold conditions (Playà-Montmany *et al.* 2021).

Materials and Methods

Bird capture and maintenance

Wintering adult Dunlins were caught using mist nets in Extremadura's rice fields, southwest Spain (39°01'N, 5°58'W), which is a key area for many nonbreeding waterbirds (Masero *et al.* 2011; Navedo *et al.* 2012). After capturing, birds were individually colour-ringed to facilitate further identification and weighed (± 0.01 g). The bill length, width and depth (both measures taken at the anterior edge of the nostrils), tarsus length, width and depth (both taken at the middle of the tarsus) were measured with a digital calliper (± 0.01 mm), while the wing length (flattened and straightened length) was measured using a wing ruler (± 0.5 mm). Eleven individuals showing the highest variability in appendage size were selected for this study (bill length CV = 8.29%; tarsus length CV = 4.27%) and transported to our bird facilities at the University of Extremadura (e.g., Gutiérrez *et al.* 2011). There, the birds were housed in an environmentally controlled room (320 cm × 260 cm × 255 cm), where they were exposed to fluorescent lighting in a 14 h light:10 h dark cycle starting at 7:00 AM. The daylight period was divided into high-tide (from 2:30 PM to 7:30 PM) and low-tide (the remaining light hours) periods simulating a diurnal tide through food availability. Live fly larvae *Protophormia terraenovae* and commercial pellets (Dibaq-Diproteq) were available *ad libitum* in several trays during the "low tide" period, and all food was removed during the "high tide" period (see details below).

The room temperature was set at 10 °C and 8 °C during the day and night, respectively, throughout the acclimation period (five weeks). A large pool (80 cm × 260 cm, 3 cm deep) provided fresh water *ad libitum* for bathing and drinking, and the rest of the ground surface was covered with wet sand. The room was equipped with a one-way window to allow vision through the window only by the observer.

Metabolic measurement protocol

Following the acclimation period, the RMR and EWL were measured at 10 °C, 25 °C and 35 °C during the "high tide" simulation period after 4 hours of fasting to ensure that the birds were in a postabsorptive state (see González-Medina *et al.* 2020). The Dunlins were weighed (± 0.1 g) before and after the metabolic measurements, and the mean body mass (M_b) was used in the analyses. T_b was measured prior to and following metabolic trials by using a calibrated laboratory thermometer (P700, Dostmann electronic GmbH, Wertheim, Germany) attached to a copper–constantan thermocouple inserted 1 cm into the cloaca. A maximum of six individuals were measured at a time. Individuals were randomly exposed to 10 °C or 25 °C using a flow rate of 1000 ml min^{-1} during three trials of 110 min each. Birds were exposed at 35 °C during two trials of 65 min each, and the flow rate was increased up to 3000 ml min^{-1} to ensure that individuals remained calm under the hot conditions (Whitfield *et al.* 2015), which was verified by the use of infrared cameras.

Gas exchange measurements

Oxygen consumption (VO_2) and EWL were measured using an open flow-through respirometry system (Sable Systems) following González-Medina et al. (2020). Briefly, each individual was placed in a polypropylene metabolic chamber inside a compressor-cooled incubator (Memmerts GmbH, Germany). Dry air (<1 kPa WVP) was pumped into the metabolic chamber at a rate of 1000 or 3000 ml min^{-1} using a mass flow controller (MFS, Sable Systems International). The water vapour density (µg ml^{-1}) and O_2 concentration (%) in the excurrent airstream were analysed using an H_2O analyser (RH300, Sable Systems) and an O_2 analyser (FC-10 Oxygen Analyser, Sable Systems), respectively. The RMR and EWL were estimated as the 2 min most stable values at each temperature using Eqs. 10.2 and 10.9, respectively, from Lighton (2008) with a respiratory quotient of 0.70 (Kvist & Lindsröm 2001). Expedata software (version 1.9.14, Sable Systems, Las Vegas, NV, USA) was used to control the multiplexer, record data, and process data for analyses.

Behavioural data collection

Behavioural observations were conducted two weeks after the respirometry measurements to ensure that individuals were re-habituated to captivity and stayed calm. Birds were exposed to each experimental room temperature (10 °C, 15 °C, 20 °C, 25 °C, 30 °C, 35 °C and 38 °C) during a single daylight period and then exposed to T_a the next day. Each experimental T_a was settled at 7:00 AM, i.e., 7.5 h before the resting period, and ended at 9:00 PM. The room temperature at night was kept 5 °C lower than the experimental temperature tested the following daylight period. There were variations between the experimental temperature set for the room and the temperature that the Dunlins experienced near the ground surface. Thus, as an approximation of the temperature experienced by birds on the ground, we measured the air temperature at Dunlin height, i.e., 2 cm above water and 5 cm above ground level, every 2 min using HOBO Micro Station Data Loggers H21-002 (Onset Computer Corporation, Bourne, Massachusetts, USA). We also recorded the water temperature (°C; 1 cm upper layer) and wet sand temperature (°C; 1 cm upper layer). The mean T_a above water and wet sand differed by 0.57±0.15 °C on average; thus, the mean value was used in posterior analyses (see below). The relative humidity ranged from 75% to 90% throughout the observational trials, and the birds did not experience air movement.

Focal behavioural observations were conducted during the high-tide period. These started at 3:30 PM, i.e., one hour after the food was removed, to allow the birds time to recover from the disturbance caused by entering the room. Each individual was observed continuously during a period of five minutes every 20 min, leading to a total of four observation bouts of 5 min each (20 min of focal observations) per individual at each T_a. Repeated observations were considered in the analyses (see below). Observations were conducted by a single researcher (NPM) through the one-way window using 10×42 binoculars. The order of observation of focal individuals was randomly chosen at the beginning of the observation period and was maintained during the following observations.

Although shorebirds usually rest during the high-tide period (no food available), individuals can be active, showing locomotion (walking) and preening behaviours. We considered that an individual was resting once it remained inactive for > 60 s. In each resting posture, we noted whether the bird was standing on one leg, standing on both legs or sitting. The bill position was noted as back rest (the bill was tucked within the back plumage) or not. We also noted panting behaviour (defined as gaping when breathing; Smit *et al.* 2016) (bill open for ≥ 5 s, see Oswald *et al.* 2019), as well as the substrate on which the Dunlins were resting (wet sand or water). We quantified the times that each individual was engaged in each behaviour and located on each substrate.

Data analysis

Bill and tarsus measurements were converted to surface area estimates following Greenberg et al. (2012). We used equations to approximate the bill surface area as an elliptical cone and the tarsi surface area as an elliptical cylinder (see equations in Greenberg *et al.* 2012). Relative bill and tarsi surface areas were calculated as the residuals of a linear regression of the bill or tarsi surface areas using the wing length (mm) as a proxy for body size (log-transformed data) (see Playà-Montmany *et al.* 2021).

Factors influencing the proportion of time that the birds exhibited back rest, unipedal posture, sitting and panting behaviours were assessed by fitting generalised linear mixed models (GLMMs) with a binomial response and logit-link function (fitted by the maximum likelihood with Laplace approximation). This calculation treated each minute of observation as a 'presence' (for example, a bird in a back rest posture) or 'absence' (a bird with the bill exposed) (see Ryeland *et al.* 2017, 2019, 2021). We modelled each behaviour by including T_a as a predictor, M_b (log-transformed) and relative bill and tarsi surface areas as covariates, and the bird identity and observation period as random factors. The global model for unipedal posture also included the substrate (two values: wet sand and water) as a predictor because it could affect the body posture (Ryeland *et al.* 2021). In the model for sitting behaviour, we did not include the substrate as a predictor because individuals only used wet sand for this behaviour. All explanatory variables were standardised prior to analysis. The quadratic term of T_a was included in models where preliminary analyses and previous studies (Ferns 1992; Ryeland *et al.* 2021) showed a quadratic relation between T_a and body posture.

The influence of T_a on the proportion of time that birds were active during the high tide period was also examined by performing a GLMM with a binomial response and logit-link function. We included the same predictors, excluding the relative bill and tarsi surface areas. M_b was included in this analysis because previous studies showed that it can influence behavioural thermoregulation (Ryeland *et al.* 2017, 2019, 2021; Pattinson *et al.* 2020).

The potential relationships between physiological thermoregulatory and morphological traits at 10 °C, 25 °C and 35 °C were analysed by fitting GLMMs, where RMR or EWL were the response variables, T_a, M_b, relative bill and tarsi surface areas were included as covariates, and individual identity was included as a random factor.

Potential collinearity among predictor variables in the global models was evaluated by calculating the variance inflation factor (VIF) using the 'car' package (Fox & Weisberg 2019). All VIF values were <5, supporting the absence of collinearity (Zuur *et al.* 2010). We first built global models using the 'lme4' package (Bates *et al.* 2014) for each analysis. Model selection was performed based on the Akaike information criterion for small sample sizes (AIC_c) to identify the top model(s) (all models with $\Delta AIC_c < 2$) and AICc weights (w_i) to further distinguish between the top models (Burnham & Anderson 2002). We used the 'dredge' function in the R package MuMIn (Barton 2018) for this procedure. For cases in which more than one model had ΔAICc < 2 but $w_i < 0.9$ (Burnham & Anderson 2002), we performed model averaging of parameter estimates (Grueber *et al.* 2011). A predictor was considered significant when the 95% confidence interval (CI) for the estimated coefficient did not overlap zero. Statistical analyses were conducted in R 4.0.2 (R Core Team, 2014), and all figures were produced using the R package 'ggplot2' (Wickham 2016).

Results

Overall, all behaviours were strongly predicted by T_a (Table 1). Both linear and quadratic terms of T_a were significant for the back rest, standing on one leg, sitting and bird activity models (Table 2). Birds increased their time spent in back rest and standing on one leg with increasing T_a values until they were exposed to 30.67 ± 0.03 °C on average. From this temperature value onwards, the use of both resting postures decreased (Figure 1a-b). Wet-sitting was mainly used above 30.67 ± 0.03 °C, after which point its use increased linearly, achieving 100% at the maximum T_a (36.52 ± 0.23 °C) (Figure 1c). Locomotor and preening activities at high tide strongly decreased from 22.03 ± 0.04 °C onwards (Figure 1d), with birds remaining active less than 5% of time above 34.81 ± 0.14 °C.

M_b significantly explained the variation in unipedal resting, sitting and locomotor activity (Table 1). The relative bill surface area and relative tarsi surface area were included in the top model explaining back rest and unipedal resting, respectively (Table 1), but none of the morphological traits had a significant effect (Table 2). Substrate had a significant effect on unipedal resting behaviour (Table 1, 2), with Dunlins more frequently using this behaviour while resting in water (β = 2.66, CI= 2.16, 2.36) than in wet sand (β =0.60, CI= 0.21, 1.00).

The final averaged model describing the use of panting included, in addition to T_a, the relative tarsi surface area and M_b (Table 1), but only T_a was significant (Table 2). Panting exclusively occurred (15.55 ± 5.24%) when the room temperature was 38 °C (36.52 ± 0.23 °C at the ground level).

Variations in RMR and EWL were not explained by the relative bill or tarsi surface area (Table 1). T_a had a significant and negative effect on the RMR (Table 2). M_b was also included in the best-fitting model explaining RMR variation, but it was not a significant predictor (Table 2). The null model was the best-fitting model for EWL (Table 1).

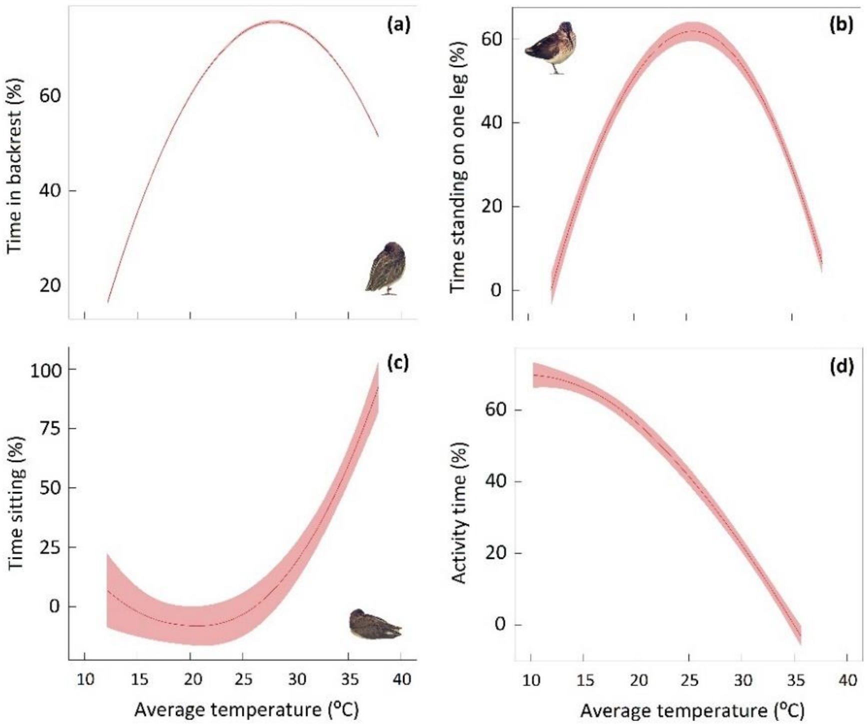

Figure 1 Model predictions for the percentage of time that Dunlins spent in (a) back rest, (b) standing on one leg (unipedal resting), (c) sitting and (d) active in Dunlins while resting in relation to average temperature (°C).

Table 1. Top-ranked candidate models explaining behavioural thermoregulation and physiological traits in dunlins at high tide (resting period). Models were selected using the Akaike Information Criterion with a correction for small samples (AICc). Only models with ΔAICc < 2 are shown.

Model	df	logLik	AICc	ΔAICc	w_i	R^2
Back rest						
$T_a + T_a^2$	5	-701.96	1414.10	0.00	0.37	0.41
$T_a + T_a^2$ + Bill index	6	-701.78	1415.90	1.72	0.16	0.41
Panting						
T_a	4	-40.59	89.30	0.00	0.30	0.55
$T_a + M_b$	5	40.04	90.30	0.98	0.18	0.55
$T_a + M_b$ + Tarsi index	6	-39.33	91.00	1.65	0.13	0.55
T_a + Tarsi index	5	-40.40	91.00	1.69	0.13	0.55
Unipedal						
$T_a + T_a^2$ + Substrate	6	-547.17	1106.60	0.00	0.32	0.78
$T_a + T_a^2$ + Substrate + Tarsi index	7	-546.86	1108.10	1.50	0.15	0.78
$T_a + T_a^2$ + Substrate + M_b	7	-546.97	1108.40	1.72	0.14	0.78
Sitting						
$T_a + T_a^2$	5	-233.29	476.80	0.00	0.34	0.97
$T_a + T_a^2 + M_b$	6	-232.79	477.90	1.09	0.20	0.97
Activity						
$T_a + T_a^2$	5	-488.13	986.50	0.00	0.62	0.79
$T_a + T_a^2 + M_b$	6	-487.56	987.40	0.95	0.38	0.79
RMR						
$T_a + M_b$	5	37.08	-61.90	0.00	0.71	0.79
T_a	4	34.73	-60.00	1.91	0.27	0.69
EWL						
Null	3	21.55	-36.30	0.00	0.86	0.00

Table 2. Model-averaged parameter estimates (± SE) for predictors and 95% confidence intervals (CI) of thermoregulatory behaviours and physiological traits in dunlins at high tide (resting period).

Model	Estimate	CI (95 %)	SE
Back rest			
Intercept	1.01	0.56, 1.46	0.23
T_a	0.51	0.35, 0.66	0.08
T_a^2	-0.83	-1.02, -0.64	0.10
Bill index	0.03	-0.16, 0.22	0.10
Panting			
Intercept	93.75	-150.36, -37.15	28.75
T_a	61.26	22.02, 100.51	19.94
M_b	1.24	-3.02, 5.50	2.17
Tarsi index	0.60	-2.24, 3.44	1.45
Unipedal			
Intercept	0.60	0.21, 1.00	0.20
T_a	0.23	0.06, 0.41	0.09
T_a^2	-1.55	-1.76, -1.34	0.12
Substrate Water	2.06	1.68, 2.43	0.19
Tarsi index	0.02	-0.11, 0.16	0.07
M_b	-0.02	-0.13, 0.10	0.06
Sitting			
Intercept	-8.15	-9.91, -6.39	0.89
T_a	4.28	3.10, 5.46	0.60
T_a^2	2.79	2.08, 3.50	0.36
M_b	0.21	-0.66, 1.09	0.44
Activity			
Intercept	-1.21	-1.81, -0.61	0.31
T_a	-1.79	-2.05, -1.54	0.13
T_a^2	-0.67	-0.87, -0.47	0.10
M_b	0.10	-0.30, 0.51	0.20
RMR			
Intercept	0.29	0.26, 0.32	0.01
T_a	-0.11	-0.13, -0.08	0.01
M_b	0.04	-0.01, 0.09	0.03

Discussion

Thermoregulation plays a major role in organism homeostasis. When exposed to extreme T_a, endotherms adjust body heat production and heat interchange through behavioural and physiological mechanisms. Among the behavioural strategies used to dissipate body heat at high T_a, our experimental data showed that Dunlins dealt with high T_a values during the daily resting period by using specific body postures, substrate selection and panting. Our data also suggested that Dunlins minimised body heat production at high T_a values by decreasing locomotor activity, being inactive most of the time at T_a > 30 °C. However, during cold exposure, Dunlins only seemed to rely on heat production by maintaining high levels of locomotor activity (our model predicted Dunlins to spend > 60% of time active in cold conditions). Intraspecific variations in bill and leg surface areas did not explain either body posture adjustments or the RMR and EWL.

Dunlins, like other birds inhabiting open habitats at temperate latitudes, experience cold winters with commonly high-speed winds, the latter of which greatly contributes to increased body heat loss by forced convection (Wiersma & Piersma 1994). Wintering in temperate latitudes should, therefore, impose the need to implement behavioural and physiological strategies to maintain T_b (e.g., Wolf 2000; Ryeland *et al.* 2017, 2019, 2021; Cooper *et al.* 2019). Shorebirds have previously been shown to consistently display body postural adjustments to minimise body heat loss at low T_a values (see Ryeland *et al.* 2017, 2019). However, we found that Dunlins used back rest and unipedal resting less than expected when exposed to temperatures below the lower critical value of the thermoneutral zone (19.8 °C according to Kelly & Weathers 2002). In the absence of wind near the ground level, captive Dunlins did not experience heat loss by forced convection (wind), and they seemed to be able to cope with lower temperatures (12 °C on average) mainly by increasing heat production through locomotor activity. Most shorebirds roost communally in flocks ranging from tens to thousands of birds, and in windy cold environments, they can reduce heat loss by flocking and facing the wind (Wiersma & Piersma 1994). However, it has also been shown that shorebirds such as the red knot *Calidris canutus* can compensate for thermoregulation costs at low temperatures by using heat generated as a by-product of walking or running (Bruinzeel & Piersma 1998), and presumably, flight would have a similar or stronger effect (Rogers *et al.* 2006). Our findings confirmed this large compensation to maintaining homeothermy by using locomotor activity in cold and windless environments. Last, when remaining inactive in cold conditions, Dunlins barely used unipedal resting or sitting (see Figure 1b-c), suggesting bipedal standing as the main body posture adopted under cold conditions. Even unipedal resting, when used, was mainly adopted in water, which suggests that birds select favourable microhabitats to reduce the energetic costs of thermoregulation. The thermal conductance of wet sand is higher than that of water and increases with increasing humidity content (Monteith & Unsworth 1990). Thus, resting in water suggests reduced body heat transfer favouring heat savings.

At temperatures within thermoneutrality (e.g., from 20 °C to 30 °C), no additional energy or water is allocated for T_b maintenance (Wiersma & Piersma 1994); thus, non-thermoregulatory responses should be expected within this range of T_a. We found Dunlins standing on one leg and tucking the bill while exposed to thermoneutral conditions. Back rest is commonly adopted by several shorebird species, including Dunlins, while resting or sleeping at high tide (e.g., Klassen 1990; Dominguez 2003). Previous studies conducted with the flamingo *Phoenicopterus ruber*, for example, showed unipedal resting to be a less energetically demanding posture that favours muscle relaxation and body balance (see Chang & Ting 2017). Thus, within the thermoneutral zone, a back rest posture and unipedal resting could have been selected by Dunlins as being more comfortable for resting (Klaassen 1990; Dominguez 2003; Chang & Ting 2017).

At high T_a values (>35 °C), Dunlins increased the time of bill exposure, as this may favour body heat dissipation by radiation. This result is analogous to that found by Ryeland et al. (2017), in which shorebirds reduced their back rest behaviour at high T_a values to favour heat flux into the environment. In addition to adjusting their bill position, as T_a increased, Dunlins remained sitting in wet sand most of the time, which is a previously observed behaviour known as 'wet-sitting' (see Ryeland *et al.* 2021). Previous studies with wild shorebirds highlighted the importance of sitting in wet substrates under heat stress, as this is an effective mechanism to avoid hyperthermia (Battley *et al.* 2003; Rogers *et al.* 2006; Ryeland *et al.* 2021). Ryeland et al. (2021), for example, showed that several coastal shorebird species spent more time wet-sitting at high tide when roosting at ~30 °C. By selecting this microhabitat and body posture, shorebirds may favour body heat loss by conduction across the leg surface and the lower body, as both surfaces directly contact the wet substrate (e.g., Ferns 1992; Ryeland *et al.* 2021). Sitting can also be less energetically expensive than standing, contributing to the balance of energy budgets under these conditions (Tickle *et al.* 2012; Pavlovic *et al.* 2019). The maximum temperature registered on the surface of the wet sand inside the room was ~37 °C, which was lower than the core T_b (~39 °C) measured in Dunlins when exposed to 35 °C inside the metabolic chambers.

Therefore, the thermal gradient (T_a-T_b) between the wet substrate and the body would allow dry heat transfer from the body to the wet sand when sitting, reducing the body heat burden of the birds (Rogers *et al.* 2006; Ryeland *et al.* 2021). At the highest T_a value, this gradient should have been minimised, and Dunlins additionally dissipated heat by using panting (forced evaporative water loss) (Amat & Masero 2004; McKechnie & Wolf 2019) while wet-sitting. Models predicting panting/gular flutter behaviours in arid-zone bird species found that panting (behavioural response present in 50% of observations) occurred at ~37 °C and ~41 °C in drinking and nondrinking species, respectively (Smit *et al.* 2016). Our experimental birds had access to freshwater *ad libitum*, and they started to use this avian respiratory heat dissipation behaviour at ~37 °C, supporting model predictions for drinking species. Finally, we did not observe heat-avoidance behaviours such as ptiloerection (raising of the 'back' feathers) and wing-dropping (defined as holding the wings away from the body), which have both been described in small-sized wild shorebirds (Amat & Masero 2004; Battley *et al.* 2003). Feather erecting may increase convective or evaporative cooling (Battley *et al.* 2003), while wing-dropping could be a mechanism to increase the surface area of the body to enhance radiative and convective dry heat loss by exposing thermal windows under the wing (Smit *et al.* 2016). The absence of ground-level wind inside the room could explain why Dunlins did not use both heat-avoidance behaviours.

Inactivity is response shared among a large fraction of the world's avifauna to minimise the impacts of heat stress (e.g., Wolf 2000; Davies 1982; Silva *et al.* 2015; Cooper *et al.* 2019), which we know mainly from studies performed in passerine species from arid habitats and Mediterranean climates (Kelly *et al.* 2004; Thompson *et al.* 2018; Cooper *et al.* 2019). However, although this thermoregulatory response to thermal stress has been largely overlooked in non-passerine species such as shorebirds, our results indicated that changes in locomotor activity are a common response used to overcome thermoregulatory challenges, as Dunlins adjust locomotor activity to increase or minimise metabolic heat production at low and high T_a values, respectively. Inevitably, some of these thermoregulatory behaviours involve trade-offs with other fitness-improving activities, such as antipredator behaviours or foraging (du Plessis *et al.* 2012). For example, the time allocated to sitting cannot be spent being alert to predators (Ryeland *et al.* 2017, 2019; Timmis *et al.* 2022), which makes sitting individuals much more vulnerable (Ryeland *et al.* 2017, 2019; Timming *et al.* 2022). These constraints associated with thermal behaviours can be accentuated by the current global warming, which forces birds to spend longer periods of time adopting behavioural strategies to alleviate thermal stress.

We found no significant influence of relative appendage sizes on either RMR or EWL. This absence of significant effects of bill and leg sizes on thermal physiological traits and thermoregulatory behaviours contrasts with the results shown by previous comparative studies (e.g., Smit *et al.*, 2016; Ryeland *et al.* 2017, 2019, 2021; Thompson *et al.* 2018; Pattinson *et al.* 2020). These studies involved several species that displayed enormous variation in morphological trait sizes, which could explain the lack of these significant relationships in our single-species study (e.g., Ryeland *et al.* 2017, 2019, 2021; Pavlovic *et al.* 2019; Pattinson *et al.* 2020). For example, the CV obtained by Ryeland et al. (2019) for tarsus length using many shorebird species was approximately 53%, while in our Dunlin sample it was ~4%. Therefore, this circumstance could explain the lack of explanatory power of the appendage sizes in explaining variation in the use of thermoregulatory behaviours and physiological traits.

In conclusion, we provided a better understanding of the physiological and behavioural responses to thermal stress in a small bird species inhabiting open landscapes. Our findings indicated that captive Dunlins advocated for behavioural strategies that included body postural adjustments, microhabitat selection and locomotor activity to defend T_b under challenging T_a values. In hot environmental conditions, Dunlins used thermoregulatory behaviours that strongly favoured conductive (sitting) and radiative (bill exposition) dry heat transfer from the body to the surroundings, while in cold environments, individuals remained active for longer periods of time to favour metabolic heat production. Our study showed that panting was only performed at the highest T_a values, supporting that the birds favoured behavioural responses over this costly physiological response. Unexpectedly, relative bill and leg sizes were reported to be unrelated to thermoregulatory behaviours and physiological traits, probably due to the low intraspecific variability. Last, previous studies (Ryeland *et al.* 2020) supported the importance of wetland margin substrate in the thermoregulation of several shorebird species, as the time spent sitting was significantly mediated by the substrate upon which they roosted. Our experimental findings emphasise the positive role of the substrate type, such as wet sand, in minimising heat stress in shorebirds, which is remarkably relevant to shorebirds, as they face a reduction in wetland habitat availability along with increasing T_a values due to global warming (Ryeland *et al.* 2020).

References

Amat, J. A. & Masero, J. A. (2004) How Kentish plovers, Charadrius alexandrinus, cope with heat stress during incubation. Behavioral Ecology and Sociobiology 56(1), 26-33.

Bartholomew, G. A., Lasiewski, R. C. & Crawford, E. C. (1968) Patterns of panting and gular flutter in cormorants, pelicans, owls, and doves. The Condor 70(1), 31-34.

Barton, K (2018) MuMIn: multi-model inference. R package. Cran-R 1: 289-290.

Bates, D., Mächler, M., Bolker, B. & Walker, S. (2014) Fitting linear mixed-effects models using lme4. arXiv preprint arXiv:1406.5823

Battley, P. F., Rogers, D. I., Piersma, T., & Koolhaas, A. (2003) Behavioural evidence for heat-load problems in Great Knots in tropical Australia fuelling for long-distance flight. Emu-Austral Ornithology 103(2), 97–103.

Brodsky, L. M. & Weatherhead, P. J. (1984) Behavioural thermoregulation in wintering black ducks: roosting and resting. Canadian Journal of Zoology 62(7), 1223–1226.

Bruinzeel, L. W. & Piersma, T. (1998) Cost reduction in the cold: heat generated by terrestrial locomotion partly substitutes for thermoregulation costs in Knot Calidris canutus. Ibis 140(2): 323-328.

Burnham, K. P. & Anderson, D. R. (2002) Model selection and multimodel inference: A practical information-theoretic approach. Springer.

Calder, W. A. (1968) The diurnal activity of the Roadrunner, Geococcyx californianus. The Condor 70(1), 84-85.

Cabello-Vergel, J., Soriano-Redondo, A., Villegas, A., Masero, J. A., Sánchez-Guzmán, J. M. & Gutiérrez, J. S. (2021) Urohidrosis as an overlooked cooling mechanism in long-legged birds. Scientific Reports 11(1), 1-11.

Carr, J. M. & Lima, S, L. (2012) Heat-conserving postures hinder escape: a thermoregulation–predation trade-off in wintering birds. Behavioral Ecology 23(2), 434-441.

Cartar, R. V. & Guy, Morrison, R. I. (2005) Metabolic correlates of leg length in breeding arctic shorebirds: the cost of getting high. Journal of Biogeography 32(3), 377-382.

Chang, Y. H. & Ting, L. H. (2017) Mechanical evidence that flamingos can support their body on one leg with little active muscular force. Biology Letters 13(5), 20160948.

Cooper, C. E., Withers, P. C., Hurley, L. L. & Griffith, S. C. (2019) The Field Metabolic Rate, Water Turnover, and Feeding and Drinking Behavior of a Small Avian Desert Granivore During a Summer Heatwave. Frontiers in Physiology 10, 1405.

Davies, S. J. J. F. (1982) Behavioural adaptations of birds to environments where evaporation is high and water is in short supply. Comparative Biochemistry and Physiology Part A: Physiology, 71(4), 557–566.

Dominguez, J. (2003) Sleeping and vigilance in Black-tailed Godwit. Journal of Ethology, 21(1), 57–60.

du Plessis, K. L., Martin, R. O., Hockey, P. A., Cunningham, S. J. & Ridley, A. R. (2012) The costs of keeping cool in a warming world: implications of high temperatures for foraging, thermoregulation and body condition of an arid-zone bird. Global Change Biology 18(10), 3063-3070.

Ferns, P. N. (1992) Thermoregulatory behavior of rock doves roosting in the Negev Desert. Journal of Field Ornithology 57-65.

Fox, J. & Weisberg, S. (2019) An R Companion to Applied Regression. Sage, ThousandOaks CA, 3rd edition.

Gardner, J. L., Symonds, M. R., Joseph, L., Ikin, K., Stein, J. & Kruuk, L. E. (2016) Spatial variation in avian bill size is associated with humidity in summer among Australian passerines. Climate Change Responses 3(1), 1-11.

González-Medina, E., Cabello-Vergel, J., Playà-Montmany, N., Villegas, A., Parejo, M., Abad-Gómez, J. M., Sánchez-Guzmán, J. M. & Masero, J. A. (2020) Going to sleep with a full belly: Thermal substitution by specific dynamic action in shorebirds. Comparative Biochemistry and Physiology Part A: Molecular & Integrative Physiology 244, 110689.

Greenberg, R. & Danner, R. M. (2012) The influence of the California marine layer on bill size in a generalist songbird. Evolution: International Journal of Organic Evolution 66(12), 3825-3835.

Greenberg, R., Cadena, V., Danner, R. M. & Tattersall, G. (2012) Heat loss may explain bill size differences between birds occupying different habitats. PLoS ONE 7(7), 1–9.

Grueber, C. E., Nakagawa, S., Laws, R. J. & Jamieson, I. G. (2011) Multimodel inference in ecology and evolution: Challenges and solutions. Journal of Evolutionary Biology 24(4), 699–711.

Gutiérrez, J. S., Masero, J. A., Abad-Gómez, J. M., Villegas, A & Sánchez-Guzmán, J. M. (2011) Metabolic consequences of overlapping food restriction and cell-mediated immune response in a long-distance migratory shorebird, the little ringed plover Charadrius dubius. Journal of Avian Biology 42(3), 259-265.

Gutiérrez, J. S., Soriano-Redondo, A., Dekinga, A., Villegas, A., Masero, J. A. & Piersma, T. (2015) How salinity and temperature combine to affect physiological state and performance in red knots with contrasting non-breeding environments. Oecologia 178(4), 1077-1091.

Hagan, A. A. & Heath, J. E. (1980) Regulation of heat loss in the duck by vasomotion in the bill. Journal of Thermal Biology 5(2), 95–101.

Kelly, A., Godley, B. J. & Furness, R. W. (2004) Magpies, pica pica, at the southern limit of their range actively select their thermal environment at high ambient temperatures. Zoology in the Middle East 32(1), 13–26.

Kelly, J. P. & Weathers, W. W. (2002) Effects of feeding time constraints on body mass regulation and energy expenditure in wintering dunlin (Calidris alpina). Behavioral Ecology 13,766-775.

Klaassen, M. (1990) Short note on the possible occurrence of heat stress in roosting waders on the Banc d'Arguin, Mauritania. Ardea 78(1–2), 63–65.

Kvist, A. & Lindström, Å. (2001) Basal metabolic rate in migratory waders: intra-individual, intraspecific, interspecific and seasonal variation. Functional Ecology 15(4), 465-473.

Lighton J. R. B. (2008) Measuring Metabolic Rates: A Manual for Scientists. Oxford University Press Inc New York.

Luskick, S., Battersby, B. & Kelty, M. (1978) Behavioral thermoregulation: orientation toward the sun in herring gulls. Science 200(4337), 81-83.

Masero, J. A., Santiago-Quesada, F., Sánchez-Guzmán, J. M., Villegas, A., Abad-Gómez, J. M., Lopes, R. J., Encarnação, V., Corbacho, C. & Morán R (2011) Long lengths of stay, large numbers, and trends of the Black-tailed Godwit Limosa limosa in rice fields during spring migration. Bird Conservation Internaional 21(1), 12–24.

McKechnie, A. E. & Wolf, B. O. (2019) The physiology of heat tolerance in small endotherms. Physiology 34(5), 302-313.

Monteith, J. & Unsworth, M. (2013) Principles of environmental physics: plants, animals, and the atmosphere. Academic Press.

Navedo, J. G., Masero, J. A., Sánchez-Guzmán, J. M., Abad-Gómez, J. M., Gutiérrez, J. S., Sansón, E. G., Villegas, A., Costillo, E., Corbacho, C., & Morán, R. (2012) International importance of Extremadura, Spain, for overwintering migratory dabbling ducks: A role for reservoirs.

Bird Conservation International 22(3), 316–327.

Oswald, K. N., Smit, B., Lee, A. T. & Cunningham, S. J. (2019) Behaviour of an alpine range-restricted species is described by interactions between microsite use and temperature. Animal Behavior 157, 177-187.

Pattinson, N. B., Thompson, M. L., Griego, M., Russell, G., Mitchell, N. J., Martin, R. O., Wolf, B. O., Smit, B., Cunningham, S. J., McKechnie, A. E. & Hockey, P. A. (2020) Heat dissipation behaviour of birds in seasonally hot arid-zones: are there global patterns? Journal of Avian Biology 51(2), 1–11.

Pavlovic, G., Weston, M. A. & Symonds, M. R. E. (2019) Morphology and geography predict the use of heat conservation behaviours across birds. Functional Ecology 33(2), 286–296.

Playà-Montmany, N., González-Medina, E., Cabello-Vergel, J., Parejo, M., Abad-Gómez, J. M., Sánchez-Guzmán, J. M., Villegas, A. & Masero, J. A. (2021) The thermoregulatory role of relative bill and leg surface areas in a Mediterranean population of Great tit (*Parus major*). Ecology and Evolution 11(22), 15936-15946.

Rogers, D. I., Piersma, T. & Hassell, C. J. (2006) Roost availability may constrain shorebird distribution: Exploring the energetic costs of roosting and disturbance around a tropical bay. Biological Conservation 133(2), 225–235.

Rosa, S., Encarnaçao, A. L., Granadeiro, J. P. & Palmeirim, J. M. (2006) High water roost selection by waders: maximizing feeding opportunities or avoiding predation?. Ibis 148(1): 88-97.

Ryeland, J., Weston, M. A. & Symonds, M. R. (2017) Bill size mediates behavioural thermoregulation in birds. Funct Ecol 31(4): 885–893.

Ryeland, J., Weston, M. A. & Symonds, M. R. (2019) Leg length and temperature determine the use of unipedal roosting in birds. Journal of Avian Biology 50(5), 1–9.

Ryeland, J., Weston, M. A. & Symonds, M. R. (2021) The importance of wetland margin microhabitat mosaics; the case of shorebirds and thermoregulation. Journal of Applied Ecology 58(2), 382–391.

Silva, J. P., Catry, I., Palmeirim, J. M. & Moreira, F. (2015) Freezing heat: Thermally imposed constraints on the daily activity patterns of a free-ranging grassland bird. Ecosphere 6(7)

Smit, B., Zietsman, G., Martin, R. O., Cunningham, S. J., McKechnie, A. E. & Hockey, P. A. R. (2016) Behavioural responses to heat in desert birds: implications for predicting vulnerability to climate warming. Climate Change Responses 3(1), 1–14.

Steen, I. & Steen, J. B. (1965) The Importance of the Legs in the Thermoregulation of Birds. Acta Physiologica Scandinavica 63(3), 285–291.

Tattersall, G. J., Andrade, D. V. & Abe, A. S. (2009) Heat exchange from the toucan bill reveals a controllable vascular thermal radiator. Science 325(5939), 468–470.

Tattersall, G. J., Arnaout, B. & Symonds, M. R. (2017) The evolution of the avian bill as a thermoregulatory organ. Biological Reviews 92(3), 1630–1656.

Thompson, M. L., Cunningham, S. J. & McKechnie, A. E. (2018) Interspecific variation in avian thermoregulatory patterns and heat dissipation behaviours in a subtropical desert. Physiology & Behavior 188, 311–323.

Tickle, P. G., Nudds, R. L. & Codd, J. R. (2012) Barnacle Geese Achieve Significant Energetic Savings by Changing Posture. PLoS ONE 7(10), 1–4.

Tieleman, B. I., Williams, J. B. & Buschur, M. E. (2002) Physiological adjustments to arid and mesic environments in larks (Alaudidae). Physiological and Biochemical Zoology 75(3), 305-313.

van de Ven, T. M. F. N., Martin, R. O., Vink, T. J. F., McKechnie, A. E. & Cunningham, S. J. (2016) Regulation of heat exchange across the hornbill beak: functional similarities with toucans?. PLoS One 11(5), e0154768.

van de Ven, T. M., McKechnie, A. E. & Cunningham, S. J. (2019) The costs of keeping cool: behavioural trade-offs between foraging and thermoregulation are associated with significant mass losses in an arid-zone bird. Oecologia 191(1): 205-215.

Walsberg, G. E. (1993) Thermal consequences of diurnal microhabitat selection in a small bird. Ornis Scandinavica 174-182.

Whitfield, M. C., Smit, B., McKechnie, A. E. & Wolf, B. O. (2015) Avian thermoregulation in the heat: scaling of heat tolerance and evaporative cooling capacity in three southern African arid-zone passerines. The Journal of Experimental Biology 218(11): 1705-1714.

Wickham, H. (2016) Programming with ggplot2. In ggplot2 (pp. 241-253). Springer, Cham.

Wiersma, P. & Piersma, T. (1994) Effects of microhabitat, flocking, climate and migratory goal on energy expenditure in the annual cycle of red knots. The Condor 96(2), 257–279.

Wolf, B. (2000) Global warming and avian occupancy of hot deserts; a physiological and behavioral perspective. Revista Chilena de Historia Natural 73, 395-400.

Wolf, B. O. & Walsberg, G. E. (1996) Thermal effects of radiation and wind on a small bird and implications for microsite selection. Ecology 77(7), 2228-2236.

Zuur, A. F., Ieno, E. N. & Elphick, C. S. (2010) A protocol for data exploration to avoid common statistical problems. Methods in Ecology and Evolution 1(1), 3-14.

4

The thermoregulatory role of relative bill and leg surface areas in a Mediterranean population of Great tit (*Parus major*)

Núria Playà-Montmany, Erick González-Medina, Julián Cabello-Vergel, Manuel Parejo, José M. Abad-Gómez, Juan M. Sánchez-Guzmán, Auxiliadora Villegas and José A. Masero

Ecology and Evolution (2021) 11 (22), 15936-15946

Abstract

There is growing evidence on the role of legs and bill as 'thermal windows' in birds coping with heat stress. However, there is a lack of empirical work examining the relationship between the relative bill and/or leg surface areas and key thermoregulatory traits such as the limits of the thermoneutral zone (TNZ) or the cooling efficiency at high temperatures. Here, we explored this relationship in a Mediterranean population of Great tit (*Parus major*) facing increasing thermal stress in its environment. The lower and upper critical limits of the TNZ were found to be 17.7 ± 1.6°C and 34.5 ± 0.7°C, respectively, and the basal metabolic rate was 0.96 ± 0.12 ml O_2 min^{-1} on average. The evaporative water loss (EWL) inflection point was established at 31.85 ± 0.27°C and was not significantly different from the value of the upper critical limit. No significant relationship was observed between the relative bill or tarsi size and TNZ critical limits, breadth, mass-independent VO_2 or mass-independent EWL at any environmental temperature (from 10°C to 40°C). However, Great tit males (but not females) with larger tarsi areas (a proxy of leg surface area) showed higher cooling efficiencies at 40°C. We found no support for the hypothesis that the bill surface area plays a significant role as a thermal window in Great tits, but the leg surface areas may play a role in males' physiological responses to high temperatures. On the one hand, we argue that the studied population occupies habitats with available microclimates and fresh water for drinking during summer, so active heat dissipation by EWL might be favored instead of dry heat loss through the bill surface. Conversely, male dominance behaviors could imply a greater dependence on cutaneous evaporative water loss through the upper leg surfaces as a consequence of higher exposure to harsh environmental conditions than faced by females.

Keywords: thermoregulation, bill size, leg size, evaporative water loss, metabolic rate, Great tit

Introduction

The bill and legs of birds are multifunctional appendages that are involved in well-known roles with direct fitness costs such as foraging or locomotion (e.g., Moreno & Carrascal 1993, Tattersall *et al.* 2017). Both appendages also become key regions in body thermoregulation due to their contribution to heat and water balances, roles that have been emphasized by studies using thermographic images (e.g., Tattersall *et al.* 2009; Greenberg *et al.* 2012; Friedman *et al.* 2019). Illustrative examples are the Toco Toucan *Ramphastos toco*, which can lose up to 60% of its total body heat through its bill (Tattersall *et al.* 2009), and herons and gulls, which increase their heat loss through their legs as the ambient temperature increases (Steen & Steen 1965). This role of the bill and legs as 'thermal windows' relies on the vascular network located under the skin; this network allows body heat dissipation via radiation and convection (e.g., Steen & Steen 1965; Hagan & Heath 1980; Tattersall *et al.* 2009; Symonds & Tattersall 2010). Due to the anatomical differences between the vascular systems providing blood supply to the legs and bill (a countercurrent system in the legs and a more random and ramified vascular arrangement in the bill; Hagan & Heath 1980; Midtgård 1981; Arad *et al.* 1989; Tattersall *et al.* 2012), the relative importance of each appendage in a bird's ability to cope with thermal stress may be different (Symonds & Tattersall 2010; Tattersall *et al.* 2012; Winder *et al.* 2020). At 35°C, four species of Darwin's finches, for example, lost dry heat through their bills, while their legs became areas of heat gain (see Tattersall *et al.* 2018).

A growing number of studies have documented body size changes − including bill and leg lengths − across diverse bird taxa in response to global warming (e.g., Yom-Tov 2001; Gardner *et al.* 2011; Sheridan & Bickford 2011; Campbell-Tennant *et al.* 2015), but the underlying physiological mechanisms responsible for these changes remain poorly understood. According to 'Allen's rule' (Allen 1877), birds from warm climates tend to have larger appendages relative to their body size than those from colder climates; this feature of birds from warm climates may favor body heat dissipation in hot environments. Thus, having relatively large unfeathered appendages could increase birds' thermal tolerance (Gardner *et al.* 2016), which is becoming critically more necessary due to the increases in the frequency, severity and duration of extreme heat events (McKechnie & Wolf 2019; Stillman 2019). In this context, interest in the role of bill and leg surface areas − especially bill size − as effective mechanisms of dry heat dissipation has increased in recent years (e.g., Tattersall *et al.* 2009, 2017; Greenberg *et al.* 2012; Gardner *et al.* 2016, Ryeland *et al.* 2017, 2019, 2021).

The thermal gradient between the environmental temperature (T_a) and body temperature (T_b) seems to be key in determining a bird's capacity to lose dry heat through the bill and leg appendages (Tattersall *et al.* 2009, 2017, 2018; Greenberg *et al.* 2012; Powers *et al.* 2017). When T_a is approximately equal to T_b (39 – 42°C; Bartholomew & Cade 1963), the capacity of the bill to lose dry heat (i.e., its ability to work as a thermal radiator) starts to diminish (e.g., Powers *et al.* 2017; Tattersall *et al.* 2018). When T_a is greater than T_b, the bill stops working as a thermal radiator and can turn into a heat input source (Greenberg & Danner 2012; Gardner *et al.* 2016; Ryeland *et al.* 2017). Thus, maximum T_a has been suggested as a driver of variations in bill size (Greenberg & Danner 2012; Greenberg *et al.* 2012). Despite this, there is a lack of empirical work examining the relationship between relative bill and leg sizes and metabolic heat production or evaporative heat loss within and outside bird's thermoneutral zone (TNZ), the range of T_a in which homeothermy can be maintained without additional costs in terms of energy or water. Further studies that delve into this relationship are required for a better understanding of thermoregulation in birds in the context of global warming.

As T_a decreases or increases below the lower (T_{lc}) or above the upper (T_{uc}) critical limits of the TNZ, respectively, energy expenditure increases to maintain homeothermy (McNab 2002). T_{uc} is generally lower than T_b, so if the bill and unfeathered leg surfaces work as thermal radiators, we should expect that the larger their relative surface areas are, the greater the loss of dry heat at T_a within the range between T_{uc} and T_b, which in turn should lead to less energy consumption and lower evaporative water loss (EWL). The latter is the only avenue by which birds can maintain normothermic T_b when T_a exceeds T_b (e.g., McKechnie & Wolf 2019) and is an energetically expensive process that is affected by the environmental humidity (e.g., Smith *et al.* 2015; van Dyk *et al.* 2019). This implies a critical trade-off between the need to avoid hyperthermia and the risk of dehydration, particularly in bird species inhabiting hot and arid environments (Boyles *et al.* 2011; Smit *et al.* 2013; Oswald *et al.* 2018; Czence *et al.* 2020; Song & Beissinger 2020).

In this study, we calculated the TNZ of a Mediterranean population of Great tit (*Parus major*) (~16 g), a widespread and abundant passerine that is a well-known ecological model used to investigate the relationships between appendage morphology and ecological traits (e.g., Gosler 1987; 1993). We then examined the relationships between the relative bill and leg surface areas to body size and several thermoregulatory traits (the rate of O_2 consumption [VO_2], EWL, T_{lc}, T_{uc}, TNZ breadth, T_a inflection point of EWL and evaporative cooling efficiency). We hypothesized that when T_a exceeds T_{uc} but is lower than T_b, individuals with larger relative bill and/or leg sizes will consume less oxygen to maintain homeothermy, whereas when T_a is lower than T_{lc}, these individuals will consume more oxygen to avoid hypothermia. We further predict a lower T_a inflection point of EWL in individuals with lower relative thermal appendage sizes.

Materials and methods

All procedures were approved by the bioethical committee of the University of Extremadura, Spain (108/2016) and were conducted under the governmental license CN0032/18/ACA.

Capture and biometric measurements

The Great tit individuals examined belonged to a population located in the areas surrounding the city of Badajoz (SW Spain; 38° 56' 7.85'' N, 6° 56' 33.129''). Classified as Csa according to the Köppen Climatic Classification (mean annual T_a: 17.27 ± 0.05°C and summer mean maximum T_a: 34.18 ± 0.07°C; data from 1998 to 2018, State Meteorological Agency), this area has experienced a significant increase in the summer maximum T_a and frequency and duration of heat waves over the last three decades (Acero *et al.* 2014; 2018). A total of 24 Great tits were collected as nestlings and hand-raised in the laboratory of the University of Extremadura during spring 2017. Individuals were maintained in artificial nests where they were fed every 2 h from 8:00 AM to 10:00 PM until fledging. When birds were completely independent, they were individually identified with an alphanumeric band and moved to outdoor aviaries (5 m × 2.5 m × 2 m each) equipped with small ponds with running water, natural vegetation and live prey where they stayed during several months before metabolic trials started (winter 2019). Taking advantage of a parallel study, we added data from 8 wild-living individuals (5 juveniles and 3 adults) caught in the same study area to optimize our sample size of individuals representing each sex. These Great tits were captured in the wild by mist-nets in the late afternoon, measured at night (winter 2019), and released early the next morning.

The age and sex of the wild-living birds were determined according to their plumage characteristics (Svensson 1992), and the sex of all individuals (16 males and 16 females) was later confirmed by CHD-based molecular sexing protocols (Griffiths *et al.* 1998). Hand-raised birds were released at their place of collection several weeks after respirometry measurements.

Bill and tarsi surface areas were estimated individually following Greenberg *et al.* (2012). Briefly, we used an equation in which the bill area is approximated to an elliptical cone:

$$\left(\frac{BW + BD}{4}\right) BL \times \pi$$

where BW is the bill width, BD is the bill depth, and BL is the bill length (see figure in Svensson 1992).

Measurements of the tarsus were used to estimate the tarsi surface area as a proxy of the leg surface area using the equation for an elliptical cylinder:

$$\left(\pi\left(2\left(\left(\frac{TW}{2}\right)^2+\left(\frac{TD}{2}\right)^2\right)-\ 0.5(TW-TD)^2\right)^{\frac{1}{2}}\right)TL\times 2$$

where TW is the tarsus width, TD is the tarsus depth (both measured at the midpoint of the tarsus) and TL is the tarsus length. All bill and tarsus measurements were performed by the same person (JMAG) using a digital calliper (± 0.01 mm).

We also measured the wing length (flattened and straightened) as a proxy of body size using a wing rule (± 0.5 mm) (Gosler *et al.* 1998).

Gas exchange measurements

We measured O_2 consumption (ml min^{-1}) and EWL (mg hr^{-1}) using an open flow-through respirometry system. Each individual was placed in a polypropylene metabolic chamber (232 × 165 × 162 mm; effective volume = 3.9 L), the floor of which was covered with a 1cm mineral oil layer to avoid evaporation from excreta. The chambers were equipped with a wire mesh platform located 3 cm above this oil layer to allow individuals to perch without touching the oil. All metabolic chambers were placed in a temperature-controlled cabinet (ICP, 750 Memmert GmbH, Schwabach, Germany), where the increasing or decreasing T_a profiles (see below for details) were created automatically using control software. We introduced a calibrated thermistor probe (± 0.001°C) inside the metabolic chambers to monitor the T_a during the metabolic trials. Exterior dry air (<1 kPa WVP) was pumped from an air dryer compressor (MESTRA®) into a carboy (Lighton 2008) and then directed to the metabolic chambers using mass flow controllers (MFS, Sable Systems International, Las Vegas, Nevada, USA). Flow rates of 1000 or 3000 ml min^{-1} (depending on data collection protocol; see details below) were used during metabolic trials. Excurrent airstreams from the chambers flowed through an eight-channel multiplexer (RM-8, Sable Systems International), which automatically alternated every 360 sec between metabolic chambers containing birds as well as an additional chamber left empty to obtain baseline values. The latter were obtained for 300 sec at the start of every trial and following two metabolic chamber measurements. We subsampled the downstream air at 200 ml min^{-1} (SS3 subsampler, Sable Systems International) and pulled it sequentially through an H_2O analyzer (RH300, Sable Systems), a Drierite® column and an O_2 analyzer (FC-10 Oxygen Analyzer, Sable Systems). The data were digitalized using an analog-to-digital converter (UI2 model, Sable Systems) and recorded with a sampling interval of 1 s using Expedata software (version 1.9.14, Sable Systems). Both analyzers were zeroed and spanned weekly using standard protocols (Lighton 2008).

Data collection protocol

Gas exchange rates were measured through a wide range of T_as (10°C, 15°C, 20°C, 25°C, 30°C, 35°C, 37°C and 40°C) in a stepped manner in a maximum of six individuals at a time. The metabolic trials were performed at night (from 8:00 PM to 8:00 AM; the daily resting phase of Great tit) after the food was withheld from the birds for at least 2 h to ensure they were in a postabsorptive state (RER 0.70). To determine T_{lc}, six birds at a time were exposed alternately to an increasing or a decreasing stepped T_a profile ranging from 10°C to 30°C or vice versa. All individuals were exposed to each T_a for a minimum of 65 min using a flow rate of 1000 ml min^{-1}. For T_{uc} determination, individuals were exposed to an increasing profile of T_as (35°C, 37°C and 40°C). We used a flow rate of to 3000 ml min^{-1} to ensure maintenance of low humidity levels (<1 kPa WVP), which aided in keeping birds calm (Whitfield *et al.* 2015), and only two birds were measured per trial; they were exposed to each T_a for a minimum of 25 min. The first 65 min or 25 of the stepped T_a profiles of each protocol were used to ensure that the individuals were acclimated to the metabolic chambers (i.e., stable VO_2 and EWL traces) after handling. To ensure captive individuals recovered from the stress of handling following T_{lc} measurement, bird exposition to the highest T_as (35°C, 37°C and 40°C) was conducted after two weeks. Individual's behavior within chambers was monitored directly by an observer (we did not record videos) using infrared cameras to ensure they remained calm during the metabolic measurements. All individuals were hydrated and weighed (± 0.1 g) before and after the metabolic measurements. The mean body mass (M_b) of the birds was used in the analyses.

Data analysis

The VO_2 and EWL values at each T_a were estimated as the lowest stable 2-min (see, for example, Boratyński *et al.* 2016) values using Eqs. 10.2 and 10.9 from Lighton (2008), respectively, with a custom macro designed in Expedata. We used a respiratory quotient of 0.70 (e.g., Kvist & Lindsröm 2001). To obtain the metabolic heat production (MHP), and converted the VO_2 values to metabolic rates (Watt, W) using an energy equivalent of 20 kJ 1^{-1} O_2 (e.g., Caro & Visser 2009). The drift of water and O_2 traces was corrected using the Catmull-Rom spline correction applied to baselines. The evaporative heat loss (EHL) was calculated assuming latent heat of vaporization values for water at 35°C, 37°C and 40°C following Tracy et al. (1980). The evaporative cooling efficiency (EHL/MHP) was calculated at every T_a above T_{uc}.

We used a generalized estimating equations (GEE) approach to simultaneously identify population limits of TNZ (T_{lc} and T_{uc}) of our Great tit population (n=24) using the 'lme4' package (Bates *et al.* 2014), the 'geepack' package (Halekoh *et al.* 2006) and a modified version of the 'segmented' package (Muggeo 2009), in R 3.6.1. Then, we calculated T_{lc} and T_{uc} for each focal individual using the R packages 'lme4' and the modified version of 'segmented'. We could not obtain TNZ values for wild-living individuals since they were only measured under one of both protocols. The VO_2 values were corrected by body mass using residuals from a regression between VO_2 and body mass (log-transformed values). The TNZ breadth was calculated as the T_{uc} value minus the T_{lc} value. Mean value of VO_2 within TNZ was considered to be the basal metabolic rate (BMR). The inflection point of EWL was also calculated using 'lme4' and 'segmented' packages in R.

To obtain the relative appendage sizes (bill and tarsi index values), we computed the residuals of the regression of the bill or tarsi surface area on the wing length, as this is assumed to be the best proxy of body size in small-sized passerines, including Great tits (Gosler *et al.* 1998; Gardner *et al.* 2016). We log-transformed the variables to meet the assumptions of linearity, homoscedasticity and normality. The residuals were calculated separately for males and females due to sexual dimorphism in size. Great tit males had larger wing lengths (t_{30} = -2.27, $p < 0.05$), higher M_b values (t_{30} = -2.38, $p < 0.05$) and bill surface areas (t_{30} = -2.16, $p < 0.05$) than females, but the sexes did not differ in tarsi surface area (t_{30}

= -1.17, $p = 0.25$). We calculated mass-independent VO_2 and mass-independent EWL from the regressions of the VO_2 and EWL rates, respectively, on the mean M_b.

To ensure that the order of exposure of each individual to T_a did not affect the metabolic measurements from 10 to 30°C, we performed a *t*-test to compare the mass-independent VO_2 and mass-independent EWL values between individuals measured at the decreasing or increasing stepped T_a profiles. No significant differences were found in the analysis (all results $p > 0.09$), so the order of T_a exposure was not considered in the models.

To test the effects of the bill and tarsi indices on physiological traits (T_{lc}, T_{uc}, TNZ breadth, the T_a inflection point of EWL, EHL/MHP and the mass-independent VO_2 and mass-independent EWL at each T_a), we built a series of generalized linear models (GLMs) that included physiological traits as response variables, sex (two levels) as a fixed factor, bill and tarsi indices as covariates, and the interactions between the bill index and sex, and between the tarsi index and sex, as fixed factors. In the case of EHL/MHP, M_b was included as a covariate. Multicollinearity was tested by calculating the variance inflation factor (VIF) among all predictor variables using the 'car' package (Fox & Weisberg 2019); we confirmed no collinearity problems (all VIF values < 5; see Zuur *et al.* 2010). The model selection was based on the Akaike information criterion for small sample sizes (AIC_c) to identify the top model(s) (models within 2 ΔAICc of the top model), and the AICc weights (w_i) were used to further distinguish among the top models (Burnham & Anderson 2002). We used the function 'dredge' from the R package MuMIn (Barton 2018) for this procedure.

In cases where more than one model had $\Delta AICc < 2$ but $w_i < 0.9$ (Burnham & Anderson 2002), we performed model averaging (Grueber *et al.* 2011). A predictor was considered significant when the 95% confidence interval (CI) for the estimated coefficient did not overlap zero. We further calculated the relative importance weight (RIW) of each explanatory variable (see Table 2).

Statistical analyses were conducted in SPSS Statistics 23 (SPSS Inc., Chicago, IL, USA) and R 4.0.3 (R Core Team, 2014), and figures were produced using the R package 'ggplot2' (Wickham, 2016). Values are shown as means ± SEs.

Results

The estimated BMR was 0.96 ± 0.12 O_2 ml min^{-1}, and the TNZ breadth, T_{lc}, and T_{uc} were 16.8 ± 1.2°C, 17.7 ± 1.6°C and 34.5 ± 0.7°C, respectively (Figure 1).

The EWL inflection point was established at 31.85 ± 0.27°C (Figure 2) and was not significantly different from the T_{uc} value ($t_{23} = -1.37$, $p = 0.18$).

The null model emerged as the top-ranked model for most of the variables analysed (see Table 1). There was no detectable relationship between any of the physiological measures and either relative bill or relative tarsus surface area at any T_a despite these indices were included in the best models (95% CIs overlapped zero in all cases) (Tables 1 and 2). The null model was the best-fitting model for the mass-independent VO_2 at 10°C, 15°C and 35°C and the mass-independent EWL at 40°C (Table 1).

Only in the case of the EHL/MHP value at 40°C did we find a potential role of the leg surface area, as the interaction between the tarsi index and sex was included in the best model and was significant (Tables 1 and 2). Males with larger leg areas showed higher cooling efficiencies at 40°C ($F_{1,10}$=17.82, $p < 0.05$), but this relationship was not found to be significant in females ($F_{1,12}$=0.10, $p = 0.76$; Figure 3).

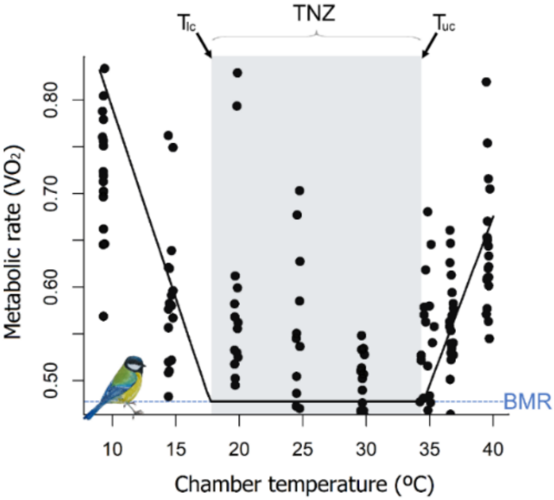

Figure 1 The relationship between metabolic rate (VO_2) (measured as mass-corrected oxygen consumption) and the environmental temperature (T_a) is mainly represented as a U-shape curve where the thermoneutral zone (TNZ) is delimited by the lower (T_{lc}) and upper (T_{uc}) critical temperatures. The TNZ of our Great tit population (n=24) was measured during the rest phase of the species. Each point represents a measurement for one individual. The lowest inflection point corresponds to the T_{lc} (17.7±1.63 °C) and the highest corresponds to the T_{uc} (34.5±0.71 °C). The breath TNZ of our population was 16.8±1.17 °C.

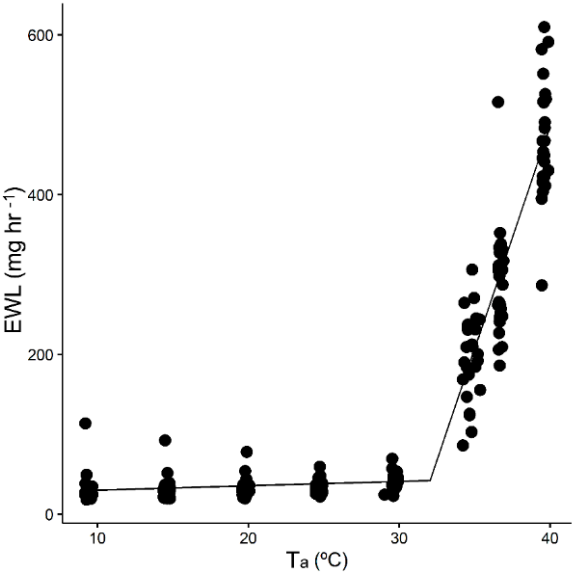

Figure 2 Evaporative water loss (EWL) in a Mediterranean population of Great tits (n=24) from 10°C to 40°C.

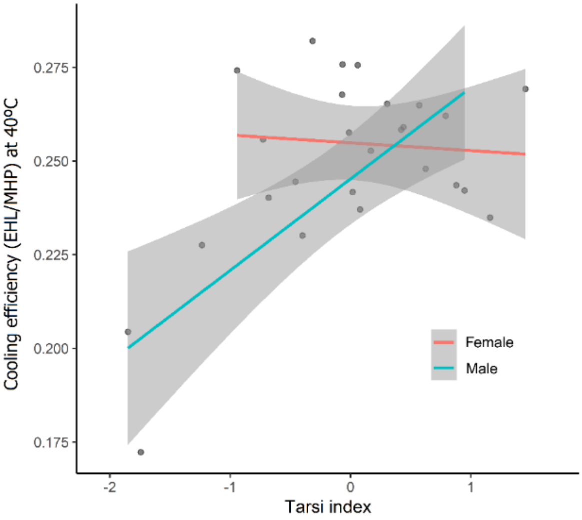

Figure 3 Evaporative cooling efficiency (EHL/MHP) in relation to tarsi index at 40°C in Great tits (log-transformed values).

Table 1. Top-ranked candidate models explaining thermoregulatory traits in a Mediterranean population of Great tits in winter, including lower critical temperature (T_{lc}), upper critical temperature (T_{uc}), thermoneutral zone (TNZ) breadth, cooling efficiency (EHL/MHP), oxygen consumption (VO_2), basal metabolic rate (BMR) and evaporative water loss (EWL).

Model	df	logLik	AICc	ΔAICc	w_i	R^2
T_{lc}						
Null	2	16.39	-28.20	0.00	0.26	0.00
Sex	3	17.57	-27.90	0.27	0.23	0.09
Bill index	3	17.03	-26.90	1.35	0.13	0.05
Bill index +Se	4	18.46	-26.80	1.41	0.13	0.16
T_{uc}						
Null	2	36.28	-68.00	0.00	0.34	0.00
Sex	3	37.32	-67.40	0.55	0.55	0.08
Inflection T_a of EWL						
Null	2	42.69	-80.80	0.00	0.37	0.00
Sex	3	43.32	-79.40	1.33	0.19	0.05
TNZ breadt						
Bill index	3	22.32	-37.40	0.00	0.28	0.13
Null	2	20.71	-36.90	0.59	0.21	0.00
Bill index + Sex + Bill index × Sex	5	24.79	-36.20	1.20	0.15	0.29
EHL/MHP at 35°C						
Tarsi index	3	53.43	-99.80	0.00	0.31	0.13
Null	2	51.56	-98.60	1.18	0.17	0.00
EHL/MHP at 37°C						
Tarsi index	3	56.10	-105.10	0.00	0.24	0.13
Null	2	54.33	-104.10	0.98	0.15	0.00
EHL/MHP at 40°C						
Tarsi index + Sex + Tarsi index × Sex	5	69.97	-126.90	0.00	0.58	0.51
Mass-independent VO_2 at 10°C						
Null	2	-39.00	82.50	0.00	0.45	0.00
Mass-independent VO_2 at 15°C						
Null	2	-39.00	82.50	0.00	0.46	0.00

(Continues)

Table 1. (Continued)

Model	**df**	**logLik**	**AICc**	**ΔAICc**	w_i	R^2
Mass-independent BMR						
Null	2	-39.00	82.50	0.00	0.38	0.00
Bill index	3	-38.60	84.10	1.69	0.16	0.03
Tarsi index	3	-38.63	84.20	1.77	0.16	0.02
Mass-independent VO_2 at 35°C						
Null	2	-34.74	74.00	0.00	0.45	0.00
Mass-independent VO_2 at 37°C						
Null	2	-35.15	74.80	0.00	0.26	0.00
Tarsi index	3	-34.25	75.60	0.78	0.18	0.07
Bill index + Tarsi index	4	-33.06	76.00	1.19	0.14	0.15
Bill index	3	-34.47	76.00	1.21	0.14	0.05
Mass-independent VO_2 at 40°C						
Null	2	-34.62	73.80	0.00	0.38	0.00
Tarsi index	3	-33.96	75.00	1.25	0.20	0.05
Mass-independent EWL at 10°C						
Null	2	-39.00	82.50	0.00	0.43	0.00
Bill index	3	-38.69	84.30	1.89	0.17	0.02
Mass-independent EWL at 15°C						
Null	2	-39.00	82.50	0.00	0.37	0.00
Bill index	3	-38.41	83.80	1.32	0.19	0.04
Mass-independent EWL at TNZ						
Null	2	-39.00	82.50	0.00	0.35	0.00
Bill index	3	-38.16	83.30	0.82	0.23	0.06
Mass-independent EWL at 35°C						
Tarsi index	3	-31.91	70.9	0.00	0.45	0.20
Mass-independent EWL at 37°C						
Null	2	-34.74	74.00	0.00	0.39	0.00
Tarsi index	3	-34.11	75.30	1.31	0.20	0.05
Mass-independent EWL at 40°C						
Null	2	-31.26	67.0	0.00	0.44	0.00

Note: Models were selected using the Akaike Information Criterion with a correction for small samples (AICc). Only models with ΔAICc < 2 are shown.

Table 2. Model-averaged parameter estimates (± SE) for predictors of thermoregulatory traits in Great tits including lower critical temperature (T_{lc}), upper critical temperature (T_{uc}), thermoneutral zone (TNZ) breadth, cooling efficiency (EHL/MHP), oxygen consumption (VO_2), basal metabolic rate (BMR) and evaporative water loss (EWL).

Model	Estimate	CI (95 %)	SE	RIW
T_{lc}				
Intercept	1.24	_	0.03	_
Bill index	0.01	-0.03, 0.11	0.03	0.35
Sex M	-0.04	-0.18, 0.03	0.05	0.48
T_{uc}				
Intercept	1.54	_	0.01	_
Sex M	-0.01	-0.08, 0.01	0.02	0.43
T_a inflection of EWL				
Intercept	1.52	_	0.01	_
Sex M	-0.01	-0.05, 0.02	0.01	0.34
TNZ breadth				
Intercept	1.22	_	0.02	_
Bill index	-0.04	-0.13, 0.01	0.04	0.68
Sex M	0.01	-0.05, 0.11	0.02	0.24
Bill index × Sex M	0.03	-0.00, 0.23	0.06	0.24
EHL/MHP at 35°C				
Intercept	0.14	_	0.01	_
Tarsi index	0.01	-0.00, 0.03	0.01	0.64
EHL/MHP at 37°C				
Intercept	0.19	_	0.01	_
Tarsi index	0.01	-0.00, 0.03	0.01	0.62
EHL/MHP at 40°C				
Intercept	0.25	_	0.00	_
Tarsi index	-0.00	-0.02, 0.01	0.01	_
Sex M	-0.01	-0.02, 0.00	0.01	_
Tarsi index × Sex M	0.03	0.01, 0.04	0.01	_
Mass-independent VO_2 at 10°C				
Intercept	-0.00	_	0.18	_
Mass-independent VO_2 at 15°C				
Intercept	-0.00	_	0.18	_

(Continues)

Table 2. (Continued)

Model	Estimate	CI (95 %)	SE	RIW
Mass-independent BMR				
Intercept	-0.00	_	0.18	_
Bill index	0.04	-0.22, 0.55	0.12	0.23
Tarsi index	0.04	-0.25, 0.60	0.13	0.22
Mass-independent VO$_2$ at 35°C				
Intercept	-0.04	_	0.18	_
Mass-independent VO$_2$ at 37°C				
Intercept	-0.01	_	0.20	_
Bill index	0.13	-0.20, 0.86	0.23	0.40
Tarsi index	-0.15	-0.80, 0.14	0.23	0.44
Mass-independent VO$_2$ at 40°C				
Intercept	0.04	_	0.19	_
Tarsi index	-0.09	-0.71, 0.21	0.18	0.35
Mass-independent EWL at 10°C				
Intercept	-0.00	_	0.18	_
Bill index	-0.04	-0.52, 0.24	0.12	0.28
Mass-independent EWL at 15°C				
Intercept	-0.00	_	0.18	_
Bill index	-0.07	-0.57, 0.18	0.15	0.34
Mass-independent EWL at TNZ				
Intercept	0.00	_	0.18	_
Bill index	0.09	-0.14, 0.61	0.17	0.40
Mass-independent EWL at 35°C				
Intercept	-0.04	_	0.19	_
Tarsi index	-0.12	-0.57, 033	0.18	0.34
Mass-independent EWL at 37°C				
Intercept	0.04	_	0.19	_
Tarsi index	0.08	-0.22, 0.71	0.18	0.34
Mass-independent EWL at 40°C				
Intercept	0.04	_	0.18	_

Note: The 95% confidence intervals (CI) and relative importance of the parameters (RIW) are also shown.

Discussion

We characterized some main thermoregulatory traits, such as TNZ breath and cooling efficiency at temperatures above T_{uc}, in a Mediterranean Great tit population. We found no evidence for the hypothesis that the bill surface area plays a significant role as a thermal window to maintain normothermia. However, the tarsi surface area − a proxy of the leg surface area− could play a relevant role in males' physiological responses to high T_as in the studied Great tit population.

Populations exposed to higher T_a values are expected to have higher critical thermal limits (e.g., Cooper & Swanson 1994; Nilsson *et al.* 2016). Our findings support this statement, as the studied Mediterranean Great tit population showed a thermoneutral zone with a higher upper critical limit (6°C higher) than Great tits from cold environments in northern Europe (see Broggi *et al.* 2005). Nevertheless, data estimated for Great tits from Russia (Gavrilov 2014) showed similar values to those found in our research (T_{lc}: 17.7°C; T_{uc}: 34.5°C), but these data must be taken with caution since the methodology used in that study to calculate the TNZ values differed from our methods and those used by other authors.

A clear link was obtained between the onset of EWL and the T_{uc}, highlighting the importance of EWL as the main mechanism of heat loss when T_a surpasses T_{uc} (Wolf & Walsberg 1996). The inflection point of EWL in Great tits contrasts with those observed in similar-sized passerines acclimated to hot and arid climates, such as the Yellow-plumed honeyeater *Ptilotula arnata* (~16 g) or the House finch *Haemorhous mexicanus* (~18 g), which showed EWL inflection points of 38°C (McKechnie *et al.* 2017, Smith *et al.* 2017). Nonetheless, it was similar to the ~35°C threshold seen in the Cape rockjumper *Chaetops frenatus* inhabiting a Mediterranean climate (Oswald *et al.* 2018). The need to use EWL as a thermoregulatory physiological mechanism may be extremely dangerous in passerines living in hot and arid zones such as deserts (McKechnie *et al.* 2021). However, forest species such as Great tits, even those inhabiting hot environments, would be subject to lower trade-offs between dehydration and hyperthermia avoidance because they normally occupy buffered habitats during summer with available microclimates and fresh water for drinking, resulting in a lower EWL inflection point. Drinking water also allows higher EWL scopes, facilitating greater body heat loss effectiveness (Czenze *et al.* 2020). Thus, in habitats where water is accessible and exposure to solar radiation can be avoided by microhabitat selection, active heat dissipation might be favored in small passerines such as Great tits instead of losing body heat through passive pathways such as radiation (Greenberg *et al.* 2012). This could explain why, contrary to our predictions, we did not find evidence of a significant effect of the bill as a thermal window. Moreover, in our Great tit population, the bill and leg surface area are only about 1% and 3% of the whole-body surface area, respectively (calculations performed following to Walsberg & King 1978). Therefore, bill surface area clearly represents only a small part of the whole-body surface, so its absolute role might be so minor that the effect size is undetectable.

Thermoregulatory behaviors reduce the need to engage in costly physiological responses (e.g., Dawson 1982; Angilletta 2009; Amat & Masero 2004; Thompson *et al.* 2018; Oswald *et al.* 2019). For example, passerine species such as the Cape rockjumper *Chaetops frenatus* or the Rufous-eared warbler *Malcorus pectoralis* increased their cool microsite use at higher T_a values (Pattinson & Smit 2017; Oswald *et al.* 2019). The behavioral mechanisms regulating T_b in the studied Great tit population have never been investigated systematically, but this population must exploit the thermal heterogeneity in their environment by selecting microhabitats with favorable T_as. We also observed, for example, Great tits adopting wing drooping inside the metabolic chambers at ~34°C (NPM pers. obs.), which occasionally matched the onset of panting. This behavior was also observed in Zebra finch (*Taeniopygia guttata*) individuals inside metabolic chambers when exposed to 40°C, favoring an increase in cutaneous evaporative heat loss (CEWL) (Wojciechowsi *et al.* 2020). However, during the metabolic trials, neither T_b nor behaviours were registered, impeding formal analyses to evaluate their possible effects on Great tit thermoregulation.

The Great tit's maximum cooling efficiency, 0.83 ± 0.06, was in accordance with previous values reported for passerines (Bartholomew *et al.* 1968, Whitfield *et al.* 2015, Smith *et al.* 2015, McKechnie *et al.* 2017) for which the maximum EHL/MHP value was < 2. At high T_as (40°C), Great tit males displayed a positive relationship between the EHL/MHP ratio and tarsi surface index. When partitioning EWL between its respiratory and cutaneous components, passerines rely mainly on respiratory evaporative water loss to deal with heat stress, but CEWL can also contribute significantly to reducing T_b in such circumstances (Wolf & Walsberg 1996; Wojciechowsi *et al.* 2020). For example, in Verdin (*Auriparus flaviceps*), a small passerine, CEWL at 50°C can be up to three times higher than at 30°C (Wolf & Walsberg 1996). The skin of the lower legs (tarsometatarsus and feet) of Great tits is not permeable to water, so CEWL through these surfaces is not possible (Bernstein 1974; Martineau & Larochelle 1988). However, CEWL could occur (in addition to other feathered parts of the skin) in the sparsely feathered surface of the upper legs, which could explain the higher EHL/MHP values recorded at 40°C in males with higher tarsi surface index values. The sex-specific differences observed in this relationship could be related to the differences in behavioral patterns previously observed between the sexes in this species; males have been observed to sing and fight for broader periods of time to defend their mates and territories (Hindle 1952). This male dominance behavior is related to increased exposure to harsh environmental conditions, and so having larger legs (and thus greater rates of CEWL) may aid males in maintaining normothermia. Sex-related behaviors have previously been related to sex-specific differences in the T_a threshold regarding the onset of heat dissipation behaviors (Kemp *et al.* 2020), which may also induce biased sexual selection over the next few decades (Miller *et al.* 2018). For example, in the nonpasserine southern yellow-billed hornbill (*Tockus leucomelas*) species, males and females have been observed showing different EWLs and RMRs at high T_a values, which is probably related to the contrasting behaviors displayed by the sexes during the breeding season (Van Jaarsveld *et al.* 2021). Future studies are needed to identify and improve our knowledge about the mechanisms that underlie these sex-specific relationships.

Overall, our study provides an improved understanding of the thermal biology of a Mediterranean population of Great tits and shows the complex interplays that may exist between the relative sizes of the unfeathered appendages and the physiological traits involved in thermoregulation. Similar studies developed with birds that occupy poorly climatically buffered habitats (i.e., habitats with reduced microclimates to escape direct solar radiation or with limited availability of freshwater) could provide clarification on the roles of the bill and legs in the thermal physiology of Mediterranean bird populations. These would also improve our ability to predict the vulnerability of these birds to global warming and extreme heat events.

References

Acero, F. J., Fernández-Fernández, M. I., Carrasco, V. M. S., Parey, S., Hoang, T. T. H., Dacunha-Castelle, D., & García, J. A. (2018) Changes in heat wave characteristics over Extremadura (SW Spain). Theoretical and Applied Climatology 133(1-2).

Acero, F. J., García, J. A., Gallego, M. C., Parey, S., & Dacunha-Castelle, D. (2014) Trends in summer extreme temperatures over the Iberian Peninsula using nonurban station data. Journal of Geophysical Research: Atmospheres 119(1), 39-53.

Allen, J. A. (1877) The influence of physical conditions in the genesis of species. Radical review 1, 108-140.

Amat, J. A., & Masero, J. A. (2004) How Kentish plovers, Charadrius alexandrinus, cope with heat stress during incubation. Behavioral Ecology and Sociobiology 56(1), 26-33.

Angilletta, M. J. (2009) Thermal adaptation: A theoretical and empirical synthesis. Oxford, UK; New York, NY: Oxford University Press.

Arad, Z., Midtgård, U., & Bernstein, M. H. (1989) Thermoregulation in turkey vultures: vascular anatomy, arteriovenous heat exchange, and behavior. The Condor 91(3), 505-514.

Bartholomew, G. A., & Cade, T. J. (1963) The water economy of land birds. The Auk 80(4), 504-539.

Bartholomew, G. A., Lasiewski, R. C., & Crawford, E. C. (1968) Patterns of panting and gular flutter in cormorants, pelicans, owls, and doves. The Condor 70(1), 31-34.

Barton, K. (2018). MuMIn: multi-model inference. R package. Cran-R, 1, 289-290.

Bates, D., Mächler, M., Bolker, B., & Walker, S. (2014) Fitting linear mixed-effects models using lme4. arXiv preprint arXiv:1406.5823.

Bernstein, M. H. (1974) Vascular responses and foot temperature in pigeons. American Journal of Physiology-Legacy Content 226(6), 1350-1355.

Boratyński, J. S., Jefimow, M., & Wojciechowski, M. S. (2016) Phenotypic flexibility of energetics in acclimated Siberian hamsters has a narrower scope in winter than in summer. Journal of Comparative Physiology B 186(3), 387-402.

Boyles, J.G., Seebacher, F., Smit, B. & McKechnie, A.E. (2011) Adaptive thermoregulation in endotherms may alter responses to climate change. Integrative and Comparative Biology 51, 676–690.

Broggi, J., Hohtola, E., Orell, M., & Nilsson, J.Å. (2005) Local adaptation to winter conditions in a passerine spreading north: A common-garden approach. Evolution 59, 1600-1603

Burnham, K. P., & Anderson, D. R. (2002) Model selection and multimodel inference: A practical information-theoretic approach. Springer.

Campbell-Tennant, D. J., Gardner, J. L., Kearney, M. R., & Symonds, M. R. (2015) Climate-related spatial and temporal variation in bill morphology over the past century in Australian parrots. Journal of Biogeography 42(6), 1163-1175.

Caro, S. P., & Visser, M. E. (2009) Temperature-induced elevation of basal metabolic rate does not affect testis growth in great tits. Journal of Experimental Biology 212(13), 1995-1999.

Cooper, S. J., & Swanson, D. L. (1994) Seasonal acclimatization of thermoregulation in the black-capped chickadee. The Condor 96(3), 638-646.

Czenze, Z. J., Kemp, R., Van Jaarsveld, B., Freeman, M. T., Smit, B., Wolf, B. O., & McKechnie, A. E. (2020) Regularly drinking desert birds have greater evaporative cooling capacity and higher heat tolerance limits than non-drinking species. Functional Ecology 34(8), 1589-1600.

Dawson, W. R. (1982). Evaporative water losses in birds. Comparative Biochemistry and Physiology 71, 495–509.

Friedman, N. R., Miller, E. T., Ball, J. R., Kasuga, H., Remeš, V., & Economo, E. P. (2019) Evolution of a multifunctional trait: shared effects of foraging ecology and thermoregulation on beak morphology, with consequences for song evolution. Proceedings of the Royal Society B 286, 20192474.

Gardner, J. L., Peters, A., Kearney, M. R., Joseph, L., & Heinsohn, R. (2011) Declining body size: a third universal response to warming?. Trends in ecology and evolution 26(6), 285-291.

Gardner, J. L., Symonds, M. R., Joseph, L., Ikin, K., Stein, J., & Kruuk, L. E. (2016) Spatial variation in avian bill size is associated with humidity in summer among Australian passerines. Climate Change Responses 3(1), 11.

Gavrilov, V. M. (2014) Ecological and scaling analysis of the energy expenditure of rest, activity, flight, and evaporative water loss in Passeriformes and non-Passeriformes in relation to seasonal migrations and to the occupation of boreal stations in high and moderate latitudes. The Quarterly Review of Biology 89(2), 107-150.

Gosler, A. G. (1987) Pattern and process in the bill morphology of the Great Tit Parus major. Ibis 129, 451-476.

Gosler, A. (1993) The Great tit. London: Hamlyn, 128.

Gosler, A. G., Greenwood, J. J. D., Baker, J. K., & Davidson, N. C. (1998) The field determination of body size and condition in passerines: a report to the British Ringing Committee. Bird Study 45(1), 92-103.

Greenberg, R., & Danner, R. M. (2012) The influence of the California marine layer on bill size in a generalist songbird. Evolution: International Journal of Organic Evolution 66(12), 3825-3835.

Greenberg, R., Cadena, V., Danner, R. M., & Tattersall, G. (2012) Heat loss may explain bill size differences between birds occupying different habitats. PloS one 7(7), e40933.

Griffiths, R., Double, M. C., Orr, K., & Dawson, R. J. (1998) A DNA test to sex most birds. Molecular Ecology 7(8), 1071-1075.

Grueber, C. E., Nakagawa, S., Laws, R. J., & Jamieson, I. G. (2011) Multimodel inference in ecology and evolution: challenges and solutions. Journal of Evolutionary Biology 24(4), 699-711.

Hagan, A. A., & Heath, J. E. (1980) Regulation of heat loss in the duck by vasomotion in the bill. Journal of Thermal Biology 5(2), 95-101.

Halekoh U, Højsgaard S & Yan J (2006) The R Package geepack for Generalized Estimating Equations. Journal of Statistical Software 15/2, 1–11.

Hindle, R. A. (1952). The behaviour of the great tit (*Parus major*) and some other related species. Behaviour. Supplement, III-201.

Fox, J. & Weisberg. S (2019) An R Companion to Applied Regression. Sage, ThousandOaks CA, 3rd edition.

Van Jaarsveld, B., Bennett, N. C., Czenze, Z. J., Kemp, R., van de Ven, T. M., Cunningham, S. J., & McKechnie, A. E. (2021) How hornbills handle heat: sex-specific thermoregulation in the southern yellow-billed hornbill. Journal of Experimental Biology, 224(4), jeb232777.

Kemp, R., Freeman, M. T., van Jaarsveld, B., Czenze, Z. J., Conradie, S. R., & McKechnie, A. E. (2020) Sublethal fitness costs of chronic exposure to hot weather vary between sexes in a threatened desert lark. Emu-Austral Ornithology 120(3), 216-229.

Kvist, A. & Lindström, Å., (2001) Basal metabolic rate in migratory waders: Intra-individual, intraspecific, interspecific and seasonal variation. Functional Ecology 15, 465–473.

Lighton, J.R.B., (2008) Measuring Metabolic Rates: A Manual for Scientists. Oxford University Press, Inc., New York.

Martineau, L., & Larochelle, J. (1988) The cooling power of pigeon legs. Journal of Experimental Biology 136(1), 193-208.

McKechnie, A. E., & Wolf, B. O. (2019) The physiology of heat tolerance in small endotherms. Physiology 34(5), 302-313.

McKechnie, A. E., Gerson, A. R., & Wolf, B. O. (2021) Thermoregulation in desert birds: scaling and phylogenetic variation in heat tolerance and evaporative cooling. Journal of Experimental Biology, 224(Suppl. 1), jeb229211.

McKechnie, A. E., Gerson, A. R., McWhorter, T. J., Smith, E. K., Talbot, W. A., & Wolf, B. O. (2017) Avian thermoregulation in the heat: evaporative cooling in five Australian passerines reveals within-order biogeographic variation in heat tolerance. Journal of Experimental Biology 220(13), 2436-2444.

McNab BK (2002) The Physiological Ecology of Vertebrates. Cornell University Press, London, UK.

Midtgård, U. (1981) The rete tibiotarsale and arteriovenous association in the hind limb of birds: a comparative morphological study on counter-current heat exchange systems. Acta Zoologica 62(2), 67-87.

Miller, C. R., Latimer, C. E., & Zuckerberg, B. (2018) Bill size variation in northern cardinals associated with anthropogenic drivers across North America. Ecology and evolution 8(10), 4841-4851.

Moreno, E., & Carrascal, L. M. (1993) Leg morphology and feeding postures in four Parus species: an experimental ecomorphological approach. Ecology 74(7), 2037-2044.

Muggeo, V. M. R. (2009) Segmented: an R package to fit regression models with broke-line relationships (pp.20-25). R News 8.1.

Nilsson, J. Å., Molokwu, M. N., & Olsson, O. (2016) Body temperature regulation in hot environments. PloS one 11(8), e0161481.

Oswald, K. N., Lee, A. T., & Smit, B. (2018) Seasonal physiological responses to heat in an alpine range-restricted bird: the Cape Rockjumper (Chaetops frenatus). Journal of Ornithology 159(4), 1063-1072.

Oswald, K. N., Smit, B., Lee, A. T., & Cunningham, S. J. (2019) Behaviour of an alpine range-restricted species is described by interactions between microsite use and temperature. Animal Behaviour 157, 177-187.

Pattinson, N. B., & Smit, B. (2017) Seasonal behavioral responses of an arid-zone passerine in a hot environment. Physiology and behavior 179, 268-275.

Powers, D. R., Langland, K. M., Wethington, S. M., Powers, S. D., Graham, C. H., & Tobalske, B. W. (2017) Hovering in the heat: effects of environmental temperature on heat regulation in foraging hummingbirds. Royal Society open science 4(12), 171056.

R Core Team (2014) R: a language and environment for statistical computing. R Foundation for Statistical Computing.

Ryeland, J., Weston, M. A., & Symonds, M. R. (2017) Bill size mediates behavioural thermoregulation in birds. Functional Ecology 31(4), 885-893.

Ryeland, J., Weston, M. A., & Symonds, M. R. (2019) Leg length and temperature determine the use of unipedal roosting in birds. Journal of Avian Biology 50(5), e02008.

Ryeland, J., Weston, M. A., & Symonds, M. R. (2021) The importance of wetland margin microhabitat mosaics; the case of shorebirds and thermoregulation. Journal of Applied Ecology 58(2), 382-391.

Sheridan, J. A., & Bickford, D. (2011) Shrinking body size as an ecological response to climate change. Nature climate change 1(8), 401-406.

Smit, B., Harding, C. T., Hockey, P. A. R. & McKechnie, A. E. (2013) Adaptive thermoregulation during summer in two populations of an arid-zone passerine. Ecology 94, 1142–1154.

Smith, E. K., O'Neill, J. J., Gerson, A. R., McKechnie, A. E., & Wolf, B. O. (2017) Avian thermoregulation in the heat: resting metabolism, evaporative cooling and heat tolerance in Sonoran Desert songbirds. Journal of Experimental Biology 220(18), 3290-3300.

Smith, E. K., O'Neill, J., Gerson, A. R., & Wolf, B. O. (2015) Avian thermoregulation in the heat: resting metabolism, evaporative cooling and heat tolerance in Sonoran Desert doves and quail. Journal of Experimental Biology 218(22), 3636-3646.

Song, S., & Beissinger, S. R. (2020) Environmental determinants of total evaporative water loss in birds at multiple temperatures. The Auk 137(1), ukz069.

Steen, I., & Steen, J. B. (1965) The importance of the legs in the thermoregulation of birds. Acta Physiologica Scandinavica 63(3), 285-291.

Stillman, J. H. (2019) Heat waves, the new normal: summertime temperature extremes will impact animals, ecosystems, and human communities. Physiology 34(2), 86-100.

Svensson, L. (1992) Identification guide to European passerines (368 pp.). Norfolk, UK: British Trust for Ornithology.

Symonds, M. R., & Tattersall, G. J. (2010) Geographical variation in bill size across bird species provides evidence for Allen’s rule. The American Naturalist 176(2), 188-197.

Tattersall, G. J., Andrade, D. V., & Abe, A. S. (2009) Heat exchange from the toucan bill reveals a controllable vascular thermal radiator. Science 325(5939), 468-470.

Tattersall, G. J., Arnaout, B., & Symonds, M. R. (2017) The evolution of the avian bill as a thermoregulatory organ. Biological Reviews 92(3), 1630-1656.

Tattersall, G. J., Chaves, J. A., & Danner, R. M. (2018) Thermoregulatory windows in Darwin's finches. Functional Ecology 32(2), 358-368.

Tattersall, G. J., Sinclair, B. J., Withers, P. C., Fields, P. A., Seebacher, F., Cooper, C. E., & Maloney, S. K. (2012) Coping with thermal challenges: physiological adaptations to environmental temperatures. Comprehensive Physiology 2(3), 2151-2202.

Thompson, M. L., Cunningham, S. J., & McKechnie, A. E. (2018) Interspecific variation in avian thermoregulatory patterns and heat dissipation behaviours in a subtropical desert. Physiology and behavior 188, 311-323.

Tracy, C. R., Welch, W. R., & Porter, W. P. (1980) Properties of air. A Manual for Use in Biophysical Ecology, 3rd ed. Technical manual. UW Laboratory for Biophysical Ecology.

van Dyk, M., Noakes, M. J., & McKechnie, A. E. (2019) Interactions between humidity and evaporative heat dissipation in a passerine bird. Journal of Comparative Physiology B 189(2), 299-308.

Walsberg, G. E., & King, J. R. (1978) The relationship of the external surface area of birds to skin surface area and body mass. Journal of Experimental Biology 76, 185-189.

Whitfield, M. C., Smit, B., McKechnie, A. E., & Wolf, B. O. (2015) Avian thermoregulation in the heat: scaling of heat tolerance and evaporative cooling capacity in three southern African arid-zone passerines. Journal of Experimental Biology 218(11), 1705-1714.

Wickham, H. (2016) Programming with ggplot2. In ggplot2 (pp. 241-253). Springer.

Winder, L. A., White, S. A., Nord, A., Helm, B., & McCafferty, D. J. (2020) Body surface temperature responses to food restriction in wild and captive great tits. Journal of Experimental Biology 223(8), jeb220046.

Wojciechowski, M. S., Kowalczewska, A., Colominas-Ciuró, R., & Jefimow, M. (2021) Phenotypic flexibility in heat production and heat loss in response to thermal and hydric acclimation in the zebra finch, a small arid-zone passerine. Journal of Comparative Physiology B 191(1), 225-239.

Wolf, B., & Walsberg, G. (1996) Respiratory and cutaneous evaporative water loss at high environmental temperatures in a small bird. Journal of Experimental Biology 199(2), 451-457.

Yom-Tov, Y. (2001) Global warming and body mass decline in Israeli passerine birds. Proceedings of the Royal Society of London. Series B: Biological Sciences 268(1470), 947-952.

Zuur, A. F., Ieno, E. N., & Elphick, C. S. (2010) A protocol for data exploration to avoid common statistical problems. Methods in ecology and evolution 1(1), 3-14.

5

How do Mediterranean bird species cope with extreme weather events? Physiological and morphological responses to simulated heat waves in Great tits (*Parus* major)

Núria Playà-Montmany, Erick González-Medina, Julián Cabello-Vergel, José M. Abad-Gómez, Manuel Parejo, Deseada Parejo, Juan M. Sánchez-Guzmán, Auxiliadora Villegas and José A. Masero

Manuscript

Abstract

Global warming is one of the greatest threats that nowadays biodiversity confronts. The global mean air temperature coupled with more frequent, long-lasting and intense heat waves are causing mass die-offs across the globe. However, the sub-lethal effects on survivors are poorly understood and remain unknown in Mediterranean songbirds. Phenotypic flexibility may help birds to efficiently buffer the consequences of these heat waves. Therefore, to fill this gap, we exposed Great tits *Parus major* to four simulated heat waves of increasing intensity (39°C, 40°C, 41°C and 42°C) and measured metabolic, hygric and thermal traits, biological biomarkers of health and morphological traits to detect potential concomitant effects. Experimental birds showed slightly higher body temperature throughout heat waves simulations and displayed a decrease of 17% in BMR and greatest oxidative damage (by 56%). At the morphological level, temperature appeared to shape contour feathers by decreasing the density of barbs and barbules of both, the pennaceous and plumulaceous sections along with showing more yellowish feathers. Thus, our results indicate Great tits buffered heat stress by plastically respond to heat waves. However, the greatest oxidative damage observed in experimental birds may suggest these immediate plastic responses may impose carry-over effects in the long term.

Keywords: hot events, plasticity, oxidative stress, corticosterone, feathers, passerines

Introduction

The increment in mean environmental temperature (T_a) caused by global warming is occurring along with increasingly frequent, intense and long-lasting extreme weather events such as severe high air temperature events (e.g., McKechnie & Wolf 2010; Stillman 2019; Molina *et al.* 2020; IPCC 2021). Future climate scenarios, in turn, anticipate an increase in the number, duration and intensity of such events worldwide (Drumond *et al.* 2020; IPCC 2021), which are expected to cause large-scale die-offs (McKechnie *et al.* 2012; Fey *et al.* 2015; Ruthrof *et al.* 2018) in both, ectotherms (Cerrano *et al.* 2000) and endotherms populations (McKechnie & Wolf 2010; McKechnie *et al.* 2021). Small endotherms - especially birds - are particularly vulnerable to these extreme heat waves due to their predominantly diurnal habits, small body mass (M_b), elevated body temperature (T_b) and high metabolic and evaporative water loss (EWL) rates (McKechnie & Wolf 2010; Boyles *et al.* 2011; McKechnie & Wolf 2019). In past years, for example, hundreds of Carnaby's black cockatoos *Calyptorhynchus latirostris* and thousands of Budgerigars *Melopsittacus undulatus* and Zebra finches *Taenopygia guttata* individuals were found dead because of heat waves (see Saunders *et al.* 2011; McKechnie *et al.* 2012, 2021). Survivors, on the other hand, are likely to experience sub-lethal effects as a result of conducting a set of behavioural, physiological and morphological changes that could negatively impact fitness (McKechnie & Wolf 2010, 2019; Saunders *et al.* 2011; McKechnie *et al.* 2012, 2021; Stillman 2019; Conradie *et al.* 2019; Danner *et al.* 2021). Therefore, exposition to increasing heat waves may elicit a significant immediate and long-term impact on biodiversity, especially in combination with a gradual and sustained increase in mean T_a (e.g., Ruthrof *et al.* 2018; Conradie *et al.* 2019; Stillman 2019).

In relation to the impact of heat waves on wild birds, most research has been conducted on species well-adapted to desert climates (e.g., Gardner *et al.* 2016, 2018; Funghi *et al.* 2019; Kemp *et al.* 2020). This research has found, for example, that repeated exposure to elevated T_a (from 35°C to 40°C) negatively impacts foraging effort (du Plessis *et al.* 2012; Smit *et al.* 2016; Funghi *et al.* 2019), body condition (du Plessis *et al.* 2012; Gardner *et al.* 2016, 2018; Funghi *et al.* 2019; Sharpe *et al.* 2019; Kemp *et al.* 2020) or nestling development (Cunningham *et al.* 2013; Andreasson *et al.* 2018). However, despite the temperate and Mediterranean species might face similar challenges during summer (e.g., Nord & Nilsson 2019; Tapper *et al.* 2020; Pipoly *et al.* 2022), the potential impacts of heat waves on Mediterranean birds remains largely unexplored and restricted to nestlings (Salaberria *et al.* 2014; Catry *et al.* 2015). This is concerning as climatic models predict that Mediterranean regions such as Iberia will experience longer and more intense heat waves exceeding 45°C (Viceto *et al.* 2019), and previous research evidenced that temperate birds are less tolerant to heat stress than desert species (Pollock *et al.* 2021; McKechnie *et al.* 2021). Thus, this imposes the need and the urgency to investigate the potential impact of heat waves on non-desert small-sized birds in order to better predict the vulnerability of these species to increasing extreme weather events associated with global warming.

Phenotypic flexibility (i.e., short-term, reversible phenotypic adjustments; sensu Piersma & Drent 2003) could be the most effective means to buffer the impacts of these extreme climatic events (e.g., Boyles *et al.* 2011; DuBois *et al.* 2020). A recent study, for example, showed that small-sized Mediterranean songbirds (passerines) exhibit pronounced seasonal phenotypic flexibility in key thermoregulatory traits, with short-term benefits in terms of energy and water savings during thermally stressful conditions (Chapter 2). This pronounced phenotypic flexibility could play a principal role in the acclimation, and therefore, in the adaptation process of Mediterranean songbirds to the new scenario of climate warming. However, this phenotypic flexibility may impose carry-over effects that result from changes in energy allocation among organismal functions, which may alter whole-organism performance, or even be insufficient when individuals confront future climates outside the range of current environmental variability (Charmantier *et al.* 2008; Kelly *et al.* 2012, Bonamour *et al.* 2019).

During extreme heat events where T_a can surpass T_b, EWL is the only avenue for birds to keep normothermic (e.g., Bartholomew & Cade 1963; Calder & King 1974; McKechnie & Wolf 2010). In order to reduce the thermal gradient (T_a-T_b) and then, minimise energy expenditure and water loss, birds may increase T_b above normothermic levels, which is known as facultative hyperthermia (McKechnie & Lovegrave 2002; Boyles *et al.* 2011; Nilsson *et al.* 2016). The limited studies to date that have assessed intraspecific variation in the physiological mechanisms of thermoregulation at high T_a have provided evidence that these mechanisms are flexible both seasonally (e.g., Noakes *et al.* 2016; Chapter 2) and in response to heat waves (Cooper *et al.* 2020; Wojciechowski *et al* 2021). This highlights the plasticity of birds to adjust their thermal physiology to cope with heat stress and avoid reaching the critical thermal maximum where hyperthermia becomes lethal (typically 46-47°C; Cade *et al.* 1965) (Gerson *et al.* 2019). Nonetheless, several physiological processes across all organization levels have been proven to be thermally sensitive in vertebrates in addition to energetics (McNab 2002) and water balance (Calder & King 1974; Wolf & Walsberg 1996), including endocrine activity (Sapolsky *et al.* 2000; Xie *et al.* 2017; Ruuskanen *et al.*

2021), oxidative status (Mujahid *et al.* 2005; Lin *et al.* 2008; Jacobs *et al.* 2020) mitochondrial function (Ton *et al.* 2021; Udino *et al.* 2021) or telomere dynamics (Simide *et al.* 2016; Zhang *et al.* 2018; Fitzpatrick *et al.* 2021).

Within this context, it is important to understand how feather and plumage structure and colouration are influenced by thermoregulatory constraints (Wolf & Walsberg 2000). Both plumage structure and colouration have proven to show plastic responses to environmental conditions, including air temperature (see Burtt & Ichida 2006; Broggi *et al.* 2011). For example, wild Great tits *Parus major* individuals from two temperate populations displayed different contour feather macrostructure, a difference which disappeared when individuals of both populations were raised under identical environmental conditions (see Broggi *et al.* 2011). Laczi *et al.* (2020), on the other hand, showed that this species developed lower brightness and UV chroma breast feathers, but higher yellow chroma, after moulting when August was warmer and drier. However, despite the crucial role of feathers on thermal insulation (Desrochers *et al.* 2009; Broggi *et al.* 2011), no studies to our knowledge had addressed the impact of extreme T_a on this morphological plastic response.

The whole-organism response to thermal stress is, therefore, complex and needs to be addressed at different levels at the same time, being key to determining the potential effects that exposition to heat waves may trigger on bird physiological and morphological status, as well as understanding their tolerance through phenotypic plasticity in order to predict impacts of heat waves on the viability of populations (McKechnie & Wolf 2019). Here, we tested the effects of simulated heat waves mimicking current extreme weather events in Iberia on physiological and morphological traits in Great tit *Parus major*, a small-sized songbird (~16g). Specifically, we assessed potential effects on key thermoregulatory traits, physiological biomarkers of health (hormones – corticosterone –, oxidative status, and telomere length), and feather structure and colouration. These heat waves, with T_a near or above the normothermic T_b of birds, are assumed to negatively impact small-sized birds' physiology. We hypothesized, therefore, that exposition to frequent and intense heat events will result in a reduction in physiological performance of Great tit inhabiting this Mediterranean area while driving morphological alterations in feathers macrostructure and/or colouration.

Materials and methods

All procedures were approved by the bioethical committee of the University of Extremadura, Spain (108/2016) and were conducted under the governmental license CN0032/18/ACA.

Capture and housing

We collected 23 Great tits nestlings at the age of 7-12 days old from 5 nests boxes located in the surroundings of Badajoz city (38° 52’41.01” N, 6°58’12.74” W), in the south-west Iberia, during spring 2017. Nestlings were marked individually with rings and were maintained in artificial nests. They were fed every 2 h (from 8:00 AM to 10:00 PM) with fly larvae, yellow mealworms larvae, Handmix (Orlux), egg mixture Oké-bird (Versele-Laga) and Uni pate (Orlux). After fledging, Great tits were randomly housed into groups of 3-4 individuals in wire cages (30 × 40 × 88 cm) equipped with a nest box, perches, feeders, and one water bowl for drinking and bathing, and under natural photoperiod (14:10 h L:D). Fresh food and water were provided daily and were available *ad libitum*. When individuals were completely independent, they were moved to outdoor aviaries located at the University of Extremadura (see details in Playà-Montmany *et al.* 2021) into groups of 5-6 individuals per aviary. To increase the sample size, four additional free-living fledglings (siblings) were captured using mist-nets in the same study area and were randomly introduced into the outdoor aviaries (one per aviary).

Experimental setup

In November 2018 Great tits were randomly assigned to an experimental group (n = 13; 9 females and 4 males) or a control group (n = 14; 7 females and 7 males). Same-sex siblings were assigned to different treatments so that we could control for genetic effects and early developmental background. Birds were housed individually in cages (see above), which in turn were housed into two climatic-controlled rooms (i.e., an ‘experimental room’ and a ‘control room’). Here they were kept on a natural photoperiod with *ad libitum* access to water and food until the start of the experiment in June 2019. During this period previous to the experiment, T_a values inside the rooms matched the outdoor T_a in Badajoz.

Simulated heat waves protocol (number, maximum T_a and duration) was designed based on the extremely hot summer that afflicted Spain in July 2017.

Concretely, we used climatic data recorded by the State Meteorological Agency weather station close to the capture sites. Experimental birds were exposed during June and July to four heat waves (five days each) of increasing intensity (39°C, 40°C, 41°C and 42°C), separated by 5 to 9 days. T_a of the control room matched that of Badajoz, with a maximum settled to 35ºC (this value is the upper critical temperature for our Great tit population; see Playà-Montmany *et al.* 2021). Room T_a was recorded every 3 min using Micro Station Data Loggers H21-002 (Onset Computer Corporation, Bourne, Massachusetts, USA) at two places, one located inside the nest box and the other outside the cage (2 m above the room floor). No differences in T_a between these positions were obtained (all results $p > 0.06$), so the average T_a between both places was used in the analysis. The maximum relative humidity recorded in the treatment and control rooms was 57.38% and 51.70% respectively. All the variables were measured before and after the treatment (heat waves), except body temperature (T_b), which was measured throughout the treatment.

Body temperature measurements

T_b of individuals of both groups was measured to the nearest 0.1°C, every 1 s, during the heat waves simulation period. Prior to starting the experiment, each bird was inserted subcutaneously with a pre-sterilized temperature-sensitive passive integrated transponder (LifeChip®) in the back (above the scapula and in the featherless area on the right side, following Nicolaus et al. 2008), using a disposable needle and under antiseptic conditions, for T_b monitoring. T_b readings were recorded by two racket antennas (model F201F-ISO, Biomark) placed inside the cage and connected to an external reader (IS1001 Multiplexing Transceiver System, Biomark). Unfortunately, due to a technical failure in a reader during the first heat wave, data from this heat wave could not be included in the analysis

Thermoregulatory traits and body mass

Following the procedure described by Playà-Montmany et al. (2021), metabolic rate (measured as oxygen consumption; VO_2) and EWL (measured in terms of water vapour production; VH_2O) within TNZ and beyond the lower critical temperature (T_{lc}) and the upper critical temperature (T_{uc}) were measured using an open flow-respirometry system prior (January 2019) and after (October 2019) treatment. Briefly, birds were placed individually in transparent polypropylene metabolic chambers (effective volume = 3.9 L) allocated inside a temperature-controlled cabinet (ICP, 750 Memmert GmbH, Schwabach, Germany) where stepped profiles of increasing or decreasing T_a (see details below) were settled automatically using control software. Exterior dry air (<1 kPa WVP) was pumped inside metabolic chambers using mass flow controllers (MFS, Sable Systems International). Water vapour density (µg ml^{-1}) and O_2 concentration (%) from excurrent airstream were analysed using an H_2O analyser (RH300, Sable Systems) and an O_2 analyser (FC-10 Oxygen Analyser, Sable Systems), respectively. We measured a maximum of six individuals in a postabsorptive state at night (from 8:00 PM to 8:00 AM). Birds were exposed alternatively to an increasing or decreasing stepped T_a profile (from 10°C to 30°C or vice versa) to determine T_{lc}, and to an increasing ramped profile of T_a (35°C, 37°C and 40°C) to obtain T_{uc}. Air flow through chambers was set up to 1000 or 3000 ml min^{-1} for T_{lc} and T_{uc} determination, respectively. Increased flow rates aid birds to remain calmed at high T_a (Whitfield *et al.* 2015). Individuals spent a minimum of 65 or 25 min at low and high T_a ($\geq$ 35°C), and first records of VO_2 and VH_2O were discarded until stable traces were obtained. Infrared cameras were used to ensure individuals remained calmed during metabolic trials. All individuals were hydrated and weighted (±0.1 g) before and after the metabolic measurements. The mean M_b of the birds was used in the analyses as previous studies showed potential effects if heat waves on body condition; see Andrew *et al.* 2017; Sharpe *et al.* 2019).

Metabolic rates (basal metabolic rate – BMR – and resting metabolic rate – RMR –) and EWL rate were estimated as the lowest stable 2-min of VO_2 and VH_2O at each T_a using Eqs. 10.2 and 10.9 from Lighton (2008), respectively, with a custom macro designed in Expedata software (version 1.9.14, Sable Systems). We used the Catmull-Rom spline correction to correct the drift of water and O_2 traces applied to baselines and using a respiratory quotient of 0.70 (e.g., Kvist & Lindsröm 2001). BMR was calculated from the mean lowest VO_2 values within TNZ (see Playà-Montmany *et al.* 2021). VO_2 values were converted to metabolic rates (Watt, W) using an energy equivalent of 20 kJ l^{-1} O_2 to obtain metabolic heat production (MHP) (e.g., Caro & Visser 2009). The evaporative heat loss (EHL) was calculated assuming latent heat of vaporization values for water at 40°C, a challenging physiological T_a above the T_{uc} of Great tit (~34°C; Playà-Montmany *et al.* 2021) following Tracy et al. (1980). The evaporative cooling efficiency (EHL/MHP) was calculated at 40°C.

Corticosterone, oxidative status and telomere length measurements

We collected the second tertial feather of the left wing to quantify corticosterone levels (CORT$_f$) before and after treatment. To re-sample the same feather after heat waves, we wait until all birds ended the moult of their body feathers (see below) to be sure that the new tertial feather was fully grown. CORT$_f$ analysis was performed by Research Support Services of the University of Extremadura (SAIUEx) following the method described by Bortolotti et al. (2008). After measuring their length (mm) and weight (µg), tertial feathers were minced with scissors into pieces (< 5mm). Six ml of methanol were added to minced feathers placed in a sonicating water bath at room temperature for 30 min followed by incubation for 10 h (overnight) in a water bath at 50°C. The methanol was separated from feathers using vacuum filtration through #4 Whatman filter paper into a new centrifuge tube. The feather bits and samples and the filter paper were washed with approximately 2 ml of additional methanol. The methanol extracts were placed in a SBHCONC/1 Sample Concentrator to dry them using a stream of nitrogen gas at 50°C. Dried extracts were stored in the freezer for posterior corticosterone measurement. The CORT$_f$ was determined using the enzyme immunoassay (EIA, Enzo Life Science, Inc.) following manufacturers' instructions. A standard curve was calculated, and plates were read using a Bio-Rad Benchmark spectrophotometer at 405 nm. Values are expressed in pg CORT per mm of the feather. Intra and inter-assay coefficients of variation were 9.04 % and 11.76 % respectively.

To measure oxidative status and telomere length, individual blood samples (20µl) were collected from the brachial vein using capillary tubes, just before and after treatment. Samples were centrifuged at 10.000 rpm for 10 min to separate plasma and red blood cells (RBC), which were frozen at -80°C until assays were conducted. Oxidative status and antioxidant capacity were measured in plasma samples, while telomere length (TL) was analysed in RBC.

The oxidative status in blood plasma was measured through the colourimetric determination of the plasma non-enzimatic antioxidant barrier and the plasmatic concentration of hydroperoxides (i.e., a reactive oxygen metabolite), using the OXY-Adsorbent test (Diacron International, Grosseto, Italy) and the d-ROMs test (Diacron International), respectively, and following protocols by Constantini & Dell'Omo (2006) and Wegman et al. (2015). Briefly, to determine antioxidant capacity, we put 5µl of diluted plasma (1:100 with distillated water), a blank and a calibrator serum in duplicate in a clear 96-well plate, and added to each 200μl of hypochlorous acid (HCLO; a potent oxidant). After incubation for 10 min at 37°C, we added 5μl of N,N-diethyl-p-phenylenediamine as chromogen and measured absorbance at 490 nm in a microplate reader (Biotek Powerwave, Winoski, VT, USA). Similarly, d-ROMs was measured by incubating 5μl of plasma, blank and calibrator in duplicate in a clear 96-well plate with a 200μl aliquot of a solution containing 0.01M acetic acid/sodium acetate buffer (pH 4.8) and N,N-diethyl-p-phenylenediamine during 75 min at 37°C. Absorbance was read immediately at 490nm. OXY and d-ROMs concentrations were obtained by comparison with reference curves of a control serum. Intraplate coefficient of variation (CV; %) based on duplicates and interplate CV based on a control sample repeated over plates were 7.08% and 11.28% respectively for OXY and 9.79% and 0.93% for d-ROMs.

Relative TL was measured by SAIUEX on DNA extracted from RBC using real-time quantitative PCR (qPCR) assay following the protocol described by Salmón et al. (2016). This technique estimates relative telomere length by determining the ratio (T/S) of telomere repeat copy number (T) to a single copy gene (glyceraldehyde 3-phosphate dehydrogenase GADPH). Briefly, DNA was extracted from RCB by using the Macherey-Nagel Whole Blood Kits (Macherey-Nagel, Bethlehem, PA, USA) and quality and purity were measured using Nanodrop 2000 Spectrophotometer (Thermo Scientific). Amplification of telomere DNA was conducted by using the primers Tebl1 (5'-CGGTTTGTTTGGGTTTGGGTTTGGGTTTGGGTTTGGGTT-3') and Tebl2 (5'-GGCTTGCCTTACCCTTACCCTTACCCTTACCCTTACCCT-3') and Great tit-specific GADPH forward (5'-TG TGATTTCAATGGTGACAGC-3) and reverse (5'-AGCTTGACA AAATGGTCGTTC-30) (Atema *et al.* 2013; Salmón *et al.* 2017). The conditions for the qPCR were: telomeres 10 min at 95°C, followed by 27 cycles of 15 s at 95°C, 30 s at 58°C and 30 s at 72°C; GAPDH 10 min at 95°C, 15 min at 95°C, 30 s at 60°C and 30 s at 72°C. Telomere and GAPDH reactions were performed in triplicates on the same plates (three plates in total). A DNA sample (from an individual not included in the study) was used as a control sample and was included in triplicate on every plate. qPCR amplifying efficiency for GAPDH and telomere was estimated from a serial dilution of the reference sample. The mean reaction efficiencies for both, GADPH and telomere amplifications were 87.25 ± 3.42% and 91.52 ± 5.45%, respectively. Relative TL was calculated following Pfaffl (2001):

$$\mathrm{TL} = \frac{((1 + \text{telomere efficiency})\Delta\mathrm{Ct}\ \text{telomere (control} - \text{sample})}{(1\ +\ \text{GAPDH efficiency})\ \Delta\mathrm{Ct}\ \text{GAPDH (control} - \text{sample}))}$$

Where telomere and GADPH efficiencies are the qPCR efficiencies of telomere and GADPH fragment, respectively; Ct is the amplification threshold cycle and ΔCt telomere (control – sample) and ΔGAPDH (control – sample) are the deviation of standard – telomere or GADPDH sequences for each sample, respectively.

Contour feather measurements

A sample of five contour feathers from the same area of the breast (left side between the central black-breast stripe and the shoulder) were collected before and after treatment for morphology and spectrophotometric analyses. Feathers were kept in individual plastic bags and stored in the dark for later analysis. All birds were non-moulting individuals when we sampled the contour feather before (on 12 February 2019) the treatment. To re-sample the same area of the breast after treatment, we wait until all birds ended the moult of their body feathers (on 26 July 2019) to be sure that they moulted that area.

The morphology of feathers was investigated with the help of a Nikon Digital camera (Sight D5 L2) connected to a binocular stereoscope microscope (Nikon SNZ 800, Tokyo, Japan). To describe feather macrostructure, we measured 9 different traits (Table 1). For each feather, the division between the pennaceous (Supplementary Figure 1A) and plumulaceous (Supplementary Figure 1B) sections of a feather was determined in both types of barbs at 20X; the total length of the feather without calamus and the length of the plumulaceous barb zone were measured at 6X (Stettenheim 2000). Barbule density measurements were calculated per feather on separate barbs, randomly chosen in the middle part of each barb to control for variation along with the feather. The number of barbules from both plumulaceous and pennaceous barbs was counted following the protocol of Broggi et al. (2011), using a fixed portion (0.43 mm) of barb and starting 0.43 mm from the rachis at 70X (Supplementary Figure 1). For length, area and barbule density (mm), feathers were photographed (Canon SX30 IS on a tripod) placed onto a stage micrometre (0.01 mm). Feather length (0.01 mm) and barbule density were measured by tracing a line along the shaft (excluding calamus), whereas area (0.1 mm^2) by encircling the feather in Analyzing Digital Images program (ADI16). The proportion (%) of barbs of the plumulaceous section with respect to all barbs was also calculated. All these variables were estimated on two randomly selected feathers per individual from the five collected in order to obtain repeatability estimates.

Reflectance was measured using a S2000 Ocean Optics equipment spectrometer (see Avilés *et al.* 2011 for details). The reflectance spectra of a minimum of two contour feathers per individual was calculated between 300 and 700 nm. Reflectance data were summarised by calculating the following three colour descriptors: brightness (spectral intensity), chroma (spectral purity) and hue (spectral colour) (Siefferman & Hill 2003, 2005). We calculated UV chroma ($R_{300\text{-}400}/R_{300\text{-}700}$), red chroma ($R_{625\text{-}700}/R_{300\text{-}700}$), yellow-red ($R_{570\text{-}700}/R_{300\text{-}700}$), and hue values in each spectral range defined as the wavelength at maximum reflectance as there were the major reflectance peaks obtained.

Data analysis

All analysis were performed in R 4.0.3 (R Core Team, 2014), and figures were produced using the R package 'ggplot2' (Wickham 2016). Values are shown as means ± SEs.

Following Playà-Montmany et al. 2021, we used generalized estimating equations (GEE) approach to simultaneously identify critical limits of TNZ (T_{lc} and T_{uc}) using the 'lme4' package (Bates *et al.* 2014) and a modified version of the 'segmented' package (Muggeo 2009). The difference between T_{uc} and T_{lc} values was used to calculate TNZ breadth. The inflection point of EWL was also calculated using 'lme4' and 'segmented' packages. We performed a *t*-test to compare VO_2 and EWL values between individuals measured at the decreasing or increasing stepped T_a profiles (from 10 to 30°C and vice versa). No significant differences were found in the analysis (all results $p > 0.5$), so the order of T_a exposure was not considered in the models. A *t*-test was also used to compare physiological and morphological traits prior to treatment.

We analyzed repeatability and source of variance in feathers using 'rptR' library to quantify the constancy of feather traits (i.e., prior to and after heat waves simulation) following Nakagawa & Schielzeth (2010). The repeatability R value was calculated using a linear mixed-effect model (LMM) based on Gaussian distribution as data did not show substantial deviation from a normal distribution. Repeatability was significant for all morphological feather traits before and after heat waves simulation with the individual as a grouping factor (prior heat waves: R=0.36-0.72, p <0.05; after heat waves: R=0.44-0.76, p<0.05) except for the area (prior heat waves simulation: R = 0.24, p =0.11, see Supplementary Table 1). Reflectance data repeatability was significant in all traits evaluated (prior: R = 0.15-0.82, p=<0.001 and after heat waves simulation:

R=0.28-0.82, $p<0.05$) except for UV hue (300-400nm) (after heat waves simulation R=0.15, $p=0.11$, see Supplementary Table 1). Average values of measurements were used for posterior analysis except for not repeatable variables that were excluded.

To test the effect of simulated heat waves on physiological and morphological variables we built a series of generalized linear mixed models (GLMMs) using 'lme4' package (Bates *et al.* 2014). We provided *p*-values with the package lmerTest (Kuznetsova *et al.* 2017) using Satterthwaite's method. Models included physiological or feather traits as response variables, treatment (two levels: control and treatment), time (two levels: before and after heat waves simulation) and the interaction term as fixed factors. Individual identity was included as a random factor to account for multiple measures in the same individuals. For modelling metabolic and hygric variables, M_b was also included as a covariate.

Maximum room T_a was reached from 1:00 PM and 6:00 PM, and we used mean T_b values registered within this time range in the analysis of this trait. Treatment, heat wave number (three levels: second, third and four heat wave) and the interaction between both terms were included as fixed factors, as well as individual identity as a random factor. Tuckey *post hoc* pairwise comparisons between groups were made using the emmeans package (Lenth *et al.* 2019).

In all cases, normality of data was inspected using Q-Q and residual plots and log-transformation was applied to satisfy assumptions of normality when necessary. Multicollinearity was tested by calculating the variance inflation factor (VIF) among all predictor variables using the 'car' package (Fox & Weisberg 2019); we confirmed no collinearity problems (all VIF values < 5; see Zuur *et al.* 2010).

Results

Individuals of the control and treatment group did not display significant differences in any of the thermoregulatory traits or M_b prior to heat waves simulations (t-test, $p > 0.11$ in all cases). There were also no significant differences in $CORT_f$, oxidative damage, antioxidant capacity and TL prior to treatment (t-test, $p > 0.18$ in all cases). Similarly, contour feathers of Great tits of control and treatment groups displayed similar macrostructure and colouration prior to heat waves simulations (t-test, $p > 0.10$ all cases), except red chroma ($t_{18}=-3.38, p < 0.01$) and yellow red chroma ($t_{21}=-2.45, p < 0.05$), which were higher (by 16% and 5%, respectively) in the treatment group.

Thermoregulatory traits and body mass

Heat waves had a significant effect on Great tits T_b (Table 1, Figure 1). Our *post hoc* analysis showed heated individuals displayed higher T_b than controls during the second (42.07 ± 0.04°C vs 41.80 ± 0.04°C) and third (42.27 ± 0.10 vs 41.96 ± 0.05), but not during fourth (42.01 ± 0.05 vs 41.96 ± 0.05) heat wave simulation. The greatest T_b in the treatment group was achieved during the third heat wave (Figure 1). T_b of the control group did not change over the course of the treatment.

BMR as well as RMR, EWL and cooling efficiency at 40°C, decreased significantly over the course of the experiment by 10%, 6%, 32% and 25%, respectively (Table 1), with experimental Great tits showing greater reduction (by 17%) in BMR. Heat waves did not affect neither M_b nor the remaining thermoregulatory variables (Table 1). Descriptive statistics of physiological and morphological data are given in Table 2.

Table 1. Summary table of the GLMM testing effects of simulated heat waves on physiological and morphological variables in Mediterranean Great tits. Significant values ($p<0.05$) are highlighted in bold.

Variables	Factors and interactions	F	df	p
Physiological variables				
T_b	Heat wave number	5.65	2,334	**0.003**
	Treatment	9.57	1,24	**0.005**
	$\log M_b$	0.34	1,22	0.57
	Heat wave simulation × Treatment	3.81	2,334	**0.02**
BMR	Treatment	6.58	1,47	**0.01**
	Time	36.51	1,47	**<0.001**
	$\log M_b$	6.55	1,47	**0.01**
	Treatment × Time	1.33	1,47	0.25
RMR	Treatment	0.23	1,24	0.63
	Time	4.66	1,30	**0.04**
	$\log M_b$	2.65	1,30	0.11
	Treatment × Time	0.08	1,25	0.78

(Continues)

Table 1. (Continued)

Variables	Factors and interactions	F	df	p
Physiological variables				
EWL within TNZ	Treatment	1.77	1,24	0.20
	Time	0.12	1,27	0.73
	logM_b	6.40	1,28	**0.02**
	Treatment × Time	0.87	1,25	0.36
EWL at 40°C	Treatment	0.35	1,25	0.56
	Time	139.14	1,34	**<0.001**
	M_b	2.33	1,38	0.14
	Treatment × Time	2.32	1,25	0.14
Cooling efficiency at 40°C	Treatment	0.37	1,25	0.55
	Time	104.70	1,32	**<0.001**
	M_b	0.05	1,33	0.82
	Treatment × Time	2.52	1,25	0.12
TNZ	Treatment	0.56	1,31	0.45
	Time	4.67	1,31	**0.04**
	Treatment × Time	0.03	1,31	0.87
T_{lc}	Treatment	0.31	1,14	0.59
	Time	3.17	1,13	0.10
	Treatment × Time	1.11	1,13	0.31
T_{uc}	Treatment	1.95	1,21	0.18
	Time	1.21	1,14	0.65
	Treatment × Time	0.90	1,14	0.36
M_b	Treatment	0.38	1,25	0.54
	Time	31.16	1,25	**<0.001**
	Treatment × Time	3.55	1,25	0.07

(Continues)

Table 1. (Continued)

Variables	Factors and interactions	F	df	p
Corticosterone				
$CORT_f$	Treatment	0.21	1,20	0.65
	Time	0.02	1,19	0.90
	Treatment × Time	2.93	1,19	0.10
Oxidative status				
Antioxidant capacity	Treatment	0.02	1,20	0.88
	Time	18.14	1,20	**<0.001**
	Treatment × Time	2.04	1,20	0.17
Oxidative damage	Treatment	0.09	1,21	0.77
	Time	10.40	1,21	**0.004**
	Treatment × Time	5.04	1,21	**0.04**
Telomere length				
TL	Treatment	0.34	1,47	0.56
	Time	15.16	1,47	**<0.001**
	Treatment × Time	0.57	1,47	0.45
Feather morphology				
Density of plumulaceous barbs (per mm)	Treatment	15.67	1,25	**<0.001**
	Time	10.17	1,25	**<0.001**
	Treatment × Time	19.77	1,25	**<0.001**
Density of pennaceous barbs (per mm)	Treatment	0.03	1,25	0.86
	Time	6.61	1,25	**0.01**
	Treatment × Time	11.20	1,25	**0.002**
Density of plumulaceous barbules (per 0.1 mm)	Treatment	7.0	1,25	0.13
	Time	33.82	1,25	**<0.001**
	Treatment × Time	15.38	1,25	**<0.001**

(Continues)

Table 1. (Continued)

Variables	Factors and interactions	F	df	p
Feather morphology				
Density of pennaceous barbules (per 0.1 mm)	Treatment	1.16	1,25	0.29
	Time	31.5	1,25	**<0.001**
	Treatment × Time	38.15	1,25	**<0.001**
Proportion of plumulaceous barbs (%)	Treatment	1.33	1,25	0.25
	Time	0.18	1,25	0.66
	Time × Treatment	0.01	1,25	0.90
Length of the plumulaceous barb zone	Treatment	1.35	1,25	0.25
	Time	0.06	1,25	0.79
	Treatment × Time	0.55	1,25	0.46
Length of the pennaceous barb zone	Treatment	0.005	1,25	0.94
	Time	0.009	1,25	0.92
	Treatment × Time	0.39	1,25	0.53
Length of the feather (mm)	Treatment	0.24	1,25	0.62
	Time	0.05	1,25	0.82
	Treatment × Time	0.91	1,25	0.34
Feather coloration				
Log Plumage brightness	Treatment	0.49	1,28	0.49
	Time	22.80	1,25	**<0.001**
	Treatment × Time	2.05	1,27	0.16
UV chroma	Treatment	6.80	1,29	**0.01**
	Time	12.12	1,24	**0.002**
	Treatment × Time	5.76	1,25	**0.02**

(Continues)

Table 1. (Continued)

Variables	Factors and interactions	F	df	p
Feather coloration				
Red chroma	Treatment	18.95	1,28	**<0.001**
	Time	0.00	1,25	0.10
	Treatment × Time	0.02	1,26	0.89
Yellow red chroma	Treatment	14.23	1,23	**0.001**
	Time	2.12	1,22	0.16
	Treatment × Time	0.64	1,22	0.43
Log red hue	Treatment	7.70	1,27	**0.01**
	Time	22.09	1,25	**<0.001**
	Treatment × Time	1.48	1,26	0.23
Log yellow red hue	Treatment	7.70	1,27	**<0.001**
	Time	22.09	1,25	0.42
	Treatment × Time	1.48	1,26	0.66

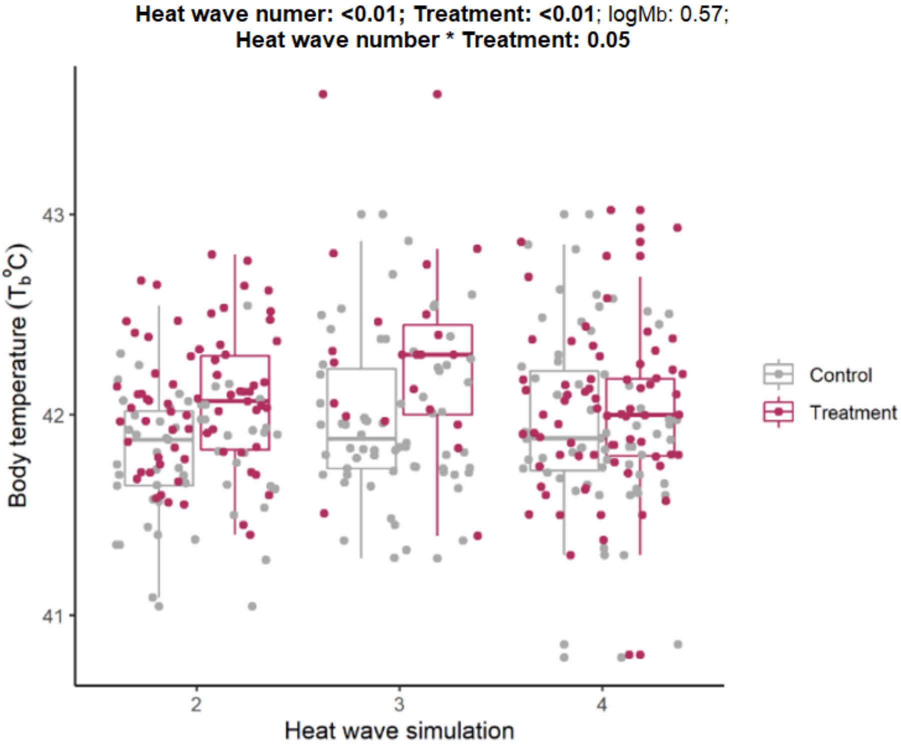

Figure 1 Effect of simulated heat waves on body temperature (T_b) in Mediterranean Great tits (n total in second heat wave = 23, n control = 11, n treatment =12; third heat wave = 17, n control = 12, n treatment = 5; and fourth heat wave = 23, n control = 11, n treatment = 12). The first and third quartile bound the boxes, the central line represents the median and whiskers represents 1.5 the interquartile range (default provided by R function 'boxplot').

Table 2. Descriptive statistics for Mediterranean Great tits physiological and morphological variables prior and after heat waves simulation.

Variables	Control						Treatment					
	Before heat waves			After heat waves			Before heat waves			After heat waves		
	n	Mean	ES	n	Mean	ES	N	Mean	ES	n	Mean	ES
Metabolic variables												
BMR	14	0.98	0.02	13	0.86	0.02	13	0.94	0.02	12	0.76	0.03
RMR at 40°C	14	1.15	0.02	14	1.07	0.04	13	1.113	0.05	11	1.02	0.04
EWL within TNZ	14	43.97	3.21	14	45.33	2.01	13	40.97	2.52	13	38.14	2.90
EWL at 40°C	14	450.59	12.34	14	323.15	13.56	13	449.07	20.51	13	288.81	15.49
Cooling efficiency at 40°C	14	0.79	0.02	14	0.61	0.02	13	0.79	0.02	13	0.56	0.03
TNZ breadth	9	16.54	1.12	9	13.21	1.20	11	17.37	1.48	6	14.53	1.76
T_{lc}	9	16.07	1.44	9	19.96	0.93	11	18.27	1.44	6	19.29	1.44
T_{uc}	9	32.61	1.37	9	33.16	0.95	11	35.64	1.13	6	33.82	1.30
M_b	14	16.54	1.12	14	16.12	0.42	13	16.55	0.42	13	16.02	0.31
Corticosterone												
$CORT_f$	13	18.85	1.66	11	21.13	1.61	13	22.23	1.88	11	19.70	1.58

(Continues)

Table 2. (Continued)

	Control						Treatment					
Variables	**Before heat waves**			**After heat waves**			**Before heat waves**			**After heat waves**		
	n	**Mean**	**ES**	**n**	**Mean**	**ES**	**N**	**Mean**	**ES**	**n**	**Mean**	**ES**
Oxidative status												
Antioxidant capacity	13	252.12	12.91	13	225.69	16.20	9	261.95	23.51	9	208.81	15.87
Oxidative damage	13	175.99	18.42	13	192.53	14.75	10	144.31	16.89	10	236.54	25.08
Telomere length												
TL	14	0.87	0.02	12	0.80	0.02	12	0.90	0.2	13	0.79	0.03
Feather morphology												
Density of plumulaceous barbs (per mm)	14	6.82	0.26	14	7.10	0.21	13	6.93	0.23	13	5.21	0.19
Density of pennaceous barbs (per mm)	14	4.05	0.17	14	4.22	0.14	13	4.75	0.36	13	3.45	0.18
Density of plumulaceous barbules (per 0.1 mm)	14	7.32	0.14	14	7.09	0.09	13	7.44	0.06	13	6.29	0.17

(Continues)

Table 2. (Continued)

Variables	Control						Treatment					
	Before heat waves			After heat waves			Before heat waves			After heat waves		
	n	Mean	ES	n	Mean	ES	N	Mean	ES	n	Mean	ES
Feather morphology												
Density of pennaceous barbules (per 0.1 mm)	14	5.23	0.12	14	5.29	0.10	13	5.74	0.12	13	4.53	0.11
Proportion of plumulaceous barbs (%)	14	0.60	0.01	14	0.60	0.01	13	0.59	0.01	13	0.59	0.01
Length of the plumulaceous barb zone	14	7.84	0.20	14	7.60	0.31	13	7.98	0.30	13	8.10	0.20
Length of the pennaceous barb zone	14	8.81	0.41	14	8.53	0.33	13	8.53	0.58	13	8.74	0.38
Length of the feather (mm)	14	16.66	0.46	14	16.13	0.55	13	16.51	0.57	13	16.84	0.46

(Continues)

Table 2. (Continued)

Variables	Control						Treatment					
	Before heat waves			After heat waves			Before heat waves			After heat waves		
	n	Mean	ES	n	Mean	ES	N	Mean	ES	n	Mean	ES
Feather colouration												
Plumage brightness	14	12239.58	944.98	15	14992.52	731.96	12	11817.71	1061.28	12	17135.22	571.23
UV chroma	14	0.24	0.00	14	0.26	0.00	13	0.24	0.00	12	0.24	0.00
Red chroma	14	0.21	0.00	15	0.22	0.01	13	0.25	0.01	12	0.25	0.00
Yellow-red chroma	14	0.36	0.01	15	0.35	0.01	12	0.38	0.01	12	0.37	0.00
Red hue	14	41.34	3.14	15	51.85	3.52	13	46.98	3.69	12	66.41	1.70
Yellow red hue	14	41.34	3.14	15	51.85	3.52	13	46.98	3.69	12	66.41	1.70

Feather CORT, oxidative status and telomere length

Neither simulated heat waves nor time had a significant influence on CORT_f (Table 1). Time, however, had a significant effect on d-ROMs and antioxidant capacity, with a significant interaction between treatment and time in the case of d-ROMs (Table 1). Antioxidant capacity decreased in both groups at the end of the treatment (Table 1, Figure 2A), but oxidative damage increased by 56% in birds exposed to heat waves while no significant variation was observed in control group (Table 2, Figure 2B). Telomeres shortened over time in both treated and untreated group, but TL was unaffected by heat waves (Table 1, Figure 4).

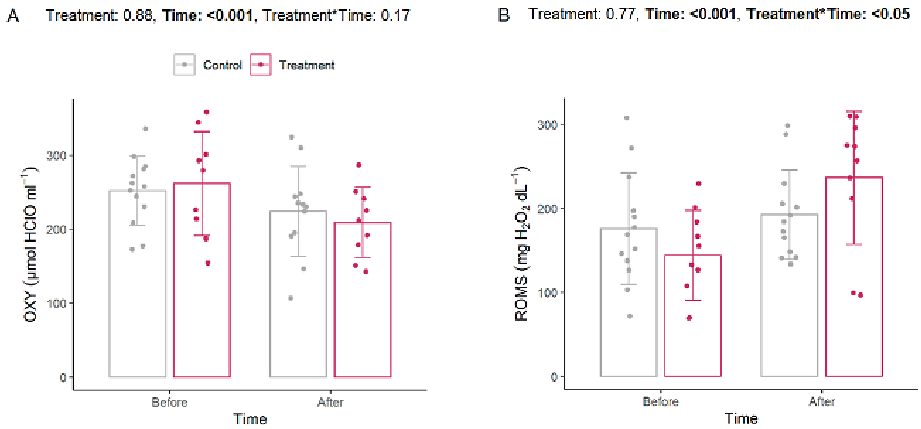

Figure 2 (A) Antioxidant capacity (OXY), and (B) oxidative damage (d-ROMs) in Mediterranean Great tits prior (n total OXY = 22, n control = 13, n treatment = 9; n total d-ROMs = 23, n control = 13, n treatment = 10) and after (n total OXY = 22, n control = 13, n treatment = 9; n total d-ROMs = 23, n control = 13, n treatment = 10) heat wave simulation of both, control and treatment group. Mean ± SE are shown along with individual points.

Feather structure and colouration

Barb and barbule density of plumulaceous and pennaceous parts of the contour feathers decreased more significantly over time in the treatment group than in the control group, while there were no differences in other feather traits between groups (Table 1, Figure 3). Individuals exposed to heat waves showed a significant reduction in the density of plumulaceous barbs (per mm) by 1.72, in the density of pennaceous barbs (per mm) by 1.30, in the density of plumulaceous barbules (per 0.1mm) by 1.15 and the density of pennaceous barbules (per 0.1mm) by 1.21 (Figure 3) when compared to the control group.

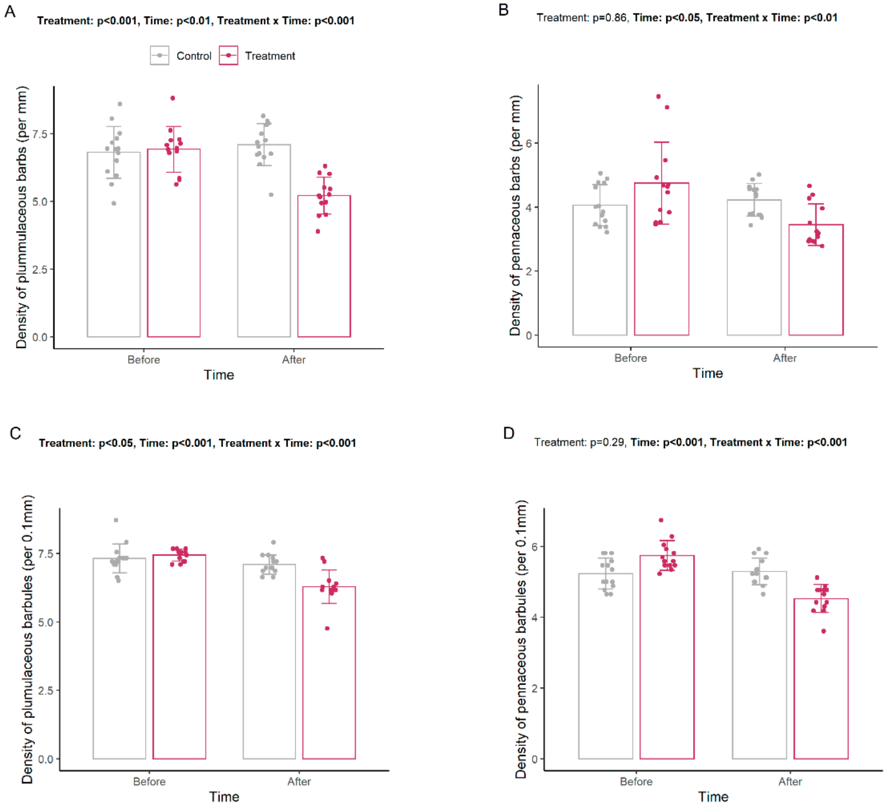

Figure 3 Heat wave simulation effect on feather macrostructure in Great tits (prior and after heat wave simulation: n total = 27, n control = 14, n treatment = 13): (A) density of plumulaceous barbs (per mm), (B) density of pennaceous barbs (per mm), (C) density of plumulaceous barbules (per 0.1mm) and, (D) density of pennaceous barbules (per 0.1mm). Mean ± SE are shown along with individual points.

Treatment group displayed greater values for red hue and yellow red hue (both by 41%) in the new contour feathers after heat waves simulation (Figure 4). The interaction term was significant for UV chroma (Table 1), being higher in the control group after moulting. Plumage brightness and red hue changed over time in both groups (Table 1), with birds showing greater values after moulting their contour feathers.

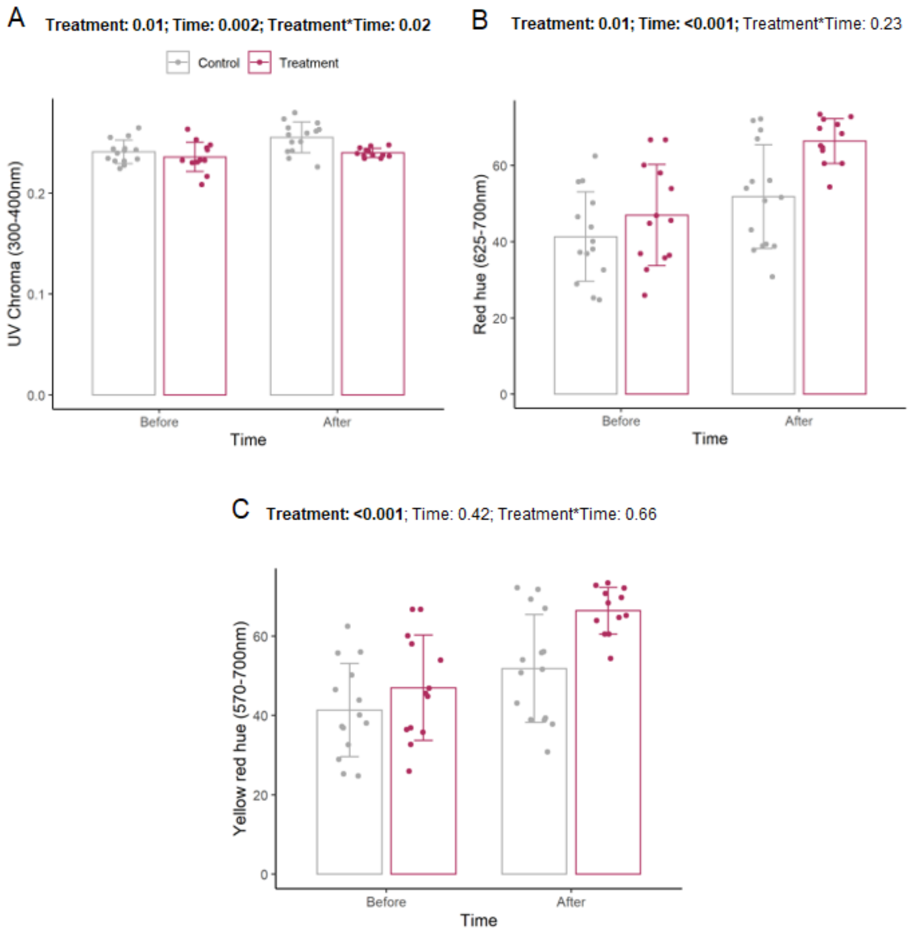

Figure 6 (A) UV chroma, (B) red hue and (C) yellow red hue in Mediterranean Great tits prior (n total UV chroma = 27, n control = 14, n treatment = 13; n total red hue = 27, n control = 14, n treatment = 13; n total yellow red hue = 27, n control = 14, n treatment = 13) and after (n total yellow red hue = 26, n control = 14, n treatment = 12; n total red hue = 27, n control = 15, n treatment = 12; n total yellow red hue = 23; n control = 11, n treatment = 12). Mean ± SE are shown along with individual points.

Discussion

The accuracy of assessments of vulnerability to extreme heat events will be improved by considering multiple characteristics of species' thermal physiology. We investigated how heat waves affect a suite of traits including those that are assumed to represent aspects of tolerance to high temperatures in songbirds and other small-sized endotherms. Current Iberian populations of resident songbirds, including Great tits, have notably high within-population phenotypic flexibility across a range of thermal traits (Chapter 3). Our experimental findings supported the notion of strong phenotypic adjustments to cope with extreme heat conditions, which facilitated T_b and BMR adjustments and changes in contour feather morphology to favour thermoregulation. However, these adjustments were not without costs for the whole organism, as they led to increased oxidative stress.

There is a large body of literature supporting the flexibility of thermoregulatory traits in endotherms to cope with changing environmental conditions (e.g., Schlichting & Pigliucci 1998; Piersma & Drent 2003; Lovette & Fitzpatrick 2016). Facultative hyperthermia – T_b values above the normothermic range of ~40-41°C during the active phase, and reaching levels as high as 45-47°C (Tieleman & Williams 1999; Gerson *et al.* 2019) – is an effective mechanism to cope with high T_a, as it provides a favourable gradient for heat loss, which translates into energy and water savings (Tieleman & Williams 1999; McKechnie & Wolf 2010, 2019; Nilsson *et al.* 2016; Gerson *et al.* 2019; Ton *et al.* 2021). Facultative hyperthermia is a well-known strategy for arid-zone birds to avoid overheating (Thompson *et al.* 2018; Gerson *et al.* 2019). While nocturnal facultative hypothermia has been demonstrated in a number of small songbirds from temperate regions, including Great tits (Broggi *et al.* 2004; Nord *et al.* 2009; Nilsson *et al.* 2020), no experimental studies assessed T_b responses to heat waves in small Mediterranean songbirds. Our novel data suggested that Great tits potentially use facultative hyperthermia as an effective via of heat dissipation, as it was recently suggested (Chapter 2).

Although thermoregulatory demands are expected to increase metabolic rate, BMR downregulation in birds facing physiological challenges, including heat stress, is assumed to be an energy-saving mechanism to maintain M_b above a critical level and maximize fitness (e.g., Gutiérrez *et al.* 2011; McKechnie 2008; Gerson *et al.* 2019). In our experiment, BMR decreased in both Great tit groups, but a greater reduction occurred in the treatment group. This strong BMR downregulation together with potential facultative hyperthermia might be key components of the pathways to maintain M_b and for facing other challenges posed by heat waves to Mediterranean songbirds. Studies assessing the effect of elevated T_a on birds M_b show inconsistent results (Andrew *et al.* 2017; Oswald *et al.* 2021; Ton *et al.* 2021). Our results are in line with previous research conducted in a small songbird well-adapted to arid areas as the Zebra finch *Taeniopygia guttata*, where the impact at M_b and other traits due to exposition to T_a exceeding 40°C during several consecutive was non-significant (Cooper *et al.* 2020). Sharpe et al. (2019), on the other hand, assessing the impact of heat waves on the small songbird Jacky winters *Microeca fascinans*, found that exposure to T_a above 42°C resulted in M_b loss (about 2%), but individuals were able to regain M_b between heat wave periods (minimum of 4-6 cooler days) and without long-term negative effects. It must be noted that in our experimental conditions Great tits had no water and food constraints, so heat waves may have not forced birds to significant dehydration nor faster energy reserve mobilisation, being able to maintain or regain M_b during the cooler days between heat waves.

Given that unpredictable extreme weather events such as heat waves may result in HPA activation (Moagi *et al.* 2021), we expected an elevation in CORT in feathers grown during heat waves, as the endocrine system is a vital component of animals' reaction to environmental perturbations (Bortolotti *et al.* 2008; Xie *et al.* 2017; Ruuskanen *et al.* 2021). However, recent studies reported mixed responses of CORT to heat stress in birds. For example, while high daily maximum air temperatures were associated with elevated faecal glucocorticoid metabolites (fGCM) in free-living Pied babblers *Turdoides bicolor* (Moagi *et al.* 2021), Ngcamphalala et al. (2021) found no evidence for an increase in fGCM concentrations in response to hot conditions ranging from 42 to 44°C in captive individuals of the same and other species, consistent to our results in Great tits. The lack of influence of heat waves on $CORT_f$ deposition supports the idea that they did not elicit a general stress response in Great tits, which may be because they had constant access to unlimited food and water during experiment that permits birds to replenish body water and offset increased EWL required for evaporative cooling, removing a potential source of stress associated with high temperatures (Xie *et al.* 2017; Brischoux *et al.* 2020).

Increased whole-body T_b, dehydration and greater mitochondrial activity have been proposed as causes of alterations in the oxidative status of ecto- and endotherms in response to extreme T_a (Beaulieau & Constantini 2014; Stachlschmidt *et al.* 2017; Jacobs *et al.* 2020). In birds, while there is considerable evidence from poultry species that oxidative damage increases in response to heat stress (e.g., Sahin *et al.* 2003; Lin *et al.* 2008) data in wild species are scarce (Jimenez *et al.* 2020). Markers of oxidative damage in experimental Great tits increased after heat waves simulation compared to control individuals, while antioxidant capacity decreased in both groups over the course of the experiment, although despite no significant effect, the drop was more conspicuous in treatment Great tits (20% vs 10%). Thus, the incapability to compensate for increased ROS production with antioxidant scavengers resulted in greater oxidative stress in heated individuals. At the molecular level, high levels of ROS can damage DNA, proteins and lipids, impairing cellular function and biological structures feasibility (Skrip & McWilliams 2016). While prolonged exposure to increasingly intense and frequent heat waves could eventually trigger telomere shortening due to oxidative stress (Zhang *et al.* 2018; Chatelain *et al.* 2020), we did not find an effect of heat waves in TL of Great tits either, since, both treatment and control individuals showed shorter telomeres at the end of the experiment. A previous study in Great tit (Stier et al. 2021), however, showed increases T_a of 2°C during postnatal growth accelerated telomere shortening, but this was not explained by oxidative stress. These contrasting findings might be related to the age of Great tits, as during postnatal development birds were not capable of fully thermoregulating and increased energy demand. Thus, at least in the short-term, the cellular function of Mediterranean Great tits appeared to be unaffected by heat waves exposition, but we cannot rule out that oxidative damage ultimately translates into telomere shortening in the long-term future as result of longer and more intense heat waves occurrence.

It is well established that feathers play a key role in thermoregulation (Walsberg 1988), but it is difficult to establish which macrostructure might favour heat loss, as several feather characteristics have been proven to alter heat flux (e.g., Broggi *et al.* 2011; Pap *et al.* 2017; Sándor *et al.* 2022). A lower proportion of barbs and barbules in the plumulaceous section allow a greater volume of air to be in contact with the body, and a higher density of barbs in the pennaceous section allows this air to be trapped (Butler *et al.* 2008). The reduced density of barbs and barbules in the pennaceous region in our heated individuals, therefore, might favour greater air pockets to be released, enhancing body heat loss. Nevertheless, this issue remains unsolved as previous research showed mixed results (see Broggi *et al.* 2011; Pap *et al.* 2017; Sándor *et al.* 2022). Sándor et al. (2022), for example, found longer plumulaceous and pennaceous sections, as well as reduced barb density, in urban Great tits exposed to warm conditions, whilst Pap et al. (2017) found species inhabiting colder environments also have a longer plumulaceous section, low barb density and reduced pennaceous barbule density. If we consider the lower density of barbs in the pennaceous section to be related to increased body heat dissipation, we can assume this morphological change in the contour feathers of treatment birds could be an adaptive advantage by decreasing the risk of lethal hyperthermia and energy expenditure (Nord & Wilsson 2019).

Experimental individuals also displayed more yellowish contour feathers. The characteristic yellow breast of the Great tit is a carotenoid-based-plumage (Quesada & Senar 2007). Carotenoids, in turn, become key to immune function and antioxidant defence which may trade-off with sexual signalling (Bertrand *et al.* 2006). As animals cannot synthesise carotenoids (Fox 1976), this colour signals the ability of birds to obtain high-quality food (Møller *et al.* 2000). However, both groups had access to similar food availability. Thus, a plausible explanation of colour differences might be related to feather structure. As experimental birds reduced the density of barbs and barbules, a greater concentration of carotenoids may have occurred leading to a more intense yellow. Anyway, the greatest yellow and yellow red hue values observed in heated birds suggest carotenoids to be related to this stressor. In fact, a recent review showed a clear relationship between carotenoid-based-plumage and temperature (Prasetya *et al.* 2020). This way, carotenoids may have a relevant role in bird thermal balance, but this is being overlooked and the actual physiological mechanism that alters carotenoid deposition or reallocation remains largely undescribed (Fitze *et al.* 2009). Further studies are needed to shed some light on this issue as several intertwined pathways might be taken place. Lastly, we obtained UV chroma to be significantly affected, but we have no reasonable explanation for the results obtained as significant variation was registered in the control group.

References

Andreasson, F., Nord, A., & Nilsson, J. Å. (2018) Experimentally increased nest temperature affects body temperature, growth and apparent survival in blue tit nestlings. Journal of Avian Biology 49(2), jav-01620.

Andrew, S. C., Hurley, L. L., Mariette, M. M., & Griffith, S. C. (2017) Higher temperatures during development reduce body size in the zebra finch in the laboratory and in the wild. Journal of evolutionary biology 30(12), 2156-2164.

Atema, E., Oers, K. V., & Verhulst, S. (2013) GAPDH as a control gene to estimate genome copy number in great tits, with cross-amplification in blue tits. Ardea 101, 49-54.

Avilés, J. M., Parejo, D., & Rodríguez, J. (2011) Parental favouritism strategies in the asynchronously hatching European Roller (*Coracias garrulus*). Behavioral Ecology and Sociobiology 65(8), 1549-1557.

Bartholomew, G. A. & Cade, T. J. (1963) The water economy of land birds. Auk 80, 504-539.

Bates, D., Mächler, M., Bolker, B., & Walker, S. (2014) Fitting linear mixed-effects models using lme4. Journal of statistical software 67, 1-48.

Beaulieu, M., & Costantini, D. (2014) Biomarkers of oxidative status: missing tools in conservation physiology. Conservation Physiology 2(1).

Bertrand, S., Faivre, B., & Sorci, G. (2006) Do carotenoid-based sexual traits signal the availability of non-pigmentary antioxidants?. Journal of Experimental Biology 209(22), 4414-4419.

Bonamour, S., Chevin, L. M., Charmantier, A., & Teplitsky, C. (2019) Phenotypic plasticity in response to climate change: the importance of cue variation. Philosophical Transactions of the Royal Society B 374(1768), 20180178.

Bortolotti, G. R., Marchant, T. A., Blas, J., & German, T. (2008) Corticosterone in feathers is a long-term, integrated measure of avian stress physiology. Functional Ecology 22(3), 494-500.

Boyles, J.G., Seebacher, F., Smit, B. & McKechnie, A.E. (2011) Adaptive thermoregulation in endotherms may alter responses to climate change. Integrative and Comparative Biology 51, 676–690.

Broggi, J., Gamero, A., Hohtola, E., Orell, M., & Nilsson, J. Å. (2011) Interpopulation variation in contour feather structure is environmentally determined in great tits. PloS one 6(9), e24942.

Burtt Jr, E. H., & Ichida, J. M. (2006) Selection for feather structure. Acta Zoologica Sinica 52, 131-135.

Butler, L. K., Rohwer, S., & Speidel, M. G. (2008) Quantifying structural variation in contour feathers to address functional variation and life history trade-offs. Journal of Avian Biology, 39(6), 629-639.

Cade, T. J., Tobin, C. A., & Gold, A. (1965) Water economy and metabolism of two estrildine finches. Physiological Zoology 38(1), 9-33.

Calder, W. A., & J. R. King. (1974) Thermal and caloric relations of birds. In d. S. Farner and J. R. King [eds.], Avian biology Vol. IV. Academic Press, New York.

Caro, S. P., & Visser, M. E. (2009) Temperature-induced elevation of basal metabolic rate does not affect testis growth in great tits. Journal of Experimental Biology 212(13), 1995-1999.

Catry, I., Catry, T., Patto, P., Franco, A. M., & Moreira, F. (2015) Differential heat tolerance in nestlings suggests sympatric species may face different climate change risks. Climate Research 66(1), 13-24.

Cerrano, C., Arillo, A., Azzini, F., Calcinai, B., Castellano, L., Muti, C., Valisano, L., Zega, G. & Bavestrello, G. (2005) Gorgonian population recovery after a mass mortality event. Aquatic Conservation: Marine and Freshwater Ecosystems 15(2), 147-157.

Charmantier, A., McCleery, R. H., Cole, L. R., Perrins, C., Kruuk, L. E., & Sheldon, B. C. (2008) Adaptive phenotypic plasticity in response to climate change in a wild bird population. science 320(5877), 800-803.

Chatelain, M., Drobniak, S. M., & Szulkin, M. (2020) The association between stressors and telomeres in non-human vertebrates: a meta-analysis. Ecology letters 23(2), 381-398.

Conradie, S. R., Woodborne, S. M., Cunningham, S. J., and McKechnie, A. E. (2019) Chronic, sublethal effects of high temperatures will cause severe declines in southern African arid-zone birds during the 21st century. Proceedings of the National Academy of Science, 201821312

Cooper, C. E., Hurley, L. L., & Griffith, S. C. (2020) Effect of acute exposure to high ambient temperature on the thermal, metabolic and hygric physiology of a small desert bird. Comparative Biochemistry and Physiology Part A: Molecular & Integrative Physiology 244, 110684.

Costantini, D., & Dell'Omo, G. (2006) Effects of T-cell-mediated immune response on avian oxidative stress. Comparative Biochemistry and Physiology Part A: Molecular & Integrative Physiology 145(1), 137-142.

Cunningham, S. J., Gardner, J. L., & Martin, R. O. (2021) Opportunity costs and the response of birds and mammals to climate warming. Frontiers in Ecology and the Environment 19(5), 300-307.

Cunningham, S. J., Martin, R. O., Hojem, C. L., & Hockey, P. A. (2013) Temperatures in excess of critical thresholds threaten nestling growth and survival in a rapidly-warming arid savanna: a study of common fiscals. PLoS One 8(9), e74613.

Danner, R. M., Coomes, C. M., & Derryberry, E. P. (2021) Simulated heat waves reduce cognitive and motor performance of an endotherm. Ecology and evolution 11(5), 2261-2272.

DesRochers, D. W., Reed, J. M., Awerman, J., Kluge, J. A., Wilkinson, J., van Griethuijsen, L. I., Aman, J. & Romero, L. M. (2009) Exogenous and endogenous corticosterone alter feather quality. Comparative Biochemistry and Physiology Part A: Molecular & Integrative Physiology 152(1), 46-52.

Drumond, A., Liberato, M. L., Reboita, M. S., & Taschetto, A. S. (2019) Weather and climate extremes: Current developments. Atmosphere 11(1), 24.

du Plessis, K. L., Martin, R. O., Hockey, P. A., Cunningham, S. J., & Ridley, A. R. (2012) The costs of keeping cool in a warming world: Implications of high temperatures for foraging, thermoregulation and body condition of an arid-zone bird. Global Change Biology 18(10), 3063-3070.

DuBois, K., Williams, S. L., & Stachowicz, J. J. (2020) Previous exposure mediates the response of eelgrass to future warming via clonal transgenerational plasticity. Ecology 101(12), e03169.

Fey, S. B., Siepielski, A. M., Nusslé, S., Cervantes-Yoshida, K., Hwan, J. L., Huber, E. R., Fey M. J., Catenazzi, A. & Carlson, S. M. (2015) Recent shifts in the occurrence, cause, and magnitude of animal mass mortality events. Proceedings of the National Academy of Sciences 112(4), 1083-1088.

Fitze, P. S., Cote, J., San-Jose, L. M., Meylan, S., Isaksson, C., Andersson, S., Rossi, J-M., & Clobert, J. (2009) Carotenoid-based colours reflect the stress response in the common lizard. PLoS One 4(4), e5111.

Fitzpatrick, L. J., Olsson, M., Pauliny, A., While, G. M., & Wapstra, E. (2021) Individual telomere dynamics and their links to life history in a viviparous lizard. Proceedings of the Royal Society B 288(1951), 20210271.

Fox, D. L. (1976) Animal Biochromes and Structural Colours: Physical, Chemical, Distribution & Physiological Features of Coloured Bodies in the Animal World. University of California Press.

Fox, J., & Weisberg, S. (2019) An R companion to applied regression, 3rd ed. Sage.

Funghi, C., McCowan, L. S., Schuett, W., & Griffith, S. C. (2019) High air temperatures induce temporal, spatial and social changes in the foraging behaviour of wild zebra finches. Animal Behaviour 149, 33-43.

Gardner, J. L., Amano, T., Sutherland, W. J., Clayton, M., & Peters, A. (2016) Individual and demographic consequences of reduced body condition following repeated exposure to high temperatures. Ecology 97(3), 786-795.

Gardner, J. L., Rowley, E., de Rebeira, P., de Rebeira, A., & Brouwer, L. (2018) Associations between changing climate and body condition over decades in two southern hemisphere passerine birds. Climate Change Responses 5(1), 1-14.

Gerson, A. R., McKechnie, A. E., Smit, B., Whitfield, M. C., Smith, E. K., Talbot, W. A., McWhorter, T. J. & Wolf, B. O. (2019) The functional significance of facultative hyperthermia varies with body size and phylogeny in birds. Functional Ecology 33(4), 597-607.

IPCC (2021) Summary for Policymakers. In: Climate Change 2021: The Physical Science Basis. Contribution of Working Group I to the Sixth Assessment Report of the Intergovernmental Panel on Climate Change. Cambridge University Press. https://www.ipcc.ch/report/ar6/wg1

Jacobs, P. J., Oosthuizen, M. K., Mitchell, C., Blount, J. D., & Bennett, N. C. (2020) Heat and dehydration induced oxidative damage and antioxidant defenses following incubator heat stress and a simulated heat wave in wild caught four-striped field mice *Rhabdomys dilectus*. PloS one 15(11), e0242279.

Kelly, M. W., Sanford, E. & Grosberg, R. K. (2012) Limited potential for adaption to climate change in a broadly distributed marine Crustacean. Proceedings of the Royal Society B: Biological Sciences 279, 349–356.

Kemp, R., Freeman, M. T., van Jaarsveld, B., Czenze, Z. J., Conradie, S. R., & McKechnie, A. E. (2020) Sublethal fitness costs of chronic exposure to hot weather vary between sexes in a threatened desert lark. Emu-Austral Ornithology 120(3), 216-229.

Kuznetsova, A., Brockhoff, P. B., & Christensen, R. H. (2017) lmerTest package: tests in linear mixed effects models. Journal of statistical software 82(13), 1-26.

Kvist, A., & Lindström, Å. (2001) Basal metabolic rate in migratory waders: Intra-individual, intraspecific and seasonal variation. Functional Ecology 15, 465-473.

Laczi, M., Hegyi, G., Nagy, G., Pongrácz, R., & Török, J. (2020) Yellow plumage colour of Great Tits Parus major correlates with changing temperature and precipitation. Ibis 162(1), 232-237.

Lenth, R., Singmann, H., Love, J., Buerkner, P., & Herve, M. (2019) Package 'emmeans'.

Lighton, J.R.B. (2008) Measuring Metabolic Rates: A Manual for Scientists. Oxford
University Press, Inc., New York

Lin, H., De Vos, D., Decuypere, E., & Buyse, J. (2008) Dynamic changes in parameters of redox balance after mild heat stress in aged laying hens (*Gallus gallus domesticus*). Comparative Biochemistry and Physiology Part C: Toxicology & Pharmacology 147(1), 30-35.

Lovette, I. J., & Fitzpatrick, J. W. (Eds.). (2016) Handbook of bird biology. John Wiley & Sons.

McKechnie, A. E. (2008) Phenotypic flexibility in basal metabolic rate and the changing view of avian physiological diversity: a review. Journal of Comparative Physiology B, 178(3), 235-247.

McKechnie, A. E., & Lovegrove, B. G. (2002) Avian facultative hypothermic responses: a review. The Condor 104(4), 705-724.

McKechnie, A. E., & Wolf, B. O. (2010) Climate change increases the likelihood of catastrophic avian mortality events during extreme heat waves. Biology letters 6(2), 253-256.

McKechnie, A. E., & Wolf, B. O. (2019) The physiology of heat tolerance in small endotherms. Physiology 34(5), 302-313.

McKechnie, A. E., Gerson, A. R., & Wolf, B. O. (2021) Thermoregulation in desert birds: scaling and phylogenetic variation in heat tolerance and evaporative cooling. Journal of Experimental Biology 224(Suppl_1), jeb229211.

McKechnie, A. E., Hockey, P. A., & Wolf, B. O. (2012) Feeling the heat: Australian landbirds and climate change.

McNab, B. K. (2002) The Physiological Ecology of Vertebrates: A View from Energetics. Ithaca, New York: Cornell University Press. P. 587.

Molina, M. O., Sánchez, E., & Gutiérrez, C. (2020) Future heat waves over the Mediterranean from an Euro-CORDEX regional climate model ensemble. *Scientific reports*, 10(1), 1-10.

Møller, A. P., Biard, C., Blount, J. D., Houston, D. C., Ninni, P., Saino, N., & Surai, P. F. (2000) Carotenoid-dependent signals: indicators of foraging efficiency, immunocompetence or detoxification ability. Avian and Poultry Biology Reviews 11(3), 137-159.

Muggeo, V. M. R. (2009) Segmented: An R package to fit regression models with broken-line relationships (pp. 20–25). R News 8.1. https://cran.rproject.org/package=segmented

Mujahid, A., Yoshiki, Y., Akiba, Y., & Toyomizu, M. (2005) Superoxide radical production in chicken skeletal muscle induced by acute heat stress. Poultry Science 84(2), 307-314.

Nakagawa, S., & Schielzeth, H. (2010) Repeatability for Gaussian and non-Gaussian data: a practical guide for biologists. Biological Reviews 85(4), 935-956.

Nilsson, J. Å., Molokwu, M. N., & Olsson, O. (2016) Body temperature regulation in hot environments. PloS one 11(8), e0161481.

Noakes, M. J., Wolf, B. O., & McKechnie, A. E. (2016) Seasonal and geographical variation in heat tolerance and evaporative cooling capacity in a passerine bird. Journal of Experimental Biology 219(6), 859-869.

Nord, A., & Nilsson, J. Å. (2019) Heat dissipation rate constrains reproductive investment in a wild bird. Functional Ecology 33(2), 250-259.

Oswald, K. N., Smit, B., Lee, A. T., Peng, C. L., Brock, C., & Cunningham, S. J. (2021) Higher temperatures are associated with reduced nestling body condition in a range-restricted mountain bird. Journal of Avian Biology 52(8).

Pap, P. L., Vincze, O., Wekerle, B., Daubner, T., Vágási, C. I., Nudds, R. L., Dyke, G. J. & Osváth, G. (2017) A phylogenetic comparative analysis reveals correlations between body feather structure and habitat. Functional ecology 31(6), 1241-1251.

Pfaffl, M. W. (2007) Relative quantification. In Real-time PCR (pp. 89-108). Taylor & Francis.

Piersma, T., & Drent, J. (2003) Phenotypic flexibility and the evolution of organismal design. Trends in Ecology & Evolution 18(5), 228-233.

Pipoly, I., Preiszner, B., Sándor, K., Sinkovics, C., Seress, G., Vincze, E., Bókony, V. & Liker, A. (2022) Extreme hot weather has stronger impacts on avian reproduction in forests than in cities. Frontiers in Ecology and Evolution 10.

Playà-Montmany, N., González-Medina, E., Cabello-Vergel, J., Parejo, M., Abad-Gómez, J. M., Sánchez-Guzmán, J. M., Villegas, A. & Masero, J. A. (2021) The thermoregulatory role of relative bill and leg surface areas in a Mediterranean population of Great tit (*Parus major*). Ecology and evolution 11(22), 15936-15946.

Pollock, H. S., Brawn, J. D., & Cheviron, Z. A. (2021) Heat tolerances of temperate and tropical birds and their implications for susceptibility to climate warming. Functional Ecology 35(1), 93-104.

Prasetya, A. M., Peters, A., & Delhey, K. (2020) Carotenoid-based plumage colour saturation increases with temperature in Australian passerines. Journal of Biogeography 47(12), 2671-2683.

Quesada, J., & Senar, J. C. (2007) The role of melanin-and carotenoid-based plumage coloration in nest defence in the great tit. Ethology 113(7), 640-647.

Ruthrof, K. X., Breshears, D. D., Fontaine, J. B., Froend, R. H., Matusick, G., Kala, J., Miller, B. P., Mitchell, P. J., Wilson, S. K., van Keulen, M., Enright, N. J., Law, D. J., wernberg, T. & Hardy, G. E. S. J. (2018) Subcontinental heat wave triggers terrestrial and marine, multi-taxa responses. Scientific Reports 8(1), 1-9.

Ruuskanen, S., Hsu, B. Y., & Nord, A. (2021) Endocrinology of thermoregulation in birds in a changing climate. Molecular and Cellular Endocrinology 519, 111088.

Sahin, K., Onderci, M., Sahin, N., Gursu, M. F., & Kucuk, O. (2003) Dietary vitamin C and folic acid supplementation ameliorates the detrimental effects of heat stress in Japanese quail. The Journal of nutrition 133(6), 1882-1886.

Salaberria, C., Celis, P., López-Rull, I., & Gil, D. (2014) Effects of temperature and nest heat exposure on nestling growth, dehydration and survival in a Mediterranean hole-nesting passerine. Ibis 156(2), 265-275.

Salmón, P., Nilsson, J. F., Nord, A., Bensch, S., & Isaksson, C. (2016) Urban environment shortens telomere length in nestling great tits, *Parus major*. Biology Letters 12(6), 20160155.

Salmón, P., Nilsson, J. F., Watson, H., Bensch, S., & Isaksson, C. (2017) Selective disappearance of great tits with short telomeres in urban areas. Proceedings of the Royal Society B: Biological Sciences 284(1862), 20171349.

Sándor, K., Seress, G., Sinkovics, C., Péter, Á., & Liker, A. (2022) Differences in feather structure between urban and forest great tits: constraint or adaptation?. Journal of Avian Biology, e02922.

Sapolsky, R. M., Romero, L. M., & Munck, A. U. (2000) How do glucocorticoids influence stress responses? Integrating permissive, suppressive, stimulatory, and preparative actions. Endocrine reviews 21(1), 55-89.

Saunders, D. A., Mawson, P., & Dawson, R. (2011) The impact of two extreme weather events and other causes of death on Carnaby's black cockatoo: a promise of things to come for a threatened species?. Pacific Conservation Biology 17(2), 141-148.

Schlichting, C., & Pigliucci, M. (1998) Phenotypic evolution: a reaction norm perspective.

Sharpe, L., Cale, B., & Gardner, J. L. (2019) Weighing the cost: the impact of serial heatwaves on body mass in a small Australian passerine. Journal of Avian Biology 50(11).

Siefferman, L., & Hill, G. E. (2003) Structural and melanin coloration indicate parental effort and reproductive success in male eastern bluebirds. Behavioral ecology 14(6), 855-861.

Siefferman, L., & Hill, G. E. (2005) Evidence for sexual selection on structural plumage coloration in female eastern bluebirds (*Sialia sialis*). Evolution 59(8), 1819-1828.

Simide, R., Angelier, F., Gaillard, S., & Stier, A. (2016) Age and heat stress as determinants of telomere length in a long-lived fish, the Siberian sturgeon. Physiological and Biochemical Zoology 89(5), 441-447.

Smit, B., Zietsman, G., Martin, R. O., Cunningham, S. J., McKechnie, A. E., & Hockey, P. A. R. (2016) Behavioural responses to heat in desert birds: implications for predicting vulnerability to climate warming. Climate Change Responses 3(1), 1-14.

Stahlschmidt, Z. R., French, S. S., Ahn, A., Webb, A., & Butler, M. W. (2017) A simulated heat wave has diverse effects on immune function and oxidative physiology in the corn snake (*Pantherophis guttatus*). Physiological and Biochemical Zoology 90(4), 434-444.

Stettenheim, P. R. (2000) The integumentary morphology of modern birds—an overview. American Zoologist 40(4), 461-477.

Stier, A., Hsu, B. Y., Cossin-Sevrin, N., Garcin, N., & Ruuskanen, S. (2021) From climate warming to accelerated cellular ageing: an experimental study in wild birds. bioRxiv.

Stillman, J. H. (2019) Heat waves, the new normal: summertime temperature extremes will impact animals, ecosystems, and human communities. Physiology 34(2), 86-100.

Tapper, S., Nocera, J. J., & Burness, G. (2020) Experimental evidence that hyperthermia limits offspring provisioning in a temperate-breeding bird. Royal Society open science 7(10), 201589.

Thompson, M. L., Cunningham, S. J., & McKechnie, A. E. (2018) Interspecific variation in avian thermoregulatory patterns and heat dissipation behaviours in a subtropical desert. Physiology & behavior 188, 311-323.

Tieleman, B. I., & Williams, J. B. (1999) The role of hyperthermia in the water economy of desert birds. Physiological and Biochemical Zoology 72(1), 87-100.

Ton, R., Stier, A., Cooper, C. E., & Griffith, S. C. (2021) Effects of heat waves during post-natal development on mitochondrial and whole body physiology: an experimental study in zebra finches. Frontiers in physiology 12, 554.

Tracy, C. R., Welch, W. R., & Porter, W. P. (1980) Properties of air. A manual for use in biophysical ecology, 3rd ed. Technical manual UW Laboratory for Biophysical Ecology.

Udino, E., George, J. M., McKenzie, M., Pessato, A., Crino, O. L., Buchanan, K. L., & Mariette, M. M. (2021) Prenatal acoustic programming of mitochondrial function for high temperatures in an arid-adapted bird. Proceedings of the Royal Society B 288(1964), 20211893.

Viceto, C., Cardoso Pereira, S., & Rocha, A. (2019) Climate change projections of extreme temperatures for the Iberian Peninsula. Atmosphere 10(5), 229.

Walsberg, G. E. (1988) Heatflow through avian plumages: the relative importance of conduction, convection, and radiation. Journal of Thermal Biology 13, 8992

Wegmann, M., Voegeli, B., & Richner, H. (2015) Oxidative status and reproductive effort of great tits in a handicapping experiment. Behavioral Ecology 26(3), 747-754.

Whitfield, M. C., Smit, B., McKechnie, A. E., & Wolf, B. O. (2015) Avian thermoregulation in the heat: scaling of heat tolerance and evaporative cooling capacity in three southern African arid-zone passerines. The Journal of experimental biology 218(11), 1705-1714.

Wickham, H. (2016) Programming with ggplot2. In ggplot2 (pp. 241–253). Springer.

Wojciechowski, M. S., Kowalczewska, A., Colominas-Ciuró, R., & Jefimow, M. (2021) Phenotypic flexibility in heat production and heat loss in response to thermal and hydric acclimation in the zebra finch, a small arid-zone passerine. Journal of Comparative Physiology B 191(1), 225-239.

Wolf, B., & Walsberg, G. (1996) Respiratory and cutaneous evaporative water loss at high environmental temperatures in a small bird. The Journal of experimental biology 199(2), 451-457.

Xie, S., Romero, L. M., Htut, Z. W., & McWhorter, T. J. (2017) Stress responses to heat exposure in three species of Australian desert birds. Physiological and Biochemical Zoology 90(3), 348-358.

Zhang, Q., Han, X., Hao, X., Ma, L., Li, S., Wang, Y., & Du, W. (2018) A simulated heat wave shortens the telomere length and lifespan of a desert lizard. Journal of thermal biology 72, 94-100.

Zuur, A. F., Ieno, E. N., & Elphick, C. S. (2010) A protocol for data exploration to avoid common statistical problems. Methods in Ecology and Evolution 1(1), 3–14.

Supplementary material: Appendix 2

Supplementary Table 1. Repeatability calculations for feather traits of Great tit individuals before and after heat waves. Repeatability (R) was performed as per Nakagawa and Schielzeth (2010) using the 'rptR' package for R and restricted maximum likelihood method. Estimation of repeatability was conducted with a linear mixed-effect model based on Gaussian distribution. Significant values are highlighted in bold.

Variables	Before heat waves		After heat waves	
	R	P	R	P
Feather structure				
Density of plumulaceous barbs (per mm)	0.44	**0.01**	0.64	**<0.001**
Density of pennaceous barbs (per mm)	0.65	**<0.001**	0.76	**<0.001**
Density of plumulaceous barbules (per 0.1 mm)	0.36	**0.03**	0.46	**0.01**
Density of pennaceous barbules (per 0.1 mm)	0.40	**0.02**	0.63	**<0.001**
Proportion of plumulaceous barbs (%)	0.50	**0.003**	0.51	**0.002**
Length of the plumulaceous barb zone	0.38	**0.02**	0.54	**0.001**
Length of the pennaceous barb zone	0.73	**<0.001**	0.75	**<0.001**
Length of the feather (mm)	0.55	**0.001**	0.75	**<0.001**
Area (mm^2)	0.24	0.11	0.44	**0.01**
Feather reflectance				
Brightness	0.54	**<0.001**	0.28	**0.01**
UV chroma	0.45	**<0.001**	0.81	**<0.001**
Red chroma	0.78	**<0.001**	0.78	**<0.001**
Yellow red chroma	0.69	**<0.001**	0.82	**<0.001**
Red hue	0.64	**<0.001**	0.76	**<0.001**
Yellow red hue	0.64	**<0.001**	0.76	**<0.001**

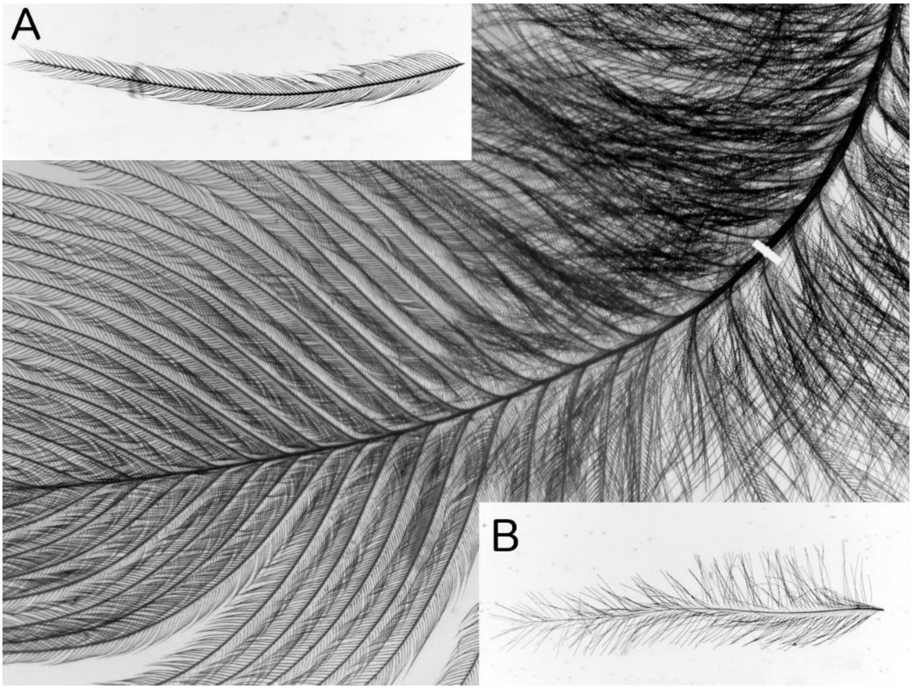

Supplementary Figure 1 Illustration of a contour feather obtained from an individual of Great tit. The distal part of the feather (left side of the white stripe on the rachis) shows the barbs of the pennaceous part, in detail in (A). The plumulaceous part is shown on the right side and detailed in (B).

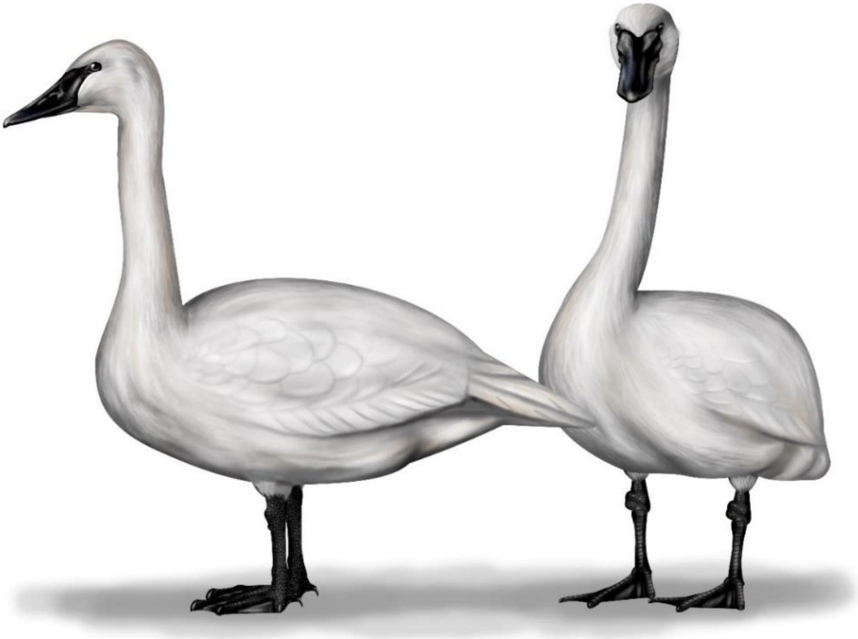

6

Spot size, distance and emissivity errors in field applications of infrared thermography

Núria Playà-Montmany and Glenn J. Tattersall

Methods in Ecology and Evolution (2021) 12(5), 828-840

Abstract

Infrared thermography is increasingly emerging as an analytical approach within the thermal ecology research community, providing unique and rapid temperature information crucial to understanding how plants and animals exchange heat with their environment. What is difficult to appreciate are the numerous ways in which thermography may still yield inaccurate (*i.e.,* deviation from the "correct" value) information if certain tenets are not followed. In this paper, we examine, demonstrate, and discuss these tenets with an aim to provide methodological advice to ecologists interested in employing thermography. We found that spot size and distance strongly influenced the surface temperature estimates of known, calibrated temperatures sources, with similar results observed in maximum eye temperature measurements in wild birds. We also report on how the angle of incidence affects the apparent emissivity of various biological surfaces (fur, feather, skin, leaves), another source of uncertainty in thermography. The variation in temperature caused by variation in distance and uncertainty in emissivity are large enough to raise flags for field applications of thermography where accuracy is necessary but control over study subjects is limited. Since accurate emissivity and distance parameters are crucial to thermography calculations, our results should serve as a framework to assist ecologists in better experimental design with respect to the use of thermography.

Keywords: thermal imaging, temperature measurement, non-invasive, distance, spot size, emissivity, error, variability

Introduction

Sources of potential error in infrared thermography are varied (Minkina & Dudzik 2009), although likely not fully appreciated and rarely acknowledged in many biological thermography research studies, especially those aimed at using non-invasive approaches with animals in the field. Recent attention has been paid to the technical aspects of infrared thermography (Chukwuka *et al.* 2019), error assessment in ecological thermography (Kim *et al.* 2018), repeatability of thermographic measurements in animal studies (Byrne *et al.* 2017), atmospheric emissivity errors in environmental thermography (OuYang *et al.* 2010), distance effects on between camera variability (Faye *et al.* 2016), assessment of environmental and microhabitat heterogeneity in plants (Scheffers *et al.* 2017; Mollinari *et al.* 2019), measurement of environmental temperatures in intertidal zones (Lathlean & Seuront 2014), and calculation of biophysical parameters such as stomatal conductance (Leinonen *et al.* 2006; Guilioni *et al.* 2008). Since the goal in ecological thermography is often to assess a surface temperature to infer an internal temperature or state, with many applications relying on maximum surface temperature extraction from moving targets with irregular and non-flat surfaces, accurate temperature estimation can be a challenge. It may be tempting to rely on manufacturer ratings of accuracy, but it behoves researchers to be aware that accuracy and precision are different concepts (Selvik & Abrahamsen 2017) and that devices that may appear precise are not necessarily accurate. For example, accuracy typically refers to how close an instrument is in providing the true value, whereas precision refers to the extent that repeated measurements agree with or are consistent with one another (see Table 1 for definitions).

Table 1. Definition of key terms in infrared thermal imaging.

Term	Definition
Accuracy	Accuracy refers to how close an instrument is in providing the true value. Typically reported as ±°C
Precision	Precision refers to the extent that repeated measurements agree with or are consistent with one another. Typically reported as ± °C.

(Continues)

Table 1. (Continued)

Term	Definition
Field of View (FOV)	FOV refers to the area that an imaging device actually captures at a given distance. It is often reported in Horizontal x Vertical degree units and thus is an angular measurement. HFOV refers specifically to the total width that the image sensor captures, and thus a wide angle lens has a large HFOV, while a telephoto lens has a small HFOV.
Instantaneous Field of View (IFOV)	IFOV refers to the smallest detail that can be detected within the FOV, at a specified distance. It is often reported in angular units milliradians.
Spot Size	Spot size is trigonometrically converted from the IFOV, and corresponds to the size of the smallest object whose temperature can be accurately assessed, at a set distance. By convention, the practically measurable spot size is 3 times the true spot size, due to vibration and uncertainty over spatial alignment of the spot being measured and the sensor pixel.
Microbolometer	A microbolometer is a particular type of detector used in long-wave infrared thermal imaging, where when radiation strikes the detector, the material is heated, thus changing its resistance. Typical infrared camera sensors consist of an array of these microbolometers that determine the spatial and imaging resolving capacity of the sensor.

(Continues)

Table 1. (Continued)

Term	Definition
Non-uniformity correction	In microbolometers, each sensor can undergo random, electronic drift over time, leading to non-uniform, gaussian noise in the detected image. These sensors require periodic, non-uniformity correction, where by the entire sensor array measures a common object (the shutter).
Blackbody	A blackbody is an idealised physical body that absorbs all incident radiation, and in thermal equilibrium this same body will emit a constant and known amount of electromagnetic black body radiation. Typically, it is used to calibrate infrared thermal imaging cameras.
Radiometric	Radiometric refers to electromagnetic radiation and is used in reference to file saving conventions being radiometric *vs.* non-radiometric. A radiometric file is one that retains the raw electromagnetic radiation information, whereas a non-radiometric file is one that retains no information on the radiance captured.
Lossless	Lossless data storage refers to a file compression technique that leads to no loss of quality in the raw data. For example, JPG files are not lossless, whereas TIFF files are lossless. Radiometric JPG files are a manufacturer-specific (FLIR) file type that retain the raw, captured radiance information.

To illuminate potential sources of uncertainty in field applications of thermography, we highlight the typical steps (see Figure 1) from object capture through to image presentation that contribute to error and uncertainty (see also Fernandez-Cuevas *et al.* 2015). Biological variation is the first source of variation (Figure 1a), being related to unmeasured physiological and morphological variation in insulation, tissue conductance, internal temperature; these cannot be controlled non-invasively. Errors and uncertainties that are external to the organism involve the physical environment (Figure 1b), namely the local ambient temperature, wind speed, and solar radiation, all of which impact surface temperatures through well understood heat transfer mechanisms (Jessen 2001). Less appreciated are the errors regarding emissivity (Figure 1c) of biological surfaces (Tracy 1979), which are often assumed from other studies due to difficulty in non-destructive measurements (Dodd 1981). With high emissivity (*i.e.,* >0.95) assumed of many biological surfaces (although values ranging from 0.91 to 0.97 have been reported for plant materials; Jones & Vaughan 2010), the error in temperature estimates may be small, but certainly not trivial especially when reflected temperature differs substantially from surface temperature (Tattersall 2016); more critical is that the angle of incidence of the object to the camera is known to alter the effective or apparent emissivity predictably and systematically (Holst 2000). These effects might not be obvious (although see Figure 2 for an example of this effect in avian thermography), but will contribute to errors in surface temperature estimation (Jiao *et al.* 2016) due to the difficulty in maintaining fixed angles on moving targets and because biological surfaces are rarely perfectly flat geometric shapes. Uncertainty related to object distance (Figure 1d) manifests from atmospheric influences, which follow Beer's law; for long-wave infrared (8-12 μm), it is primarily the water vapour in the atmosphere that absorbs infrared radiation and thereby attenuates the true target signal. Thermal imaging camera algorithms (Figure 1e) account for the degree of radiation absorption, provided the distance to target and atmospheric humidity are known (Minkina & Dudzik 2009). Users of thermography rely on these manufacturer's algorithms to account for most of the direct physical effects mentioned above, these algorithms convert the measured radiance into an estimated temperature based on ideal conditions measuring a calibrated blackbody radiation source. Many users may be unaware of this aspect, considering thermal cameras as temperature sensors, rather than radiance flux sensors that estimate surface temperature according to numerous assumptions. Indeed, Faye *et al.* (2016) demonstrated that temperatures were under-estimated as distance to object was increased in field thermography applications, even when using the appropriate calculation algorithms.

Final sources of variation in thermal imaging involve the quality of the camera, lens, and sensor (Figure 1f). The spatial and thermal resolution of the lens and camera not only allow for capture of fine details but are critical in resolving the true temperature of these details, since these properties set the minimum spot size the camera can reasonably measure (see Table 1 for definitions). Thus, low resolution, wide angle lens cameras, or cameras at far distance cannot properly resolve small, point heat sources present on a surface because the large spot size has averaged over a larger instantaneous field of view

(IFOV) to obtain a single temperature value for a particular pixel. Indeed, Holst (2000) recommends that the chosen spot size be ~3 times smaller than the desired minimum object size to obtain accurate pixel-based temperature resolution. Additional considerations in the variability pathway are still important (Figure 1g), reflecting good laboratory practice: cameras need to be calibrated to a blackbody source at the factory and should have electronic thermal stability controls and non-uniformity correction to account for electronic drift common in microbolometer based imagers; images should be captured to a lossless, radiometric image file for any post-capture processing or analysis (Figure 1h); finally, images should be in focus (Figure 1i) for accurate temperature assessment (Tattersall 2016). Although not critical to analysis, thermal images are typically displayed as false colour images, partly for visual appeal but importantly to communicate temperature differences. The scale or choice of colours can affect interpretation since the colour palette used can enhance small temperature differences and thereby inflate negligible responses that otherwise would seem mundane with simple grayscale imagery (Figure 1j). Since infrared thermography has begun to be used in ever wider applications and in increasingly challenging conditions, it is vital that researchers are aware of these common pitfalls and uncertainties and adopt a consistent approach to data collection and data sharing in order to ensure their data are internally consistent and accurate; this manuscript is written to serve as a place to start that discussion.

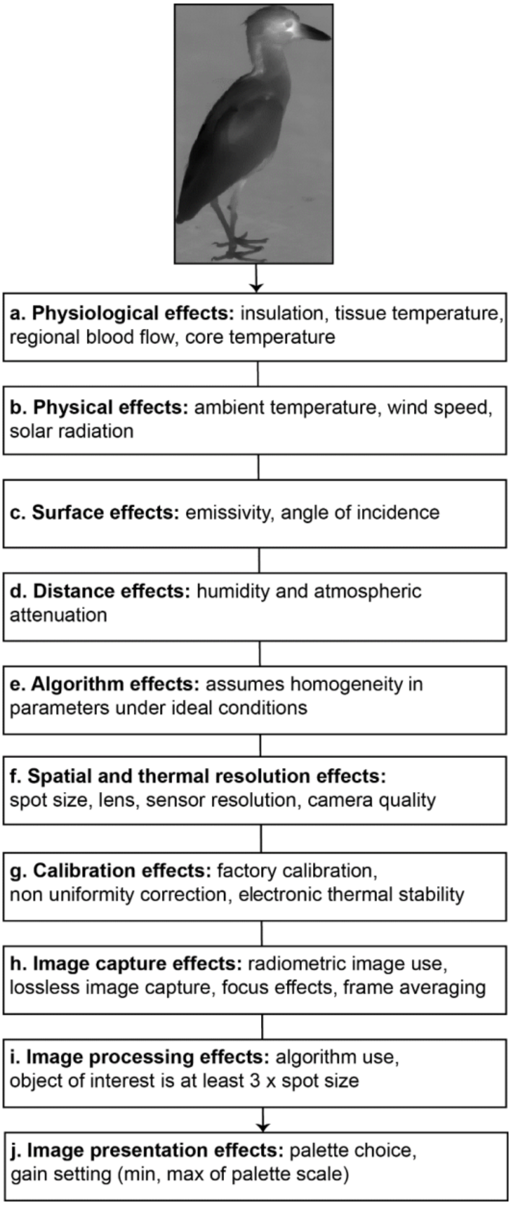

Figure 1 Conceptual workflow depicting the possible contributions to uncertainty in surface temperature estimation using thermal imaging starting from the object (top) to the presentation of the image (bottom). Each box depicts a step where assumptions or estimations are required.

In this study, we assess the degree of error of research grade thermal imaging cameras by manipulating typical parameters within a user's control, namely distance, angle, and external temperature. Formally we report on: 1) inter-camera temperature differences of a known object temperature, 2) how camera spot size and object distance impact the temperature estimates of a known, calibrated radiation source, and 3) the influence of angle of incidence on emissivity measurements of various biological materials (fur, feathers, reptile skin, leaves).

Material and Methods

Thermal Infrared Cameras

We used two research grade thermal cameras (see Table 2) with three lenses of different focal length to capture thermal images at various distances (see below) to estimate accuracy and error under a range of conditions. Since each lens is calibrated routinely by the manufacturer, these lens/camera combinations serve as 3 systematic sources of variance. The first thermal camera was a FLIR SC660 (FLIR SC660, FLIR Systems Inc., Wilsonville, Oregon, USA) with a lens of focal length of 75 mm (24°), and equipped with an uncooled microbolometer sensor that converts infrared radiation into temperature in the range of -40 to +120°C. The resolution is 640 × 480 pixels, and at 0.3 m, the instantaneous field of view (IFOV) or spatial resolution is 0.65 mrad. The measurement accuracy of the thermal camera was ±1°C or ±1% of reading for limited temperature range. The second thermal camera was the FLIR T1030sc (FLIR T1030sc, FLIR Systems Inc., Wilsonville, Oregon, USA) used with two different lenses, the wide angle lens with a focal length of 21.2 mm (45°) and an IFOV of 0.80 mrad and the telephoto lens with a focal length of 83.4 mm (12°) and an IFOV of 0.20 mrad. This thermal camera had a spectral range of 7.5 - 14 μm and its microbolometer sensor was set to detect an object temperature range from -40 to +150°C. The resolution was 1024 × 768 pixels and the measurement accuracy rated at ±1°C or ±1% of reading at 25°C for temperatures from 5°C to 150°C. Due to the potential for misinterpretation of the % of reading accuracy (*i.e.,* ±1% of 25°C is 0.25°C vs. 1% of the full scale range of 190°C is ±1.9°C), in all instances, we interpreted potential accuracy to be the greater of the values: thus, at 25°C, the worst-case accuracy for all cameras relative to the manufacturer's calibration could be as low as 0.25°C (unlikely) or as high as ±1.9°C. Images were saved in lossless radiometric JPG format (see Table 1 for definitions) or if captured as video, in FLIR's lossless radiometric video format (SEQ or CSQ).

Study System

We used a black body calibrator (BB703, Omega Company, Stamford, CT. USA) with an emissivity value of 0.95 to test the effect of distance on thermal metrics of surfaces; its target plate could achieve temperatures in the range of 11 to 400°C with an ambient temperature up to 25°C. We placed the black body calibrator in two different environments (inside vs. outside in Canadian winter) that differed according to the following environmental conditions: environmental temperature (T_a, °C), relative humidity (RH, %), wind speed (WS, $m \cdot s^{-1}$) and solar radiation (SR, $W \cdot m^{-2}$) that were collected during thermal image acquisition using a Kestrel® 4000 Pocket Weather Tracker and a Solar Meter (DBTU1300 digital solar power meter, General Tools and Instruments) pointed vertically. Collection of appropriate environmental data accompanied each thermal image. One environment was a 10 m corridor without windows in the laboratory (Brock University, St. Catharines, ON, Canada) where T_a and RH varied from 19.8 to 24.8°C and from 15.1 to 28% respectively, with WS=0 and SR=0. The second environment was outside, at the Brock University campus (43° 7' 3.84" N, 79° 14' 59.484" W). In this second environment, thermal images were acquired under a roof but under natural environmental conditions in February 2020. During the outdoor thermal image acquisition, T_a varied from -3.3 to 8.7°C, RH from 35 to 61.3%, WS from 0 to 2 m s^{-1} and SR from 23.7 to 475 W m^{-2} and the local winter photoperiod was 10-h of light. Aspects of our study design are similar to Faye *et al.* (2016), although we focused on within-camera error for the distance effects.

Table 2. Specifications for the three camera and lens combinations used in this study. All thermal cameras were calibrated within the recommended schedule of the manufacturer.

	FLIR SC660	FLIR T1030sc	FLIR 1030sc
Temperature Range	-40 to +120°C	-40 to +150°C	-40 to +150°C
Focal Length	75 mm	21.2 mm	83.4 mm

(Continues)

Table 2. (Continued)

	FLIR SC660	FLIR T1030sc	FLIR 1030sc
FOV (°)	24°	45°	12°
IFOV	0.65 mrad	0.8 mrad	0.2 mrad
Resolution	640 x 480	1024 x 768	1024 x 768
Min Focus Distance	0.3 m	0.2 m	0.6 m
Manufacturer Certified Accuracy	±1 °C or 1 % of reading	±1 °C or 1 % of reading	±1 °C or 1 % of reading

Distance and Spot Size Effects on Camera Offset (ΔT)

We used the three lenses of different focal length (21.2, 75, and 83.4 mm) described above to acquire thermal images at 0.3, 0.6, 1, 2, 3, 4, 5, 6, 7, 8, 9, and 10 m along a straight transect in front the black body calibrator, that was set up at 30, 40 and 50°C in both environments (laboratory and Brock University campus). The black body calibrator was placed 0.73 m height above ground level, at the same height of the thermal cameras that were positioned in a professional tripod (Alta Pro 263AT) to obtain an angle of view of 90° to the surface (Clark 1976) avoiding angle effects on temperature analysis. The height of the black body calibrator and the thermal cameras were not modified along each transect. The minimum focus distance of the lens of focal length 83.4 mm was 0.6 m which resulted in not acquiring thermal images of the black body calibrator at 0.3 m. We acquired 144 thermal images (2 environments × 3 black body calibrator temperatures × 12 distances) using the lenses of focal length of 21.2 and 75 mm, and 66 thermal images (2 environments × 3 black body calibrator temperatures × 11 distances) using the focal length lens of 83.4 mm. In total, we acquired 210 thermal images. Before thermal image acquisition started, the black body calibrator and the thermal cameras were switched on for 30 min to ensure temperature and sensor stabilisation, respectively.

Spot Size Calculations

Spot size is defined as the size in real dimensions that is represented by 1 pixel in captured images. We calculated spot size (mm) for each camera and distance using trigonometric formulae (Supplementary Figure 1) and details from the manufacturer's technical specifications:

$$Spot\ Size = \frac{1000 \cdot 2 \cdot d \cdot \tan\left(\frac{HFOV}{2}\right)}{p_h}$$

where d is the distance (m) from camera to object, $HFOV$ is the horizontal field of view (radians), and p_h is the sensor horizontal pixel resolution. Spot size is therefore higher for longer distances and cameras with larger fields of view, and smaller for higher resolution cameras.

Accuracy Assessment

We assessed inter-camera accuracy by comparing the estimated surface temperature of the blackbody source set to 30, 40, or 50 °C. Since our blackbody source has a stated accuracy of ±1.4°C, any measurement of the blackbody would be subject to an unknown offset of up to 1.4°C, therefore we chose the camera that was most recently factory calibrated (SC660, September 2019) as our standard. Thus, although our blackbody source was within factory specifications, it was still reading +1.2°C above set-point compared to our most accurate thermal camera, and therefore we report on the actual blackbody temperature rather than the set-point. We assume that the blackbody drift over the 2 weeks of experimentation was negligible, based on the manufacturer's reported stability (±0.3°C) and calibration sheet. During most distance comparisons, we collected data over the course of hours, so we are confident that the blackbody source temperature was stable. We verified the time course required for blackbody warm-up by conducting a separate series of ~30 minute trials to assess warm-up and stability of the blackbody source under the various environmental conditions examined (Supplementary Figure 2).

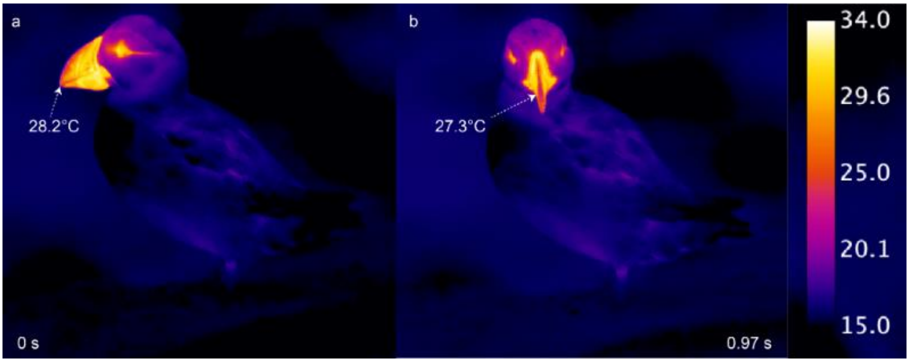

Figure 2 Sample images of the influence of angle on surface temperature estimation of the bill of an Atlantic Puffin (*Fratercula arctica*). The image in *b* was taken 0.97 seconds after the image in *a*, when the bird turned its head by ~90°. At low angle of incidence (a), the surface temperature appears 0.9°C higher than that assessed under high angle of incidence (b) conditions. Because the ambient temperature is ~16°C, the high angle under-estimates bill surface temperature due to the potential to reflect ambient temperature. This effect would be accentuated under conditions where the difference between surface and ambient conditions is greater.

Field Test of Distance Effects in Trumpeter swans

The ultimate test of the accuracy of thermography is in outdoor conditions without control over environmental conditions or object placement. This is well achieved in the field of wildlife imaging where animals are cautious of investigators, usually preventing close access. A population of Trumpeter swans (*Cygnus buccinator*) overwinters in Lake Ontario (La Salle Park, Burlington, Ontario, Canada), allowing for reasonably close access (1.5 to 10 m). Since each bird is tagged by the Trumpeter Swan Coalition (Lumsden 2018), we visited the study site with cooperation of the Conservation authorities. In total, 56 birds were imaged over the course of a 1-hour period to ensure similar environmental conditions. Unfortunately, we could not keep a constant distance to the birds, and soon noted that the effect of distance on estimated temperature was substantial. Distance was not readily measured in the field, so we adopted an indirect approach, using the area *vs*. distance relationship determined empirically in the blackbody test to allow us to estimate the distance for each image in the field from the area of the eye region, a part of the bird that was consistently measured by drawing an oval around the perimeter of the eye region excluding the feathers. Although this distance was an approximation, the values confirmed our field estimates (*i.e.,* the closest bird was appropriately calculated to be 1.5 m). Working in a public park, animals were not handled or manipulated during this study, and thus the variance in surface temperature measurements could be due to a host of biological (e.g., anticipation of food, stress, unknown pathologies) or physical parameters.

Angle Effects on Emissivity

We assessed the influence of incidence angle on apparent emissivity of numerous objects using a Leslie cube (10 cm × 10 cm × 10 cm; Supplementary Figure 3), built from welded copper sheets with tubing inlets and outlets on one side to allow for the continuous flow of thermostatically controlled water (60°C). A Leslie cube is a device used to demonstrate the different emission of radiation from surfaces held at a constant temperature. It is typically constructed as a hollow cube to be filled with hot water at a constant temperature, while the external surface consists of different materials that can be readily aimed at different angles at a device capable of recording emitted radiation. To ensure a substantial difference between emitted and reflected radiant energy from target surfaces, atmospheric temperature and reflected temperature were kept at 21° (assessed with a Kestrel 4000 portable weather thermometer). The reflected temperature was kept as close to room temperature by using a hanging cloth drape to reduce any point source reflected radiation (i.e., experimenter). The thermal imaging camera (FLIR SC660) was kept at 0.4 m for optimal accuracy.

We adhered target materials to one side of the Leslie cube (Supplementary Figure 3), using heat transfer paste on non-adhesive materials to assist with thermal equilibration. Materials examined were black electrical tape, Liquid Paper™, bond paper, Cassowary eggshell (*Casuarius casuarius*), peacock tail feather (*Pavo cristatus*), Canada goose feather (*Branta canadensis*), lizard skin (*Pogona vitticeps*), snake skin (*Crotalus durissus*), mink fur (*Neovison vison*), flamingo flower leaf (*Anthurium scherzerianum*), palm leaf (*Chamaedorea elegans*), polka dot plant leaf (*Hypoestes phyllostachya*), poinsettia leaf (*Euphorbia pulcherrima*), and peace lily leaf (*Spathiphyllum wallisii*). We verified that electrical tape and Liquid Paper exhibited similar emissivities (0.95) by painting a small section of electrical tape and verifying no difference in surface temperature estimates when the Leslie cube was filled with warm water (60°C). Thereafter, we painted Liquid Paper™ onto a small section of the biological surfaces to obtain their apparent emissivities by first comparing to this known emissivity. All materials were initially observed at incident angles of 0°, and a surface temperature estimated for each surface under this starting condition. Thermal images were then captured while rotating the Leslie cube every 5 degrees up to 75 degrees. Apparent emissivity (e_{app}) at each angle was determined using FLIR's built-in emissivity calculator tool, which uses radiance to temperature conversion algorithms to estimate the apparent surface emissivity required to produce the true temperature of the surface (determined from the initial 0° measurement).

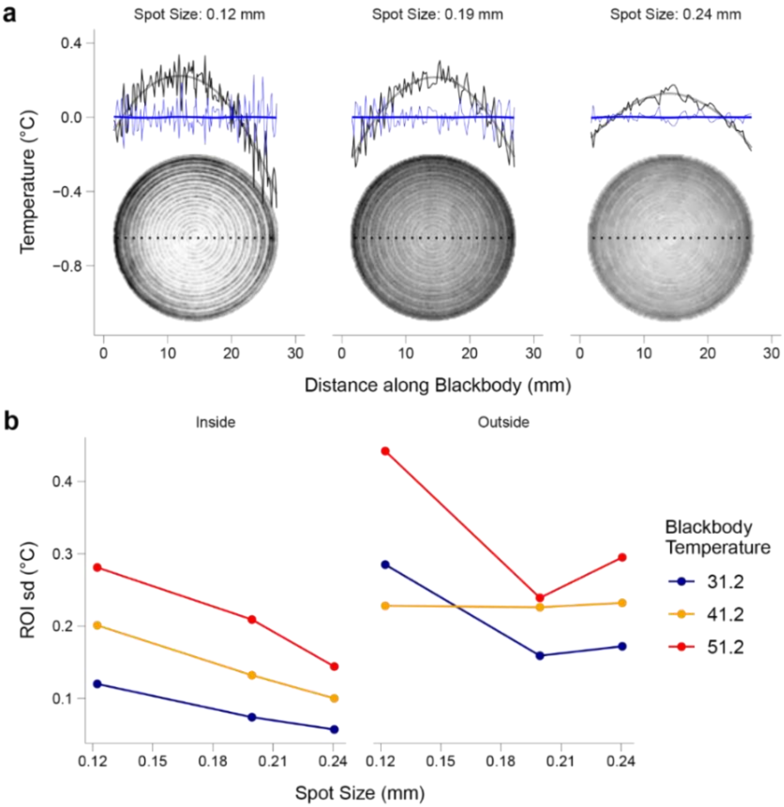

Figure 3 Camera spot size influences resolution and variability. Top graph (a) shows how 3 different spot sizes (0.12, 0.19, and 0.24 mm) depict the spatial resolution of a blackbody calibration source. Inset images are the same object captured at the minimum focal distance. Line profiles depict the temperature (grey, normalized to mean temperature; blue, residual of line profile) along a line transecting the mid-line of the image (dotted line). Bottom graph (b) depicts the variability (sd) of a region of interest (ROI) drawn around the entire image.

Image Analysis Process

Thermal imaging analysis was performed using FLIR's research analysis software (ResearchIR) and customised macros and functions in ImageJ (Tattersall 2019). We set all appropriate environmental parameters during thermal imaging analysis (emissivity, distance, atmospheric temperature, reflected temperature, and relative humidity). The emissivity of the black body calibrator was 0.95, atmospheric temperature was set to T_a and we assumed reflected environmental temperature to be equal to T_a (to minimize temperature measurement error resulting from background temperature). For the blackbody calibration source, a circular region of interest (ROI) over the entire black body calibrator region was digitally drawn to obtain surface average and maximum temperature and standard deviation, while avoiding the extreme edge of the blackbody source due to possible edge scattering artefacts. For analysis of the swan thermal images, we extracted only the maximum temperature in the periorbital region near the eye, often used as a proxy for core temperature (Jerem *et al.* 2015). For the materials emissivity assessments, ROIs were drawn over a central section of the material at each angle increment until the material was no longer visible (>75°).

Statistical Analysis

We performed linear modelling in R (R Core Team 2016) to assess the influence of predictor variables (distance, indoor/outdoor) on the offset temperature estimates of blackbody temperature (i.e., ΔT), where the offset refers to the difference in thermal image temperature compared to the closest range (0.3 or 0.6 m). Since spot size and distance strongly correlate, we used AIC values to compare competing models including either spot size or distance, although we also report the effect of distance for ease of interpretation and future field implementation. Visual inspection of residuals and quantile-quantile plots revealed no deviations from normality. For the influence of angle on emissivity, we fit loess smooths though the relationship between apparent emissivity and angle of incidence in order to facilitate calculation of threshold angles leading to a 0.05 or 0.1 decline in apparent emissivity (analogous to a 5 and 10% error). Plots were generated using the ggplot2 package (Wickham 2016).

Results

Camera Accuracy and Thermal Resolution

Although the blackbody calibration source required time to warm up (Supplementary Figure 2), our measurements were always taken during steady-state conditions. Estimates of accuracy reflect the best-case scenario (closest distance and indoors) given these devices. All cameras were technically accurate according to the manufacturer's specifications, deviating from each other by less than 1°C at the minimum focal distance (Supplementary Figure 4). Lower spot size lenses were clearly able to resolve spatial variation in the blackbody surface (Figure 3), manifesting in higher region of interest (ROI) variability. ROI variability of the blackbody source was higher outdoors compared to indoor conditions.

Distance and Spot Size Effects on ! T

Spot size yielded lower AIC scores (AIC=425.7 vs 460.4) than distance in a 2-way linear model with Camera as a fixed intercept ($\Delta T \sim$ Spot Size × Location + Camera *vs.* $\Delta T \sim$ Distance × Location + Camera; Figure 4), therefore we report the statistical results for spot size (Table 3). ΔT was negatively associated with spot size ($\beta_{spotsize} = -0.37$ °C/mm; $P<0.001$) and this effect was more profound when measurements were made outside ($\beta_{Outside} = -0.89$°C; $P<0.001$; $\beta_{Spotsize \times Outside} = -0.18$°C/mm; $P<0.001$).

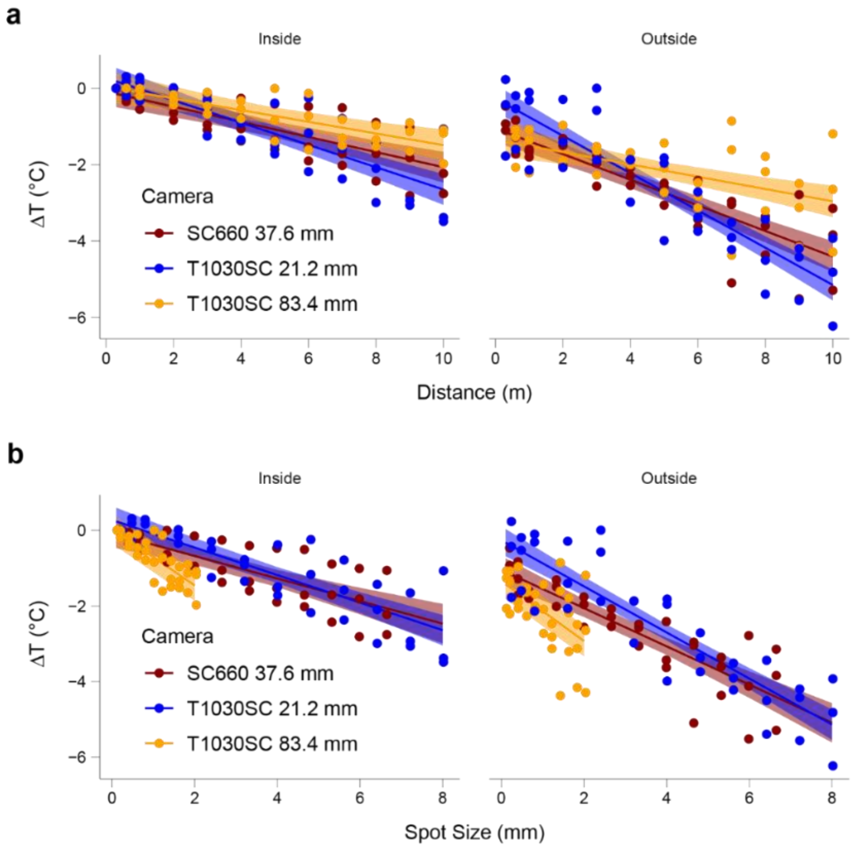

Figure 4 Distance from blackbody calibration source negatively influences the offset temperature (ΔT = difference in from indoor condition at minimum focal distance), with greater impact when under low ambient temperature conditions. A 2-way interaction between Spot Size × Location significantly influenced ΔT ($P < 0.001$). Under outdoor conditions, at 10 m, underestimation of temperature can be as higher as 6°C. The same data are plotted against distance (a) and spot size (b), since spot size is determined by distance to object, lens focal length, and sensor resolution.

Table 3. Model estimates from a linear model (ΔT ~ Spot Size × Location + Camera – 1) describing the influence of spot size, place of measurement and camera model in estimating the temperature difference (ΔT) from the true blackbody temperature. The reference (*i.e.,* intercept) camera in this model is the SC660.

Predictor	Estimate	CI	t	p
Spot Size (mm)	-0.37	-0.43 – -0.32	-12.51	**<0.001**
Location$_{\text{Inside}}$	0.14	-0.11 – 0.38	1.09	0.278
Location$_{\text{Outside}}$	-0.89	-1.14 – -0.65	-7.16	**<0.001**
Camera$_{\text{T1030SC 21.2 mm}}$	0.29	0.07 – 0.51	2.64	**0.009**
Camera$_{\text{T10130SC 83.4 mm}}$	-0.59	-0.83 – -0.35	-4.89	**<0.001**
Spot Size × Location$_{\text{Outside}}$	-0.18	-0.25 – -0.10	-4.47	**<0.001**
Observations	216			
Adjusted r^2	0.911			

Distance Effects in Wild Birds

Maximum eye temperatures among Trumpeter swans imaged in the field were negatively associated with distance to the camera (Figure 5a; β = -0.581°C/m; $F_{1,55}$=9.1; P=0.0039; r^2=0.126). We also tracked a single swan walking toward us over a ~45 second period (Figure 5b; Supplementary Video 1); maximum periorbital temperature was ~10°C cooler when measured at a distance (~10-15 m) compared to the close up images (1.5 m).

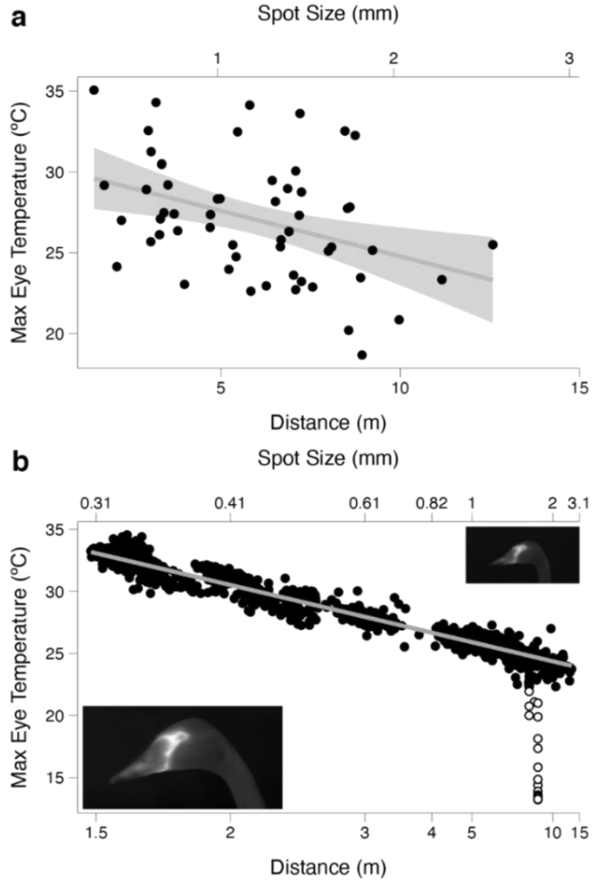

Figure 5 Maximum eye temperature in Trumpeter swans captured on a winter day. Top panel (a) represents eye temperatures from swans in a large aggregation (N=56). Lower panel (b) depicts the maximum temperature from a thermal video (30 frames/second) of a Trumpeter swan slowly walking toward the camera (see Supplementary Video 1). Inset thermal images are representative for close and far images. Distance was estimated from the area of pixels subtending the eye region, based on an empirical size:distance relationship for a known object. Maximum temperature represents the value of a single pixel in the periorbital region. White points represent a brief period where the camera was out of focus (excluded from the regression line shown in grey), showing how focus dramatically affects temperature estimates. Maximum temperature is inversely proportional to distance (spacing in the x-axis scale in b reflects distance^{-1} and spot size^{-1}).

Angle Effects on Emissivity

Increased angle of incidence led to declines in the apparent emissivity, but the strength of this effect varied depending on the nature of the tested materials (Figure 6). Initially, this effect manifests in an error in the apparent temperature as high as 8°C at the steepest angles, if the emissivity for the 0° angle is used to calculate temperature (Figure 6). Physical materials that were easy to adhere to the copper plate and had minimal roughness yielded smooth, monotonic angle effects on emissivity that became progressively steeper as angle increased. The biological materials were more varied, with certain materials showing only shallow declines in emissivity. Especially coarse materials with surface structure (lizard and snake skins), showed slightly irregular and materially different declines in emissivity. Thinner biological materials (feathers, leaves) that were easy to adhere to the Leslie cube to facilitate even heat transfer showed relatively smooth, monotonic decreases in emissivity with increasing angle of incidence. In general, any angles greater than 55 degrees led to a 5% decline in emissivity (see Table 4 for details).

Table 4. Emissivity values for various materials at 0° angle of incidence along with critical threshold angles of incidence.

Material	Emissivity	Critical Angle ($e_{-0.05}$; °)*	Critical Angle ($e_{-0.10}$; °)*
Black electrical tape	0.950	54.7	62.8
Liquid Paper™	0.953	41.5	63.7
Bond paper	0.901	63.0	68.4
Cassowary egg shell	0.910	55.0	62.2
Goose feather	0.959	38.7	58.4
Peacock feather	0.963	46.5	65.4
Lizard skin	0.941	64.8	74.5
Snake skin	0.959	54.8	67.2
Mink fur	0.919	56.1	>75
***Anthurian* leaf**	0.946	52.6	62.4
***Cycas* leaf**	0.948	58.0	66.2

(Continues)

Table 4. (Continued)

Material	Emissivity	Critical Angle ($e_{-0.05}$; °)*	Critical Angle ($e_{-0.10}$; °)*
***Hypoestes* leaf**	0.959	56.7	67.2
***Euphorbia* leaf**	0.966	56.1	65.3
***Spathiphyllum* leaf**	0.968	53.5	65.3
Average	0.946	55.6	66.1

*the threshold angle of incidence leading to a decline in emissivity of 0.05 or 0.10.

Discussion

Infrared thermal imaging has revolutionised thermal ecology (McCafferty 2007; Hristov *et al.* 2008; Tattersall & Cadena 2010; Tattersall 2016). The ease of capturing detailed surface temperatures has enhanced entire fields of research, ranging from welfare-related assessments of vasomotion and affective state (Herborn *et al.* 2015), to field thermal energetics (Tattersall *et al.* 2018), to pathological screening (Soerensen & Pedersen 2015), to live monitoring of evapotranspiration (Leinonen *et al.* 2006; Gutierrez *et al.* 2018), and to assessment of environment thermal heterogeneity (Scheffers *et al.* 2017; Mollinari *et al.* 2019). The downside of the relative ease of any technology, however, is that the onus is on the user to appreciate the limits to manufacturer stated accuracies apply to specific condition (Chukwuka *et al.* 2019). These accuracies have only been measured under prescribed conditions quite atypical of the field. We provide a framework to interpreting thermal imaging data and have examined how easily ignored parameters (distance, camera type, angle of incidence, emissivity) can influence the validity of the temperatures reported.

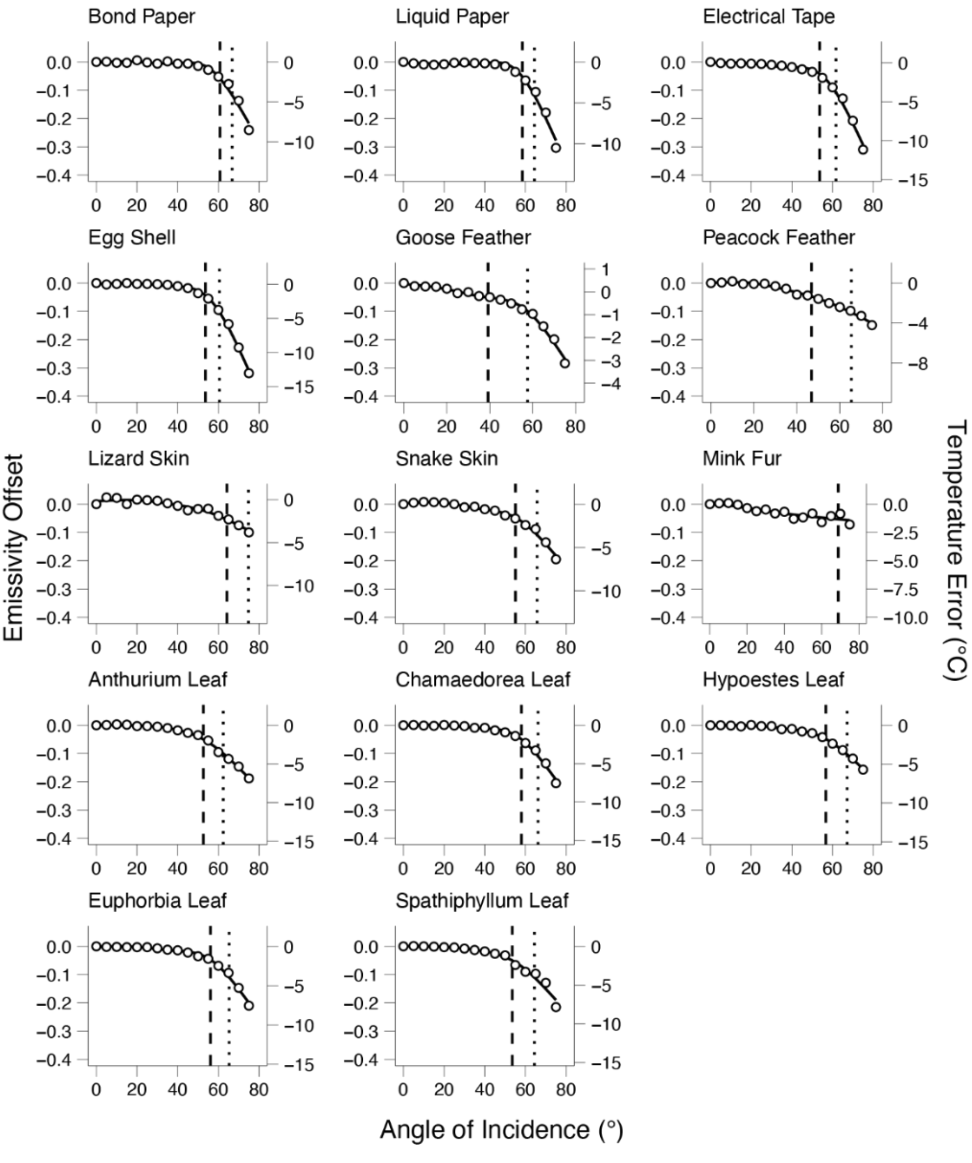

Figure 6 Apparent emissivity estimates (offset relative to true emissivity at 0°) for various physical, animal, and plant materials as a function of angle of incidence. Vertical lines represent the threshold angles corresponding to a 0.05 (dashed) and a 0.10 (dotted) decline in emissivity. Right hand y-axes depict the level of temperature error present if the apparent emissivity was not used, appropriate to the experimental conditions.

Camera Accuracy and Thermal Resolution

Under ideal conditions, all cameras performed within the manufacture's upper stated accuracy parameters, which is not itself remarkable. At close range, all three accurately estimated blackbody temperature within ±1°C of each other, even when measured non-synchronously. Points of confusion with this technology arise from the different quoted manufacturer accuracies (i.e., ±% of signal, ±% of full range of signal, or ±°C). In the case of these cameras, it appears that these devices are consistent with the most accurate quoted manufacturer range of ±1°C. Accuracy indoors erred on the positive side, whereas accuracy when measuring outside in the winter erred on the negative side (Supplementary Figure 4), suggesting contributions to accuracy result from the differences in the local environmental conditions. Thus, even under ideal conditions (close range examination of a stable black body calibration source), different cameras will not lead to identical temperature estimates, suggesting that studies involving different cameras or studies that span wide environmental conditions should consider, at minimum, that this level of uncertainty will be present in their analysis. In terms of thermal resolution, smaller spot size lenses captured higher variability from the same blackbody source (Figure 3), which is consistent with their enhanced resolving capacity. Thus, from a technical perspective the lenses behaved unremarkably and according to the manufacturer specifications.

Distance and Spot Size Underestimate Temperature

We demonstrated that even when incorporating the appropriate object parameters in the thermal image software, increasing distance away from our calibration source led to a linear increase in the apparent error in temperature (i.e*.,* ΔT was negatively related to distance and spot size), consistent with Faye *et al.* (2016) who compared thermal image variability from a point source. What is interesting about the distance and spot size effects is that the ΔT estimates can rise to as high as 6°C at only 10 m, which very much exceeds the manufacturer's upper level accuracy estimate of ±1.9°C, even when used in the laboratory. In addition to the clear effect of distance using a known object source temperature, we also observed that birds imaged from different distances exhibited similar effects on temperature estimates, although there remained considerable unexplained variance in maximum eye temperature (r^2=0.14; Figure 5). Because we imaged during the winter under cold ambient conditions, the surface temperatures estimated were likely lower as a result of the lower reflected temperature influencing the spot size limitations at further distances.

Spot Size Effects

Resolving fine details in long-wave infrared imaging is challenging due to numerous technical constraints. The response time of LWIR thermal cameras is slow (often in milliseconds range), which can pose challenges for capturing rapidly moving objects. For still imaging, the minimum resolvable spot size is determined by physical conditions (usually distance) and the optics of the imaging device. A commonly reported parameter from thermal imaging systems is the instantaneous field of view (IFOV), which is the angle (q) over which the detector integrates incoming radiation and reported as horizontal and vertical by the manufacturer. Under ideal conditions, the effective measuring IFOV (MIFOV) is the same as IFOV, although Holst (2000) recommends that due to phasing effects (i.e., slight vibration during image capture) and uncertainty of spot alignment with each pixel (Supplementary Figure 1), there are limits to the smallest measurable size and the target should be assumed to subtend up to 3×3 pixels, and thus:

$$\theta_{MIFOV} = 3 \cdot \theta_{IFOV}$$

In the case of capturing maximum eye temperature on animals from a distance, if we assume that the size of a surface blood vessel providing the source of heat has a size of 0.5 mm (Porter & Witmer 2016), then the appropriate minimum spot size would be 0.17 mm, which is not achievable even with any of the high quality research cameras used in this study at distances greater than 1 m (Figure 4). Clearly, caution is warranted when using thermography for accurate temperature assessment if distance effects are not fully controlled or considered, especially so when the surface temperature is suspected to be greatly different from the background temperature. Users of IRT should carefully assess the minimum spot size they plan to measure a priori, and design their data collection appropriately, setting minimum object distances according to the specifications of the equipment.

Angle of Incidence and Emissivity of Biological Surfaces

We also describe a range of influences of angle of incidence on emissivity, with the general response as expected (Holst 2000), with emissivity declining progressively with increasing angle of incidence; at angles over 50°, the emissivity estimates decline more steeply (Table 4). Rough surfaces, like reptile skin, did not show as large a decline in emissivity with angle of incidence, likely because the 3-dimensional structure scatters and reflects light (Xu *et al.* 2019) which appears to augment the emissivity at steep angles. Overall, these declines in emissivity highlight how changing angles in thermography would alter the estimated surface temperature if a constant emissivity is assumed. For example, we illustrated this effect from images captured of an Atlantic puffin 0.97 seconds apart (Figure 2), showing how a steep change in angle due to head movement can alter the bill temperature by ~1°C. Practically speaking, in the field, the angle of incidence is difficult to control when animals move and attempting to precisely measure these angles complicated by complex geometry of the body surface. In terms of complex environmental imaging, as might be present when capturing a leaves on a plant, not every surface has the same angle of incidence to the camera sensor, and attention to this source of variation seems warranted. However, the advantage to knowing how the apparent emissivity changes is that if the actual angle is known, then the appropriate calculations can be conducted to determine the actual surface temperature rather than the apparent one.

Recommendations for data reporting in field thermography

Some thermography applications primarily focus on detection of warm bodies without the need for accurate thermal data (Karp 2020), and thus issues raised in this study are not as germane. In contrast, recent attention to the use of thermography as a rapid, non-invasive tool for transiently capturing maximum surface temperatures highlights the need to evaluate the conditions wherein non-laboratory thermal images are captured. Indeed, a recent study on calves demonstrated that eye temperatures measured in field conditions with infrared thermal imaging only weakly correlate to core temperature and were not strongly predictive of pyrexia (Bell *et al.* 2020). These results contrast with those employing thermography to assess the potential for eye temperature changes to assess stress and welfare (Herborn *et al.* 2015; Jerem *et al.* 2015). Therefore, throughout this paper, we have attempted to demonstrate how many of the parameters in thermography are influenced by study design constraints. Given the broad range of disciplines using thermography, it will be difficult to standardise all reporting parameters and conditions, but we recommend at minimum reporting to include: distance to object, object emissivity, angle of incidence (or declare if the angle of incidence is greater than 45 degrees), atmospheric and reflected temperatures, wind speed or wind conditions, relative humidity, solar radiation or cloud conditions (see Table 5). Finally, if these specifics are unavailable for all images, then two approaches are advised. The first is to use objects of known temperature and emissivity (e.g., a portable black body calibrator) to estimate error empirically under typical measurement conditions and report on this uncertainty. The alternative approach would be to conduct an error analysis, modelling the range of uncertainty in the estimated temperatures across the range of possible parameter uncertainty (see Supplementary Figure 5; Tattersall 2016).

Conclusions

Infrared thermography is used in a range of disciplines, although there has been recent adoption in field of thermal ecology. We outlined in this paper various, common sources of variation in measurement and biological error that should be considered when planning a study with this technology. For animal thermography, variation in anatomical and physiological attributes such as insulation, tissue conductance, distance to blood vessels, and regional blood flow will all influence surface temperature. Other physiological contributions to surface temperature accuracies relate to thermoregulatory concepts and the extent to which peripheral temperatures are a by-product of core temperature regulation. Relying on maximum eye (i.e., periorbital region) temperature to precisely reflect internal temperatures in wild animals should be used very cautiously. Not only has this metric been shown to change with stress and with respect to relevant welfare indicators, but due to the widespread use of fever scanning in humans, a naïve adopter of thermography may be given the impression that core temperature can be extracted from maximum eye temperature. Since camera spot size is crucial to accurately assess small objects, the camera needs to be close enough to properly render the object of interest in sufficient detail to capture the true temperature, and the angle of incidence to the camera should be kept as low as possible for accurate data; this applies to all field based thermography, whether focussed on plants or animal biology. Controlling these parameters in the field is often a challenge, and so we recommend that care is made to record and analyse these potential causes of variation in field thermographic research. The general advice we can offer all field biologists using thermography is to conduct *a priori* calculations on what the minimum size of the object interest would be and to collect images at appropriate distances. Controlling angle of incidence is perhaps easier to manage with stationary objects and a challenge to control with moving targets, but especially difficult to achieve when imaging complex objects. In these cases, careful image quality control should result in minimally acceptable angles for the purposes of minimising emissivity errors.

Table 5. Recommended practises to follow and parameters to consider for field and laboratory thermal imaging studies.

	Recording Parameters	Reporting Parameters	Presenting Images
Essential	- Radiometric lossless files - Research grade software - Research grade camera - Ensure robust image focus - Use lens with spot size appropriate to object of interest	- Distance to object (m) - Emissivity (assumed or measured) - Uncertainty over angle of incidence - Atmospheric and reflected temperatures (°C) - Spotsize (mm) - Camera accuracy (±°C)	- Compare images at similar ranges (*i.e.,* max-min) values - Report temperature scale bar in image
Recommended	- Capture thermal videos to assist with focus challenges - Record sample of known temperature in field of view for empirical accuracy	- Solar radiation (W/m^{2}) - Wind speed (m/s) - Cloud cover (0-1)	- Use standard thermal palettes (greyscale, ironbow, rainbow) - Provide sample images in manuscripts - Share raw images for open access initiatives

References

Bell, D.J., Macrae, A.I., Mitchell, M.A., Mason, C.S., Jennings, A. & Haskell, M.J. (2020) Comparison of thermal imaging and rectal temperature in the diagnosis of pyrexia in pre-weaned calves using on farm conditions. Research in Veterinary Science 131, 259-265.

Byrne, D.T., Berry, D.P., Esmonde, H. & McHugh, N. (2017) Temporal, spatial, inter-, and intra-cow repeatability of thermal imaging. Journal of Animal Science 95, 970-979.

Chukwuka, C.O., Virens, J. & Cree, A. (2019) Accuracy of an inexpensive, compact infrared thermometer for measuring skin surface temperature of small lizards. Journal of Thermal Biology 84, 285-291.

Dodd, C.K. (1981) Infrared reflectance in chameleons (Chamaeleonidae) from Kenya. Biotropica 13, 161-164.

Faye, E., Dangles, O. & Pincebourde, S. (2016) Distance makes the difference in thermography for ecological studies. Journal of Thermal Biology 56, 1-9.

Fernandez-Cuevas, I., Marins, J.C.B., Lastras, J.A., Carmona, P.M.G., Carlo, S.P., Garcia-Concepcion, M.A. & Sillero-Quintana, M. (2015) Classification of factors influencing the use of infrared thermography in humans: A review. Infrared Physics & Technology 71, 28-55.

Guilioni, L., Jones, H.G., Leinonen, I. & Lhomme, J.P. (2008) On the relationships between stomatal resistance and leaf temperatures in thermography. Agricultural and Forest Meteorology 148, 1908-1912.

Gutierrez, S., Diago, M.A.P., Fernandez-Novales, J. & Tardaguila, J. (2018) Vineyard water status assessment using on-the-go thermal imaging and machine learning. Plos One 13.

Herborn, K.A., Graves, J.L., Jerem, P., Evans, N.P., Nager, R., McCafferty, D.J. & McKeegan, D.E.F. (2015) Skin temperature reveals the intensity of acute stress. Physiology & behavior 152, 225-230.

Holst, G.C. (2000) Common sense approach to thermal imaging. SPIE Optical Engineering Press; JCD Publishing, Bellingham, Wash., Winter Park, Fla.

Hristov, N.I., Betke, M. & Kunz, T.H. (2008) Applications of thermal infrared imaging for research in aeroecology. Integrative and Comparative Biology 48, 50-59.

Jerem, P., Herborn, K., McCafferty, D., McKeegan, D. & Nager, R. (2015) Thermal imaging to study stress non-invasively in unrestrained birds. Jove-Journal of Visualized Experiments 10.

Jessen, C. (2001) Temperature Regulation in Humans and Other Mammals. Springer-Verlag, Berlin.

Jiao, L., Dong, D.M., Zhao, X.D. & Han, P.C. (2016) Compensation method for the influence of angle of view on animal temperature measurement using thermal imaging camera combined with depth image. Journal of Thermal Biology 62, 15-19.

Jones, H.G. & Vaughan, R.A. (2010) Remote sensing of vegetation : principles, techniques, and applications. Oxford University Press, Oxford; New York.

Karp, D. (2020) Detecting small and cryptic animals by combining thermography and a wildlife detection dog. Scientific reports 10, 5220.

Kim, Y., Still, C.J., Roberts, D.A. & Goulden, M.L. (2018) Thermal infrared imaging of conifer leaf temperatures: Comparison to thermocouple measurements and assessment of environmental influences. Agricultural and Forest Meteorology 248, 361-371.

Lathlean, J. & Seuront, L. (2014) Infrared thermography in marine ecology: methods, previous applications and future challenges. Marine Ecology Progress Series 514, 263-277.

Leinonen, I., Grant, O.M., Tagliavia, C.P.P., Chaves, M.M. & Jones, H.G. (2006) Estimating stomatal conductance with thermal imagery. Plant Cell and Environment 29, 1508-1518.

Lumsden, H.G. (2018) Some behaviour patterns of Trumpeter Swans. Ontario Birds 36, 174-192.

McCafferty, D.J. (2007) The value of infrared thermography for research on mammals: previous applications and future directions. Mammal Review 37, 207-223.

Minkina, W. & Dudzik, S. (2009) Infrared thermography : errors and uncertainties. J. Wiley, Chichester, West Sussex, U.K. ; Hoboken, NJ.

Mollinari, M.M., Peres, C.A. & Edwards, D.P. (2019) Rapid recovery of thermal environment after selective logging in the Amazon. Agricultural and Forest Meteorology 278, 12.

OuYang, X.Y., Wang, N., Wu, H. & Li, Z.L. (2010) Errors analysis on temperature and emissivity determination from hyperspectral thermal infrared data. Optics Express 18, 544-550.

Porter, W.M.R. & Witmer, L.M. (2016) Avian cephalic vascular anatomy, sites of thermal exchange, and the Rete Ophthalmicum. Anatomical Record-

Advances in Integrative Anatomy and Evolutionary Biology 299, 1461-1486.

R Core Team (2016) R: A language and environment for statistical computing. R Foundation for Statistical Computing, Vienna, Austria.

Scheffers, B.R., Edwards, D.P., Macdonald, S.L., Senior, R.A., Andriamahohatra, L.R., Roslan, N., Rogers, A.M., Haugaasen, T., Wright, P. & Williams, S.E. (2017) Extreme thermal heterogeneity in structurally complex tropical rain forests. Biotropica 49, 35-44.

Selvik, J.T. & Abrahamsen, E.B. (2017) On the meaning of accuracy and precision in a risk analysis context. Proceedings of the Institution of Mechanical Engineers Part O-Journal of Risk and Reliability 231, 91-100.

Soerensen, D.D. & Pedersen, L.J. (2015) Infrared skin temperature measurements for monitoring health in pigs: a review. Acta Veterinaria Scandinavica 57, 11.

Tattersall, G.J. (2016) Infrared thermography: A non-invasive window into thermal physiology. Comparative Biochemistry and Physiology A Molecular and Integrative Physiology 202, 78-98.

Tattersall, G.J. (2019) ThermimageJ: ImageJ functions and macros for working with thermal image files. https://github.com/gtatters/ThermImageJ.

Tattersall, G.J. & Cadena, V. (2010) Insights into animal temperature adaptations revealed through thermal imaging. Imaging Science Journal 58, 261-268.

Tattersall, G.J., Chaves, J.A. & Danner, R.M. (2018) Thermoregulatory windows in Darwin's finches. Functional Ecology 32, 358-368.

Tracy, C.R. (1979) Emissivity, a little explored variable. The Behavioral Significance of Color (ed. E.H. Burtt), pp. 28-32. Garland STPM Press, New York.

Wickham, H. (2016) ggplot2: Elegant Graphics for Data Analysis. Springer-Verlag, New York.

Xu, B.B., Peng, Z.W., Wu, Z.P., Zhang, X.A. & Wang, Y.H. (2019) Quantitative infrared spectroscopy of environmentally sensitive and rough materials. Review of Scientific Instruments 90, 8.

Appendix 3: Supplementary Material

Supplementary Video 1. Video to accompany Figure 5 in main text of a Trumpeter swan walking toward the thermal camera over a 45 second period. The video shows the maximum periorbital temperature (+ sign on video) location throughout rising as the birds gets closer to the camera and thus represents a larger object to the camera sensor. Calibration bar on the right represents the temperature scale (°C).

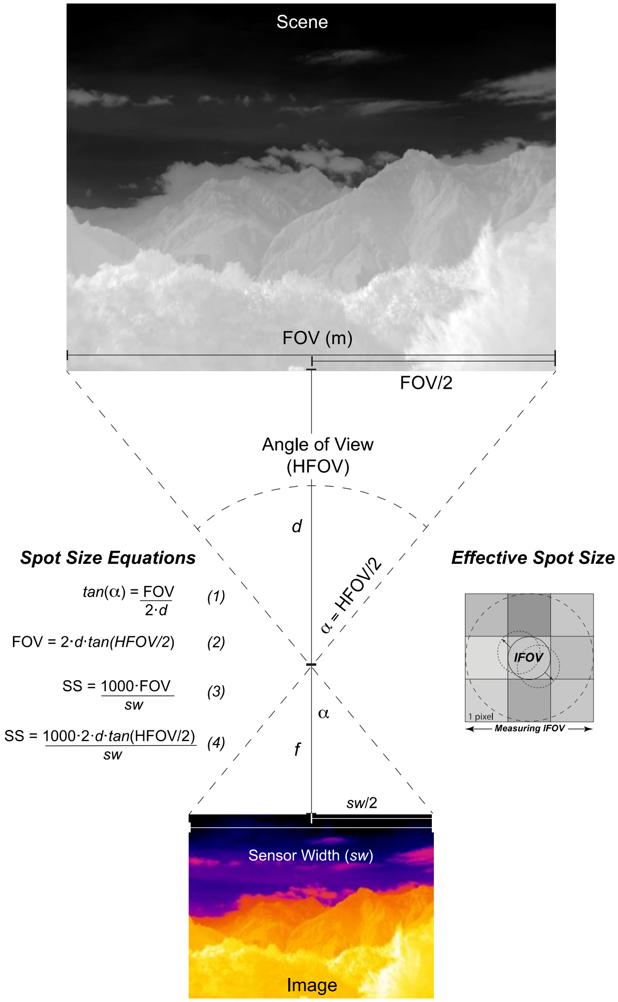

Supplementary Figure 1. Depiction of the process involved in calculating spot size for a given imaging system. Using information on the field of view (FOV; m), the camera lens angle of view (HFOV, degrees), and sensor width (sw; pixels), and distance (d; m) to object, one can solve for spot size (SS; mm), using equation 4. Although spot size is simply FOV divided by sensor width, equations 1-3 depict the relationships among the above variables allowing for the calculation of spot size from typically provided manufacturer information. Effective spot size is more conservatively 3 times larger because the true spot is unlikely to remain aligned precisely due to slight motion artefacts (see 3×3 pixel array, where IFOV is instantaneous field of view).

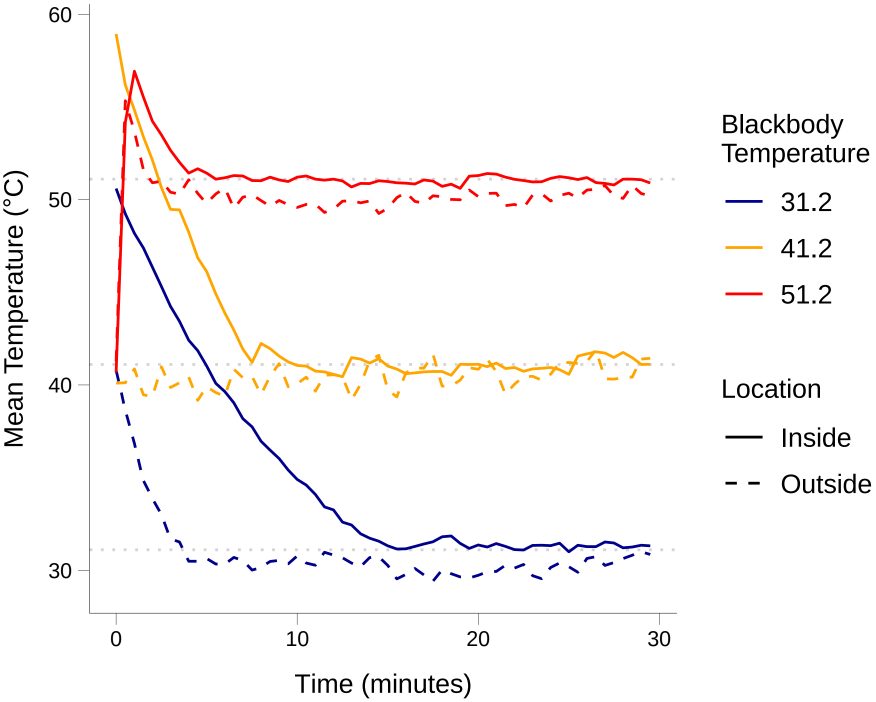

Supplementary Figure 2. Time lapse temperature traces (mean ± sd) of the blackbody source from the onset of switching the device on under indoor (ambient temperature 20-22°C) and outdoor (ambient temperature 0 to 5°C) conditions and with 3 different blackbody temperatures. To derive the temperatures, an ROI was drawn around the blackbody source and mean and standard deviation of temperature from the ROI extracted every 30 seconds. The blackbody source was typically stable within 15 minutes.

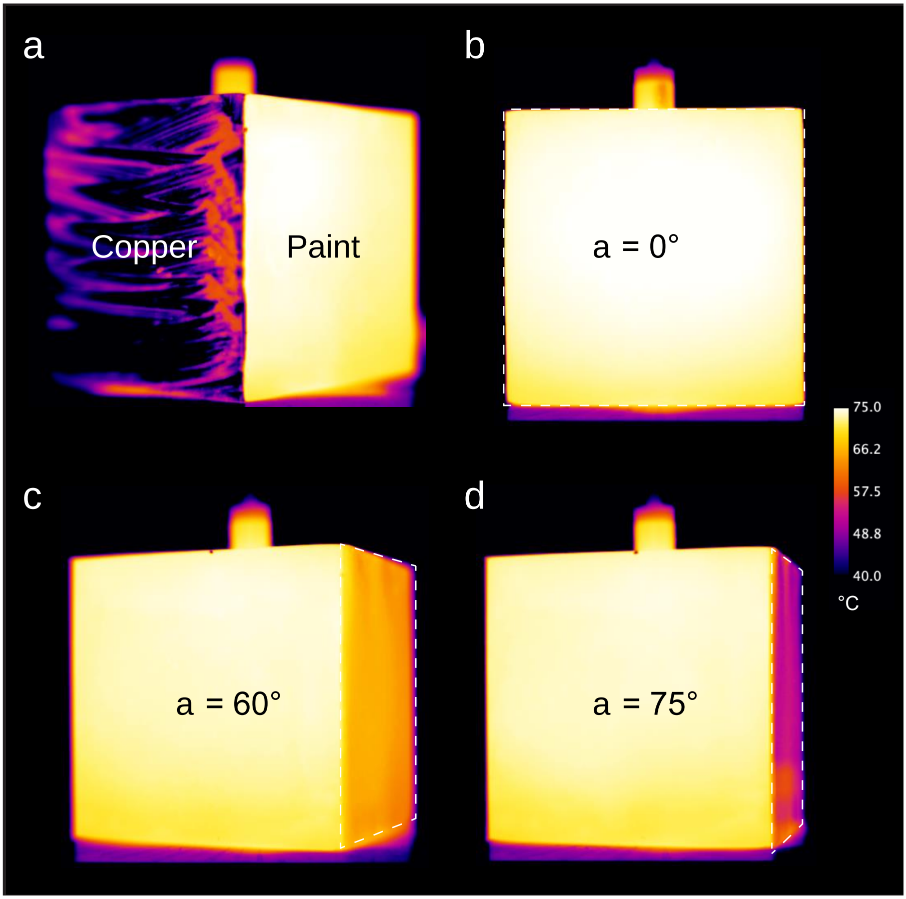

Supplementary Figure 3. Thermal images of a copper Leslie cube demonstrating the effect of angle of incidence on emissivity, and the resultant potential error in temperature estimation. One side of the Leslie cube is unpainted copper, while the other sides are painted with a material with emissivity of 0.95 (a: depicts both sides visible at 45° angle of incidence). The white dotted outlined regions in each panel refer to the side being measured with respect to 0° (b), 60° (c), and 75° angle of incidence. At higher angles of incidence, the same surface appears cooler (note the colour within the dotted region) since the reflectivity of the cooler ambient radiation increases.

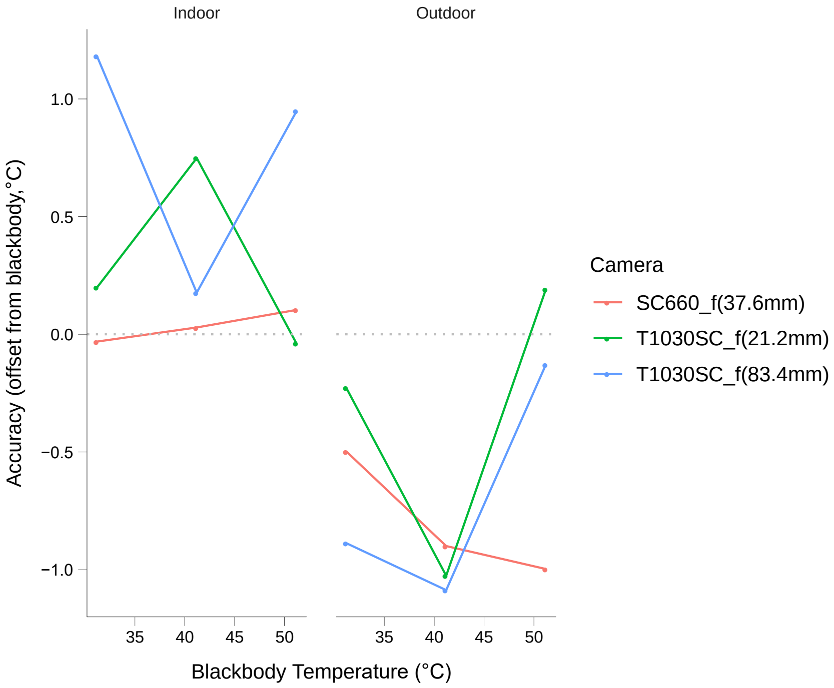

Supplementary Figure 4. Inter-camera differences in temperature accuracy are approximately ±1°C, consistent with the upper limit of manufacturer stated accuracies. Accuracy differences at different blackbody temperatures may reflect the non-synchronous nature of the image collection, capturing some of the inherent variation in the blackbody source. In studies using or comparing multiple cameras, it is important to assess whether these inherent differences contribute to apparent biological variation in temperature.

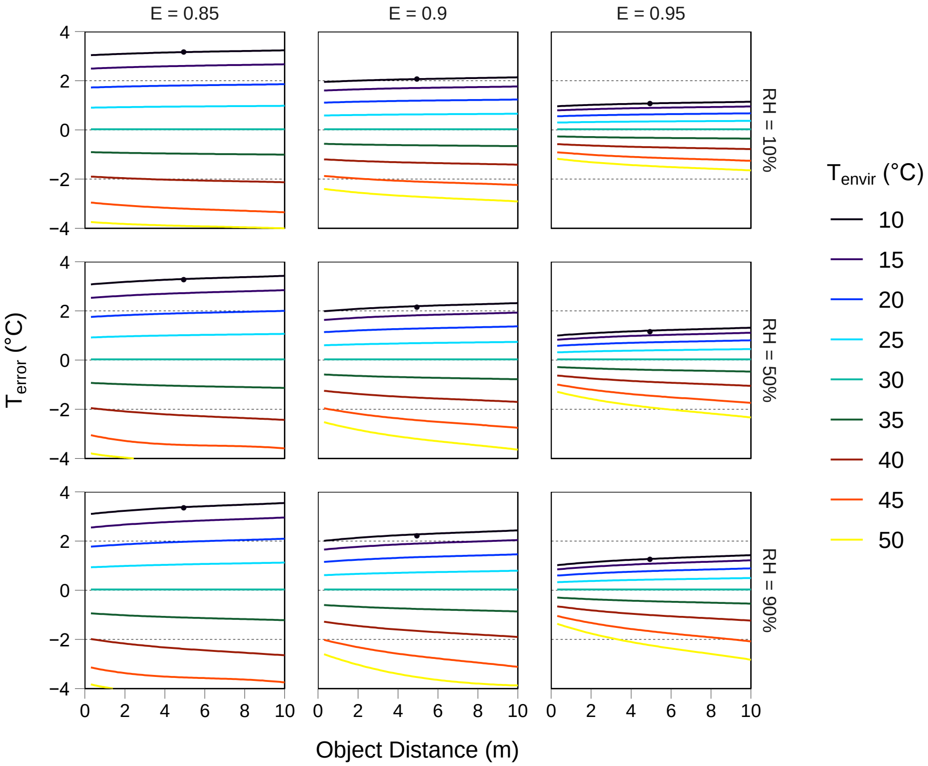

Supplementary Figure 5. Predicted systematic error (T_{error} = Estimated Temperature – Actual Temperature), based on the premise that incorrect values (*i.e.,* uncertainty or omission) for various parameters are used. The true value is that of a 30°C grey body with e = 0.95 measured at 0.3 m with environmental (atmospheric and reflected) temperatures of 30°C and relative humidity of 50%. Based on standard thermal imaging algorithms (Minkina and Dudzik, 2009), we calculated the temperatures for 2 different emissivities (0.85, and 0.9) representing two 'erroneous' emissivities to compare to a true emissivity (0.95), under different object distance and environmental conditions (atmospheric and reflected temperature ranged from 10 to 50°C, and relative humidity at 10, 50, and 90%). The algorithm converts the radiance captured by the camera sensor into a temperature estimate by accounting for radiation path loss and reflected radiation impinging on the surface. To assist in interpretation, a single point (black circle) depicts the temperature error for an object (true e = 0.95) at 5m distance under the different emissivities and humidities, but with an incorrect environment temperature of 10°C included. Simple errors in object parameters can lead to substantial inaccuracies.

7

General conclusions

General conclusions

1. We demonstrated that resident Mediterranean songbirds adjust their thermoregulatory physiology to seasonal variations. We found that they increased strongly their basal metabolic rate, the slope of evaporative water loss and the slope below the lower critical temperature during winter. These metabolic adjustments suggest a high seasonal flexibility in thermoregulatory traits that increases metabolic heat production as well as cold tolerance in winter while promotes water savings in summer.
2. Trans-Saharan songbirds displayed during summer higher lower and upper critical temperatures than its resident counterparts, jointly with narrower thermoneutral zone breadth. Therefore, migratory songbirds displayed more efficient thermoregulatory mechanisms at high T_a, which supports the climatic variability hypothesis as well as these migratory species would be more resilient to global warming than resident species inhabiting in the same Mediterranean region.
3. Using the Dunlin *Calidris alpina* as a model species, we showed that shorebirds adjusted their body posture jointly with locomotor activity according to the T_a during the resting period. Dunlins coped with high temperatures (>30 °C) by minimising locomotor activity and by sitting in wet substrate (sand) and ultimately panting while wet-sitting when challenged with temperatures above 37 °C.
4. The substrate type available for roosting in wetland margins is assumed to be important for bird thermoregulation, and our experimental findings emphasise the role of this factor in minimising heat stress in wetland species.
5. No relationships were found between physiological thermal traits and the relative size of bill in Mediterranean Great tits *Parus major*. However, males - but not females - with higher leg surface areas displayed higher cooling efficiencies at 40°C. This sex-dependent pattern suggests that male dominance behaviours could imply a greater dependence on cutaneous evaporative water loss through the leg surfaces as a consequence of higher exposure to harsh environmental conditions than faced by females.
6. We proposed that forest species such as Great tits would not be subjected to significant trade-offs between dehydration and hyperthermia avoidance because they normally occupy buffered habitats during summer with available microclimates and fresh water for drinking and thus, evaporative water loss could be favoured rather than dry heat loss through the bill surface.

7. Heat waves elicited plastic responses at both, physiological and morphological level in Great tits. Experimental birds displayed higher T_b values throughout heat waves simulation while showing a reduction of 17% on BMR and a greatest oxidative damage (by 56%) once experiments ended. Furthermore, Great tits exposed to heat waves also showed a decrease in barb and barbule density of plumulaceous and pennaceous section of contour feathers and more yellowish feathers.
8. Our results suggest Mediterranean Great tits to effectively buffer immediate stress triggered by heat waves through phenotypic flexibility, although we cannot discard long-term carry-over effects on fitness as climatic models anticipate more severe heat waves.
9. We showed the significant impact that distance and angle of incidence from a target object can exert on the quality of data collected through thermal imaging. Spot size and distance from the target object greatly influenced temperature measured. Indeed, we obtained an error of 6°C at a 10m distance.
10. Contrary to the distance effect, the angle at which an animal states in front of the camera cannot be controlled. This way, the angle of incidence becomes one of the main sources of error when taking thermal images. In this thesis we showed that the angle of incidence, generally over 50°, to the camera sensor can impact emissivity, being especially affected by smooth surfaces, which displayed a higher decline in emissivity when increased the angle of incidence.

Conclusiones generales

1. Demostramos que los paseriformes mediterráneos residentes ajustaron su fisiología termorreguladora a las variaciones estacionales. Encontramos que estos aumentan en gran medida su tasa metabólica basal, la pendiente de pérdida de agua por evaporación, así como la pendiente por debajo de la temperatura crítica inferior durante el invierno. Estos ajustes metabólicos sugieren una alta flexibilidad estacional en los rasgos termorreguladores que aumentan la producción metabólica de calor al igual que la tolerancia al frío en invierno, mientras que permite un ahorro hídrico en verano.
2. Las aves paseriformes migratorias transaharianas mostraron temperaturas críticas inferiores y superiores más altas que sus homólogos residentes durante el verano, junto con una amplitud de la zona termoneutral más estrecha. Por lo tanto, las especies migratorias presentaron mecanismos termorreguladores más eficientes a T_a elevadas, lo que apoya la hipótesis de variabilidad climática, además estas especies serían más resistentes al calentamiento global en comparación con las especies residentes que habitan en la misma región mediterránea.
3. Utilizando el Correlimos común *Calidris alpina* como especie modelo, demostramos que las aves limícolas ajustan su postura corporal conjuntamente con la actividad locomotora en función de la T_a durante el periodo de descanso. Los individuos que fueron expuestos experimentalmente a temperaturas elevadas (>30°C) minimizaron la actividad locomotora (sentándose en un sustrato húmedo [arena]) y, jadearon mientras permanecían sentados cuando se expusieron a temperaturas superiores a 37°C.
4. Se presupone que el tipo de sustrato disponible durante el descanso en los márgenes de los humedales es importante para la termorregulación de las aves que ocupan estos hábitats, y nuestros resultados experimentales enfatizan el papel de este para minimizar el estrés térmico en estas especies.
5. No se encontraron relaciones entre los rasgos térmicos fisiológicos y el tamaño relativo del pico en los Carboneros comunes mediterráneos *Parus major*. Sin embargo, los machos – pero no las hembras – con una mayor superficie de las patas mostraron una eficiencia de enfriamiento superior a 40°C. Este patrón dependiente del sexo sugiere que los comportamientos de dominancia de los machos podrían implicar una mayor dependencia de la pérdida de agua por evaporación cutánea a través de las superficies de las

patas, como consecuencia de una mayor exposición a las duras condiciones ambientales a las que se enfrentan las hembras.

6. Especies forestales como el Carbonero común no están sujetas a compromisos entre mantenerse hidratados y evitar la hipertermia porque normalmente ocupan hábitats con microclimas disponibles y agua fresca para beber durante el verano, y por tanto, podría favorecerse la pérdida de agua por evaporación en lugar de la pérdida de calor seco a través de la superficie del pico.
7. Las olas de calor desencadenaron respuestas plásticas tanto a nivel fisiológico como morfológico. Las aves experimentales mostraron valores de T_b más altos a lo largo de la simulación de las olas de calor, al tiempo que mostraron una reducción del 17% en la tasa metabólica basal y un aumento del 56% en el daño oxidativo. Además, los Carboneros comunes expuestos a olas de calor también mostraron una disminución de la densidad de barbas y bárbulas de la sección plumulacea y pennacea de las plumas de contorno además de plumas más amarillentas.
8. Nuestros resultados sugieren que los Carboneros comunes mediterráneos pueden amortiguar eficazmente el estrés inmediato provocado por las olas de calor mediante la flexibilidad fenotípica, aunque no podemos descartar efectos de arrastre a largo plazo sobre la aptitud, ya que los modelos climáticos predicen olas de calor más severas.
9. Demostramos el gran impacto que la distancia y el ángulo de incidencia, de un objeto de estudio, pueden ejercer sobre la calidad de los datos recogidos mediante imágenes térmicas. El *spot size* y la distancia desde el objeto influyeron en gran parte a la temperatura medida. De hecho, obtuvimos un error de 6°C a una distancia de 10m.
10. Al contrario que el efecto de la distancia, no se puede controlar el ángulo en el que un animal se sitúa frente a la cámara. De este modo, el ángulo de incidencia se convierte en una de las principales fuentes de error al tomar imágenes térmicas. En esta tesis probamos que el ángulo de incidencia, generalmente superior a 50°, respecto al sensor de la cámara puede afectar a la emisividad, viéndose especialmente afectada por las superficies lisas, que mostraban una mayor disminución de la emisividad al aumentar el ángulo de incidencia.

Addresses of co-authors

Auxiliadora Villegas [1,2]
Deseada Parejo[2,3]
Erick González-Medina[1]
Glenn J. Tattersall[4]
Jorge S. Gutiérrez[1,2]
José A. Masero[1,2]
José M. Abad-Gómez[1]
Juan M. Sánchez-Guzmán[1,2]
Julián Cabello-Vergel[1]
Manuel Parejo[1]

[1]Conservation Biology Research Group, Facultad de Ciencias, Universidad de Extremadura, Badajoz, Spain.
[2]Ecology in the Anthropocene, Associated Unit CSIC-UEX, Facultad de Ciencias, Universidad de Extremadura, Badajoz, Spain.
[3]Department of Functional and Evolutionry Ecology, EEZA-CSIC, Almería, Spain.
[4]Department of Biological Science, Brock University, St. Catharines, ON, Canada.






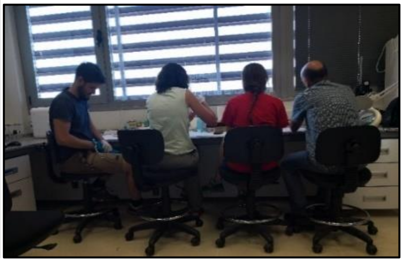


SEO
BirdLife
#AvesDeBarrio

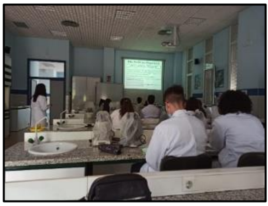




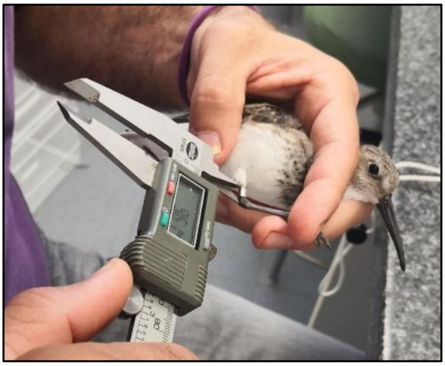


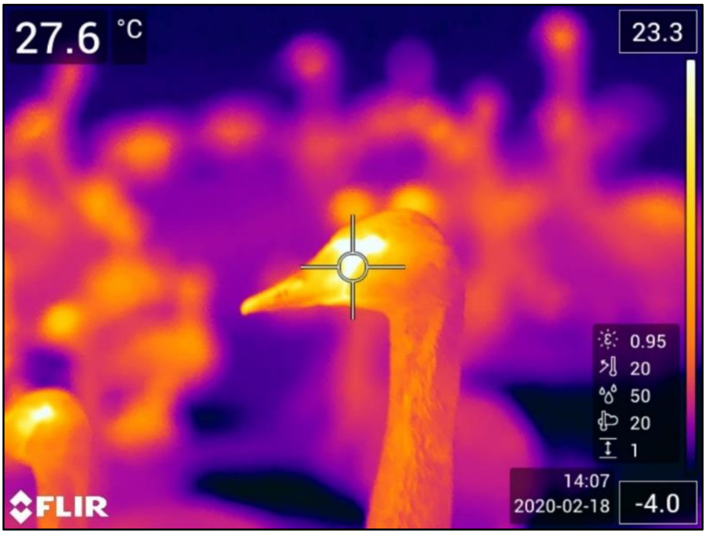
27.6 °C
23.3
0.95
20
50
20
1
14:07
2020-02-18
-4.0
FLIR

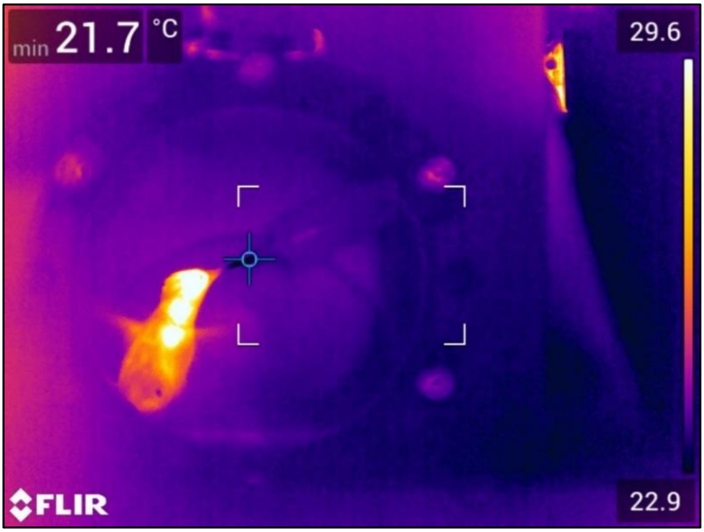
min 21.7 °C
29.6
22.9
FLIR

1. **Playà-Montmany, N.**, González-Medina, E., Cabello-Vergel, J., Parejo, M., Abad-Gómez, J. M., Sánchez-Guzmán, J. M., Villegas, A., Gutiérrez, J. S. and Masero, J. A. (2022) Mediterranean songbirds show pronounced variation in thermoregulatory traits. Submitted to Ecology Letters.

2. **Playà-Montmany, N.**, González-Medina, E., Cabello-Vergel, J., Parejo, M., Abad-Gómez, J. M., Sánchez-Guzmán, J. M., Villegas, A and Masero, J. A. (2022) Behavioural and physiological responses to experimental temperature changes in a long-billed and long-legged bird: a role for relative appendage size. Submitted to Behavioral Ecology and Sociobiology.

3. **Playà-Montmany, N.**, González-Medina, E., Cabello-Vergel, J., Parejo, M., Abad-Gómez, J. M., Sánchez-Guzmán, J. M., Villegas, A. and Masero, J. A. (2021) The thermoregulatory role of relative bill and leg surface areas in a Mediterranean population of Great tit (*Parus major*). Ecology and Evolution 11(22), 15936-15946.

4. **Playà-Montmany, N.**, González-Medina, E., Cabello-Vergel, J., Abad-Gómez, J. M., Parejo, M., Parejo, D., Sánchez-Guzmán, J. M., Villegas, A. and Masero, J. A. (2022) How do Mediterranean bird species cope with extreme weather events? Physiological and morphological responses to simulated heat waves in Great ttis (*Parus major*). Manuscript.

5. **Playà-Montmany, N.** and Tattersall, G. J. (2021) Spot size, distance and emissivity errors in field applications of infrared thermography. Methods in Ecology and Evolution 12(5), 828-840.